

**ERROR MINIMIZATION OF REDUCED MODELS OF LARGE-SCALE
SYSTEMS BY SOLVING TIME AND FREQUENCY RESTRICTED LYAPUNOV
EQUATIONS**

The thesis submitted to the
Department of Mathematics, BUET, DHAKA-1000
in partial fulfilment of the requirements for the degree of

MASTER OF SCIENCE

IN

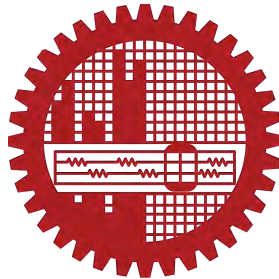
MATHEMATICS

By

KIFE INTASAR BIN IQBAL

Student ID: 1018092512F

Registration No. 1018092512, Session: October-2018



Under the supervision

of

Dr. Mohammed Forhad Uddin

Professor

Department of Mathematics

Bangladesh University of Engineering and Technology (BUET)
Dhaka-1000, Bangladesh

The thesis entitled

**ERROR MINIMIZATION OF REDUCED MODELS OF LARGE-SCALE
SYSTEMS BY SOLVING TIME AND FREQUENCY RESTRICTED LYAPUNOV
EQUATIONS**

Submitted by

KIFE INTASAR BIN IQBAL

Student ID: 1018092512F, Registration No. 1018092512, Session: October-2018 has been accepted as satisfactory in partial fulfillment for the degree of Master of Science in Mathematics on

BOARD OF EXAMINERS

1. 

Dr. Mohammed Forhad Uddin
Professor
Department of Mathematics, BUET, Dhaka

**Chairman
(Supervisor)**

2. 

Dr. Khandker Farid Uddin Ahmed
Professor and Head
Department of Mathematics, BUET, Dhaka

**Member
(Ex-Officio)**

3. 


Dr. Md. Abdul Hakim Khan
Professor
Department of Mathematics, BUET, Dhaka

Member

4. 

Dr. Khandker Farid Uddin Ahmed
Professor
Department of Mathematics, BUET, Dhaka

Member

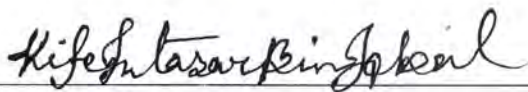
5. 

Dr. Mohammad Monir Uddin
Associate Professor
Department of Mathematics and Physics
North South University, Dhaka-1229

**Member
(External)**

DECLARATION OF AUTHORSHIP

I, Kife Intasar Bin Iqbal, declare that this thesis titled, **ERROR MINIMIZATION OF REDUCED MODELS OF LARGE-SCALE SYSTEMS BY SOLVING TIME AND FREQUENCY RESTRICTED LYAPUNOV EQUATIONS** and the work presented in this thesis is the outcome of the investigation carried out by the author under the supervision of Dr. Mohammed Forhad Uddin, Professor, Department of Mathematics, Bangladesh University of Engineering and Technology (BUET), Dhaka-1000 in accordance with the requirement of the University's Regulations and Code of Practice for Research Degree Programs and that it has not been submitted anywhere for any other academic award.



Kife Intasar Bin Iqbal

Date: 28/08/2021

ACKNOWLEDGMENTS

I would like to express my deepest gratitude to my supervisor Prof. Dr. Mohammed Forhad Uddin for his guidance on this thesis showing me the path of conducting successful research and above all for always being there as my mentor. I shall forever cherish the memories of working with him. I am very thankful to him for introducing me in this highly fascinating research area and complete this thesis successfully.

I would like to express my gratitude to all of my teachers for their valuable suggestions and thankful to my department head Dr. Khandker Farid Uddin Ahmed for giving me the opportunity to use our computational lab as well as other facilities during my research period. Moreover, I am grateful to all of the staffs of the department of mathematics for their supportive attitudes and friendly behaviours to me during any necessity of mine.

I am cordially grateful to Dr. Md. Abdul Hakim Khan and Dr. Khandker Farid Uddin Ahmed for being on my defense committee, reading my thesis and giving me valuable suggestions for improvements. Their treasured supports were really influential in sharpening my experiment methods and making myself thoughtful to understand mathematics deeply.

Especially, I am extremely thankful and highly indebted to Dr. Mohammad Monir Uddin for his generous assistance, cooperation and precious guidance during my research periods. He shared his wisdom with me in analyzing subject matters and at the same time valued my thinking approach to synthesize those topics. His priceless suggestions drove me towards better ways of thinking, his reviews enriched me in solving problems, and his support gave me strength at the time of my disappointment. The knowledge, I have achieved from him, is an asset in my life.

I want to show my cordial gratefulness to Bangladesh Bureau of Educational Information and Statistics (BANBEIS), Dhaka, Bangladesh for their financial support under the project ID: MS20191055 throughout this research work.

Finally, I express my best regards to my mother for her support and motivations. Her heartfelt wishes for me gave me energy in my research study.

ABSTRACT

The usage of mathematical models of physical systems are increasing day by day in various disciplines of science and engineering for simulation, optimization, or control. Descriptor systems is a special kind of formation of physical systems arisen in many practical oriented fields whose dynamics maintain Differential- Algebraic Equations. Such type of systems are originated by finite elements or difference methods which becomes huge and complex to analyze along with the increment of the fineness of the grid resolution. As a result, the necessity of model order reduction comes up in order to minimize the complexity of the models during controlling by preserving the input-output relation of the original large-scale models. However, although reducing the dimension of large-scale models on infinite time and frequency domains has a great theoretical significance, the reduced order models of original large-scale models on restricted time and frequency intervals are more demandable to the analyzers and engineers for practical investigation.

This dissertation elaborately discusses the model generations for data extraction to form the large-scale state-space systems and the projection based techniques to calculate the approximate low-rank solutions of the original state-space systems on definite time and frequency intervals. We impose relevant governing equations to create physical as well as data models. Balanced truncation is one of the most notable methods for the reduction of the model dimensions of linear time-invariant systems which requires computing the numerical solutions of two Lyapunov equations, commonly known as Gramians. Among some widely used approaches, Rational Krylov Subspace Method is one of the most effective procedures for finding the Gramians of the Lyapunov equations of the large-scale sparse dynamical systems which has already been developed to compute the low-rank time and frequency indefinite solutions. Besides, it has been also reformed to compute the low-rank approximation of the standard Lyapunov equations on limited time and frequency intervals for small-dense state-space systems.

However, in this thesis, we establish algorithms intending to obtain the low-rank solutions of the Lyapunov equations on restricted time and frequency intervals constructed centering around large-scale sparse index-I and index-II descriptor systems by creating no explicit projection. Moreover, we develop algorithm to compute the matrix exponential through power series expansion avoiding typical Schur decomposition in order to retain the sparsity for less memory consumption and analyze the existing algorithms of matrix logarithm computation. For gaining the fastest convergent solutions, we do a comparative analysis of the existing shift parameters essential for solving the linear time-invariant systems. We also develop algorithms for getting low-rank solutions on finite time interval with non-homogeneous initial condition, i.e., non-zero initial value. Although balanced truncation gives the guarantee to preserve the stability of the reduced order models deduced from the stable full models on infinite time and frequency domains, it fails to give the stable time and frequency restricted reduced order models of stable original systems.

Hence, an algorithm is proposed here as a remedy to this problem.

At the final stage, the numerical outcomes by applying our proposed algorithms on various types of existing data models including our generated models are exhibited to demonstrate the efficiency and exactness by minimizing the errors on the restricted time and frequency intervals. In addition, the comparative analysis between the domain restricted and unrestricted reduced order models are performed to show that on limited time and frequency intervals, our proposed algorithms give better approximations of the original large-scale sparse systems.

TABLE OF CONTENTS

	Page
List of Tables	viii
List of Figures	x
List of Algorithms	xii
1 Introduction	1
1.1 Motivation	1
1.2 Thesis outline	4
2 Background	5
2.1 Theory of systems and control	5
2.1.1 State-space representation of dynamical system	6
2.1.2 Duhamel’s principle and Solution of the Generalized LTI system	7
2.1.3 Input-output relation, Step response, and Transfer function of LTI system	7
2.1.4 Descriptor system	9
2.1.5 Controllability and Observability Gramians on infinite time domain	10
2.1.6 System stability	11
2.1.7 Controllability and Observability Gramians on restricted time interval . .	12
2.1.8 Controllability and Observability Gramians on restricted frequency interval	13
2.1.9 Difficulties in system’s stability on restricted time and frequency intervals	16
2.1.10 System Hankel’s singular values	16
2.1.11 System’s realizations	17
2.2 Concept of matrix computation	17
2.2.1 Eigenvalue Problem	17
2.2.2 Sparsity Pattern and projection	18
2.2.3 Important matrix decomposition	19
2.2.3.1 Eigenvalue decomposition	19
2.2.3.2 Schur decomposition	19
2.2.3.3 QR decomposition	19
2.2.3.4 Singular value decomposition	20
2.2.3.5 Arnoldi decomposition	20
2.2.4 Matrix exponential	21
2.2.4.1 Eigenvalue decomposition method	21

2.2.4.2	Power series expansion	22
2.2.5	Matrix square root	22
2.2.5.1	Schur decomposition method	22
2.2.5.2	Power series expansion	22
2.2.5.3	Denman-Beaver method	23
2.2.6	Matrix logarithm	23
2.2.6.1	Eigenvalue decomposition method	23
2.2.6.2	Power series expansion	24
2.3	Available methods for solving Lyapunov equation	24
2.3.1	Methods for dense system	24
2.3.1.1	Bartels-Stewart's method	24
2.3.1.2	Hammarling's method	25
2.3.1.3	Matrix sign function method	25
2.3.2	Methods for sparse systems	26
2.3.2.1	Low Rank LDL^T factor- Alternating Direction Implicit method	26
2.3.2.2	Krylov subspace method	27
2.4	Model order reduction techniques	28
2.4.1	Square root balanced truncation	29
2.4.2	Interpolatory projection method	31
3	Generation of Data Models	33
3.1	Piezoelectric Tonpiliz Transducer	33
3.2	Power system model	39
3.3	Existing data models	43
3.3.1	Brazilian Interconnected Power Systems	43
3.3.2	Oseen Model	44
4	Solution of Lyapunov Equations on Restricted Time Intervals by Iterative Method	46
4.1	Rational Krylov Subspace Method	46
4.2	Selection of Shift Parameter	49
4.3	Computation of Matrix Exponential	49
4.4	Calculating Residual Norm	52
4.5	Formulation and Solution of Time Restricted Index-I Descriptor System	53
4.5.1	Investigation on Solving Time Restricted Index-I Descriptor System with Non-homogeneous Initial Condition	57
4.6	Formulation and Solution of Time Restricted Index-II Descriptor System	59
4.7	Numerical Outcomes	62
4.7.1	Numerical Results from Index-I Descriptor System	62
4.7.2	Numerical Results from Index-I Descriptor System on Non-homogeneous Time intervals	66
4.7.3	Numerical Results from Index-II Descriptor System	67

5	Solution of Lyapunov Equations on Restricted Frequency Intervals by Iterative Method	70
5.1	Rational Krylov Subspace Method for Generalised Frequency-restricted Lyapunov Equation	70
5.2	Selection of Shift Parameters Using Genetic Algorithm	71
5.3	Computation of Matrix Logarithm	75
5.4	Calculating Residual Norm	76
5.5	Solution of Frequency Restricted Index-I Descriptor System	77
5.6	Solution of Frequency Restricted Index-II Descriptor System	77
5.7	Numerical Outcomes	77
5.7.1	Numerical Results from Index-I Descriptor System	78
5.7.2	Numerical Results from Index-II Descriptor System	81
5.7.3	Numerical Results after Plugging in Gene Shift Parameters	82
6	Error Minimization of Reduced Order Model using the Solutions of Lyapunov Equations	85
6.1	Square Root Balanced Truncation of Index-I System	85
6.2	Square Root Balanced Truncation of Index-II System	87
6.3	Retrieve of the Stability of the Reduced Order Models	87
6.4	Error Calculation of Reduced Order Systems	88
6.4.1	Error Calculation of Index-I Reduced Order Model	88
6.4.2	Error Calculation of Index-II Reduced Order Model	90
6.5	Numerical Outcomes	90
6.5.1	Error of Index-I system on Restricted Time Intervals	91
6.5.2	Error of Index-II system on Restricted Time Intervals	92
6.5.3	Error of Index-I system on Restricted Frequency Intervals	94
6.5.4	Error of Index-II system on Restricted Frequency Intervals	96
6.5.5	Error of Stable system	97
7	Conclusion and Future Work	106
7.1	Conclusion	106
7.2	Future Work	107
	Bibliography	109

LIST OF TABLES

TABLE	Page
3.1 Dimension of Piezoelectric Tonpiliz transducer	38
3.2 Dimension of Electric power system	41
3.3 Dimension of Brazilian Interconnected Power System	44
3.4 Dimension of Oseen model	44
4.1 Computational time of Matrix Exponential	51
4.2 Required Time for the computation of linear systems of sparse and dense system . . .	64
4.3 Residual norms of time restricted and unrestricted CG and OG on nominated time intervals	66
4.4 Residual norms of time restricted and unrestricted CG and OG on nominated time intervals	68
4.5 Required Time for the computation of linear systems of sparse and dense index-II system	68
4.6 Residual norms of time restricted and unrestricted CG and OG on nominated time intervals	69
5.1 Residual norms of frequency restricted and unrestricted CG and OG on nominated frequency intervals	79
5.2 Residual norms of frequency restricted and unrestricted CG and OG on nominated frequency intervals	81
5.3 Residual norms of frequency restricted and unrestricted CG and OG on nominated frequency intervals	82
5.4 Effect of various key parameters on selecting shift parameters	83
6.1 Competitive numerical analysis on absolute & relative errors of the time-restricted (t) and time-unrestricted (∞) Gramians under nominated time intervals	91
6.2 Competitive numerical analysis on absolute & relative errors of the time-restricted (t) and time-unrestricted (∞) Gramians under non-homogeneous time intervals	91
6.3 Competitive numerical analysis on absolute & relative errors of the time-restricted (t) and time-unrestricted (∞) Gramians under nominated time intervals	93
6.4 Competitive numerical analysis on absolute & relative errors of the frequency-restricted (Ω) and frequency-unrestricted (∞) Gramians under nominated frequency intervals .	95
6.5 Competitive numerical analysis on absolute & relative errors of the frequency-restricted (Ω) Gramians between Gene shift and RKSM shift under nominated frequency intervals	96

6.6	Competitive numerical analysis on absolute & relative errors of the frequency-restricted (Ω) and frequency-unrestricted (∞) Gramians under nominated frequency intervals .	97
-----	----------------------------------------------------------------------------------------------------------------------------------------------------------------------------------------------	----

LIST OF FIGURES

FIGURE	Page
1.1 Work flow of this thesis	2
2.1 Diagram of state-space representation of linear system	5
2.2 (a) Sparse Pattern (b) Dense Pattern	18
2.3 Model reduction (image source [1])	29
3.1 Mesh of Piezoelectric Tonpilz Transducer	33
3.2 Acoustic field pressure on output Probe points Vs. Time [0-10 sec]	36
3.3 External field pressure	37
3.5 Sound pressure	38
3.4 External fluid pressure	38
3.6 Transfer function of Piezoelectric Tonpilz transducer	39
3.7 Distributed Line	41
3.8 Capacitor	41
3.9 Control diagram of Tap Changer	42
3.10 Connection of tap changer	42
3.11 Current and Voltage Profile through single wire transmission line	42
3.12 Current and Voltage Profile through triple wires transmission line	43
3.13 Transfer function of electric power system	43
3.14 Mesh structure of simple channel flow	44
3.15 Velocity profile of simple channel flow	45
3.16 Pressure profile of simple channel flow	45
4.1 (a) Dense Pattern and (b) Sparse Pattern of Power system model	63
4.2 (a) Dense Pattern and (b) Sparse Pattern of Piezoelectric Tonpilz Transducer model	63
4.3 (a) Dense Pattern and (b) Sparse Pattern of BIPS-1693 model	63
4.4 Convergence tendency of (a) CG and (b) OG of BIPS-606	64
4.5 Convergence tendency of (a) CG and (b) OG of BIPS-1142	65
4.6 Convergence tendency of (a) CG and (b) OG of BIPS-1693	65
4.7 Convergence tendency of (a) CG and (b) OG of Piezo Tonpilz Transducer	66
4.8 Convergence tendency of (a) CG and (b) OG of BIPS-606 on non-homogeneous time interval	67
4.9 Convergence tendency of (a) CG and (b) OG of BIPS-606 on non-homogeneous time interval	67

4.10 (a) Dense Pattern and (b) Sparse Pattern of Ossen model	68
4.11 Convergence tendency of (a) CG and (b) OG of Ossen model	69
5.1 Flow chart of genetic algorithm	73
5.2 Convergence tendency of (a) CG and (b) OG of BIPS-606	79
5.3 Convergence tendency of (a) CG and (b) OG of BIPS-1142	80
5.4 Convergence tendency of (a) CG and (b) OG of BIPS-1693	80
5.5 Convergence tendency of (a) CG and (b) OG of Piezo Tonpilz Transducer	81
5.6 Convergence tendency of (a) CG and (b) OG of Ossen model	82
5.7 Convergence tendency of (a) CG and (b) OG of BIPS-606 by Gene Shift	83
5.8 Convergence tendency of (a) CG and (b) OG of Piezo Tonpilz Transducer by Gene Shift	84
6.1 Mesh of reduced order Piezoelectric Tonpilz Transducer	92
6.2 Acoustic field pressure on output Probe points Vs. Time [0-10 sec] of reduced order Piezo Tonpilz Transducer	92
6.3 (a) Approximation of full models and (b) Absolute (c) Relative errors of reduced order BIPS-1142 Model on time interval [0,5]	93
6.4 External field pressure of reduced order Piezo Tonpilz Transducer	94
6.5 Sound pressure of reduced order Piezo Tonpilz Transducer	94
6.6 (a) Approximation of full models and (b) Absolute (c) Relative errors of reduced order Piezo Tonpilz Transducer Model on time interval [0,10]	95
6.7 External fluid pressure of reduced order Piezo Tonpilz Transducer	96
6.8 (a) Approximation of full models and (b) Absolute (c) Relative errors of reduced order BIPS-606 Model on time interval [2,5]	98
6.9 (a) Approximation of full models and (b) Absolute (c) Relative errors of reduced order Ossen Model on time interval [0,6]	99
6.10 (a) Approximation of full models and (b) Absolute (c) Relative errors of reduced order BIPS-1693 Model on frequency interval [3,7]	100
6.11 (a) Approximation of full models and (b) Absolute (c) Relative errors of reduced order Power System Model on frequency interval [0,5]	101
6.12 Comparative error analysis between full and reduced order models using existing RKSM shift and proposed Gene shift on frequency interval [-2,2]	102
6.13 (a) Approximation of full models and (b) Absolute (c) Relative errors of reduced order Ossen Model on frequency interval [-3,3]	103
6.14 Time domain analysis of stable and unstable reduced order system	104
6.15 Eigenvalues observation of stable and unstable reduced order models	104
6.16 Comparison between unstable and stable model on frequency intervals [1,3]	105

LIST OF ALGORITHMS

ALGORITHM	Page
1 Step response.	8
2 Arnoldi algorithm	21
3 Low rank LDL^T factorization ADI method	27
4 Square root balanced truncation	30
5 Time-restricted IRKA	32
6 RKSM for solving time-restricted controllability Gramian (2.19a) of generalised system (2.2) on time interval $[0, t_f]$	48
7 Computation of Matrix Exponential.	50
8 RKSM for solving time-restricted controllability Gramian (2.19a) of index-I system (2.10) on time interval $[0, t_f]$	54
9 Change in Algorithm (8) for solving time-restricted controllability Gramian (4.15) of index-I system (2.10) on time interval $[t_0, t_f]$	59
10 RKSM for solving time-restricted controllability Gramian (2.19a) of index-II system (2.11) on time interval $[0, t_f]$	61
11 RKSM for solving frequency-restricted controllability Gramian (2.33a) of generalised system (2.2) on frequency interval $[\Omega_0, \Omega_f]$	72
12 Selection of Shift Parameters using Genetic Algorithm	74
13 RKSM for solving frequency-restricted controllability Gramian (2.33a) of index-I system (2.10) on frequency interval $[\Omega_0, \Omega_f]$	76
14 RKSM for solving frequency-restricted controllability Gramian (2.33a) of index-II system (2.11) on frequency interval $[\Omega_0, \Omega_f]$	78
15 Square root balanced truncation for index-I system (2.10)	86
16 Square root balanced truncation for index-II system (2.11)	87
17 Stability preservation of reduced order index-I and index-II system matrices (6.1) and (6.3)	88

1.1 Motivation

Mathematical simulation is a very powerful and popular approach in the field of scientific experiments to investigate scientific concepts what is required mathematical data models for analysis converted from physical models. Often, these types of practically oriented mathematical models are designated by Linear Time-Invariant (LTI) continuous-time systems which are subject to supplementary algebraic constraints, constructed as descriptor systems [2] represented by Differential-Algebraic Equations (DAEs). There are several well-established discretization methods to obtain this type of data system among which Finite Element Method (FEM) is widely used in the model designing sector. Such kind of discretizational procedure generates a satisfactory number of grid points for resolving the geometrical details as accurately as possible what is the reason behind the dimension of the mathematical data models becoming extremely huge and sparse [1, 3–5]. As a result, these types of memory-hungry large-scale systems demand numerous computational efforts which is a major hindrance for smooth simulation due to the memory as well as time limitation. Therefore, it is inevitable to substitute the higher dimensional models with the equivalent lower dimensional data models what is possible by imposing the methods, ordinarily known as Model Order Reduction (MOR) [6–9].

The primary goal of MOR is to construct lower-dimensional systems in the replacement of higher dimensional systems for reducing the time and space complexities during simulation whose input-output responses are approximately as same as the responses of the original large models [10]. During the conversion of mathematical data models from physical models solving a large number of Ordinary or Partial Differential Equations (ODEs or PDEs), there is an immense amount of spare data included in the models which are unessential to characterize the input-output of any physical device [11]. With a view to eliminating those redundant data from the original data models, MOR is imposed what decreases the entire sizes of the systems suitable for scientific analysis. However, at the time of dealing with real-life related problems, the requirement of model simulation on small time and frequency intervals arises instead of analysing on entire domains [12]. Therefore, although the MOR on infinite domains has great theoretical significance, it is less practically important comparing with the MOR of the data models on limited time and frequency domains.

Generally, two well-established techniques [3, 4, 6], namely, Gramian based methods and moment based methods are very popular to the analyzers for MOR what are sub-divided into several

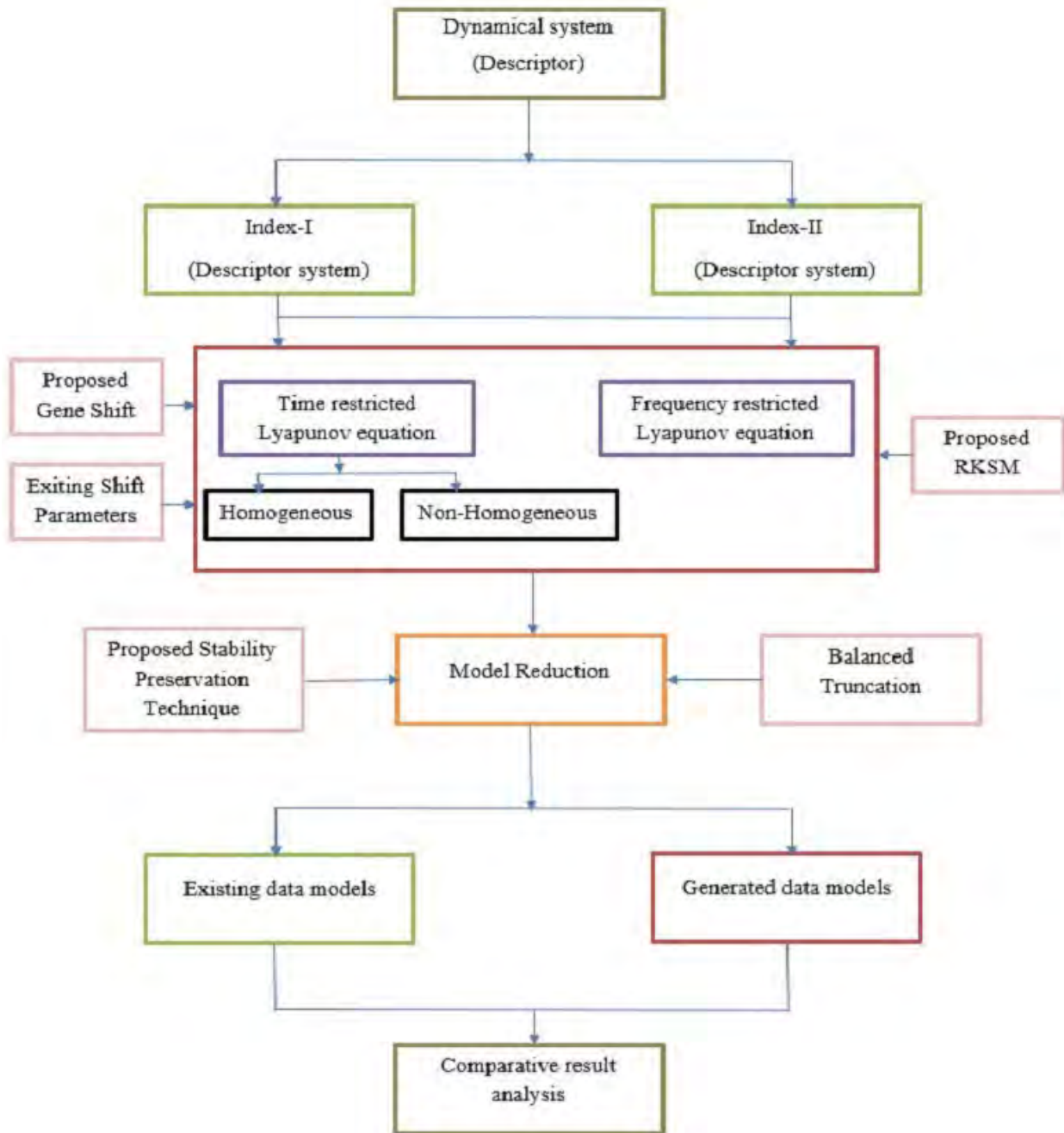


Figure 1.1: Work flow of this thesis

theoretically proven methods such as singular perturbation approximation [13], optimal Hankel norm approximation [14], rational Krylov method [15, 16], Balanced Truncation (BT) [17, 18]. Among them, the usage of BT is increasing day by day for the MOR of large-scale sparse dynamical systems because it gives the guarantee of stability preservation of the reduced order models on infinite domains and also has a global error bound [2, 11, 17].

However, BT requires the solutions of two continuous-time Lyapunov equations, commonly known as Controllability Gramian (CG) and Observability Gramian (OG) [9, 10]. There are diverse iterative methods like Low-Rank Cholesky Factor Alternating Direction Implicit (LRCF-ADI) [19, 20], cyclic low-rank Smith method [21, 22], projection methods [23–26], matrix sign function

[27, 28] besides direct solver methods such as Bartels-Stewart method [29, 30] and Hammarling method [31, 32] developed over the last few decades as the remedy to find out the solution of Lyapunov equation on infinite domains. Among all of these, Rational Krylov Subspace Method (RKSM) [33] is one of the most popular projection-based iterative methods modified as the solver of the Lyapunov equations in [25, 34] that computes the low-rank factors of the approximate solutions of the Lyapunov equations. RKSM has already been developed in [11, 35, 36] with a view to solving the Lyapunov equations on infinite domains constructed centering around large-scale sparse descriptor systems.

Nevertheless, to cope with solving the realistic problems, it is more important to find out the solutions of the Lyapunov equations of large-scale descriptor systems on restricted time and frequency intervals rather than solving them on finite intervals. Therefore, it is a contemporary need to solve the Lyapunov equations of large-scale descriptor systems on restricted time and frequency intervals. The structures of Lyapunov equations on finite time and frequency intervals based on dense standard systems were introduced in [12]. The authors of [37, 38] investigated the methods for solving them for large standard case only. However, in [39, 40], it was extended to the generalized case also. But none of them discussed how to find out the solutions by keeping the system matrices sparse because all of them created explicit projectors for projecting the system matrices converting the matrices to dense. As a result, it increases the computational time to compute the low-rank approximations of the solutions of the time and frequency limited Lyapunov equations.

On the other hand, we propose algorithms to solve the Lyapunov equations centering on two special kinds of descriptor systems, known as index-I and index-II descriptor systems, on restricted time and frequency intervals using RKSM without constructing any explicit projector, i.e., projecting the system matrices implicitly. We also develop algorithms for computing matrix exponential by modifying the existing typical computational procedures [41] and analyze the existing algorithms of matrix logarithm [42], necessary for solving time and frequency limited Lyapunov equations in order to get faster solution. As a result, our proposed algorithms, which also work for both stable and unstable systems, successfully decrease the entire computational periods. Moreover, we also conduct a competitive analysis among the existing shift parameters, the essential ingredient for solving Lyapunov equations by RKSM, to seek out the better shift parameter for fast convergence. After that, we apply BT using our computed low-rank solution factors for MOR on restricted time and frequency intervals.

Although reduced order models of stable original models on infinite domains imposing BT become stable, there is no guarantee to get stable reduced models on finite time or frequency domains [12] from stable full models. Therefore, there are several techniques developed to make the reduced unstable systems stable [37, 43]. But, unfortunately, none of them gives the reduced order models stable and more accurate than the infinite reduced models simultaneously. From that necessity, we develop an algorithm for stability preservation of unstable reduced models that gives more accurate approximations of full original models on nominated time and frequency intervals at the same time. In addition, we also develop an algorithm for solving the Lyapunov equations on restricted time interval having non-homogeneous initial values, i.e., non-zero starting points by modifying our proposed algorithm working for homogeneous time intervals, i.e., consisting of zero initial values. Finally, we conduct a detail numerical experiment to show the efficiency of

our proposed algorithms on restricted time and frequency intervals while the intervals outside the particular time and frequency boundaries are out of our prime concern. The flow chart 1.1 systematically summarizes our entire workflow throughout this thesis.

1.2 Thesis outline

The thesis is organized as follows:

In Chapter 2, the backgrounds of our research work are discussed. A vast description of the basics of control theory and descriptor systems alongside the model order reduction techniques is included in this chapter. A short review and derivation of the existing methods for generalised systems are given and some essential matrix computational processes are discussed in it.

Chapter 3 provides the way of the generation of data models from physical models and convert them to the state-space systems for analytical purposes. It also discusses the existing data models available on different control theory platforms used in this thesis for numerical analysis.

Chapter 4 gives a broad description of the solution of Lyapunov equations centering around two types of descriptor systems; index-I and index-II, on restricted time intervals using RKSM methods. It also deals with the solutions of Lyapunov equations on non-homogeneous time intervals. At here, an efficient procedure of the computation of matrix exponential is proposed.

Chapter 5 is the consequence of Chapter 4 which mainly discusses the solution of Lyapunov equations on nominated frequency intervals. For finding efficient solutions, a new approach of the selection of shift parameters by the genetic algorithm is described in this chapter. Moreover, an elaborate discussion on the matrix logarithm computation is also be included here for finding fast convergent solutions.

One of the main parts of this thesis is provided in Chapter 6 where the topics on model order reduction are discussed using the solutions of time and frequency restricted Lyapunov equations. To remove the instability difficulties of time and frequency restricted reduced-order models, a projection-based computational remedy is proposed what fixes both instability and error minimization problems. Chapter 7 consists of the conclusion and a brief discussion on the futuristic possibilities and the sectors of improvement of this research work.

Introduction

This chapter aims to introduce major concepts from the literature. We start our discussion with some essential properties of Linear Time-Invariant (LTI) continuous-time systems as well as their classes what is followed by the introduction of some basic computational procedures of matrix relevant to our thesis contexts. After that, a brief introduction of the existing methods for the solutions of Lyapunov equations on infinite time domains is given alongside the discussion on available model order reduction techniques. The derivations of Lyapunov equations on restricted time and frequency domains are also shown in this chapter. It is noted that the background theories are only discussed for non-descriptor generalized systems since we develop the model reduction approach for large-scale descriptor systems on time and frequency intervals in the rest of the chapters of this thesis. We avoid attaching some of the proofs of the theorems, lemmas, propositions, etc. by referring to the related literature.

2.1 Theory of systems and control

This section describes the fundamental concepts of the systems and their realizations from the points of view of the system theory and linear algebra. All the discussion are centered on generalized state-space dynamical systems what are extended to the descriptor forms, a special form of the generalized systems, in a subsequent manner.

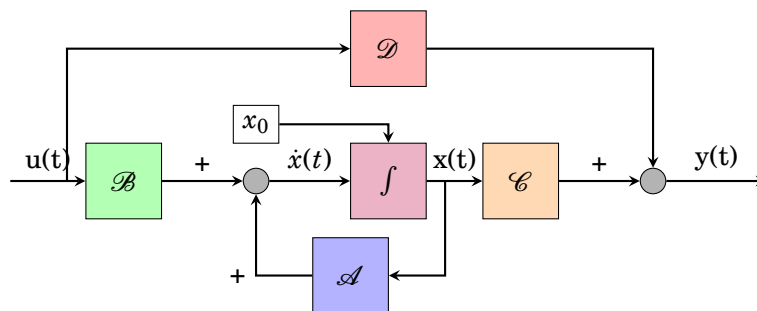


Figure 2.1: Diagram of state-space representation of linear system

2.1.1 State-space representation of dynamical system

The great mathematician Henri Poincaré is the pioneer of the representation of any physical dynamic system linearly as a compact combination of variable, known as the state variable x , with the output response to any given set of input u written as:

$$\dot{x}(t) = g(x, u, t)$$

where, $\dot{x}(t)$ represents the ordinary derivation of x with respect to time t . Any system having n states can be expressed as the form of n state equations as:

$$\begin{aligned} \dot{x}_1(t) &= g_1(x, u, t), \\ \dot{x}_2(t) &= g_2(x, u, t), \\ &\vdots \\ \dot{x}_n(t) &= g_n(x, u, t) \end{aligned}$$

what easily describes as the linear differential equations with constant coefficients [10] written as the following matrix form:

$$\begin{bmatrix} \dot{x}_1(t) \\ \dot{x}_2(t) \\ \vdots \\ \dot{x}_n(t) \end{bmatrix} = \begin{bmatrix} \mathcal{A}_{11} & \mathcal{A}_{12} & \dots & \mathcal{A}_{1n} \\ \mathcal{A}_{21} & \mathcal{A}_{22} & \dots & \mathcal{A}_{2n} \\ \vdots & \vdots & \ddots & \vdots \\ \mathcal{A}_{n1} & \mathcal{A}_{n2} & \dots & \mathcal{A}_{nn} \end{bmatrix} \begin{bmatrix} x_1(t) \\ x_2(t) \\ \vdots \\ x_n(t) \end{bmatrix} + \begin{bmatrix} \mathcal{B}_{11} & \mathcal{B}_{12} & \dots & \mathcal{B}_{1k} \\ \mathcal{B}_{21} & \mathcal{B}_{22} & \dots & \mathcal{B}_{2k} \\ \vdots & \vdots & \ddots & \vdots \\ \mathcal{B}_{n1} & \mathcal{B}_{n2} & \dots & \mathcal{B}_{nk} \end{bmatrix} \begin{bmatrix} u_1(t) \\ u_2(t) \\ \vdots \\ u_k(t) \end{bmatrix}$$

or, simply as:

$$\dot{x}(t) = \mathcal{A}x(t) + \mathcal{B}u(t)$$

Meanwhile, the corresponding output of n states of the particular system can be written as following:

$$\begin{bmatrix} y_1(t) \\ y_2(t) \\ \vdots \\ y_n(t) \end{bmatrix} = \begin{bmatrix} \mathcal{C}_{11} & \mathcal{C}_{12} & \dots & \mathcal{C}_{1n} \\ \mathcal{C}_{21} & \mathcal{C}_{22} & \dots & \mathcal{C}_{2n} \\ \vdots & \vdots & \ddots & \vdots \\ \mathcal{C}_{l1} & \mathcal{C}_{l2} & \dots & \mathcal{C}_{ln} \end{bmatrix} \begin{bmatrix} x_1(t) \\ x_2(t) \\ \vdots \\ x_n(t) \end{bmatrix} + \begin{bmatrix} \mathcal{D}_{11} & \mathcal{D}_{12} & \dots & \mathcal{D}_{1k} \\ \mathcal{D}_{21} & \mathcal{D}_{22} & \dots & \mathcal{D}_{2k} \\ \vdots & \vdots & \ddots & \vdots \\ \mathcal{D}_{l1} & \mathcal{D}_{l2} & \dots & \mathcal{D}_{lk} \end{bmatrix} \begin{bmatrix} u_1(t) \\ u_2(t) \\ \vdots \\ u_k(t) \end{bmatrix}$$

Or,

$$y(t) = \mathcal{C}x(t) + \mathcal{D}u(t)$$

Therefore, the entire Linear Time-Invariant (LTI) system having n states can be written in the form of

$$\begin{aligned} \dot{x}(t) &= \mathcal{A}x(t) + \mathcal{B}u(t); \quad x(t_0) = x_0, \quad t \geq t_0, \\ y(t) &= \mathcal{C}x(t) + \mathcal{D}u(t) \end{aligned} \tag{2.1}$$

Figure 2.1 illustrates the entire Working strategy of any dynamical systems. However, the system (2.1) is known as standard dynamical LTI system which can be generalized as:

$$\begin{aligned} \mathcal{E}\dot{x}(t) &= \mathcal{A}x(t) + \mathcal{B}u(t); & x(t_0) &= x_0, & t &\geq t_0, \\ y(t) &= \mathcal{C}x(t) + \mathcal{D}u(t) \end{aligned} \quad (2.2)$$

where, $x(t) \in \mathbb{R}^{n \times n}$, $u(t) \in \mathbb{R}^{n \times k}$, $y(t) \in \mathbb{R}^{l \times n}$ are the states, inputs, and outputs of the system with initial condition $x(t_0) = x_0$. It is noted that $\mathcal{E} \in \mathbb{R}^{n \times n}$ is invertible matrix and $\mathcal{D} \in \mathbb{R}^{l \times k}$ is the direct transmission map what remains a null matrix in most of the real data models. However, the first and second equations of (2.2) are widely known as state and output equations respectively. The system (2.2) becomes Single-Input, Single-Output (SISO), if $k = l = 1$. Otherwise, it is called Multi-Input, Multi-Output (MIMO) systems.

Generally, the LTI system randomly appears physical modeling whose system matrices \mathcal{A} , \mathcal{B} , \mathcal{C} , \mathcal{D} are independent of time. If the system matrices change with respect of time as well as state n or input u , it becomes non-linear. In this thesis, we only focus on LTI system.

2.1.2 Duhamel's principle and Solution of the Generalized LTI system

The state equation of the general LTI system (2.2) can be reformed as the standard state equation like the system (2.1) as:

$$\dot{x}(t) = \mathcal{A}_s x(t) + \mathcal{B}_s u(t); \quad x(t_0) = x_0 \quad (2.3)$$

where, $\mathcal{A}_s = \mathcal{E}^{-1}\mathcal{A}$ and $\mathcal{B}_s = \mathcal{E}^{-1}\mathcal{B}$. Now integrating (2.3) with respect to τ after multiplying both sides by integrating factor $e^{-\mathcal{A}_s t}$, we can get the solution applying the initial condition as:

$$x(t) = e^{\mathcal{A}_s(t-t_0)}x_0 + \int_{t_0}^t e^{\mathcal{A}_s(t-\tau)}\mathcal{B}_s u(\tau)d\tau \quad (2.4)$$

which is known as Duhamel's principle for ordinary differential equation. The derivation of this solution can be found in [11]. Now, plugging in this derived solution in the output equation of (2.2), we reform the output $y(t)$ as:

$$y(t) = \mathcal{C}e^{\mathcal{A}_s(t-t_0)}x_0 + \int_{t_0}^t \mathcal{C}e^{\mathcal{A}_s(t-\tau)}\mathcal{B}_s u(\tau)d\tau + \mathcal{D}u(t), \quad (2.5)$$

where, $e^{\mathcal{A}_s(t-\tau)}$ is known as state transition matrix.

2.1.3 Input-output relation, Step response, and Transfer function of LTI system

The response of the system having initial value x_0 and input $u(t)$ can be characterized from (2.4) and (2.5). The common responses of generalized LTI system on time domain are step-response and impulse response.

Definition 2.1 (Unit step function [9]). The unit step function is defined as

$$u_{step}(t) = \begin{cases} 0, & \text{if } t < 0 \\ 1, & \text{if } t \geq 0 \end{cases}$$

Algorithm 1: Step response.

Input: $\mathcal{E}, \mathcal{A}, \mathcal{B}, \mathcal{C}, \mathcal{D}, T_0$ (initial point of plotting domain), T_f (final point of plotting domain), N (Total no. of points).

Output: stp .

- 1 Compute $h = \frac{T_f - T_0}{N}$
- 2 Compute LU decomposition as

$$[L, U, P, Q] = lu(\mathcal{E} - h\mathcal{A})$$

- 3 **for** $i=1:N$ **do**
- 4 $x = Q(U \setminus (L \setminus (P(\mathcal{E}x + h\mathcal{B}))))$
- 5 $stp = \mathcal{C}x + \mathcal{D}$

When subjected to the step input, the system will initially have an undesirable output known as transient response occurred for the approaching of the system to its final output value. If the time goes to infinity, system response is called steady-state response what will be occurred if the transient response has end. The computational process of step responses known as implicit Euler method is summarized in Algorithm (1).

The response of the generalized system on frequency domain is popularly known as frequency response derived by applying the Laplace transformation [2, 44] as:

$$\begin{aligned} L(\dot{x}(t)) &= \int_0^{\infty} \dot{x}(t)e^{-st} dt \\ &= e^{-st} \left[x(t) \right]_0^{\infty} + s \int_0^{\infty} x(t)e^{-st} dt \\ &= sL(x(t)) - x(0) = sX(s) - x_0 \end{aligned}$$

Now combining this finding with (2.2), it can be written as:

$$s\mathcal{E}X(s) - x_0 = \mathcal{A}X(s) + \mathcal{B}U(s), \quad (2.6a)$$

$$Y(s) = \mathcal{C}X(s) + \mathcal{D}U(s) \quad (2.6b)$$

Considering the initial value $x_0 = 0$ and inserting the value of $X(s)$ from (2.6a) to (2.6b), we can rewrite

$$Y(s) = \mathcal{G}(s)U(s), \quad \text{where, } \mathcal{G}(s) := \mathcal{C}(s\mathcal{E} - \mathcal{A})^{-1}\mathcal{B} + \mathcal{D} \quad (2.7)$$

$\mathcal{G}(s)$ is known as the transfer function of the SISO dynamical system. For the MIMO system, it becomes

$$\mathcal{G}(s) = \begin{bmatrix} \mathcal{G}_{11} & \mathcal{G}_{12} & \dots & \mathcal{G}_{1k} \\ \mathcal{G}_{21} & \mathcal{G}_{22} & \dots & \mathcal{G}_{2k} \\ \vdots & \vdots & \ddots & \vdots \\ \mathcal{G}_{l1} & \mathcal{G}_{l2} & \dots & \mathcal{G}_{lk} \end{bmatrix} \quad (2.8)$$

where $\mathcal{G}_{ij} = \mathcal{C}(i, :)(s\mathcal{E} - \mathcal{A})^{-1}\mathcal{B}(:, j) + \mathcal{D}(i, j)$ with $i = 1, 2, \dots, l$ and $j = 1, 2, \dots, k$. Transfer function is one of the key factors of the control theory since the input-output relation of the dynamical system. However, on complex frequency domain, the transfer function (2.7) can be written as

$$\mathcal{G}(i\omega) := \mathcal{C}(i\omega\mathcal{E} - \mathcal{A})^{-1}\mathcal{B} + \mathcal{D} \quad (2.9)$$

where, $\omega \in \mathbb{R}$ is the frequency and i is the value on imaginary axis.

Definition 2.2 (Proper and Improper transfer function [2, 9]). The transfer function (2.7) is called proper, or strictly proper respectively if $\lim_{s \rightarrow \infty} < \infty$, or $\lim_{s \rightarrow \infty} = 0$. Otherwise, it is recognized as improper.

2.1.4 Descriptor system

Currently, there are many data models derived from the real-world physical models where \mathcal{E} is found as singular form, i.e., $\det(\mathcal{E}) = 0$ [4, 7, 45]. Such type of special dynamical system is known as descriptor or singular system what consists of both differential and algebraic part [9] having regular matrix pencil

$$(\lambda \mathcal{E} - \mathcal{A}) \neq 0$$

Assuming two invertible matrices κ and η , the above matrix pencil can be reformed as following Weierstress canonical form:

$$\mathcal{E} = \kappa \begin{bmatrix} \mathcal{I} & 0 \\ 0 & \mathbf{n} \end{bmatrix} \eta, \quad \mathcal{A} = \kappa \begin{bmatrix} \mathcal{A}_i & 0 \\ 0 & \mathcal{I}_n \end{bmatrix} \eta$$

where, \mathbf{n} is nilpotent matrix of nilpotency index p such that $\mathbf{n}^p = 0$. In [46], the properties of the descriptor systems containing differential-algebraic part, represented by Differential-Algebraic Equations (DAEs), with their derivative procedure are broadly discussed. Depending on the sparsity pattern of \mathcal{E} , the system matrices of large-scale descriptor systems can be divided into sub-blocks. In this thesis, we mainly focus on such kinds of special structured descriptor system of the form

$$\underbrace{\begin{bmatrix} \mathcal{E}_i & \mathcal{E}_{ii} \\ 0 & 0 \end{bmatrix}}_{\mathcal{E}} \underbrace{\begin{bmatrix} \dot{g}(t) \\ \dot{r}(t) \end{bmatrix}}_{\dot{x}(t)} = \underbrace{\begin{bmatrix} \mathcal{A}_i & \mathcal{A}_{ii} \\ \mathcal{A}_{iii} & \mathcal{A}_{iv} \end{bmatrix}}_{\mathcal{A}} \underbrace{\begin{bmatrix} g(t) \\ r(t) \end{bmatrix}}_{x(t)} + \underbrace{\begin{bmatrix} \mathcal{B}_i \\ \mathcal{B}_{ii} \end{bmatrix}}_{\mathcal{B}} u(t) \quad (2.10a)$$

$$y(t) = \underbrace{\begin{bmatrix} \mathcal{C}_i & \mathcal{C}_{ii} \end{bmatrix}}_{\mathcal{C}} \underbrace{\begin{bmatrix} g(t) \\ r(t) \end{bmatrix}}_{x(t)} + \mathcal{D}u(t) \quad (2.10b)$$

and

$$\underbrace{\begin{bmatrix} \mathcal{E}_i & 0 \\ 0 & 0 \end{bmatrix}}_{\mathcal{E}} \underbrace{\begin{bmatrix} \dot{g}(t) \\ \dot{r}(t) \end{bmatrix}}_{\dot{x}(t)} = \underbrace{\begin{bmatrix} \mathcal{A}_i & \mathcal{A}_{ii} \\ \mathcal{A}_{iii} & 0 \end{bmatrix}}_{\mathcal{A}} \underbrace{\begin{bmatrix} g(t) \\ r(t) \end{bmatrix}}_{x(t)} + \underbrace{\begin{bmatrix} \mathcal{B}_i \\ \mathcal{B}_{ii} \end{bmatrix}}_{\mathcal{B}} u(t) \quad (2.11a)$$

$$y(t) = \underbrace{\begin{bmatrix} \mathcal{C}_i & \mathcal{C}_{ii} \end{bmatrix}}_{\mathcal{C}} \underbrace{\begin{bmatrix} g(t) \\ r(t) \end{bmatrix}}_{x(t)} + \mathcal{D}u(t) \quad (2.11b)$$

where, $g(t) \in \mathbb{R}^{n_i}$ represents the differential part, $r(t) \in \mathbb{R}^{n_{ii}}$ represents the algebraic part, the full dimension of the system is $n = n_i + n_{ii}$, $\mathcal{A}_i \in \mathbb{R}^{n_i \times n_i}$, $\mathcal{A}_{ii} \in \mathbb{R}^{n_{ii} \times n_{ii}}$, $\mathcal{A}_{iii} \in \mathbb{R}^{n_{ii} \times n_i}$, $\mathcal{A}_{iv} \in \mathbb{R}^{n_{ii} \times n_{ii}}$ are the sub-blocks of \mathcal{A} , $\mathcal{B}_i \in \mathbb{R}^{n_i \times k}$, $\mathcal{B}_{ii} \in \mathbb{R}^{n_{ii} \times k}$ are the sub-blocks of \mathcal{B} , and $\mathcal{C}_i \in \mathbb{R}^{l \times n_i}$, $\mathcal{C}_{ii} \in \mathbb{R}^{l \times n_{ii}}$

are the sub-blocks of \mathcal{C} .

The descriptor system (2.10) is well-known as index-I system having $\det(\mathcal{A}_{iv}) \neq 0$, whereas the system (2.11) is called index-II system containing \mathcal{A}_{iv} block as zero including $\det(\mathcal{A}_{iii}\mathcal{A}_{ii}) \neq 0$. Any descriptor system having \mathcal{A}_{iv} as zero and $\det(\mathcal{A}_{iii}\mathcal{A}_{ii}) = 0$ is known as index-III system which is practically rare.

2.1.5 Controllability and Observability Gramians on infinite time domain

Controllability and observability are two prime topics in control theory what plays an important roles in the MOR technique, especially Gramian-based Mor technique [10, 47].

Definition 2.3 (Controllable system [2, 6, 11]). The LTI dynamical system (2.2) is said to be controllable system on time domain $(t_0 = 0) \leq t < (t_f = \infty)$, if for any initial state $x(0) = x_0$ and final state x_f , there exists a input $u(t)$ such that the solution (2.4) satisfies $x(t_f) = x_f$. Otherwise, it becomes uncontrollable.

However, a system is fully controllable if $X^{full} = \mathbb{R}^n$ [48], where X^{full} indicates the set of all controllable states. Centering on the concept of the controllability of a system, the following theorems are established:

Theorem 2.1. *The below axioms are equivalent for the system matrix pair $(\mathcal{A}_s, \mathcal{B}_s)$ of the system (2.2):*

- $(\mathcal{A}_s, \mathcal{B}_s)$ is controllable.
- The controllability matrix $\mathbf{C}(\mathcal{A}_s, \mathcal{B}_s) = [\mathcal{B}_s, \mathcal{A}_s\mathcal{B}_s, \mathcal{A}_s^2\mathcal{B}_s, \dots, \mathcal{A}_s^{n-1}\mathcal{B}_s]$ has full rank.
- The controllability Gramian on infinite time domain

$$\mathcal{P}_\infty = \int_0^\infty e^{\mathcal{A}_s t} \mathcal{B}_s \mathcal{B}_s^T e^{\mathcal{A}_s^T t} dt \quad (2.12)$$

is positive semi-definite, i.e., no eigenvalue is on the negative x -half plane for any $t > 0$.

- The matrix $[\mathcal{A} - s\mathcal{E}, \mathcal{B}]$ has full rank n for all $s \in \mathbb{C}$.
- The reduced order pair $(\tilde{\mathcal{A}}_s, \tilde{\mathcal{B}}_s)$ is controllable, where $\tilde{\mathcal{A}}_s = \mathcal{T} \mathcal{A}_s \mathcal{T}^{-1}$ and $\tilde{\mathcal{B}}_s = \mathcal{T} \mathcal{B}_s$ for any non-singular $\mathcal{T} \in \mathbb{R}^{n \times n}$.

Proof. All of the proofs of above axioms are available in [6, 10]. ■

On the other hand, observability is the dual concept of the controllability what is defined as follow:

Definition 2.4 (Observable system [2, 6, 11]). The dynamical system (2.2) becomes an observable system on time domain $(t_0 = 0) \leq t < (t_f = \infty)$, if for a given input $u(t)$ initial state $x(0) = x_0$ can be uniquely determined from the system's output (2.5).

If $Y^{full} = \mathbb{R}^n$, where Y^{full} is the set of all observable states, then a system is completely observable [48]. The following theorems are constructed based on the concept of the observability of a system :

Theorem 2.2. *The below axioms are equivalents for the system matrix pair $(\mathcal{A}_s, \mathcal{C})$ of the system (2.2):*

- $(\mathcal{A}_s, \mathcal{C})$ is observable.

- The observability matrix $\mathbf{O}(\mathcal{A}_s, \mathcal{C}) = \begin{bmatrix} \mathcal{C} \\ \mathcal{C}\mathcal{A}_s \\ \mathcal{C}\mathcal{A}_s^2 \\ \vdots \\ \mathcal{C}\mathcal{A}_s^{n-1} \end{bmatrix}$ has full rank.

- The observability Gramian on infinite time domain

$$\mathcal{Q}_\infty = \int_0^\infty e^{\mathcal{A}_s^T t} \mathcal{C}^T \mathcal{C} e^{\mathcal{A}_s t} dt \quad (2.13)$$

is positive semi-definite, i.e., no eigenvalue is on the negative x -half plane for any $t > 0$.

- The matrix $\begin{bmatrix} \mathcal{A} - s\mathcal{E} \\ \mathcal{C} \end{bmatrix}$ has full rank n for all $s \in \mathbb{C}$.

- The reduced order pair $(\tilde{\mathcal{A}}_s, \tilde{\mathcal{C}})$ is observable, where $\tilde{\mathcal{A}}_s = \mathcal{T} \mathcal{A}_s \mathcal{T}^{-1}$ and $\tilde{\mathcal{C}} = \mathcal{C} \mathcal{T}^{-1}$ for any non-singular $\mathcal{T} \in \mathbb{R}^{n \times n}$.

Proof. All of the proofs of above axioms are available in [6, 10]. ■

It has been shown in [49, 50] that the controllability Gramian (2.12) is the solution of the Continuous-time Algebraic Lyapunov Equation (CALE):

$$\mathcal{E} \mathcal{P}_\infty \mathcal{A}^T + \mathcal{A} \mathcal{P}_\infty \mathcal{E}^T = - \underbrace{\mathcal{B} \mathcal{B}^T}_{\alpha_c} \quad (2.14)$$

which is well-known as the controllability Lyapunov equation. Likewise, the observability Gramian (2.13) is the solution of continuous-time algebraic observability Lyapunov equation:

$$\mathcal{E}^T \mathcal{Q}_\infty \mathcal{A} + \mathcal{A}^T \mathcal{Q}_\infty \mathcal{E} = - \underbrace{\mathcal{C}^T \mathcal{C}}_{\alpha_o} \quad (2.15)$$

2.1.6 System stability

Stability is a very vital characteristic property of any dynamical system since an unstable system can never be controlled. Therefore, stability analysis is a must-needed topic in control theory.

Definition 2.5 (Stable system [2, 6, 11]). The dynamical system (2.2) is called stable or Hurwitz-stable if all of the members of the eigenvalue set λ of its system matrix pair $(\mathcal{A}, \mathcal{E})$ are on the open left half of the complex plane, i.e., $\lambda \in \mathbb{C}^-$. In other word, if both of the Lyapunov equations (2.14) and (2.15) have unique solution, the dynamic system (2.2) is said to be asymptotically stable.

The LTI system (2.2) can be stabilizable if there exists a matrix $\mathcal{K} \in \mathbb{R}^{k \times n}$ such that $(\mathcal{A}_s - \mathcal{B}_s \mathcal{K})$ is stable [11].

Theorem 2.3 (Lyapunov Stability Theorem [6, 10]). *The system (2.2) is asymptotically stable on infinite time domain if and only if for any symmetric positive semi-definite matrix α_c indicated in (2.14), there exists a unique symmetric positive definite matrix \mathcal{P}_∞ indicated in (2.12) satisfying the Lyapunov equation (2.14).*

Proof. The proof is found in [6, 10]. ■

However, if α_o in (2.13) is symmetric positive semi-definite, the observability Lyapunov equation (2.13) also satisfies the theorem (2.3).

For the stable dynamical system, both of the Gramians $\mathcal{P}_\infty, \mathcal{Q}_\infty$ can be explained physically in the following ways [14]:

- The minimum energy of the input for the controllability Gramian is

$$\mathcal{J}_c = \int_{-\infty}^0 u^T(t)u(t)dt, \quad x(0) = x_0, \quad t \leq 0,$$

is equivalent to $\mathcal{J}_c = x_0^T \mathcal{P}_\infty^{-1} x_0$, what indicates any state $x_0 = x(t)$ required more energy to control lying in an eigenspace of \mathcal{P}_∞^{-1} corresponding to large eigenvalues.

- The obtained energy from output for the observability Gramian under the zero input is

$$\mathcal{J}_o = \int_0^\infty y^T(t)y(t)dt, \quad x(0) = x_0, \quad t \geq 0,$$

is equivalent to $\mathcal{J}_o = x_0^T \mathcal{Q}_\infty x_0$, what indicates the difficulty of observing any state $x_0 = x(t)$ lying in an eigenspace of \mathcal{Q}_∞ corresponding to small eigenvalues.

2.1.7 Controllability and Observability Gramians on restricted time interval

It is important to construct Controllability Gramian (CG) and Observability Gramian (OG) on restricted time interval for dealing with real data problems. Time-restricted Gramian is defined as follows:

Definition 2.6 (Time-restricted Gramian [12]). The time-restricted CG (\mathcal{P}) and OG (\mathcal{Q}) with respect to time $t \in \mathbb{R}^+$ on time interval $[t_0, t_f]$ for the system (2.2) are defined as:

$$\mathcal{P} = \mathcal{E} \int_{t_0}^{t_f} e^{\mathcal{E}^{-1}\mathcal{A}t} \mathcal{E}^{-1} \mathcal{B}(\mathcal{E}^{-1}\mathcal{B})^T e^{(\mathcal{E}^{-1}\mathcal{A})^T t} dt \mathcal{E}^T \quad (2.16a)$$

$$\mathcal{Q} = \int_{t_0}^{t_f} e^{(\mathcal{E}^{-1}\mathcal{A})^T t} \mathcal{C}^T \mathcal{C} e^{\mathcal{E}^{-1}\mathcal{A}t} dt \quad (2.16b)$$

Theorem 2.4. *The time-restricted CG (2.16a) is the solution of the time-restricted Continuous-time Algebraic Controllability Lyapunov Equation (CACLE) on time interval $[t_0, t_f]$:*

$$\mathcal{A}\mathcal{P}\mathcal{E}^T + \mathcal{E}\mathcal{P}\mathcal{A}^T + \mathcal{E}e^{\mathcal{E}^{-1}\mathcal{A}t_0} \mathcal{E}^{-1} \mathcal{B}(\mathcal{E}^{-1}\mathcal{B})^T e^{(\mathcal{E}^{-1}\mathcal{A})^T t_0} \mathcal{E}^T - \mathcal{E}e^{\mathcal{E}^{-1}\mathcal{A}t_f} \mathcal{E}^{-1} \mathcal{B}(\mathcal{E}^{-1}\mathcal{B})^T e^{(\mathcal{E}^{-1}\mathcal{A})^T t_f} \mathcal{E}^T = 0 \quad (2.17)$$

Proof. Plugging in the value of \mathcal{P} , we get

$$\begin{aligned}
 \mathcal{A} \left[\mathcal{E} \int_{t_0}^{t_f} e^{\mathcal{E}^{-1}\mathcal{A}t} \mathcal{E}^{-1} \mathcal{B} (\mathcal{E}^{-1} \mathcal{B})^T e^{(\mathcal{E}^{-1}\mathcal{A})^T t} dt \mathcal{E}^T \right] \mathcal{E}^T + \mathcal{E} \left[\mathcal{E} \int_{t_0}^{t_f} e^{\mathcal{E}^{-1}\mathcal{A}t} \mathcal{E}^{-1} \mathcal{B} (\mathcal{E}^{-1} \mathcal{B})^T e^{(\mathcal{E}^{-1}\mathcal{A})^T t} dt \mathcal{E}^T \right] \mathcal{A}^T + \\
 \mathcal{E} e^{\mathcal{E}^{-1}\mathcal{A}t_0} \mathcal{E}^{-1} \mathcal{B} (\mathcal{E}^{-1} \mathcal{B})^T e^{(\mathcal{E}^{-1}\mathcal{A})^T t_0} \mathcal{E}^T - \mathcal{E} e^{\mathcal{E}^{-1}\mathcal{A}t_f} \mathcal{E}^{-1} \mathcal{B} (\mathcal{E}^{-1} \mathcal{B})^T e^{(\mathcal{E}^{-1}\mathcal{A})^T t_f} \mathcal{E}^T \\
 = \mathcal{E} \int_{t_0}^{t_f} \frac{d}{dt} \left[e^{\mathcal{E}^{-1}\mathcal{A}t} \mathcal{E}^{-1} \mathcal{B} (\mathcal{E}^{-1} \mathcal{B})^T e^{(\mathcal{E}^{-1}\mathcal{A})^T t} dt \right] \mathcal{E}^T + \\
 \mathcal{E} e^{\mathcal{E}^{-1}\mathcal{A}t_0} \mathcal{E}^{-1} \mathcal{B} (\mathcal{E}^{-1} \mathcal{B})^T e^{(\mathcal{E}^{-1}\mathcal{A})^T t_0} \mathcal{E}^T - \mathcal{E} e^{\mathcal{E}^{-1}\mathcal{A}t_f} \mathcal{E}^{-1} \mathcal{B} (\mathcal{E}^{-1} \mathcal{B})^T e^{(\mathcal{E}^{-1}\mathcal{A})^T t_f} \mathcal{E}^T \\
 = \mathcal{E} \left[e^{\mathcal{E}^{-1}\mathcal{A}t} \mathcal{E}^{-1} \mathcal{B} (\mathcal{E}^{-1} \mathcal{B})^T e^{(\mathcal{E}^{-1}\mathcal{A})^T t} \right]_{t_0}^{t_f} \mathcal{E}^T + \\
 \mathcal{E} e^{\mathcal{E}^{-1}\mathcal{A}t_0} \mathcal{E}^{-1} \mathcal{B} (\mathcal{E}^{-1} \mathcal{B})^T e^{(\mathcal{E}^{-1}\mathcal{A})^T t_0} \mathcal{E}^T - \mathcal{E} e^{\mathcal{E}^{-1}\mathcal{A}t_f} \mathcal{E}^{-1} \mathcal{B} (\mathcal{E}^{-1} \mathcal{B})^T e^{(\mathcal{E}^{-1}\mathcal{A})^T t_f} \mathcal{E}^T \\
 = \mathcal{E} e^{\mathcal{E}^{-1}\mathcal{A}t_0} \mathcal{E}^{-1} \mathcal{B} (\mathcal{E}^{-1} \mathcal{B})^T e^{(\mathcal{E}^{-1}\mathcal{A})^T t_0} \mathcal{E}^T - \mathcal{E} e^{\mathcal{E}^{-1}\mathcal{A}t_f} \mathcal{E}^{-1} \mathcal{B} (\mathcal{E}^{-1} \mathcal{B})^T e^{(\mathcal{E}^{-1}\mathcal{A})^T t_f} \mathcal{E}^T - \\
 \mathcal{E} e^{\mathcal{E}^{-1}\mathcal{A}t_0} \mathcal{E}^{-1} \mathcal{B} (\mathcal{E}^{-1} \mathcal{B})^T e^{(\mathcal{E}^{-1}\mathcal{A})^T t_0} \mathcal{E}^T + \mathcal{E} e^{\mathcal{E}^{-1}\mathcal{A}t_f} \mathcal{E}^{-1} \mathcal{B} (\mathcal{E}^{-1} \mathcal{B})^T e^{(\mathcal{E}^{-1}\mathcal{A})^T t_f} \mathcal{E}^T = 0
 \end{aligned}$$

■

Similarly, it can be shown that the OG (2.16b) is the solution of the time-restricted Continuous-time Algebraic Observability Lyapunov Equation (CAOLE):

$$\mathcal{A}^T \mathcal{Q} \mathcal{E} + \mathcal{E}^T \mathcal{Q} \mathcal{A} + e^{(\mathcal{E}^{-1}\mathcal{A})^T t_0} \mathcal{C}^T \mathcal{C} e^{\mathcal{E}^{-1}\mathcal{A}t_0} - e^{(\mathcal{E}^{-1}\mathcal{A})^T t_f} \mathcal{C}^T \mathcal{C} e^{\mathcal{E}^{-1}\mathcal{A}t_f} = 0 \quad (2.18)$$

However, if the initial value of the time interval is zero, i.e., $[t_0 = 0, t_f]$, then 2.17 and 2.18 are reformulated as:

$$\mathcal{A} \mathcal{P} \mathcal{E}^T + \mathcal{E} \mathcal{P} \mathcal{A}^T + \mathcal{B} \mathcal{B}^T - \mathcal{E} e^{\mathcal{E}^{-1}\mathcal{A}t_f} \mathcal{E}^{-1} \mathcal{B} (\mathcal{E}^{-1} \mathcal{B})^T e^{(\mathcal{E}^{-1}\mathcal{A})^T t_f} \mathcal{E}^T = 0 \quad (2.19a)$$

$$\mathcal{A}^T \mathcal{Q} \mathcal{E} + \mathcal{E}^T \mathcal{Q} \mathcal{A} + \mathcal{C}^T \mathcal{C} - e^{(\mathcal{E}^{-1}\mathcal{A})^T t_f} \mathcal{C}^T \mathcal{C} e^{\mathcal{E}^{-1}\mathcal{A}t_f} = 0 \quad (2.19b)$$

2.1.8 Controllability and Observability Gramians on restricted frequency interval

For frequency response analysis on restricted frequency interval $[-\Omega, \Omega]$, we need construct frequency-restricted CG and OG what are defined as follows:

Definition 2.7 (Frequency-restricted Gramian [12]). The frequency-restricted CG (\mathcal{M}) and OG (\mathcal{N}) with respect to frequency $\Omega \subset \mathbb{R}$ on frequency interval $[-\Omega, \Omega]$ for the system (2.2) are defined as:

$$\mathcal{M} = \frac{\mathcal{E}}{2\pi} \int_{-\Omega}^{\Omega} \Phi(i\Omega) \mathcal{B} \mathcal{B}^T \Phi^*(i\Omega) d\Omega \mathcal{E}^T \quad (2.20a)$$

$$\mathcal{N} = \frac{1}{2\pi} \int_{-\Omega}^{\Omega} \Theta^*(i\Omega) \mathcal{E}^T \mathcal{C}^T \mathcal{C} \mathcal{E} \Theta(i\Omega) d\Omega \quad (2.20b)$$

where, $\Phi(i\Omega) = (i\Omega \mathcal{E} - \mathcal{A})^{-1}$, $\Theta(i\Omega) = (\mathcal{E} i\Omega - \mathcal{A})^{-1}$ and $\Phi^*(i\Omega)$, $\Theta^*(i\Omega)$ are the complex conjugate transposes of the respective $\Phi(i\Omega)$, $\Theta(i\Omega)$.

Theorem 2.5 (Parseval's Theorem). If $\Phi(\Omega)$ and $\overline{\Phi(\Omega)}$ are the Fourier transformations of $F(t)$ and $\overline{F(t)}$ respectively, then

$$\int_0^{\infty} F(t) \overline{F(t)} dt = \frac{1}{2\pi} \int_{-\infty}^{\infty} \Phi(\Omega) \overline{\Phi(\Omega)} d\Omega$$

Proof. Taking inverse Fourier transformation from time interval $[0, \infty)$ to frequency interval $(-\infty, \infty)$

$$\int_0^\infty F(t)dt = \frac{1}{2\pi} \int_{-\infty}^\infty e^{i\Omega t} \Phi(\Omega) d\Omega$$

whose complex conjugate is:

$$\int_0^\infty \overline{F(t)} dt = \frac{1}{2\pi} \int_{-\infty}^\infty e^{-i\Omega t} \overline{\Phi(\Omega)} d\Omega$$

Now, we can get-

$$\begin{aligned} \int_0^\infty F(t) \overline{F(t)} dt &= \frac{1}{2\pi} \int_0^\infty F(t) \int_{-\infty}^\infty e^{-i\Omega t} \overline{\Phi(\Omega)} d\Omega dt \\ &= \frac{1}{2\pi} \int_{-\infty}^\infty \int_0^\infty F(t) e^{-i\Omega t} dt \overline{\Phi(\Omega)} d\Omega \\ &= \frac{1}{2\pi} \int_{-\infty}^\infty \Phi(\Omega) \overline{\Phi(\Omega)} d\Omega \end{aligned}$$

■

Using Fourier transformation from frequency interval $(-\infty, \infty)$ to time interval $[0, \infty)$

$$\begin{aligned} \int_{-\Omega}^\Omega \mathbf{F}(i\Omega) d\Omega &= \int_0^\infty e^{-i\Omega t} e^{\mathcal{E}^{-1}\mathcal{A}t} dt \\ &= \int_0^\infty e^{-(i\Omega - \mathcal{E}^{-1}\mathcal{A})t} dt \\ &= - \left[\frac{e^{-(i\Omega - \mathcal{E}^{-1}\mathcal{A})t}}{i\Omega - \mathcal{E}^{-1}\mathcal{A}} \right]_0^\infty \\ \Rightarrow \int_{-\Omega}^\Omega \mathbf{F}(i\Omega) d\Omega &= (i\Omega \mathcal{E} - \mathcal{A})^{-1} \mathcal{E} \end{aligned}$$

Now imposing the above Theorem (2.5) and the Fourier transformation of $e^{\mathcal{E}^{-1}\mathcal{A}}$ on CG (2.12), we can get CG on infinite frequency domain for the generalized system (2.2) as:

$$\mathcal{M}_\infty = \frac{\mathcal{E}}{2\pi} \left[\int_{-\infty}^\infty \Phi(i\Omega) \mathcal{B} \mathcal{B}^T \Phi^*(i\Omega) d\Omega \right] \mathcal{E}^T \quad (2.21)$$

where, $\Phi(i\Omega) = (i\Omega \mathcal{E} - \mathcal{A})^{-1}$ and $\Phi^*(i\Omega)$ is the complex conjugate transpose. Likewise, the infinite OG can be written as:

$$\mathcal{N}_\infty = \frac{1}{2\pi} \left[\int_{-\infty}^\infty \Theta^*(i\Omega) \mathcal{E}^T \mathcal{C}^T \mathcal{C} \Theta(i\Omega) d\Omega \right] \quad (2.22)$$

where, $\Theta(i\Omega) = (\mathcal{E}i\Omega - \mathcal{A})^{-1}$ and $\Theta^*(i\Omega)$ is the complex conjugate transpose. Therefore, on finite frequency interval $[-\Omega, \Omega]$, the frequency-restricted CG and OG are written as (2.20a) and (2.20b). However, it is shown in [51] that (2.20a) and (2.20b) can be partially decomposed as:

$$\mathcal{M} = \frac{1}{2\pi} \int_{-\Omega}^\Omega (\mathcal{E} \Phi(i\Omega) \mathcal{M}_\infty + \mathcal{M}_\infty \Phi^*(i\Omega) \mathcal{E}^T) d\Omega \quad (2.23)$$

$$\mathcal{N} = \frac{1}{2\pi} \int_{-\Omega}^\Omega (\Theta^*(i\Omega) \mathcal{E}^T \mathcal{N}_\infty + \mathcal{N}_\infty \mathcal{E} \Theta(i\Omega) \mathcal{E}) d\Omega \quad (2.24)$$

We can rewrite (2.23) and (2.24) after integration as:

$$\mathcal{M} = \mathcal{E} \phi(i\Omega) \mathcal{M}_\infty + \mathcal{M}_\infty \phi^*(i\Omega) \mathcal{E}^T \quad (2.25)$$

$$\mathcal{N} = \xi^*(i\Omega) \mathcal{E}^T \mathcal{N}_\infty + \mathcal{N}_\infty \mathcal{E} \xi(i\Omega) \mathcal{E} \quad (2.26)$$

where [39],

$$\begin{aligned}\phi(i\Omega) &= \frac{1}{2\pi} \int_{-\Omega}^{\Omega} (\Phi(i\Omega)d\Omega) \\ &= \frac{1}{2\pi} \int_{-\Omega}^{\Omega} \frac{1}{i\Omega\mathcal{E} - \mathcal{A}} d\Omega \\ &= \frac{1}{2\pi i} \left[\ln(i\Omega\mathcal{E} - \mathcal{A}) \right]_{-\Omega}^{\Omega} \mathcal{E}^{-1}\end{aligned}\quad (2.27)$$

$$\implies \phi(i\Omega) = \frac{i}{2\pi} [\ln(-i\Omega\mathcal{E} - \mathcal{A}) - \ln(i\Omega\mathcal{E} - \mathcal{A})] \mathcal{E}^{-1}.$$

$$\therefore \phi^*(i\Omega) = \frac{i}{2\pi} \mathcal{E}^{-T} [\ln(-i\Omega\mathcal{E} - \mathcal{A}) - \ln(i\Omega\mathcal{E} - \mathcal{A})]^T \quad (2.28)$$

and,

$$\xi(i\Omega) = \frac{1}{2\pi} \int_{-\Omega}^{\Omega} (\Theta(i\Omega)d\Omega) = \frac{i}{2\pi} \mathcal{E}^{-1} [\ln(-\mathcal{E}i\Omega - \mathcal{A}) - \ln(\mathcal{E}i\Omega - \mathcal{A})] \quad (2.29)$$

$$\xi^*(i\Omega) = \frac{i}{2\pi} [\ln(-\mathcal{E}i\Omega - \mathcal{A}) - \ln(\mathcal{E}i\Omega - \mathcal{A})]^T \mathcal{E}^{-T} \quad (2.30)$$

Theorem 2.6. *The frequency-restricted CG (2.25) is the solution of the frequency-restricted Continuous-time Algebraic Controllability Lyapunov Equation (CACLE) on frequency interval $[-\Omega, \Omega]$:*

$$\mathcal{A}\mathcal{M}\mathcal{E}^T + \mathcal{E}\mathcal{M}\mathcal{A}^T + \mathcal{E}\phi(i\Omega)\mathcal{B}\mathcal{B}^T + \mathcal{B}\mathcal{B}^T\phi^*(i\Omega)\mathcal{E}^T = 0 \quad (2.31)$$

Proof. Plugging in the value of \mathcal{M} , we get-

$$\begin{aligned}\mathcal{A} \left[\mathcal{E}\phi(i\Omega)\mathcal{M}_{\infty} + \mathcal{M}_{\infty}\phi^*(i\Omega)\mathcal{E}^T \right] \mathcal{E}^T + \mathcal{E} \left[\mathcal{E}\phi(i\Omega)\mathcal{M}_{\infty} + \mathcal{M}_{\infty}\phi^*(i\Omega)\mathcal{E}^T \right] \mathcal{A}^T + \\ \mathcal{E}\phi(i\Omega)\mathcal{B}\mathcal{B}^T + \mathcal{B}\mathcal{B}^T\phi^*(i\Omega)\mathcal{E}^T \\ = \mathcal{E}\phi(i\Omega) \left[\mathcal{A}\mathcal{M}_{\infty}\mathcal{E}^T + \mathcal{E}\mathcal{M}_{\infty}\mathcal{A}^T \right] + \left[\mathcal{A}\mathcal{M}_{\infty}\mathcal{E}^T + \mathcal{E}\mathcal{M}_{\infty}\mathcal{A}^T \right] \phi^*(i\Omega)\mathcal{E}^T + \\ \mathcal{E}\phi(i\Omega)\mathcal{B}\mathcal{B}^T + \mathcal{B}\mathcal{B}^T\phi^*(i\Omega)\mathcal{E}^T \\ = -\mathcal{E}\phi(i\Omega)\mathcal{B}\mathcal{B}^T - \mathcal{B}\mathcal{B}^T\phi^*(i\Omega)\mathcal{E}^T + \mathcal{E}\phi(i\Omega)\mathcal{B}\mathcal{B}^T + \mathcal{B}\mathcal{B}^T\phi^*(i\Omega)\mathcal{E}^T = 0\end{aligned}$$

■

Similarly, it can be shown that the OG (2.26) is the solution of the frequency-restricted Continuous-time Algebraic Observability Lyapunov Equation (CAOLE):

$$\mathcal{A}^T \mathcal{N}\mathcal{E} + \mathcal{E}^T \mathcal{N}\mathcal{A} + \xi^*(i\Omega)\mathcal{E}^T \mathcal{C}^T \mathcal{C} + \mathcal{C}^T \mathcal{C} \xi(i\Omega) = 0 \quad (2.32)$$

Moreover, for any frequency interval $[\Omega_0, \Omega_f]$ the frequency-restricted CG (2.31) and OG (2.32) can be reformed as according to [12, 37]:

$$\mathcal{A}\mathcal{M}\mathcal{E}^T + \mathcal{E}\mathcal{M}\mathcal{A}^T + \mathcal{E}\phi(i\omega)\mathcal{B}\mathcal{B}^T + \mathcal{B}\mathcal{B}^T\phi^*(i\omega)\mathcal{E}^T = 0 \quad (2.33a)$$

$$\mathcal{A}^T \mathcal{N}\mathcal{E} + \mathcal{E}^T \mathcal{N}\mathcal{A} + \xi^*(i\omega)\mathcal{E}^T \mathcal{C}^T \mathcal{C} + \mathcal{C}^T \mathcal{C} \xi(i\omega) = 0 \quad (2.33b)$$

where, $\phi(i\omega) = (\phi(i\Omega_f) - \phi(i\Omega_0))$ and $\xi(i\omega) = (\xi(i\Omega_f) - \xi(i\Omega_0))$.

2.1.9 Difficulties in system's stability on restricted time and frequency intervals

Reconstructing the CACLE (2.17) on restricted time interval as Equation (2.14), we can get-

$$\mathcal{A}\mathcal{P}\mathcal{E}^T + \mathcal{E}\mathcal{P}\mathcal{A}^T = \underbrace{\begin{bmatrix} \mathcal{E}e^{\mathcal{E}^{-1}\mathcal{A}t_f}\mathcal{E}^{-1}\mathcal{B} & \mathcal{E}e^{\mathcal{E}^{-1}\mathcal{A}t_0}\mathcal{E}^{-1}\mathcal{B} \end{bmatrix}}_{\mathcal{B}} \underbrace{\begin{bmatrix} 1 & 0 \\ 0 & -1 \end{bmatrix}}_{\alpha} \underbrace{\begin{bmatrix} \mathcal{E}e^{\mathcal{E}^{-1}\mathcal{A}t_f}\mathcal{E}^{-1}\mathcal{B} & \mathcal{E}e^{\mathcal{E}^{-1}\mathcal{A}t_0}\mathcal{E}^{-1}\mathcal{B} \end{bmatrix}^T}_{\mathcal{B}^T} \quad (2.34)$$

According to Theorem (2.3), the system (2.2) on finite time interval represented by (2.34) will be stable, if the right side is strictly positive semi-definite. But, unfortunately, the one of the eigenvalues of α is on the negative x -half plane what makes the right side negative definite. Therefore, the system on limited time interval is not stable despite it may be stable on infinite time domain.

Similarly, the CACLE (2.33a) on restricted frequency interval can be reformed as Equation (2.14):

$$\mathcal{A}\mathcal{P}\mathcal{E}^T + \mathcal{E}\mathcal{P}\mathcal{A}^T = \underbrace{\begin{bmatrix} \mathcal{E}\phi(i\omega)\mathcal{B} & \mathcal{B} \end{bmatrix}}_{\mathcal{B}} \underbrace{\begin{bmatrix} 0 & -1 \\ -1 & 0 \end{bmatrix}}_{\beta} \underbrace{\begin{bmatrix} \mathcal{E}\phi(i\omega)\mathcal{B} & \mathcal{B} \end{bmatrix}^T}_{\mathcal{B}^T} \quad (2.35)$$

what also represents the entire system unstable on limited frequency interval as one of the eigenvalues of β is on the negative x -half plane.

2.1.10 System Hankel's singular values

The system Hankel's singular values or simply Hankel's Singular Values (HSVs) is very important topic in the balancing based model reduction what are considered as the measurement of energy at every state in a dynamic system. The HSVs are the basis of balancing based model reduction, in which low energy states are discarded and high energy states are preserved. The Hankel's operator maps can be expressed as:

$$\mathcal{H} : u(t) \rightarrow \int_{-\infty}^0 \mathcal{E}e^{\mathcal{E}^{-1}\mathcal{A}(t-\tau)}\mathcal{E}^{-1}\mathcal{B}u(\tau)d\tau$$

which has a finite number of singular values essential for model reduction of large-scale system. It has been shown in [14] that HSVs are the positive square roots of the eigenvalues of the product of the CG and OG :

$$\sigma_i = \sqrt{\lambda_i(\mathcal{P}\mathcal{Q})} \text{ or } \sqrt{\lambda_i(\mathcal{M}\mathcal{N})}, \quad i = 1, 2, \dots, n, \quad (2.36)$$

where, λ_i denotes the eigenvalues. However, as the time-restricted CG (\mathcal{P}) and OG (\mathcal{Q}) as well as frequency-restricted CG (\mathcal{M}) and OG (\mathcal{N}) are not positive semi-definite, their Cholesky decomposition is never possible what is the reason HSVs (σ) cannot be expressed in the way shown in [2, 11, 52].

2.1.11 System's realizations

Any dynamic system has realization if the system matrices $\mathcal{E}, \mathcal{A}, \mathcal{B}, \mathcal{C}, \mathcal{D}$ satisfy the transfer function (2.7). The transfer function (2.7) is invariant under state-space or coordinate transformations $\tilde{x}(t) = \mathcal{T}x(t)$, where \mathcal{T} is non-singular matrix. After the transformation, we obtain a transformed system where

$$(\mathcal{E}, \mathcal{A}, \mathcal{B}, \mathcal{C}, \mathcal{D}) \Leftrightarrow (\mathcal{T}\mathcal{E}\mathcal{T}^{-1}, \mathcal{T}\mathcal{A}\mathcal{T}^{-1}, \mathcal{T}\mathcal{B}, \mathcal{C}\mathcal{T}^{-1}, \mathcal{D})$$

Therefore, the transformed invariant transfer function under the transformation \mathcal{T} is

$$\begin{aligned} \tilde{\mathcal{G}}(s) &= (\mathcal{C}\mathcal{T}^{-1})(s\mathcal{T}\mathcal{E}\mathcal{T}^{-1} - \mathcal{T}\mathcal{A}\mathcal{T}^{-1})^{-1}\mathcal{T}\mathcal{B} + \mathcal{D} \\ &= \mathcal{C}(s\mathcal{E} - \mathcal{A})^{-1}\mathcal{B} + \mathcal{D} = \mathcal{G}(s) \end{aligned}$$

Therefore, the transfer function of the transformed system is as same as the transfer function of the original system. Since the input-output (I/O) relations is unchanged under coordinate transformations, a system may have infinitely many realizations.

Definition 2.8 (Minimal transfer function [9–11]). A state space realization of a transfer function (2.7) is minimal if and only if the system is fully controllable and observable.

Definition 2.9 (Balanced realization [10, 11]). The realization of a system (2.2) is said to be balanced if its CG (\mathcal{P}) or (\mathcal{M}) and OG (\mathcal{Q}), (\mathcal{N}) is equal to each other and diagonal such that

$$\mathcal{P} = \mathcal{Q} = \text{diag}\{\sigma_i\}, \text{ or } \mathcal{M} = \mathcal{N} = \text{diag}\{\sigma_i\}, \text{ where } i = 1, 2, \dots, n,$$

Among many realizations, there exist a realizations where the dimension (r) of the system is minimum, i.e., consisting of minimum number of degree of freedoms (DoFs) what is known as McMillan degree of the system.

2.2 Concept of matrix computation

This section briefly describes some basic concepts of matrix computation relevant to this thesis subject.

2.2.1 Eigenvalue Problem

The finding of eigenvalues $\lambda \in \mathbb{R}, \text{ or } \mathbb{C}$ including $x \in \mathbb{R}^n \text{ or } \mathbb{C}^n$ satisfying

$$\mathcal{A}x = \lambda \mathcal{E}x, \quad x \neq 0,$$

where $\mathcal{A} \in \mathbb{R}^{n \times n} \text{ or } \mathbb{C}^{n \times n}$, $\mathcal{E} \in \mathbb{R}^{n \times n} \text{ or } \mathbb{C}^{n \times n}$ is known as eigenvalue problem. The scalar λ is called eigenvalues, i.e., $\det(\lambda \mathcal{E} - \mathcal{A})x = 0$, whereas x is called the eigenvectors of corresponding eigenvalues.

Definition 2.10 (Spectrum and trace of a matrix). The set of all eigenvalues of \mathcal{A} associated with \mathcal{E} is called the spectrum of \mathcal{A} denoted by $\Lambda(\mathcal{A}, \mathcal{E})$.

On the other hand, the sum of all the diagonal elements of the matrix \mathcal{A} is known as its trace.

The maximum modulus of the eigenvalues is called spectral radius denoted by $\rho(\mathcal{A}) = \max_{\lambda \in \rho(\mathcal{A})} |\lambda|$.

Any system’s stability depends on the positive definiteness of the matrix α (see 2.1.6) what can be defined as follows:

Definition 2.11 (Positive semi-definite). A square matrix α is said to be positive semi-definite if $x^T \alpha x \geq 0$ for every non-zero column vector x of real numbers. Similarly, if α is Hermitian, i.e., $\alpha = \bar{\alpha}^*$, then it will be positive semi-definite if $x^* \alpha x \geq 0$ for every non-zero column vector X of complex numbers.

However, any linear transformation $\mathcal{T} : \mathbb{R}^n \rightarrow \mathbb{R}^n$, or $\mathcal{T} : \mathbb{C}^n \rightarrow \mathbb{C}^n$ on a subspace $S \subset \mathbb{R}^n$, or $S \subset \mathbb{C}^n$ is said to be invariant if $\mathcal{A}x \in S$ for every $x \in S$.

2.2.2 Sparsity Pattern and projection

When we talk about large-scale matrix, there is a term ‘sparse’ included because of most of the entities of practical large-scale matrix being zero. The sparsity of any matrix depends on the ratio of the zero-valued entities against the total number of elements of a matrix. For instance, a matrix $a_{100 \times 100}$ has a sparsity ratio 9000 : 10000. That means, it contains 9000 non-zero elements and 1000 zero elements whereas the total entities is 10000.

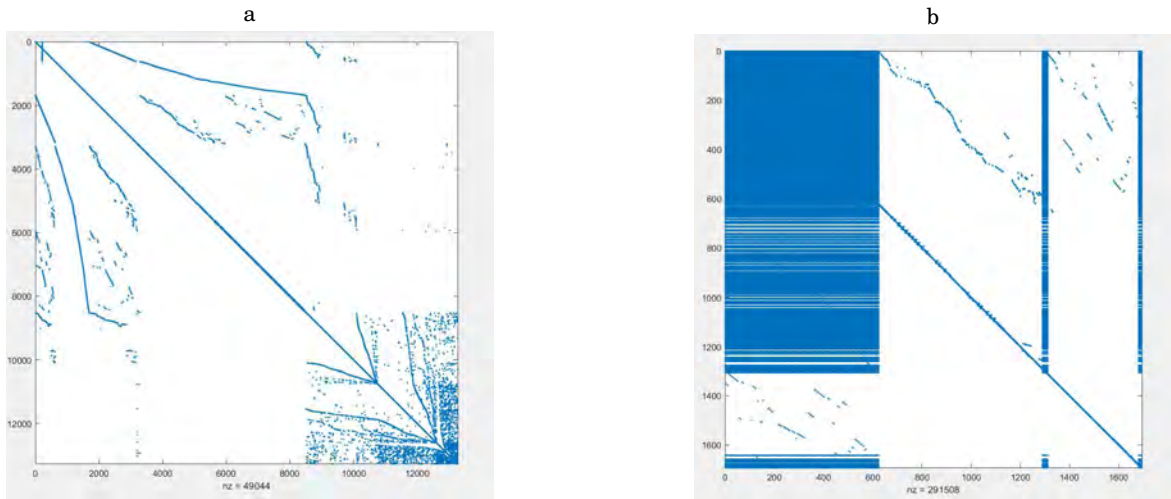


Figure 2.2: (a) Sparse Pattern (b) Dense Pattern

Practically, when a system is developed, most of the entities of the system matrices are zero, that means, the system becomes sparse. Figure (2.2) shows the sparse and dense forms of a system matrix having 2866249 entities in total. When it is sparse, the number of non-zero elements is only 49044. But after converting to dense form, the number of non-zero entities becomes 291508.

Projection is a very important topic in the control theory which is often required for converting any large-scale sparse matrix to equivalent small-scale matrix.

Definition 2.12 (Projection [6, 9, 10]). Projection is a linear transformation \mathcal{V} on a vector space $S \subset \mathbb{R}$ or $S \subset \mathbb{C}$ written as $\mathcal{V} : S \rightarrow S$ such that $\mathcal{V}^2 = \mathcal{V}$

A square matrix Γ is said to be an orthogonal projector if $\Gamma^2 = \Gamma = \Gamma^T$ for real and $\Gamma^2 = \Gamma = \Gamma^H$ for complex matrix. H denotes the complex conjugate transpose. Otherwise, the projector is recognized as oblique.

If a subspace S with dimension r can be written as $S = \text{Range}(\Gamma)$ and $\mathcal{V} = [\mathcal{V}_1, \dots, \mathcal{V}_r]$ is the set of basis of subspace S , then Γ is a projector onto S expressed as $\Gamma = \mathcal{V}(\mathcal{V}^T \mathcal{V})^{-1} \mathcal{V}^T$.

- The square matrix $\mathcal{I} - \Gamma$ is called complementary projector.
- Let S' be another r dimensional subspace and $S' = \text{range}(\mathcal{W})$ then $\Gamma = \mathcal{V}(\mathcal{W}^T \mathcal{V})^{-1} \mathcal{W}^T$ is called an oblique projector.

2.2.3 Important matrix decomposition

Matrix decomposition is a vital tool in the field of matrix computation what is a factorization process to factorize a matrix into a product of two or more matrices. Some of the important matrix decompositions are briefly introduced below:

2.2.3.1 Eigenvalue decomposition

Eigenvalue decomposition [53–55] factorizes a matrix into a canonical form to represent the matrix in terms of its eigenvalues and eigenvectors. A square matrix $\mathcal{A} \in \mathbb{R}^n$, or $\mathcal{A} \in \mathbb{C}^n$ can be factorized through eigenvalue decomposition as:

$$\mathcal{A} = \mathbf{V} \Lambda \mathbf{V}^{-1},$$

where, $\Lambda \in \mathbb{R}^n$, or $\Lambda \in \mathbb{C}^n$ is an diagonal matrix containing the eigenvalues of \mathcal{A} and $\mathbf{V} \in \mathbb{R}^n$, or $\mathbf{V} \in \mathbb{C}^n$ is the eigenvectors of \mathcal{A} .

2.2.3.2 Schur decomposition

The Schur decomposition of a square matrix $\mathcal{A} \in \mathbb{R}^n$, or $\mathcal{A} \in \mathbb{C}^n$ is defined as [53, 55]:

$$\mathcal{A} = \mathbf{U} \mathbf{T} \mathbf{U}^T,$$

where, $\mathbf{U} \in \mathbb{R}^n$, or $\mathbf{U} \in \mathbb{C}^n$ is unitary matrix, \mathbf{T} is upper triangular matrix containing the eigenvalues of \mathcal{A} at its diagonal.

2.2.3.3 QR decomposition

The QR decomposition of a matrix $\mathcal{A} \in \mathbb{R}^{n \times m}$, or $\mathcal{A} \in \mathbb{C}^{n \times m}$ is defined as [53, 55]:

$$\mathcal{A} = \mathbf{Q} \mathbf{R},$$

where \mathbf{Q} is an orthogonal matrix and \mathbf{R} is an upper triangular matrix. There are several methods existed for computing \mathbf{QR} decomposition such as Gram-Schmidt orthogonal process, household transformation. Generally, \mathbf{QR} decomposition is used to solve the eigenvalue problem and least square problem.

2.2.3.4 Singular value decomposition

The most widely used matrix decomposition in linear control systems is Singular Value Decomposition (SVD) [55–57], what can be written mathematically for a rectangular matrix $\mathcal{A} \in \mathbb{R}^{n \times m}$, or $\mathcal{A} \in \mathbb{C}^{n \times m}$

$$\mathcal{A} = \mathbf{U}\mathbf{\Sigma}\mathbf{V}^T,$$

where, $\mathbf{U} \in \mathbb{R}^{n \times n}$, or $\mathbf{U} \in \mathbb{C}^{n \times n}$ and $\mathbf{V} \in \mathbb{R}^{m \times m}$, or $\mathbf{V} \in \mathbb{C}^{m \times m}$ are unitary matrices and the diagonal entries σ_i of $\mathbf{\Sigma} \in \mathbb{R}^{n \times m}$, or $\mathbf{\Sigma} \in \mathbb{C}^{n \times m}$ are called singular values of \mathcal{A} arranged in chronological way, i.e., $\sigma_1 \geq \sigma_2 \geq \sigma_3 \geq \dots \sigma_k, k = \min(m, n)$.

The thin SVD of \mathcal{A} is obtained by taking only the first n singular values. SVD holds the following properties:

- If the $\mathcal{A}^T \mathcal{A}$ is symmetric positive semi-definite, the singular values σ_i are the square roots of the eigenvalues of $\mathcal{A}^T \mathcal{A}$.
- If l be the number of singular values, then $\text{rank}(\mathcal{A}) = l$.
- For symmetric \mathcal{A} , $\sigma_i = \|\lambda(\mathcal{A})\|$.
- $\|\mathcal{A}\|_2 = \sigma_1$ and $\|\mathcal{A}\|_F = \sqrt{(\sigma_1^2 + \sigma_2^2 + \dots + \sigma_k^2)}$

2.2.3.5 Arnoldi decomposition

Arnoldi decomposition is a typical large sparse matrix algorithm [58, 59] which makes the matrix map vectors instead of accessing the elements of the matrix directly. The prime tool of this method is Krylov subspace which is defined as:

Definition 2.13 (Krylov subspace [9, 11, 25]). The Krylov subspace \mathcal{K}_m associated with $\mathcal{A} \in \mathbb{R}^{n \times n}$, or $\mathcal{A} \in \mathbb{C}^{n \times n}$ and $\mathcal{V} \in \mathbb{R}^{n \times k}$, or $\mathcal{V} \in \mathbb{C}^{n \times k}$ can be written as:

$$\mathcal{K}_m(\mathcal{A}, \mathcal{V}) = \left[\mathcal{V}, \mathcal{A}\mathcal{V}, \dots, \mathcal{A}^{m-1}\mathcal{V} \right]$$

Lemma 2.1. Let, the column of $\mathcal{V}_{m+1} = \left[\mathcal{V}_m \quad v_{m+1} \right]$ form an orthogonal basis, then there exists an upper Hessenberg matrix $\hat{\mathcal{H}}_m \in \mathbb{R}^{m+1 \times m}$, defined as,

$$\hat{\mathcal{H}}_m = \begin{bmatrix} h_{11} & h_{12} & \dots & h_{1m} \\ h_{21} & h_{22} & \dots & h_{2m} \\ 0 & h_{32} & \dots & h_{3m} \\ \vdots & \ddots & \ddots & \vdots \\ 0 & 0 & \dots & h_{m+1,m} \end{bmatrix}$$

such that

$$\mathcal{A}\mathcal{V}_m = \mathcal{V}_{m+1}\hat{\mathcal{H}}_m \tag{2.37}$$

Conversely, if a matrix \mathcal{V}_{m+1} of orthogonal columns satisfies Equation (2.37), then the columns of \mathcal{V}_{m+1} form a basis for the Krylov subspace \mathcal{K}_m .

Algorithm 2: Arnoldi algorithm

Input: \mathcal{A} , initial matrix \mathcal{B}
Output: $\mathcal{H}_m \in \mathbb{R}^{n \times m}$, or $\mathcal{H}_m \in \mathbb{C}^{n \times m}$ such that $\mathbf{X}_m = \mathcal{H}_m \mathcal{H}_m^T$

- 1 set initial basis vector $v_1 = \frac{\mathcal{B}}{\|\mathcal{B}\|}$, $\mathcal{V}_1 = v_1$
- 2 **for** $k = 2, \dots, m$ **do**
- 3 Set $v_k = \mathcal{A}v_{k-1}$
- 4 **for** $j = 1$ **to** $k - 1$ **do**
- 5 compute inner product $h_{j,k-1} = v_j^T v_k$
- 6 subtract projection $v_k = v_k - (h_{j,k-1} v_j)$
- 7 compute $h_{k+1,k} = \|v_k\|$ and new basis vector $v_{k+1} = \frac{v_k}{h_{k+1,k}}$
- 8 $\mathcal{H}_k = \begin{bmatrix} \mathcal{H}_{k-1} & h_k \\ 0 & h_{k+1,k} \end{bmatrix}$
- 9 $\mathcal{V}_{k+1} = \begin{bmatrix} \mathcal{V}_k & v_{k+1} \end{bmatrix}$
- 10 Partition $\mathcal{H}_m = \begin{bmatrix} \hat{\mathcal{H}}_m \\ h_{m+1,m} e_m^T \end{bmatrix}$

From Equation (2.37), for Hessenberg matrix it can be elaborated as:

$$\mathcal{A}\mathcal{V}_m = \begin{bmatrix} \mathcal{V}_m & v_{m+1} \end{bmatrix} \begin{bmatrix} \mathcal{H}_m \\ h_{m+1,m} e_m^T \end{bmatrix} = \mathcal{V}_m \mathcal{H}_m + \underbrace{h_{m+1,m} v_{m+1} e_m^T}_{em}, \quad (2.38)$$

where, \mathcal{H}_m is found removing the last row from $\hat{\mathcal{H}}_m$ and e_m is a matrix of the last k columns of the mk identity matrix.

After m steps, $h_{m+1,m}$ will be vanished and after some iteration, em term of (2.38) converges to zero. Therefore, Equation (2.38) can rewrite as:

$$\mathcal{H}_m = \mathcal{V}_m^T \mathcal{A}\mathcal{V}_m \quad (2.39)$$

Hence, \mathcal{H}_m represents the projection onto the Krylov subspace $\mathcal{K}_m(\mathcal{A}, \mathcal{V})$.

Definition 2.14 (Ritz value and Ritz vector [58]). The eigenvalues λ_m of \mathcal{H}_m are called Ritz values and if \tilde{v} is eigenvectors of \mathcal{H}_m associated with λ_m , then $\mathcal{V}_m \tilde{v}$ is called Ritz vectors belong to λ_m .

2.2.4 Matrix exponential

Matrix exponential is an essential part of the system on definite time interval (see (2.1.7)) and also a challenging part of computation for the large scale sparse system matrices. There are several techniques available for the matrix computation what are briefly described below:

2.2.4.1 Eigenvalue decomposition method

If a square matrix $\mathcal{A} \in \mathbb{R}^n$, or $\mathcal{A} \in \mathbb{C}^n$ is diagonalizable, its exponent can be easily computed through eigenvalue decomposition (see (2.2.3.1)) as:

$$e^{\mathcal{A}} = \mathbf{V} e^{\Lambda} \mathbf{V}^{-1},$$

where, Λ contains the eigenvalues of \mathcal{A} at its diagonal.

However, converting \mathcal{A} to Jordan canonical form \mathbf{J} , matrix exponent is computed as:

$$e^{\mathcal{A}} = \mathbf{P}e^{\mathbf{J}}\mathbf{P}^{-1},$$

The main problem of the decomposition method is that it consumes more memory during dealing with large-sparse matrix and convert the sparse matrix dense before computing.

2.2.4.2 Power series expansion

Power series is the ideal process to computing matrix exponent as it retains the sparsity pattern at the time of computation. As a result, it consumes less memory during computation. For any square matrix $\mathcal{A} \in \mathbb{R}^n$, or $\mathcal{A} \in \mathbb{C}^n$, the Taylor series expansion of \mathcal{A} at convergence point 0 is:

$$e^{\mathcal{A}} = \mathcal{I} + \mathcal{A} + \frac{\mathcal{A}^2}{2!} + \frac{\mathcal{A}^3}{3!} + \dots + \frac{\mathcal{A}^n}{n!} = \sum_{k=0}^{\infty} \frac{\mathcal{A}^k}{k!}, \quad (2.40)$$

where, $\mathcal{I}_{n \times n}$ is an identity matrix. However, Taylor series is very slowly convergent to zero. Therefore, Padé approximation is a better remedy of matrix exponent what gives surprisingly fast convergent approximation of the matrix exponent written as:

$$\left(1 + \sum_{k=1}^i b_k \mathcal{A}^k\right) f(\mathcal{A}) = \sum_{k=0}^j a_k \mathcal{A}^k, \quad (2.41)$$

where, $f(\mathcal{A})$ indicates the Taylor series of matrix exponent of \mathcal{A} . a_k, b_k are the coefficients numerators and denominators respectively of the rational polynomial $P = \frac{a_k \mathcal{A}^k}{b_k \mathcal{A}^k}$.

2.2.5 Matrix square root

The computation of matrix square root is related to finding matrix logarithm. Some well-known square root computational procedures are given below:

2.2.5.1 Schur decomposition method

If any matrix \mathcal{A} is diagonalizable, then its square-root can be computed by Schur decomposition (see (2.2.3.2)) as:

$$\mathcal{A}^{\frac{1}{2}} = \mathbf{U}\mathbf{T}^{\frac{1}{2}}\mathbf{U}^T,$$

where, the eigenvalues of \mathcal{A} is the diagonal entities of the upper triangular matrix \mathbf{U} .

2.2.5.2 Power series expansion

The power series of the square root of a matrix \mathcal{A} can be written as:

$$\mathcal{A}^{\frac{1}{2}} = \sum_{k=0}^{\infty} (-1)^k \frac{2k!}{(1-2k)(k!)^2 4^k} (\mathcal{A} - \mathcal{I})^k$$

It gives a convergent approximation if it satisfies the Gelfand's condition $\lim_{k \rightarrow \infty} \left\| \mathcal{A}^k \right\|^{\frac{1}{k}} < 1$, that means, the spectrum of \mathcal{A} is within the disk $D(1,1) \subset \mathbb{C}$. It works perfectly well if matrix \mathcal{A} is positive semi-definite.

2.2.5.3 Denman-Beaver method

Denman-Beaver method [60] is an iterative method for finding square root of a square matrix \mathcal{A} starting with $Y_0 = \mathcal{A}$, $Z_0 = \mathcal{I}$ as:

$$\begin{aligned} Y_{k+1} &= \frac{1}{2}(Y_k + Z_k^{-1}) \\ Z_{k+1} &= \frac{1}{2}(Z_k + Y_k^{-1}) \end{aligned}$$

The main problem of this method is that it gives no guarantee to give convergent approximation. But if it gives convergent approximation, then Y_k converges quadratically to $\mathcal{A}^{\frac{1}{2}}$ and Z_k converges to $\mathcal{A}^{-\frac{1}{2}}$. However, recently in [42], the authors implied inverse scaling method for finding convergent approximation through this method what works well practically.

However, another problem is that it needs to perform matrix inversion which is inefficient while working with large-scale matrix.

2.2.6 Matrix logarithm

Matrix logarithm is an inevitable part for defining any system on finite frequency interval (see (2.1.8)) and still there is no efficient method for computing logarithm of large-sparse matrix, especially matrix of complex entities. However, in this thesis we mainly focus on complex matrix logarithm. The logarithm of a square matrix $\mathcal{A} \in \mathbb{C}^n$ can be written as:

$$\begin{aligned} \ln(\mathcal{A}) &= \ln(x + iy) = \ln(re^{i\theta}) \\ &= \frac{1}{2}\ln(x^2 + y^2) + i \arctan\left(\frac{y}{x}\right), \end{aligned}$$

where, $r = (x^2 + y^2)^{\frac{1}{2}}$ and $\theta = \arctan(\frac{y}{x})$. This is known as principle value of logarithm which is only possible if the real part of all of the eigenvalues are on the positive x -half plane. Otherwise, we get general value of logarithm written as:

$$\ln(\mathcal{A}) = \frac{1}{2}\ln(x^2 + y^2) + i(2k\pi + \arctan(\frac{y}{x})), \quad k = 1, 2, \dots, n.$$

Some established methods of finding finding logarithm are given as following:

2.2.6.1 Eigenvalue decomposition method

If $\mathcal{A} \in \mathbb{C}^n$ is diagonalizable, its logarithm can be calculated by eigenvalue decomposition (see (2.2.3.1)) as:

$$\ln(\mathcal{A}) = \mathbf{V}\ln(\Lambda)\mathbf{V}^{-1},$$

where, Λ contains the eigenvalues of \mathcal{A} at its diagonal. The main problem of the decomposition method is that it consumes more memory during dealing with large-sparse matrix and convert the sparse matrix dense before computing.

2.2.6.2 Power series expansion

If a matrix \mathcal{A} is sufficiently close to the identity matrix \mathcal{I} of same dimension, i.e., $\|\mathcal{A} - \mathcal{I}\| < 1$, then its Taylor series can be written as:

$$\ln(\mathcal{A}) = (\mathcal{A} - \mathcal{I}) - \frac{(\mathcal{A} - \mathcal{I})^2}{2} + \frac{(\mathcal{A} - \mathcal{I})^3}{3} + \dots + (-1)^{n-1} \frac{(\mathcal{A} - \mathcal{I})^n}{n} = \sum_{k=1}^n (-1)^{k-1} \frac{(\mathcal{A} - \mathcal{I})^k}{k} \quad (2.42)$$

However, for faster convergence, we can apply Padé approximation (2.41) here also where $f(\mathcal{A})$ denotes the Taylor series of matrix logarithm of \mathcal{A} .

2.3 Available methods for solving Lyapunov equation

The solution of Lyapunov equation (2.14) is a key element in control theory for analysing system's stability, finding equivalent low-rank approximation [6, 9, 10]. There are several methods established over the decades among which some directly solve the Lyapunov equation constructed centering on small dense systems and some give approximate solution by iteration during dealing with large-scale sparse systems. However, in this section, we only describe the methods appropriate for finding the solution on limited time and frequency intervals. We convert the general case to standard as $\mathcal{A}_s = \mathcal{E}^{-1}\mathcal{A}$ and $\mathcal{B}_s = \mathcal{E}^{-1}\mathcal{B}$ for describing in a convenient way. For the description of the methods available for the solution of infinite domains, one may see [2, 9, 11].

2.3.1 Methods for dense system

These solvers are appropriate for small dense systems. If the system becomes large, they need more computational time and increase the computational cost what is quite inefficient in the field of matrix computation.

2.3.1.1 Bartels-Stewart's method

The Bartels-Stewart method [29, 30] provided the first numerically standard technique to solve the dense small Lyapunov equations. Bartels-Stewart algorithm transformed a matrix \mathcal{A}_s into \mathcal{H} by imposing Schur decomposition $\mathcal{H} = \mathbf{U}^T \mathcal{A}_s \mathbf{U}$, where \mathbf{U} is orthogonal and \mathcal{H} is quasi upper-triangular, while in the Hessenberg-Schur algorithm, \mathcal{A}_s is reduced only to upper Hessenberg form. Therefore, the controllable Lyapunov equation (2.17) on definite time interval $[t_f, t_0]$ can be written as:

$$\mathcal{H} \tilde{\mathcal{P}} + \tilde{\mathcal{P}} \mathcal{H}^T = \mathbf{U}^T e^{\mathcal{H}t_f} \mathcal{B}_s \mathcal{B}_s^T e^{\mathcal{H}^T t_f} \mathbf{U} - \mathbf{U}^T e^{\mathcal{H}t_0} \mathcal{B}_s \mathcal{B}_s^T e^{\mathcal{H}^T t_0} \mathbf{U}$$

Similarly, on limited frequency $[\Omega_f, \Omega_0]$, the controllable Lyapunov equation (2.33a) can be expressed as:

$$\mathcal{H} \tilde{\mathcal{M}} + \tilde{\mathcal{M}} \mathcal{H}^T + \mathbf{U}^T \phi(i\omega) \mathcal{B}_s \mathcal{B}_s^T \mathbf{U} + \mathbf{U}^T \mathcal{B}_s \mathcal{B}_s^T \phi^*(i\omega) \mathbf{U} = 0$$

These equations can be solved through backward substitutions so that $\tilde{\mathcal{P}} = \mathbf{U}^T \mathcal{P} \mathbf{U}$ and $\tilde{\mathcal{M}} = \mathbf{U}^T \mathcal{M} \mathbf{U}$.

In this method, the system matrix \mathcal{A}_s is transformed to real Schur form and then solves backward for the solution of the transformed Lyapunov equations. The solutions $\tilde{\mathcal{P}}$ and $\tilde{\mathcal{M}}$ are obtained by a congruence transformation.

2.3.1.2 Hammarling's method

Another exact method is Hammarling method [31, 32] which is only applicable if the right side $\mathcal{B}\alpha\mathcal{B}^T$ of (2.34) and $\mathcal{B}\beta\mathcal{B}^T$ of (2.35) is symmetric positive semi-definite which is not naturally possible for the Lyapunov equation on definite time and frequency interval (see (2.1.9)). However, recently few works have been done for converting a negative definite matrix to positive semi-definite [37, 39, 43]. After applying one of those methods, we may convert $\mathcal{B}\alpha\mathcal{B}^T$ and $\mathcal{B}\beta\mathcal{B}^T$ to positive semi-definite which is mandatory to impose Hammarling method for solving Lyapunov equations on limited time and frequency intervals.

This algorithm first transforms \mathcal{A}_s to lower triangular form for calculating the lower triangular matrix Cholesky factor R, S of the solution \mathcal{P} and \mathcal{M} such that $\mathcal{P} = RR^T$ and $\mathcal{M} = SS^T$ in the recursive manner. Like the previous exact method, this method is also required Schur decomposition of \mathcal{A}_s or Hessenberg decomposition of \mathcal{B}_s .

2.3.1.3 Matrix sign function method

Matrix sign function is the most popular approach to solve dense Lyapunov equations what can be written for a matrix \mathcal{A}_s as following:

$$\text{sign}(\mathcal{A}_s) = \mathcal{V}\mathbf{D}\mathcal{V}^{-1}$$

where, $\mathbf{D} = \text{diag}(d_1, d_2, \dots, d_n)$ and

$$d = \begin{cases} 1 & \text{Re}(\lambda_n) > 0 \\ -1 & \text{Re}(\lambda_n) < 0 \end{cases}$$

where, λ is the eigenvalues of \mathcal{A}_s . The Lyapunov equations (2.17) and (2.33a) on restricted time and frequency intervals can be decomposed as :

$$\begin{bmatrix} \mathcal{A}_s & \mathbf{P} \\ 0 & -\mathcal{A}_s^T \end{bmatrix} = \begin{bmatrix} \mathcal{I} & \mathcal{P} \\ 0 & \mathcal{I} \end{bmatrix} \begin{bmatrix} \mathcal{A}_s & 0 \\ 0 & -\mathcal{A}_s^T \end{bmatrix} \begin{bmatrix} \mathcal{I} & -\mathcal{P} \\ 0 & \mathcal{I} \end{bmatrix}$$

and

$$\begin{bmatrix} \mathcal{A}_s & \mathbf{M} \\ 0 & -\mathcal{A}_s^T \end{bmatrix} = \begin{bmatrix} \mathcal{I} & \mathcal{M} \\ 0 & \mathcal{I} \end{bmatrix} \begin{bmatrix} \mathcal{A}_s & 0 \\ 0 & -\mathcal{A}_s^T \end{bmatrix} \begin{bmatrix} \mathcal{I} & -\mathcal{M} \\ 0 & \mathcal{I} \end{bmatrix}$$

where, $\mathbf{P} = e^{\mathcal{A}_s t_0} \mathcal{B}_s \mathcal{B}_s^T e^{\mathcal{A}_s^T t_0} - e^{\mathcal{A}_s t_f} \mathcal{B}_s \mathcal{B}_s^T e^{\mathcal{A}_s^T t_f}$ and $\mathbf{M} = -\phi(i\omega) \mathcal{B}_s \mathcal{B}_s^T - \mathcal{B}_s \mathcal{B}_s^T \phi^*(i\omega)$.

Hence, if \mathcal{A}_s is asymptotically stable, then [28, 61]

$$\text{sign}(\mathcal{A}_s) = \mathcal{V} \text{sign} \left(\begin{bmatrix} \mathcal{A}_s & 0 \\ 0 & -\mathcal{A}_s^T \end{bmatrix} \right) \mathcal{V}^{-1}$$

The matrix sign function is computed by the following formula:

$$X_0 = \mathcal{A}_s = \begin{bmatrix} \mathcal{A}_s & \mathbf{P} \\ 0 & -\mathcal{A}_s^T \end{bmatrix}, \quad X_{k+1} = \frac{(X_k + X_k^{-1})}{2}, \quad k = 0, 1, 2, \dots$$

It is shown in [61, 62] that $X_k \rightarrow \text{sign}(\mathcal{A}_s)$ as $k \rightarrow \infty$. Although this method requires approximately the same amount of work space as the requirement of Bartels-Stewart method [63], the matrix sign function method is more appropriate for parallelization as well as application than generalized Bartels-Stewart method [62].

However, the disadvantage of the matrix sign function method is that an explicit matrix inversion is required in every iteration which may lead to significant round-off error for ill-conditioned X_k if the eigenvalues of the matrix pencil $\lambda - \mathcal{A}_s$ lie close to the imaginary axis. As a result, it cannot be directly utilized for projected generalized Lyapunov equation.

2.3.2 Methods for sparse systems

These method are appropriate for large-scale sparse systems. In these types of methods, the low-rank approximations of the original solution of the Lyapunov equations are calculated what are comparatively more cost efficient than the direct methods previously described.

2.3.2.1 Low Rank LDL^T factor- Alternating Direction Implicit method

The Alternating Direction Implicit (ADI) method is a powerful method arisen from the solution methods for parabolic and elliptic partial differential equations what was first applied for solving Lyapunov equation in [64]. However, at here we reform ADI method for the Lyapunov equation (2.34) on definite time interval $[t_0, t_f]$ as:

$$\begin{aligned} (\mathcal{A}_s + \mu_j \mathcal{I}) \mathcal{P}_{j-\frac{1}{2}} &= \mathcal{B}_s \alpha \mathcal{B}_s^T - \mathcal{P}_{j-1} (\mathcal{A}_s - \mu_j \mathcal{I})^T \\ (\mathcal{A}_s + \mu_j \mathcal{I}) \mathcal{P}_j &= \mathcal{B}_s \alpha \mathcal{B}_s^T - \mathcal{P}_{j-\frac{1}{2}}^T (\mathcal{A}_s - \mu_j \mathcal{I})^T \end{aligned}$$

with $\mathcal{P}_0 = 0$ and the shift parameters $\mu_1, \mu_2, \dots, \mu_j \in \mathbb{C}^-$ computed following the procedure described in [65].

In [66], the authors simplified the typical ADI method by converting it for finding low-rank Cholesky factors of the solution (\mathcal{P}) of Lyapunov equation. But the problem is that we cannot perform Cholesky factorization on the solution of the Lyapunov equation as it is positive indefinite (see (2.1.9)). Therefore, a better remedy is to perform LDL^T factorization instead of Cholesky decomposition [67].

Therefore, the solution \mathcal{P} can be written as :

$$\begin{aligned} \mathcal{P} \approx L_j D_j L_j^T &= -2\text{Re}(\mu_j) (\mathcal{A}_s + \mu_j \mathcal{I})^{-1} G_s S G_s^T (\mathcal{A}_s + \mu_j \mathcal{I})^{-T} + \\ &\{ (\mathcal{A}_s + \mu_j \mathcal{I})^{-1} (\mathcal{A}_s - \mu_j \mathcal{I}) L_{j-1} D_{j-1} L_{j-1}^T (\mathcal{A}_s - \mu_j \mathcal{I})^T (\mathcal{A}_s + \mu_j \mathcal{I})^{-T} \}, \end{aligned}$$

Algorithm 3: Low rank LDL^T factorization ADI method

Input: \mathcal{A}_s , ADI shift $\mu_j \in \mathbb{C}, G_s, S$, tolerance ϵ
Output: L_j, D_j such that $\mathcal{P} \approx L_j D_j L_j^T$

- 1 Initiate $X_0 = G_s, j = 1$
- 2 **while** $\|X_{j-1} S X_{j-1}^T\| \geq \epsilon \|G_s S G_s^T\|$ **do**
- 3 Solve $\mathcal{V}_j = (\mathcal{A}_s + \mu_j \mathcal{S})^{-1} X_{j-1}$
- 4 **if** μ_j is real **then**
- 5 $X_j = X_{j-1} - 2\mu_j \mathcal{V}_j$
- 6 $L_j = [L_{j-1}, \mathcal{V}_j]$
- 7 **else**
- 8 $n_j = \sqrt{2}, \delta_j = \frac{\text{Re}(\mu_j)}{\text{Im}(\mu_j)}$
- 9 $X_{j+1} = X_{j-1} - 4\text{Re}(\mu_j)(\text{Re}(\mathcal{V}_j) + \delta_j \text{Im}(\mathcal{V}_j))$
- 10 $L_{j+1} = [L_{j-1}, n_j(\text{Re}(\mathcal{V}_j) + \delta_j \text{Im}(\mathcal{V}_j)), n_j \sqrt{\delta_j^2 + 1} \text{Im}(\mathcal{V}_j)]$
- 11 $j = j + 1$
- 12 $D_j = -2\text{diag}(\text{Re}(\mu_1), \dots, \text{Re}(\mu_j)) \otimes S$

where,

$$L_j = \left[(\mathcal{A}_s + \mu_j \mathcal{S})^{-1} G_s, (\mathcal{A}_s + \mu_j \mathcal{S})^{-1} (\mathcal{A}_s - \mu_j \mathcal{S}) L_{j-1} \right]$$

$$D_j = \begin{bmatrix} -2\text{Re}(\mu_j) S & 0 \\ & \ddots \\ 0 & D_{j-1} \end{bmatrix}$$

$$G_s S G_s^T = \mathcal{B}_s \alpha \mathcal{B}_s^T.$$

Algorithm (3) shows the step by step procedures of LDL^T factorization-ADI method for finding the solution \mathcal{P} where the technique to compute real low-rank Gramian factor $LD^{\frac{1}{2}}$ is imposed by smartly picking the complex shift parameters described in [68].

Same algorithm can be applied for finding the low rank solution of Lyapunov equation (2.35) on definite frequency interval $[\Omega_0, \Omega_f]$ by performing the factorization as $G_s S G_s^T = \mathcal{B}_s \beta \mathcal{B}_s$.

2.3.2.2 Krylov subspace method

Projection based low-rank iterative methods are one of the most efficient methods for solving Large scale Lyapunov equations by reducing the problem dimensions. Krylov subspace method [23, 24] is frequently used developed based on Krylov subspace techniques via block Arnoldi algorithm (2) or Lanczos process introduced in [26] for smaller system what was extended for larger system in [23]. However, at here we talk about the solution of time and frequency restricted Lyapunov equations (2.17, 2.33a).

In Krylov subspace methods, an approximate solution of the Lyapunov equation (2.17) is determined in the form $\mathcal{P} \approx \mathcal{V} \tilde{\mathcal{P}} \mathcal{V}^T$. First, we need to determine the columns of $\mathcal{V}_m \in \mathbb{R}^{n \times k}$, which span an orthonormal basis for the mk -dimensional Krylov subspace defined by

$$\mathcal{K}_m(\mathcal{A}_s, \mathcal{B}_s) = \text{span}(\mathcal{B}_s, \mathcal{A}_s \mathcal{B}_s, \mathcal{A}_s^2 \mathcal{B}_s, \dots, \mathcal{A}_s^{m-1} \mathcal{B}_s)$$

Using Algorithm (2), the basis \mathcal{V}_m of the Krylov subspace \mathcal{K}_m can be computed. Ensuring the unique solution \mathcal{P}_m at each iteration of the each reduced order equation

$$\mathcal{H}_m \mathcal{P}_m + \mathcal{P}_m \mathcal{H}_m^T + \mathcal{V}_m^T e^{\mathcal{A}_s t_0} \mathcal{B}_s \mathcal{B}_s^T e^{\mathcal{A}_s^T t_0} \mathcal{V}_m - \mathcal{V}_m^T e^{\mathcal{A}_s t_f} \mathcal{B}_s \mathcal{B}_s^T e^{\mathcal{A}_s^T t_f} \mathcal{V}_m = 0$$

is the key problem which is ensured for real \mathcal{H}_m if and only if $\lambda_i + \lambda_j \neq 0$ for every pair of eigenvalues λ_i and λ_j of \mathcal{H}_m .

There are several method available for constructing the basis of Krylov subspace. In [24], Galerkin type method was imposed relying on their global Arnoldi process whereas the convergence of Arnoldi-Lyapunov methods has been studied in [69] computing the residual of corresponding \mathcal{P}_m as

$$R_m = \mathcal{A}_s \mathcal{V}_m \mathcal{P}_m \mathcal{V}_m^T + \mathcal{V}_m \mathcal{P}_m \mathcal{V}_m^T \mathcal{A}_s^T + e^{\mathcal{A}_s t_0} \mathcal{B}_s \mathcal{B}_s^T e^{\mathcal{A}_s^T t_0} - e^{\mathcal{A}_s t_f} \mathcal{B}_s \mathcal{B}_s^T e^{\mathcal{A}_s^T t_f}$$

satisfying the Galerkin condition

$$\mathcal{V}_m^T R_m \mathcal{V}_m = 0$$

In [70], the author used two pass version of the Lanczos algorithm for the reduction of memory consumption whose convergence tendency has been studied in [69].

Similarly, using projection based Krylov subspace the reduced order frequency restricted Lyapunov equation can be expressed as

$$\mathcal{H}_m \mathcal{M}_m + \mathcal{M}_m \mathcal{H}_m^T + \mathcal{V}_m^T \phi(i\omega) \mathcal{B}_s \mathcal{B}_s^T \mathcal{V}_m + \mathcal{V}_m^T \mathcal{B}_s \mathcal{B}_s^T \phi^T(i\omega) \mathcal{V}_m = 0$$

2.4 Model order reduction techniques

In control theory, the linear time invariant continuous-time system (2.2) arises during solving many real-life applications what becomes more challenging to compute for the large-scale mathematical model. As a result, reducing the size of the system from higher order to lower order is indispensable to circumvent the computational complexity which is known as model order reduction (MOR).

The aim of the model reduction is to substitute the higher dimensional system (2.2) by a substantially lower dimensional system

$$\begin{aligned} \tilde{\mathcal{E}} \dot{\tilde{x}}(t) &= \tilde{\mathcal{A}} \tilde{x}(t) + \tilde{\mathcal{B}} u(t), \\ \tilde{y}(t) &= \tilde{\mathcal{C}} \tilde{x}(t) + \tilde{\mathcal{D}} u(t), \end{aligned} \tag{2.43}$$

where, $\tilde{\mathcal{E}}, \tilde{\mathcal{A}} \in \mathbb{R}^{r \times r}$, $\tilde{\mathcal{B}} \in \mathbb{R}^{r \times k}$, $\tilde{\mathcal{C}} \in \mathbb{R}^{l \times r}$, and $\tilde{\mathcal{D}} \in \mathbb{R}^{l \times k}$. Noted that, r (reduced dimension) $\ll n$ (full dimension). The approximation is more accurate if the matrix norm

$$\|y - \tilde{y}\|$$

is sufficiently small. The transfer function of full system (2.7) is replaced by the transfer function of reduced system written as

$$\tilde{Y}(s) = \tilde{\mathcal{G}}(s) U(s), \quad \tilde{\mathcal{G}}(s) = \tilde{\mathcal{C}}(s\tilde{\mathcal{E}} - \tilde{\mathcal{A}})^{-1} \tilde{\mathcal{B}} + \tilde{\mathcal{D}} \tag{2.44}$$

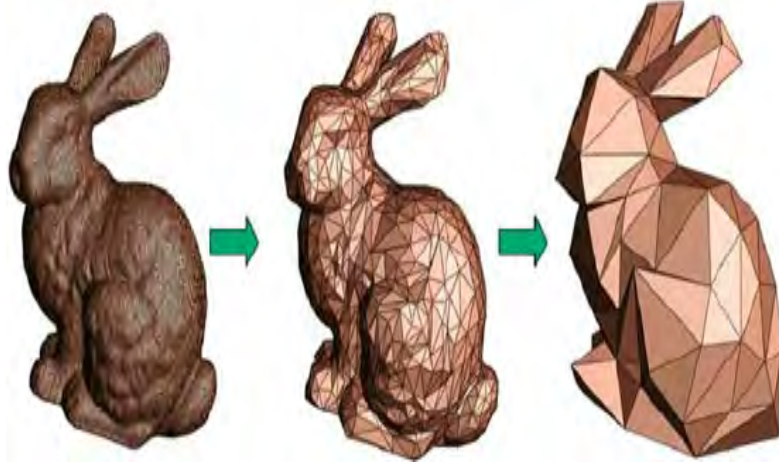


Figure 2.3: Model reduction (image source [1])

Therefore, the error between the original and reduced systems can be measured from

$$\|Y - \tilde{Y}\|_2 = \|(\mathcal{G} - \tilde{\mathcal{G}})U\|_2 \leq \|\mathcal{G} - \tilde{\mathcal{G}}\|_\infty \|U\|_2. \quad (2.45)$$

Hence, in the frequency domain, for the same input, the difference between two output responses can be bounded by

$$\|\mathcal{G} - \tilde{\mathcal{G}}\|_\infty.$$

Therefore, by minimizing $\|\mathcal{G} - \tilde{\mathcal{G}}\|_\infty$, we can guarantee that $\|Y - \tilde{Y}\|_2$ is minimized. Hence in model reduction, the approximation error between the original and reduced models can be obtained by computing the $\|\mathcal{G} - \tilde{\mathcal{G}}\|_\infty$ in certain range of the frequency domain.

Along with minimizing the approximated error, the other features like stability, passivity, symmetry, definiteness of the original system must be preserved in the reduced systems if the original system contains all of these properties.

The techniques to reduce the state space dimension are mainly classified into two classes: the Gramian-based methods and the moment matching-based methods [6, 9]. The first class includes optimal Hankel norm approximation [14], singular perturbation approximation [13], dominant subspaces projection [71], balanced truncation [17] whereas the second implements rational Krylov methods efficiently [15, 16, 43].

However, among those some of the efficient MOR methods implemented on limited time and frequency domains are discussed below:

2.4.1 Square root balanced truncation

Balanced truncation is a Gramian-based model reduction technique what basically reduces the dimensions by truncating the less important states from the systems. These states correspond to the smallest Hankel's Singular Values (HSVs) which is difficult to control but easy to observe or vice-versa [9]. This issue can be fixed by transforming the system into a balanced form (2.9), that means, the degree of controllability and observability of each state are the same.

Now if we eliminate those states of the balanced system through balancing transformation that are hard to control, we have eliminated the states that are hard to observe at the same time.

Definition 2.15 (Balancing transformation [9, 10]). A state space transformation \mathcal{T} defined in (2.1.11) is called a balancing transformation if

$$\mathcal{T}^{-T} \mathcal{P} \mathcal{T}^{-1} = \mathcal{T} \mathcal{Q} \mathcal{T}^T = \Sigma = \begin{bmatrix} \Sigma_i & \\ & \Sigma_{ii} \end{bmatrix},$$

where, \mathcal{P} and \mathcal{Q} are the controllability and observability Gramians on restricted time interval respectively, $\Sigma_i = \text{diag}(\sigma_1, \dots, \sigma_r)$, $\Sigma_{ii} = \text{diag}(\sigma_{r+1}, \dots, \sigma_n)$ are the system's HSVs.

Similarly, it is applicable for controllability and observability Gramians on restricted frequency interval \mathcal{M} and \mathcal{N} .

Since balanced truncation is a Gramian-based technique, the low-rank factors of \mathcal{P} , \mathcal{Q} found by solving Lyapunov equations (2.17) and (2.18) are required what can be constructed as:

$$\mathcal{P} = \mathcal{R}_{\mathcal{P}} \mathcal{R}_{\mathcal{P}}^T \quad \text{and} \quad \mathcal{Q} = \mathcal{L}_{\mathcal{Q}} \mathcal{L}_{\mathcal{Q}}^T, \quad (2.46)$$

where, $\mathcal{R}_{\mathcal{P}} = \mathcal{V} \mathcal{V} \Lambda^{\frac{1}{2}}$ and $\mathcal{L}_{\mathcal{Q}} = \mathcal{V} \mathcal{V} \Lambda^{\frac{1}{2}}$. \mathcal{V} and Λ are found from the eigenvalue decomposition of low-rank approximation $\tilde{\mathcal{P}}$, $\tilde{\mathcal{Q}}$ of \mathcal{P} and \mathcal{Q} respectively instead of Cholesky factorization as they are positive indefinite.

Algorithm 4: Square root balanced truncation

Input: Low rank factors $\mathcal{R}_{\mathcal{P}}$ and $\mathcal{L}_{\mathcal{Q}}$ of \mathcal{P} and \mathcal{Q} respectively

Output: Reduced order system matrices $\tilde{\mathcal{E}}$, $\tilde{\mathcal{A}}$, $\tilde{\mathcal{B}}$, $\tilde{\mathcal{C}}$, $\tilde{\mathcal{D}}$

1 Compute and partition a (thin) Singular Value Decomposition (SVD)

$$\mathcal{L}_{\mathcal{Q}}^T \mathcal{R}_{\mathcal{P}} = \begin{bmatrix} \mathbf{U}_i & \mathbf{U}_{ii} \end{bmatrix} \begin{bmatrix} \Sigma_i & \\ & \Sigma_{ii} \end{bmatrix} \begin{bmatrix} \mathbf{V}_i & \mathbf{V}_{ii} \end{bmatrix}^T, \quad (2.47)$$

where $\Sigma_i = \text{diag}(\sigma_1, \dots, \sigma_r)$ contains the largest r HSVs.

2 Construct the left and right balancing transformation matrices

$$\mathcal{T}_L := \mathcal{R}_{\mathcal{P}} \mathbf{V}_i \Sigma_i^{-\frac{1}{2}}, \quad \mathcal{T}_R := \mathcal{L}_{\mathcal{Q}} \mathbf{U}_i \Sigma_i^{-\frac{1}{2}}, \quad (2.48)$$

3 Generate reduced order system matrices as

$$\begin{aligned} \tilde{\mathcal{E}} &:= \mathcal{T}_R^T \mathcal{E} \mathcal{T}_L, & \tilde{\mathcal{A}} &:= \mathcal{T}_R^T \mathcal{A} \mathcal{T}_L, \\ \tilde{\mathcal{B}} &:= \mathcal{T}_R^T \mathcal{B}, & \tilde{\mathcal{C}} &:= \mathcal{C} \mathcal{T}_L, & \tilde{\mathcal{D}} &:= \mathcal{D} \end{aligned}$$

After computing the SVD of $\mathcal{L}_{\mathcal{Q}}^T \mathcal{R}_{\mathcal{P}}$ as (2.47), two transformation matrices \mathcal{T}_L and \mathcal{T}_R can be constructed as (2.48) for performing balanced truncation reduction technique which satisfy the properties

$$\begin{aligned} \mathcal{T}_R^T \mathcal{T}_L &= \Sigma_i^{-\frac{1}{2}} \mathbf{U}_i^T (\mathcal{L}_{\mathcal{Q}}^T \mathcal{R}_{\mathcal{P}}) \mathbf{V}_i \Sigma_i^{-\frac{1}{2}} = \Sigma_i^{-\frac{1}{2}} \mathbf{U}_i^T (\mathbf{U}_i \Sigma_i \mathbf{V}_i^T) \mathbf{V}_i \Sigma_i^{-\frac{1}{2}} = \mathcal{I} \\ \mathcal{T}_L \mathcal{T}_R^T &= \mathcal{R}_{\mathcal{P}} \mathbf{V}_i \Sigma_i^{-\frac{1}{2}} \Sigma_i^{-\frac{1}{2}} \mathbf{U}_i^T \mathcal{L}_{\mathcal{Q}}^T = \mathcal{R}_{\mathcal{P}} (\mathbf{V}_i \Sigma_i^{-1} \mathbf{U}_i^T) \mathcal{L}_{\mathcal{Q}}^T = \mathcal{R}_{\mathcal{P}} (\mathbf{U}_i \Sigma_i^{-1} \mathbf{V}_i^T)^{-1} \mathcal{L}_{\mathcal{Q}}^T = \mathcal{R}_{\mathcal{P}} (\mathcal{L}_{\mathcal{Q}}^T \mathcal{R}_{\mathcal{P}})^{-1} \mathcal{L}_{\mathcal{Q}}^T = \mathcal{I} \end{aligned}$$

As a result, \mathcal{T}_L and \mathcal{T}_R are oblique projector to one another (see (2.12)). Now approximating $x(t)$ by $\mathcal{T}_L \mathcal{T}_R^T x(t)$ in (2.2), we obtain

$$\begin{aligned}\mathcal{E} \mathcal{T}_L \mathcal{T}_R^T \dot{x}(t) &\approx \mathcal{A} \mathcal{T}_L \mathcal{T}_R^T x(t) + \mathcal{B} u(t), \\ y(t) &\approx \mathcal{C} \mathcal{T}_L \mathcal{T}_R^T x(t) + \mathcal{D} u(t)\end{aligned}$$

By considering $\tilde{x}(t) = \mathcal{T}_R^T x(t)$, an error is defined as $err = \mathcal{E} \mathcal{T}_L \dot{\tilde{x}}(t) - \mathcal{A} \mathcal{T}_L \tilde{x}(t) - \mathcal{B} u(t)$ known as residual from what can be written as $\mathcal{T}_R^T err = 0$, i.e., each column of \mathcal{T}_R^T is perpendicular to err . Putting all these value together after pre-multiplication with \mathcal{T}_R^T , we can get the reduced order system (2.43) whose reduced system matrices can be generated from the Algorithm (4).

The corresponding time-restricted Lyapunov equations converted from (2.19a and 2.19b) centering around the reduced system matrices can be written as:

$$\tilde{\mathcal{A}} \tilde{\mathcal{P}} \tilde{\mathcal{E}}^T + \tilde{\mathcal{E}} \tilde{\mathcal{P}} \tilde{\mathcal{A}}^T + \tilde{\mathcal{B}} \tilde{\mathcal{B}}^T - \tilde{\mathcal{E}} e^{\tilde{\mathcal{E}}^{-1} \tilde{\mathcal{A}} t_f} \tilde{\mathcal{E}}^{-1} \tilde{\mathcal{B}} (\tilde{\mathcal{E}}^{-1} \tilde{\mathcal{B}})^T e^{(\tilde{\mathcal{E}}^{-1} \tilde{\mathcal{A}})^T t_f} \tilde{\mathcal{E}}^T = 0 \quad (2.49a)$$

$$\tilde{\mathcal{A}}^T \tilde{\mathcal{Q}} \tilde{\mathcal{E}} + \tilde{\mathcal{E}}^T \tilde{\mathcal{Q}} \tilde{\mathcal{A}} + \tilde{\mathcal{C}}^T \tilde{\mathcal{C}} - e^{(\tilde{\mathcal{E}}^{-1} \tilde{\mathcal{A}})^T t_f} \tilde{\mathcal{C}}^T \tilde{\mathcal{C}} \tilde{\mathcal{E}} e^{\tilde{\mathcal{E}}^{-1} \tilde{\mathcal{A}} t_f} = 0 \quad (2.49b)$$

where, $\tilde{\mathcal{P}} = \mathcal{T}_R^T \mathcal{P} \mathcal{T}_R$ and $\tilde{\mathcal{Q}} = \mathcal{T}_L^T \mathcal{Q} \mathcal{T}_L$. It is easily shown that

$$\begin{aligned}\tilde{\mathcal{P}} &= \mathcal{T}_R^T \mathcal{P} \mathcal{T}_R \\ &= \Sigma_i^{-\frac{1}{2}} \mathbf{U}_i^T (\mathcal{L}_{\mathcal{Q}}^T \mathcal{R}_{\mathcal{P}}) (\mathcal{R}_{\mathcal{P}}^T \mathcal{L}_{\mathcal{Q}}) \mathbf{U}_i \Sigma_i^{-\frac{1}{2}} \\ &= \Sigma_i^{-\frac{1}{2}} \mathbf{U}_i^T (\mathbf{U}_i \Sigma_i \mathbf{V}_i^T) (\mathbf{V}_i \Sigma_i^{-\frac{1}{2}} \mathbf{U}_i^T) \mathbf{U}_i \Sigma_i^{-\frac{1}{2}} \\ &= \Sigma_i^{-\frac{1}{2}} \Sigma_i^2 \Sigma_i^{-\frac{1}{2}} = \Sigma_i\end{aligned}$$

Similarly, $\tilde{\mathcal{Q}} = \mathcal{T}_L^T \mathcal{Q} \mathcal{T}_L = \Sigma_i$. Therefore, by definition (2.9), the transferred system (2.43) is fully balanced.

Following the same procedure, the reduced frequency-restricted Lyapunov equations can be written as from (2.33a and 2.33b):

$$\tilde{\mathcal{A}} \tilde{\mathcal{M}} \tilde{\mathcal{E}}^T + \tilde{\mathcal{E}} \tilde{\mathcal{M}} \tilde{\mathcal{A}}^T + \tilde{\mathcal{E}} \tilde{\phi}(i\omega) \tilde{\mathcal{B}} \tilde{\mathcal{B}}^T + \tilde{\mathcal{B}} \tilde{\mathcal{B}}^T \tilde{\phi}^*(i\omega) \tilde{\mathcal{E}}^T = 0 \quad (2.50a)$$

$$\tilde{\mathcal{A}}^T \tilde{\mathcal{N}} \tilde{\mathcal{E}} + \tilde{\mathcal{E}}^T \tilde{\mathcal{N}} \tilde{\mathcal{A}} + \tilde{\mathcal{E}}^T \tilde{\xi}^*(i\omega) \tilde{\mathcal{C}}^T \tilde{\mathcal{C}} + \tilde{\mathcal{C}}^T \tilde{\mathcal{C}} \tilde{\xi}(i\omega) \tilde{\mathcal{E}} = 0 \quad (2.50b)$$

where $\tilde{\mathcal{M}}$ and $\tilde{\mathcal{N}}$ are frequency-limited reduced Controllability and observability Gramians.

2.4.2 Interpolatory projection method

Rational tangential interpolation is another well-developed technique for model order reduction on infinite domain introduced in [72]. In this procedure, two oblique projectors \mathcal{W} and \mathcal{V} have to be computed in such a way that the reduced transfer function $\tilde{\mathcal{G}}(s)$ tangentially interpolates the original transfer function $\mathcal{G}(s)$ at a predefined set of interpolation points and some fixed tangential direction expressed as

$$\begin{aligned}\mathcal{G}(\theta_i) b_i &= \tilde{\mathcal{G}}(\theta_i) b_i, \quad c_i^T \mathcal{G}(\theta_i) = c_i^T \tilde{\mathcal{G}}(\theta_i), \quad \text{and} \\ c_i^T \mathcal{G}(\theta_i) b_i &= c_i^T \tilde{\mathcal{G}}(\theta_i) b_i \quad \text{for } i = 1, \dots, r\end{aligned}$$

Algorithm 5: Time-restricted IRKA**Input:** $\mathcal{E}, \mathcal{A}, \mathcal{B}, \mathcal{C}, t_f$, initial reduced matrices $\tilde{\mathcal{E}}, \tilde{\mathcal{A}}$ **Output:** Reduced order system matrices $\tilde{\mathcal{E}}, \tilde{\mathcal{A}}, \tilde{\mathcal{B}}, \tilde{\mathcal{C}}$

- 1 Compute low-rank observability factors $\mathcal{L}_{\mathcal{Q}}$ such that $\mathcal{Q} = \mathcal{L}_{\mathcal{Q}}\mathcal{L}_{\mathcal{Q}}^T$ by solving time-limited observability Lyapunov equation (2.19b).
- 2 Make an initial selection of the interpolation points $\{\theta_i\}_{i=1}^r$ and the tangential directions $\{b_i\}_{i=1}^r$.
- 3 Construct the right projector
- 4 $\mathcal{V} = [(\theta_1\mathcal{E} - \mathcal{A})^{-1}(\mathcal{B}b_1 - \mathcal{E}e^{\mathcal{E}^{-1}\mathcal{A}t_f}\mathcal{B}b_1e^{\tilde{\mathcal{E}}^{-1}\tilde{\mathcal{A}}t_f}\tilde{\mathcal{E}}^T), \dots, (\theta_r\mathcal{E} - \mathcal{A})^{-1}(\mathcal{B}b_r - \mathcal{E}e^{\mathcal{E}^{-1}\mathcal{A}t_f}\mathcal{B}b_re^{\tilde{\mathcal{E}}^{-1}\tilde{\mathcal{A}}t_f}\tilde{\mathcal{E}}^T)]$
- 5 And left projector $\mathcal{W} = \mathcal{L}_{\mathcal{Q}}(\mathcal{L}_{\mathcal{Q}}^T\mathcal{V})(\mathcal{V}^T\mathcal{L}_{\mathcal{Q}}\mathcal{L}_{\mathcal{Q}}^T\mathcal{V})^{-1}$
- 6 **while not converged do**
- 7 Construct

$$\tilde{\mathcal{E}} = \mathcal{W}^T\mathcal{E}\mathcal{V}, \tilde{\mathcal{A}} = \mathcal{W}^T\mathcal{A}\mathcal{V}, \tilde{\mathcal{B}} = \mathcal{W}^T\mathcal{B}, \tilde{\mathcal{C}} = \mathcal{C}\mathcal{V}$$
- 8 Compute $y_i^* \tilde{\mathcal{A}} = \tilde{\lambda}_i y_i^* \tilde{\mathcal{E}}$
- 9 $\theta_i \leftarrow -\lambda_i, b_i^* \leftarrow -y_i^* \tilde{\mathcal{B}}$ for $i = 1, \dots, r$
- 10 Compute \mathcal{V} and \mathcal{W} as above.
- 11 $i = i + 1$
- 12 $\tilde{\mathcal{E}} = \mathcal{W}^T\mathcal{E}\mathcal{V}, \tilde{\mathcal{A}} = \mathcal{W}^T\mathcal{A}\mathcal{V}, \tilde{\mathcal{B}} = \mathcal{W}^T\mathcal{B}, \tilde{\mathcal{C}} = \mathcal{C}\mathcal{V}.$

where $b_i \in \mathbb{C}^k$ and $C_i \in \mathbb{C}^l$ are respectively right and left tangential direction and correspond to interpolation points θ_i . The rational tangential interpolation is performed using these quantities. In [73], the Iterative Rational Krylov Algorithm (IRKA)-based projection methods has been discussed for model order reduction on infinite domains, where at each iteration both interpolation points and tangential directions have been updated until the reduced system satisfies the necessary condition for \mathcal{H}_2 -optimality.

However, in this thesis we update the algorithms with a view to reducing the model order on restricted time and frequency intervals. We modify the typical IRKA algorithm by combining the procedure discussed in [74] for preserving system's stability.

Algorithm (5) shows the step by step procedures to reduce the models on finite time intervals. The same algorithm can be applicable to find out the reduced order models on limited frequency intervals where the low-ranks observability factors $\mathcal{L}_{\mathcal{N}}$ can be computed by solving frequency-limited observability Lyapunov equation (2.33b) and the right projector can be computed as

$$\mathcal{V} = [(\theta_1\mathcal{E} - \mathcal{A})^{-1}(\mathcal{E}\phi(i\omega)\mathcal{B}b_1 + \mathcal{B}b_1\tilde{\phi}(i\omega)\tilde{\mathcal{E}}^T), \dots, (\theta_r\mathcal{E} - \mathcal{A})^{-1}(\mathcal{E}\phi(i\omega)\mathcal{B}b_r + \mathcal{B}b_r\tilde{\phi}(i\omega)\tilde{\mathcal{E}}^T)]$$

GENERATION OF DATA MODELS

Introduction

Analytical control theory largely depends on linear time-invariant state-space equation constructed based on mathematical data models. In this chapter, our discussion goes on the generation of mathematical data models from physical models. We develop two data models among which the physical model of one data model is based on fluid dynamics focusing on acoustic wave equation and another is developed considering electrical power system as its physical model. We also take some existing data models for our analysis purposes.

3.1 Piezoelectric Tonpilz Transducer

Piezoelectric Tonpilz (acoustic mushroom) Transducer has a great importance in naval science which is a certain type of underwater electro-acoustic transducer. It can effectively operate as either a sound projector or a hydrophone on or under the sea surface by high power sound emission [75]. Tonpilz transducers are used in sonar technique working based on sound propagation to navigate, communicate or detect objects on or under the surface of water. The transducer consists of piezoceramic rings stacked between massive ends and pre-stressed by a central bolt. The tail and head mass lower the resonance frequency of the device.

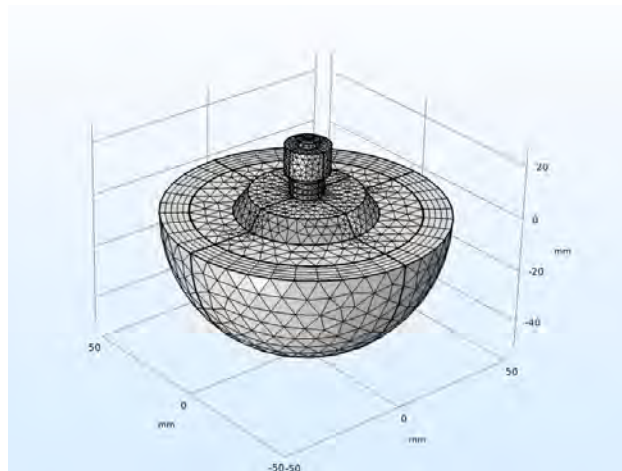


Figure 3.1: Mesh of Piezoelectric Tonpilz Transducer

We have constructed this physical model from the motivation of [76]. In this model, time domain interface of the acoustics module is used for the study. The model determines the radiated pressure field and sound pressure level. The model is developed considering the total circumstance as adiabatic, that means, it is not affected by the external temperature and it only transfers energy to the surrounding only at the time of working. The governing equations are derived from the acoustic wave equation.

The linear Euler's equation valid for acoustic processes of the small amplitude can be written as [77]

$$\rho_0 \frac{\partial u}{\partial t} = -\nabla p,$$

where, p is pressure, ρ_0 is initial density and u is fluid velocity. Taking divergence on the both side, we get

$$\nabla(\rho_0 \frac{\partial u}{\partial t}) = -\nabla^2 p, \quad (3.1)$$

From the equation of continuity of fluid, it can be written as:

$$\frac{\partial \rho}{\partial t} + \nabla(\rho u) = 0, \quad (3.2)$$

If ρ_0 is sufficiently weak function of time and assume the condensation s is very small, we can write $\rho = \rho_0 s$ and (3.2) becomes

$$\rho_0 \frac{\partial s}{\partial t} + \nabla(\rho_0 u) = 0,$$

Taking time derivative, we get-

$$\rho_0 \frac{\partial^2 s}{\partial t^2} + \nabla(\rho_0 \frac{\partial u}{\partial t}) = 0, \quad (3.3)$$

Combining, (3.1) and (3.3)

$$\nabla^2 p = \rho_0 \frac{\partial^2 s}{\partial t^2}, \quad (3.4)$$

For *adiabatic process*^{*}, the condensation s can be written with the help of the thermodynamic speed of sound c as $s = \frac{\rho_0 p}{c^2}$. Then from (3.4), we get-

$$\nabla^2 p = \frac{1}{c^2} \frac{\partial^2 p}{\partial t^2} \quad (3.5)$$

For convicting the sound field, a uniform constant volumetric force F_d needed to be added and for causing of pressure variations, a heat source F_h is also included which has the uniform strenght in all directions. Then (3.5) becomes

$$\frac{1}{\rho c^2} \frac{\partial^2 p}{\partial t^2} - \frac{1}{\rho} \nabla^2 p + \frac{1}{\rho} \nabla F_d - F_h = 0 \quad (3.6)$$

^{*}Adiabatic process is a type of thermodynamic process which occurs without transferring heat or mass between the system and its surroundings.

Since we consider the incompressible fluid domain like water, with unit outward normal \hat{n} , from the equation of continuity, we get-

$$\frac{\hat{n}}{\rho} \nabla p - \frac{\hat{n}}{\rho} F_d = 0. \quad (3.7)$$

Equations (3.6) and (3.7) are the two main governing equations of tonpilz transducer with initial condition $p(t_0, x_0) = 0$ and $\frac{\partial p}{\partial t}(t_0, x_0) = 0$, where t_0 is the initial time with initial position x_0 .

We have already known that the the relation between strain-stress of dielectric materials from Hook's law can be written as-

$$\epsilon = s\sigma$$

where, ϵ is strain, s is compliance under short circuit conditions and σ is stress what can be rewritten for elastic displacement u as-

$$\epsilon = \frac{\nabla u + u \nabla}{2} \quad (3.8)$$

The electric flux f can be written as-

$$f = \Xi \nabla \Phi \quad (3.9)$$

where, Ξ is permittivity and Φ is electric potential. Combining (3.8) and (3.9), we can write the Piezoelectric coupled equations as strain-charge form as [78]-

$$\sigma = \frac{C}{2} (\nabla u + u \nabla) + e^T \nabla \Phi \quad (3.10)$$

$$f = \frac{e}{2} (\nabla u + u \nabla) - T_d \nabla \Phi \quad (3.11)$$

where, C is elastic moduli, e is Piezoelectric tensor, T_d is dielectric tensor.

Equations (3.6), (3.7), (3.10), and (3.11) are four governing equations of Piezoelectric Tonpilz Transducer. Now considering all of the independent variables of these equations as a function of $k(t, x)$ and after *similarity transformation*[†], we can modify these equations as-

$$\left(\frac{1}{\rho c^2} k_t - \frac{1}{\rho} k_i\right) \ddot{p} + \left(\frac{1}{\rho c^2} k_{tt} - \frac{1}{\rho} k_{ii}\right) \dot{p} + \frac{1}{\rho} k_i \dot{F}_d + \frac{1}{\rho c^2} p = F_h \quad (3.12)$$

$$\frac{\hat{n}}{\rho} k_i \dot{p} - \frac{\hat{n}}{\rho} F_d = 0 \quad (3.13)$$

$$\frac{C}{2} k_i \dot{u} + \frac{C}{2} u \partial_i + e^T k_i \dot{\Phi} + e^T \Phi = \sigma \quad (3.14)$$

$$\frac{e}{2} k_i \dot{u} + \frac{e}{2} u \partial_i - T_d k_i \dot{\Phi} - T_d \Phi = f \quad (3.15)$$

[†]Similarity transformation is a mapping of a set by which each element in the set is mapped into a positive constant multiple of itself, the same constant being used for all elements.

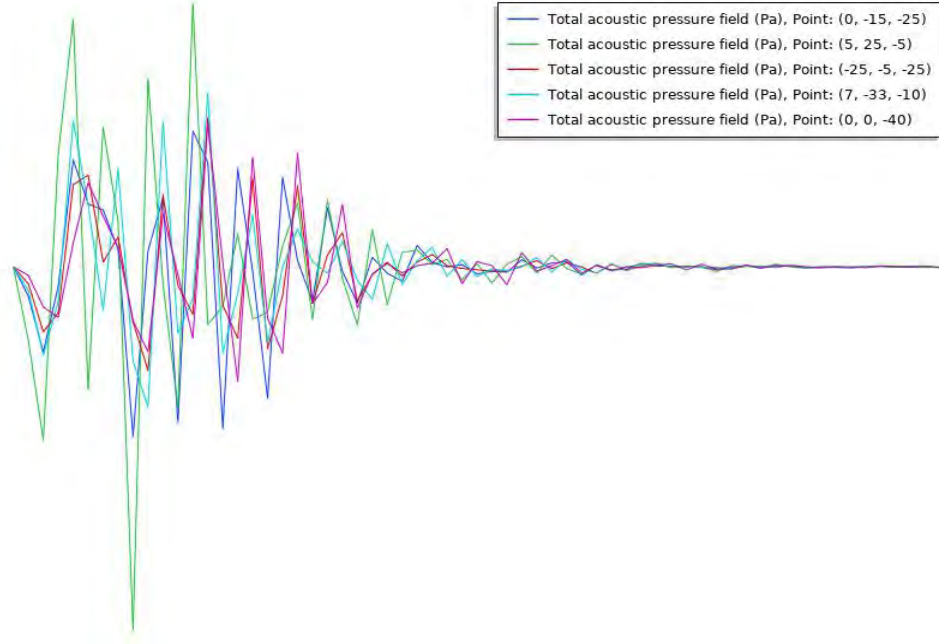


Figure 3.2: Acoustic field pressure on output Probe points Vs. Time [0-10 sec]

The above equations can be represented as state-space forms as

$$\begin{bmatrix} \frac{1}{\rho c^2} k_t - \frac{1}{\rho} k_i & 0 & 0 & 0 \\ 0 & 0 & 0 & 0 \\ 0 & 0 & 0 & 0 \\ 0 & 0 & 0 & 0 \end{bmatrix} \begin{bmatrix} \ddot{p} \\ \ddot{F}_d \\ \ddot{u} \\ \ddot{\Phi} \end{bmatrix} + \begin{bmatrix} \frac{1}{\rho c^2} k_{tt} - \frac{1}{\rho} k_{ii} & \frac{1}{\rho} k_i & 0 & 0 \\ \frac{\hat{n}}{\rho} k_i & 0 & 0 & 0 \\ 0 & 0 & \frac{C}{2} k_i & e^T k_i \\ 0 & 0 & \frac{e}{2} k_i & -T_d k_i \end{bmatrix} \begin{bmatrix} \dot{p} \\ \dot{F}_d \\ \dot{u} \\ \dot{\Phi} \end{bmatrix} + \begin{bmatrix} \frac{1}{\rho c^2} & 0 & 0 & 0 \\ 0 & -\frac{\hat{n}}{\rho} & 0 & 0 \\ 0 & 0 & \frac{C}{2} \partial_i & e^T \\ 0 & 0 & \frac{e}{2} \partial_i & -T_d \end{bmatrix} \begin{bmatrix} p \\ F_d \\ u \\ \Phi \end{bmatrix} = \begin{bmatrix} 1 \\ 0 \\ 1 \\ 1 \end{bmatrix} u \quad (3.16)$$

where $u := [F_h \ 0 \ \sigma \ f]^T$ is the input matrix of the system. Therefore, the output of this system can be written as-

$$y = \begin{bmatrix} 1 & 0 & 1 & 1 \end{bmatrix} \begin{bmatrix} p \\ F_d \\ u \\ \Phi \end{bmatrix} \quad (3.17)$$

Equations (3.16) and (3.17) are the state-space representation of the Piezoelectric Tonpilz transducer. Using simulation software, we have created the physical model of Piezoelectric Tonpilz transducer. Five output probe points have been taken for measuring the output response on the against of nine inputs.

$$\text{Considering, } \begin{bmatrix} p \\ F_d \\ u \\ \Phi \end{bmatrix} = x, \quad \begin{bmatrix} \frac{1}{\rho c^2} k_t - \frac{1}{\rho} k_i & 0 & 0 & 0 \\ 0 & 0 & 0 & 0 \\ 0 & 0 & 0 & 0 \\ 0 & 0 & 0 & 0 \end{bmatrix} = G, \quad \begin{bmatrix} \frac{1}{\rho c^2} & 0 & 0 & 0 \\ 0 & -\frac{\hat{n}}{\rho} & 0 & 0 \\ 0 & 0 & \frac{C}{2} \partial_i & e^T \\ 0 & 0 & \frac{e}{2} \partial_i & -T_d \end{bmatrix} = T,$$

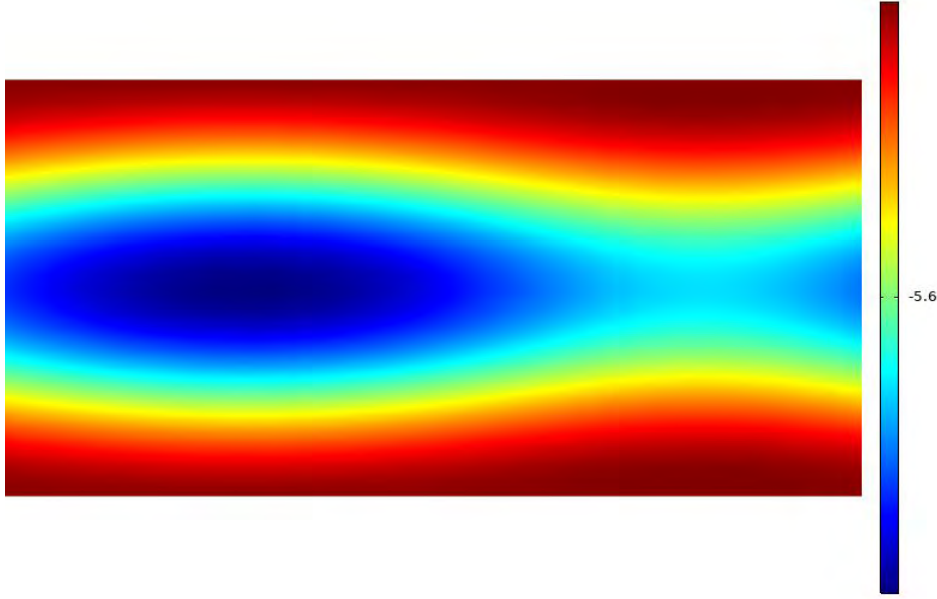


Figure 3.3: External field pressure

$$\begin{bmatrix} \frac{1}{\rho c^2} k_{tt} - \frac{1}{\rho} k_{ii} & \frac{1}{\rho} k_i & 0 & 0 \\ \frac{\hat{n}}{\rho} k_i & 0 & 0 & 0 \\ 0 & 0 & \frac{C}{2} k_i & e^T k_i \\ 0 & 0 & \frac{e}{2} k_i & -T_d k_i \end{bmatrix} = O, \quad \begin{bmatrix} 1 \\ 0 \\ 1 \\ 1 \end{bmatrix} = Z, \text{ we can rearrange Equation (3.16) as:}$$

$$G\ddot{x} + O\dot{x} + Tx = Zu. \quad (3.18)$$

Assuming, $x_2 = \dot{x}$ and $x_1 = x$, we can reform the above Equation (3.18) as

$$\underbrace{\begin{bmatrix} 0 & \mathcal{I} \\ G & O \end{bmatrix}}_{\mathcal{E}} \begin{bmatrix} \dot{x}_2 \\ \dot{x}_1 \end{bmatrix} = \underbrace{\begin{bmatrix} \mathcal{I} & 0 \\ 0 & -T \end{bmatrix}}_{\mathcal{A}} \begin{bmatrix} x_2 \\ x_1 \end{bmatrix} + \underbrace{\begin{bmatrix} 0 \\ Z \end{bmatrix}}_{\mathcal{B}} u \quad (3.19)$$

which is the first order form of the second order State equation (3.16). Considering, $\begin{bmatrix} 1 & 0 & 1 & 1 \end{bmatrix} = L$, we can rewrite the Output equation (3.17) as following:

$$y = \underbrace{\begin{bmatrix} 0 & L \end{bmatrix}}_{\mathcal{C}} \begin{bmatrix} x_2 \\ x_1 \end{bmatrix} \quad (3.20)$$

Equations (3.19) and (3.20) are the first order generalised state-space representation of the second order Piezoelectric Tonpiliz Transducer model.

The line graph (3.2) illustrates the acoustic field pressure on the selected output points on the certain segment of time. We have considered around 9200 degree of freedoms (DoFs) for giving a meshing structure of the model.

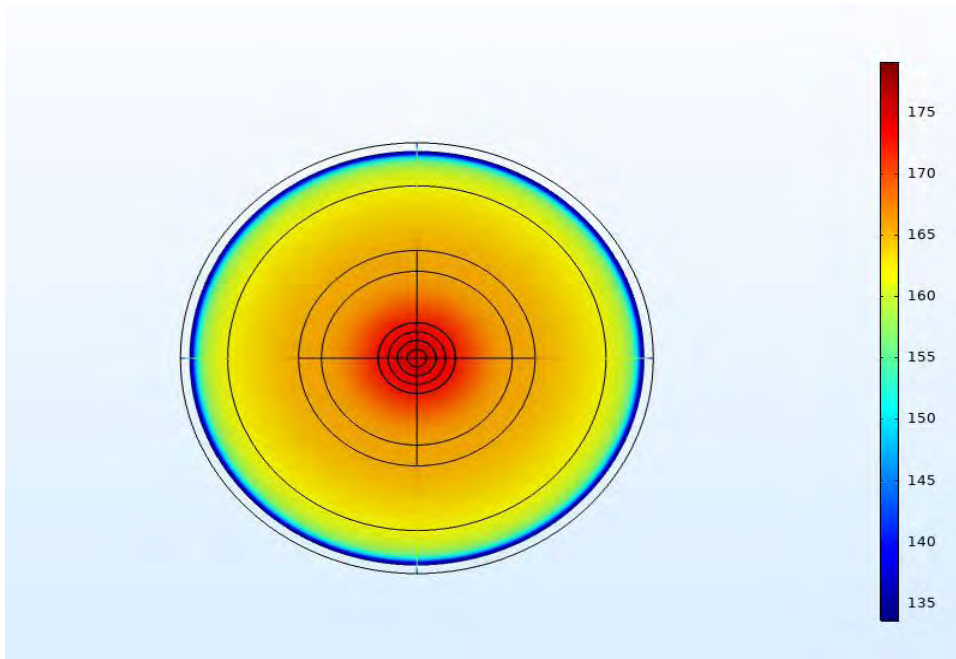


Figure 3.5: Sound pressure

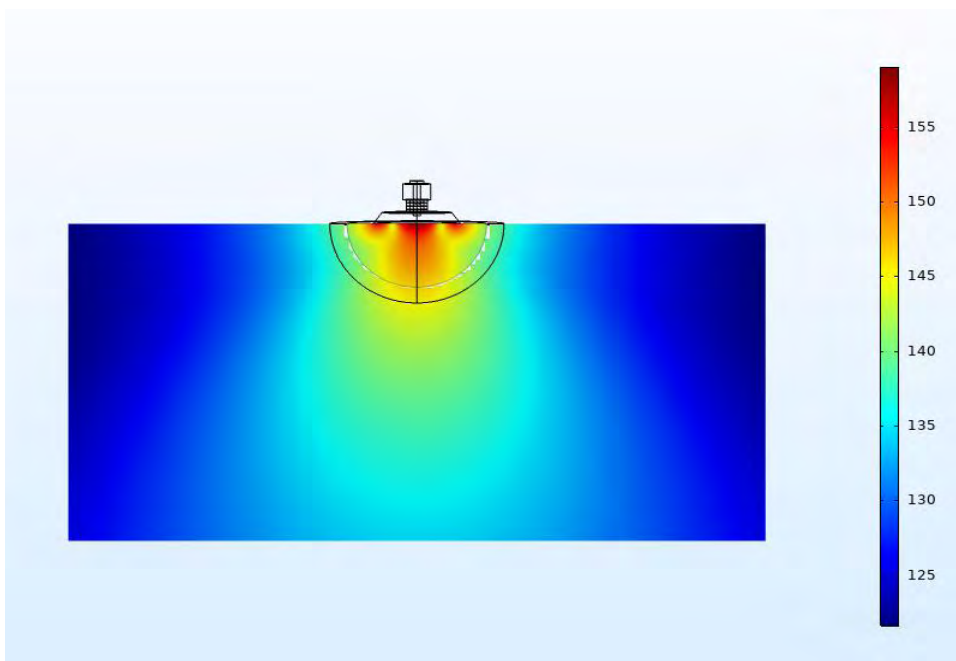


Figure 3.4: External fluid pressure

Table 3.1: Dimension of Piezoelectric Tonpilz transducer

Full	Differential	Algebraic	Input	Output
9140	3065	6075	9	5

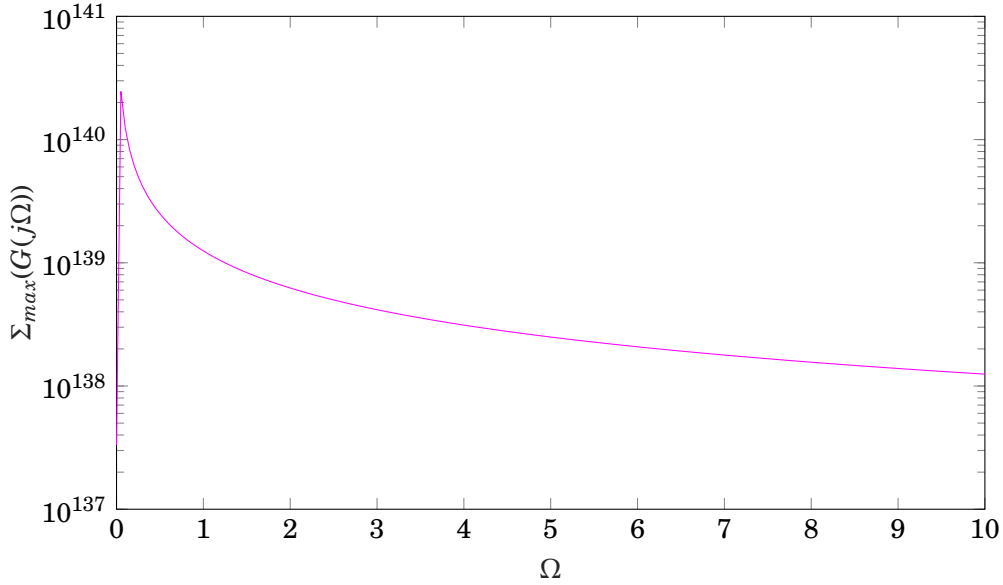


Figure 3.6: Transfer function of Piezoelectric Tonpilz transducer

After the compilation of the model and with the help of state-space equations (3.16) and (3.17), we can get a differential-algebraic state-space system having 9140 dimensional state matrix whose differential part is 3065 dimensional and algebraic part consists of 6075 dimension. The system is developed as a form of special kind of descriptor system which is known as second order index-I system. After conversion according to [2, 9], it can be formed as first order index-I descriptor system (2.10). The transfer function of the system using (2.9) is plotted as shown in the Figure (3.6).

3.2 Power system model

Electric power system model is one of the popular models in the field of model reduction what is widely used for analysis. However, we have also generated a power system model for our analytical purpose consisting of 84 buses. The data, used for generating the model, has been collected from [79]. The system is operated by 4.8 kV (kilo Volt), what is the actual operating voltage of California, USA [79]. The entire system is characterized by overhead and underground electric line. The voltage and current of this power grid is measured in Phasor Measurement Unit (PMU) whose base frequency is 60 Hz. The power load is generated with the help of constant current, impedance, on-load tap changer (OLTC) used for voltage regulation through the buses. We know from the Ohm's law that the relation among the impedance Z , voltage V and current I is

$$Z = \frac{V}{I} = \frac{i\omega LI}{I} = i\omega L, \quad (3.21)$$

where, L is inductance and ω is frequency. The voltage through the inductor with initial phase angle ϕ can be expressed as [80]

$$\begin{aligned}
 V_L &= (i\omega L)I \\
 &= \omega L e^{\frac{i\pi}{2}} I \phi \\
 &= \omega L I \cos(\omega t + \phi) \\
 &= L \frac{d}{dt}(I \sin(\omega t + \phi)) \\
 \therefore V_L &= L \frac{dI_L}{dt}
 \end{aligned} \tag{3.22}$$

Similarly, the current flow through the capacitor with capacitance C can be written as

$$\begin{aligned}
 \frac{V}{I_C} &= \frac{1}{i\omega C} \\
 I_C &= V i\omega C \\
 &= \omega C e^{\frac{i\pi}{2}} V \phi \\
 &= \omega C V \cos(\omega t + \phi) \\
 &= C \frac{d}{dt}(V \sin(\omega t + \phi)) \\
 &= C \frac{dV_C}{dt} \\
 \therefore \dot{V}_C &= \frac{1}{C} I_C
 \end{aligned} \tag{3.23}$$

From Kirchhoff's law, the entire voltage generations through the power system can be expressed as

$$\begin{aligned}
 V &= V_Z + V_L + V_C \\
 &= I_L Z + L \frac{dI_L}{dt} + V_C \\
 \therefore \dot{I}_L &= -\frac{1}{L} V_C - \frac{Z}{L} I + \frac{1}{L} V
 \end{aligned} \tag{3.24}$$

Combining (3.23) and (3.24), we get the state space equation as

$$\begin{bmatrix} \dot{V}_C \\ \dot{I}_L \end{bmatrix} = \begin{bmatrix} 0 & \frac{1}{C} \\ -\frac{1}{L} & -\frac{Z}{L} \end{bmatrix} \begin{bmatrix} V_C \\ I_L \end{bmatrix} + \begin{bmatrix} 0 \\ \frac{1}{L} \end{bmatrix} u, \tag{3.25}$$

where, $u = [V]^T$ is the input matrix of the system. The output of the power system can be written as

$$y = \begin{bmatrix} y_1 \\ y_2 \end{bmatrix} = \begin{bmatrix} \mathcal{I} & 0 \\ 0 & Z \end{bmatrix} \begin{bmatrix} V_C \\ I_L \end{bmatrix} \tag{3.26}$$

Equations (3.25) and (3.26) are the state-space representation of the electric power system.

The system is interconnected through three-phase four wire arrangement what is used star connected phase winding. The turning ratio of the voltage frequency is adjusted by On Load Tap Changer (OLTP) during operation while the frequent changing in the return ratio of transformer is utilized by Off Circuit Tap Changer (OCTC). Figure (3.9) represents the control diagram of the

Table 3.2: Dimension of Electric power system

Full	Differential	Algebraic	Input	Output
634	435	199	10	10

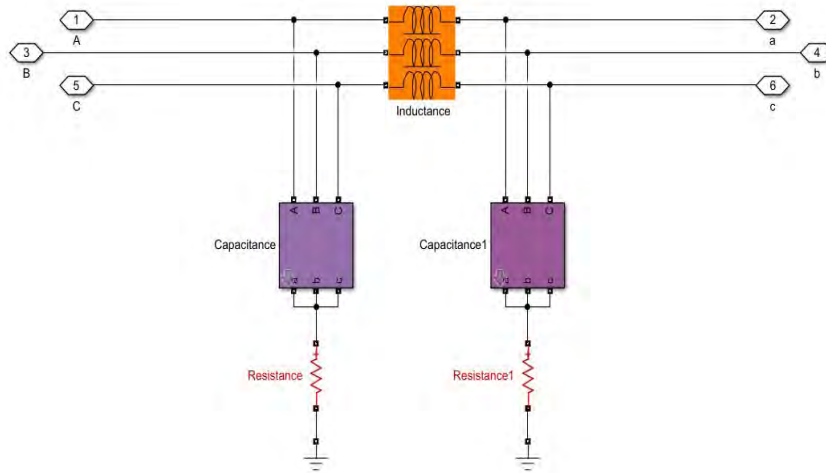


Figure 3.7: Distributed Line

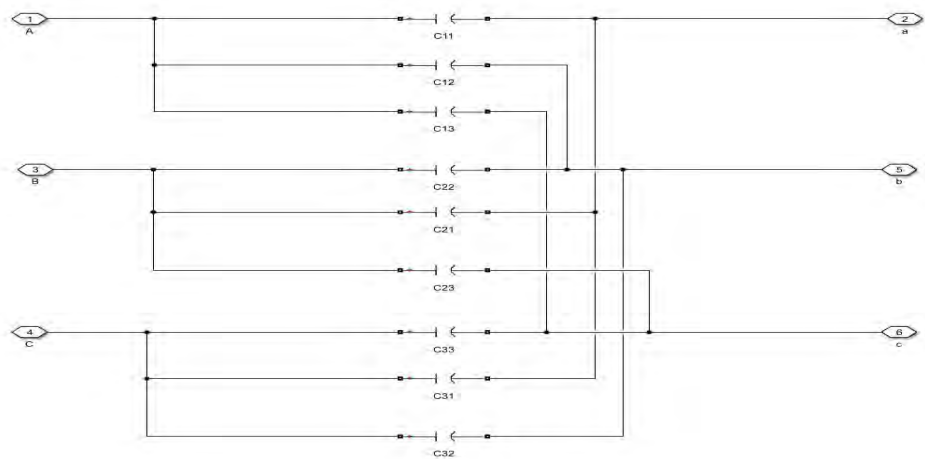


Figure 3.8: Capacitor

tap changer and Figure (3.10) illustrates the connection of the tap changers.

After the simulation of the power model and with the help of state-space equations (3.25) and (3.26), we can get a differential-algebraic state-space system having 634 dimensional state matrix whose differential part is 435 dimensional and algebraic part consists of 199 dimension. It is also structured as first order index-I descriptor system (2.10). The transfer function of the system using (2.9) is plotted as shown in the Figure (3.13).

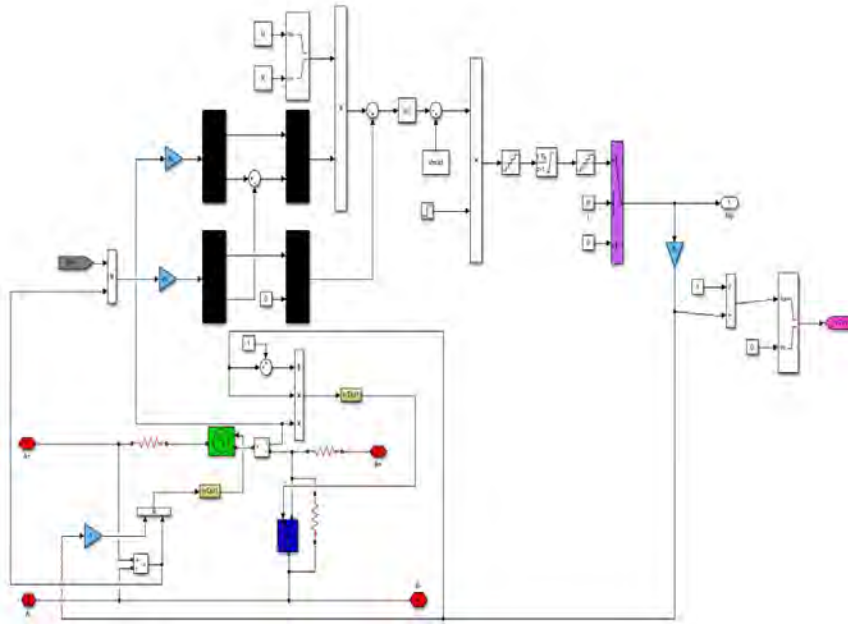


Figure 3.9: Control diagram of Tap Changer

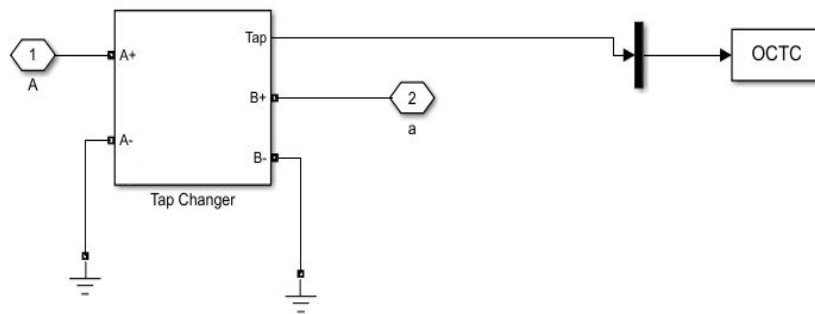


Figure 3.10: Connection of tap changer

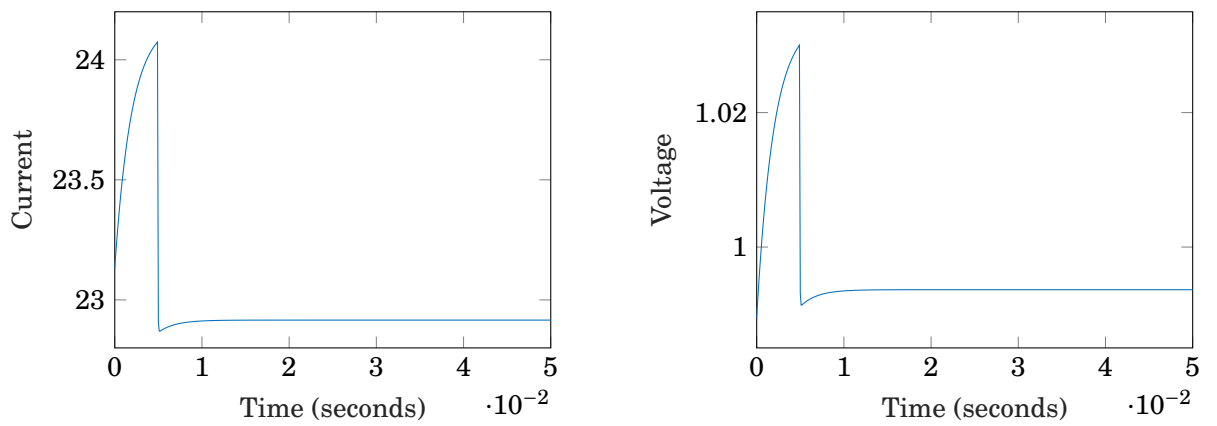


Figure 3.11: Current and Voltage Profile through single wire transmission line

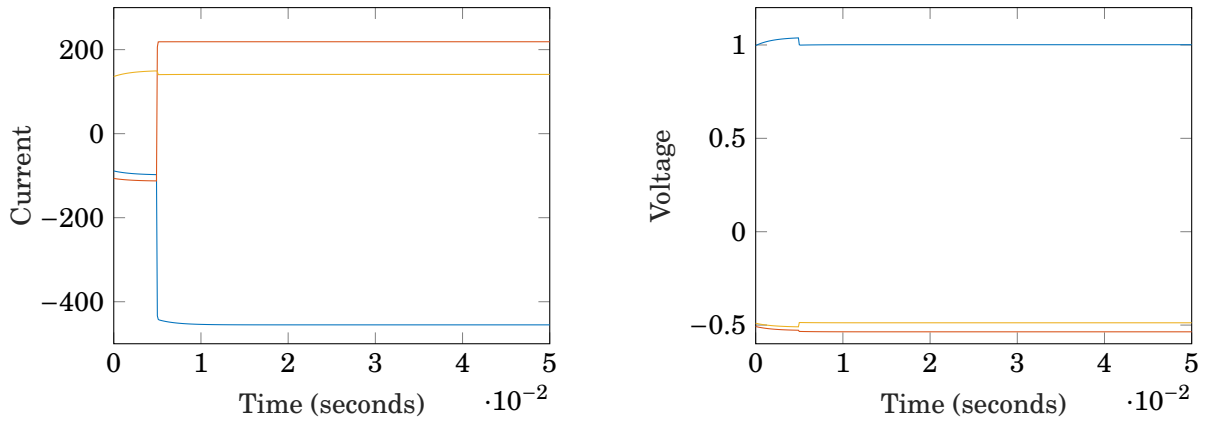


Figure 3.12: Current and Voltage Profile through triple wires transmission line

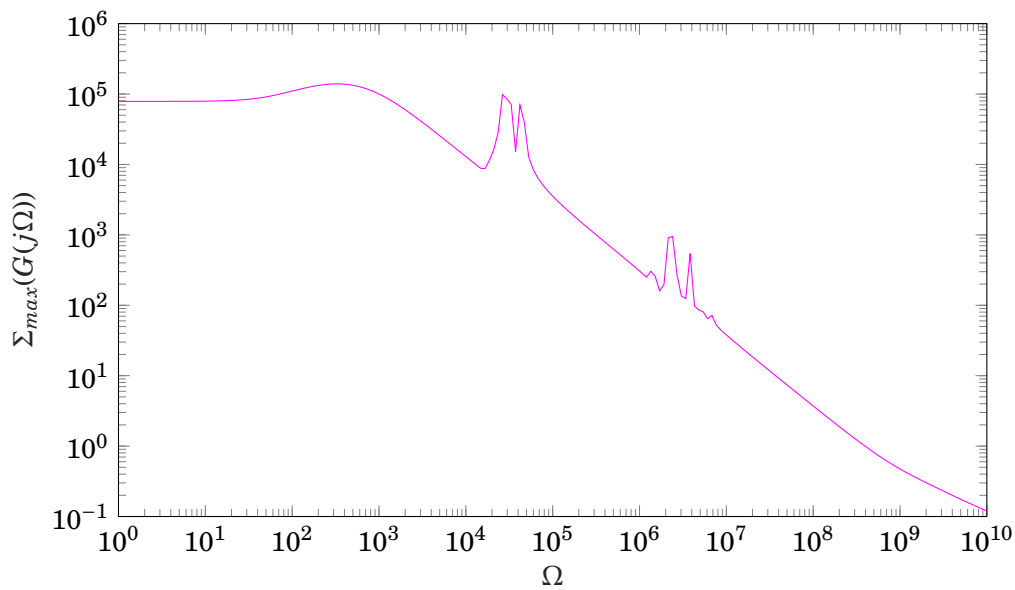


Figure 3.13: Transfer function of electric power system

3.3 Existing data models

We have also considered several existing data models for our analytical purpose besides the data models we have generated. All of the models are highly sparse and are structured as special kinds of descriptor systems.

3.3.1 Brazilian Interconnected Power Systems

The Brazilian Interconnected Power System (BIPS) models provides a number of differential-algebraic systems which have special kind of descriptor structures represented by (2.10).

Table 3.3: Dimension of Brazilian Interconnected Power System

Model	Full	Differential	Algebraic	Input	Output
BIPS-606	7135	606	6529	4	4
BIPS-1142	9735	1142	8593	4	4
BIPS-1693	13275	1693	11582	4	4

We have collected the data of three variants of BIPS models from [81] and Table (3.3) represents the dimensions of each model.

3.3.2 Oseen Model

Oseen model is a special type of data model governed by the stokes equation [82] written for incompressible fluid flow as

$$\begin{aligned} \frac{\partial v}{\partial t} &= \Delta v - \nabla p + f \\ \nabla v &= 0 \end{aligned} \tag{3.27}$$

with initial and boundary conditions

$$\begin{aligned} v(x, 0) &= v_0(x), \quad x \in \Omega \\ v(x, t) &= g(x, t), \quad (x, t) \in \partial\Omega \times (0, t_f), \end{aligned}$$

where, v is the velocity vector, p is fluid pressure, f is external force, Ω is a bounded open domain with boundary $\partial\Omega$ and t_f is the final time of time interval.

Table 3.4: Dimension of Oseen model

Full	Differential	Algebraic	Input	Output
7399	4900	2499	4	4

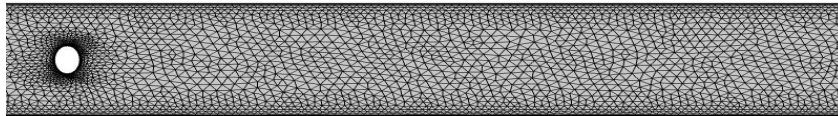


Figure 3.14: Mesh structure of simple channel flow



Figure 3.15: Velocity profile of simple channel flow

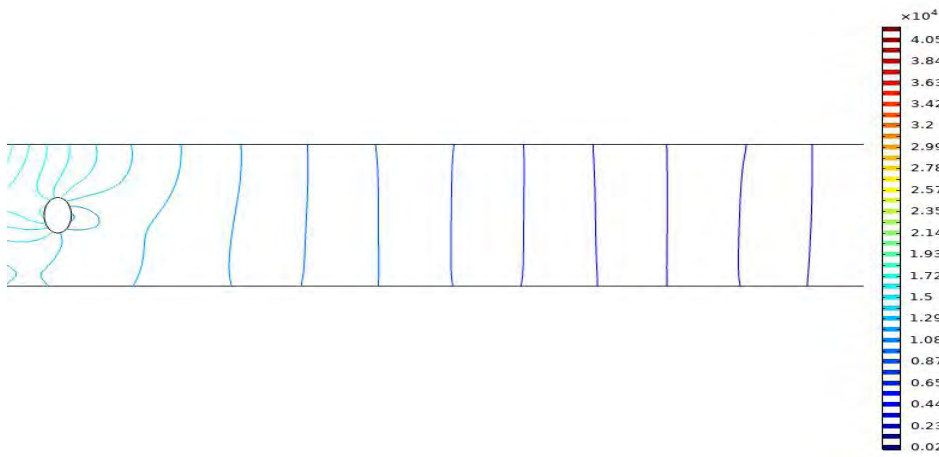


Figure 3.16: Pressure profile of simple channel flow

This model is similar with simple channel flow of incompressible fluid like water whose meshing structure can be represented by Figure (3.14). Figures (3.15) and (3.16) respectively represent velocity and pressure profiles of simple channel flow having initial velocity and pressure as zero with no slip boundary condition.

After the extraction of data model of oseen equation from physical model, we get a special type of descriptor system of the form (2.11) which is known as index-II descriptor system.

The analytical results of this thesis have been found after conducting thorough analysis using the above described data models.

SOLUTION OF LYAPUNOV EQUATIONS ON RESTRICTED TIME INTERVALS BY ITERATIVE METHOD

Introduction

One of the key operations for model order reduction is to compute the solution of the Lyapunov equation. Several works have been done through last few decades on the efficient computation of Lyapunov equation on infinite time domain [1, 2, 6, 7, 9, 11, 43]. But to cope with finding the solution of real-life oriented problems, it is more important to solve Lyapunov equation on restricted time interval rather than on infinite domain. Very few researches have been conducted on searching the solution of Lyapunov equation on finite time interval centering around dense small standard or generalised state-space systems [12, 38, 40] what are the previous topics of our discussion (see Section 2.3). But none of them discussed on the solution of the Lyapunov equations constructed on large-sparse dynamic system. In this chapter, we elaborately describe the efficient computation procedure of the low-rank solution of large-scale Lyapunov equations constructed around two special types of large-scale sparse descriptor systems of the form (2.10) and (2.11) known as index-I and index-II descriptor system respectively. For this purpose, we concentrate our attention on Rational Krylov Subspace Method (RKSM) [33, 34] because this method is computationally cheap and the convergence solution is quickly found. We rebuild the typical method for finding the Gramian of large-scale index-I and index-II descriptor systems on finite time interval. Since we deal with large-scale system, to increase the computational efficiency we compute low-rank solution factors instead of finding full-rank solution. We not only focus on the solution of Lyapunov equation on the time interval having initial point zero but our research is extended to the quest of the solution on time interval having non-homogeneous initial condition. We also inspect the procedure of computing matrix exponential inevitable part for solving time restricted Lyapunov equation by occupying less device's memory and requiring less computational time what increases the efficiency of the computational algorithms.

4.1 Rational Krylov Subspace Method

Rational Krylov Subspace Method (RKSM) was first proposed in [33] after the modification of Krylov subspace method (see Subsection 2.3.2.2). There, the author modified the Krylov subspace

$$\mathcal{K}_m(\mathcal{A}, \mathcal{B}) = \text{span}(\mathcal{B}, \mathcal{A}\mathcal{B}, \mathcal{A}^2\mathcal{B}, \dots, \mathcal{A}^{m-1}\mathcal{B})$$

by replacing with the rational function of \mathcal{A} written as

$$\mathcal{K}_m(\mathcal{A}, \mathcal{B}, \mu) = \text{span}((\mathcal{A} - \mu_1 \mathcal{I})^{-1} \mathcal{B}, (\mathcal{A} - \mu_2 \mathcal{I})^{-1} \mathcal{B}, \dots, (\mathcal{A} - \mu_{m-1} \mathcal{I})^{-1} \mathcal{B}),$$

where, $\{\mu_j\} \in \mathbb{C}$ is the set of shift parameters required for spectral transformation. If \mathcal{E} exists, the rational Krylov subspace will be reformed as

$$\begin{aligned} \mathcal{K}_m(\mathcal{E}, \mathcal{A}, \mathcal{B}, \mu) &= \text{span}((\mathcal{A} - \mu_1 \mathcal{E})^{-1} \mathcal{B}, (\mathcal{A} - \mu_2 \mathcal{E})^{-1} \mathcal{B}, \dots, (\mathcal{A} - \mu_{m-1} \mathcal{E})^{-1} \mathcal{B}) \\ &= \text{span}\left(\prod_{j=1}^m (\mathcal{A} - \mu_j \mathcal{E})^{-1} \mathcal{B}\right). \end{aligned}$$

We can compute the orthogonal basis \mathcal{V}_m of this subspace using Algorithm (2) in such a way that

$$\text{Range}(\mathcal{V}_m) = \text{span}\left(\prod_{j=1}^m (\mathcal{A} - \mu_j \mathcal{E})^{-1} \mathcal{B}\right)$$

Recalling the time restricted Lyapunov equation pairs on time interval $[0, t_f]$ (2.19)

$$\begin{aligned} \mathcal{A} \mathcal{P} \mathcal{E}^T + \mathcal{E} \mathcal{P} \mathcal{A}^T + \mathcal{B} \mathcal{B}^T - \mathcal{E} e^{\mathcal{E}^{-1} \mathcal{A} t_f} \mathcal{E}^{-1} \mathcal{B} (\mathcal{E}^{-1} \mathcal{B})^T e^{(\mathcal{E}^{-1} \mathcal{A})^T t_f} \mathcal{E}^T &= 0 \\ \mathcal{A}^T \mathcal{Q} \mathcal{E} + \mathcal{E}^T \mathcal{Q} \mathcal{A} + \mathcal{C}^T \mathcal{C} - e^{(\mathcal{E}^{-1} \mathcal{A})^T t_f} \mathcal{C}^T \mathcal{C} e^{\mathcal{E}^{-1} \mathcal{A} t_f} &= 0 \end{aligned}$$

centering around generalized state-space system (2.2)

$$\begin{aligned} \dot{x}(t) &= \mathcal{A}x(t) + \mathcal{B}u(t); \quad x(t_0) = x_0, \quad t \geq t_0, \\ y(t) &= \mathcal{C}x(t) + \mathcal{D}u(t) \end{aligned}$$

and applying the Galerkin condition on time restricted Controllability Lyapunov equation (2.19a), we can write

$$\begin{aligned} \mathcal{V}^T (\mathcal{A} \mathcal{P} \mathcal{E}^T + \mathcal{E} \mathcal{P} \mathcal{A}^T + \mathcal{B} \mathcal{B}^T - \mathcal{E} e^{\mathcal{E}^{-1} \mathcal{A} t_f} \mathcal{E}^{-1} \mathcal{B} (\mathcal{E}^{-1} \mathcal{B})^T e^{(\mathcal{E}^{-1} \mathcal{A})^T t_f} \mathcal{E}^T) \mathcal{V} &= 0 \\ (\mathcal{V}^T \mathcal{A} \mathcal{V}) (\mathcal{V}^T \mathcal{P} \mathcal{V}) (\mathcal{V}^T \mathcal{E} \mathcal{V})^T + (\mathcal{V}^T \mathcal{E} \mathcal{V}) (\mathcal{V}^T \mathcal{P} \mathcal{V}) (\mathcal{V}^T \mathcal{A} \mathcal{V})^T + (\mathcal{V}^T \mathcal{B}) (\mathcal{V}^T \mathcal{B})^T \\ - (\mathcal{V}^T \mathcal{E} \mathcal{V}) (\mathcal{V}^T e^{\mathcal{E}^{-1} \mathcal{A} t_f} \mathcal{V}) (\mathcal{V}^T \mathcal{E}^{-1} \mathcal{V} \mathcal{V}^T \mathcal{B}) (\mathcal{V}^T \mathcal{E}^{-1} \mathcal{V} \mathcal{V}^T \mathcal{B})^T (\mathcal{V}^T e^{\mathcal{E}^{-1} \mathcal{A} t_f} \mathcal{V})^T (\mathcal{V}^T \mathcal{E} \mathcal{V})^T &= 0 \end{aligned}$$

Considering $\tilde{\mathcal{P}} = \mathcal{V}^T \mathcal{P} \mathcal{V}$, $\tilde{\mathcal{E}} = \mathcal{V}^T \mathcal{E} \mathcal{V}$, $\tilde{\mathcal{A}} = \mathcal{V}^T \mathcal{A} \mathcal{V}$, $\tilde{\mathcal{B}} = \mathcal{V}^T \mathcal{B}$, the projected controllability Lyapunov equation from Equation (2.19a) can be written as

$$\tilde{\mathcal{A}} \tilde{\mathcal{P}} \tilde{\mathcal{E}}^T + \tilde{\mathcal{E}} \tilde{\mathcal{P}} \tilde{\mathcal{A}}^T + \tilde{\mathcal{B}} \tilde{\mathcal{B}}^T - \tilde{\mathcal{E}} e^{\tilde{\mathcal{E}}^{-1} \tilde{\mathcal{A}} t_f} \tilde{\mathcal{E}}^{-1} \tilde{\mathcal{B}} (\tilde{\mathcal{E}}^{-1} \tilde{\mathcal{B}})^T e^{(\tilde{\mathcal{E}}^{-1} \tilde{\mathcal{A}})^T t_f} \tilde{\mathcal{E}}^T = 0 \quad (4.1)$$

Similarly, considering $\tilde{\mathcal{C}} = \mathcal{C} \mathcal{V}$, the projected observability Lyapunov equation from Equation (2.19b) can be expressed as

$$\tilde{\mathcal{A}}^T \tilde{\mathcal{Q}} \tilde{\mathcal{E}} + \tilde{\mathcal{E}}^T \tilde{\mathcal{Q}} \tilde{\mathcal{A}} + \tilde{\mathcal{C}}^T \tilde{\mathcal{C}} - \tilde{\mathcal{E}} e^{(\tilde{\mathcal{E}}^{-1} \tilde{\mathcal{A}})^T t_f} \tilde{\mathcal{C}}^T \tilde{\mathcal{C}} e^{\tilde{\mathcal{E}}^{-1} \tilde{\mathcal{A}} t_f} = 0 \quad (4.2)$$

Since Equation (4.1) is projected small-scale equation, it can be solved by any direct solver method described in section (2.3.1). Due to the instability difficulty, the controllability Gramian becomes negative definite and we do not perform Cholesky factorization of $\tilde{\mathcal{P}}$. Instead of that, we perform eigenvalue decomposition (4.3) so that

$$\tilde{\mathcal{P}} = (\mathbf{V} \Lambda^{\frac{1}{2}}) (\mathbf{V} \Lambda^{\frac{1}{2}})^T$$

Algorithm 6: RKSM for solving time-restricted controllability Gramian (2.19a) of generalised system (2.2) on time interval $[0, t_f]$.

Input: $\mathcal{E}, \mathcal{A}, \mathcal{B}$, m_{it} (no. of iteration), t_f (endpoint of time interval), $0 < tol \ll 1$ (tolerance value), μ_1 (initial shift parameter).

Output: $\mathcal{R}_{\mathcal{P}} \in \mathbb{R}^{n \times z}$ such that $\mathcal{R}_{\mathcal{P}} \mathcal{R}_{\mathcal{P}}^T \approx \mathcal{P}$, where $z \ll n$.

1 set initial basis vector $v_1 = (\mathcal{A} - \mu_1 \mathcal{E})^{-1} \mathcal{B}$, $\mathcal{V}_1 = \frac{v}{\|v\|}$

2 **while** $j \leq m_{it}$ **do**

3 Find the next basis matrix by solving linear system $(\mathcal{A} - \mu_j \mathcal{E}) v_{j+1} = \mathcal{V}_j$.

4 Construct orthonormal vector set $\mathcal{V}_{j+1} = [\mathcal{V}_j, v_{j+1}]$ by QR decomposition (see Subsection (2.2.3.3)) using Algorithm (2).

5 Solve the projected controllability Lyapunov equation (4.1)

$$6 \quad \tilde{\mathcal{A}}_{j+1} \tilde{\mathcal{P}} \tilde{\mathcal{E}}_{j+1}^T + \tilde{\mathcal{E}}_{j+1} \tilde{\mathcal{P}} \tilde{\mathcal{A}}_{j+1}^T + \tilde{\mathcal{B}}_{j+1} \tilde{\mathcal{B}}_{j+1}^T - \tilde{\mathcal{E}}_{j+1} e^{\tilde{\mathcal{E}}_{j+1}^{-1} \tilde{\mathcal{A}}_{j+1} t_f} \tilde{\mathcal{E}}_{j+1}^{-1} \tilde{\mathcal{B}}_{j+1} (\tilde{\mathcal{E}}_{j+1}^{-1} \tilde{\mathcal{B}}_{j+1})^T e^{(\tilde{\mathcal{E}}_{j+1}^{-1} \tilde{\mathcal{A}}_{j+1})^T t_f} \tilde{\mathcal{E}}_{j+1}^T = 0$$

for finding small-scale CG \tilde{P} Where, $\tilde{\mathcal{E}}_{j+1} = \mathcal{V}_{j+1}^T \mathcal{E} \mathcal{V}_{j+1}$, $\tilde{\mathcal{A}}_{j+1} = \mathcal{V}_{j+1}^T \mathcal{A} \mathcal{V}_{j+1}$,
 $\tilde{\mathcal{B}}_{j+1} = \mathcal{V}_{j+1}^T \mathcal{B}$

7 Compute next shift parameter μ (see Section (4.2))

8 Compute residual norm (see Section (4.4))

9 **if** residual norm $\leq tol$ **then**

10 | Stop Rational Krylov iteration.

11 Operate eigenvalue decomposition

$$\tilde{\mathcal{P}} = \begin{bmatrix} \mathbf{V}_1 & \mathbf{V}_2 \end{bmatrix} \begin{bmatrix} \Lambda_1 & \\ & \Lambda_2 \end{bmatrix} \begin{bmatrix} \mathbf{V}_1 & \mathbf{V}_2 \end{bmatrix}^T \quad (4.3)$$

12 Establish low-rank controllability Gramian factor

$$\mathcal{R}_{\mathcal{P}} = \mathcal{V}_{j+1} \mathbf{V}_1 \Lambda_1^{\frac{1}{2}} \quad (4.4)$$

after truncating less effective eigenvalues Λ_2 .

Conducting Gaussian back substitution, the original controllability Gramian can be retrieved as

$$\mathcal{P} = \mathcal{V} \tilde{\mathcal{P}} \mathcal{V}^T$$

Combining the above two expression, we can write as

$$\begin{aligned} \mathcal{P} &= (\mathcal{V} \mathbf{V} \Lambda^{\frac{1}{2}}) (\mathbf{V} \Lambda^{\frac{1}{2}} \mathcal{V})^T \\ &= \mathcal{R}_{\mathcal{P}} \mathcal{R}_{\mathcal{P}}^T, \end{aligned}$$

where, $\mathcal{R}_{\mathcal{P}} = \mathcal{V} \mathbf{V} \Lambda^{\frac{1}{2}}$, is low-rank controllability Gramian factor. For increasing the more efficiency of the computation, we can eliminate the negligible eigenvalues and their corresponding eigenvectors. Algorithm (6) summarises the entire procedure of computing the low-rank solution factor of the controllability Lyapunov equation centering around generalised system.

Similarly, by taking the transpose of the system matrices, we can compute the low-rank observability Gramian factor $\mathcal{L}_{\mathcal{Q}}$ by solving projected observability Lyapunov equation (4.2) such that $\mathcal{Q} = \mathcal{L}_{\mathcal{Q}} \mathcal{L}_{\mathcal{Q}}^T$ using the same Algorithm (6).

4.2 Selection of Shift Parameter

Shift parameter selection is one of the vital parts in RKSM method. Without proper selection of shift parameter, it is impossible to find out convergent solution on nominated time interval. So a vast research has been conducted on this topic. However, which procedure we have followed partially in this thesis for finding shift parameter has been proposed in [83] known as optimized RKSM shift parameter. The shift parameter sequences have been calculated by rational function [34, 83]

$$\mathcal{B} - (\mathcal{A} - \mu\mathcal{E})\mathcal{V}_m(C_p - \mu\mathcal{E})^{-1}\mathcal{V}_m^T\mathcal{B} = \frac{f_m(\mathcal{E}, \mathcal{A})\mathcal{B}}{f_m(\mu)},$$

$$f_m(z) = \prod_{j=1}^m \frac{z - \lambda_j}{z + \mu_j},$$

where, λ_j and μ_j are the interpolating points. It has been observed in [34] that the characteristic polynomial of C_p minimizes $\|p(\mathcal{E}, \mathcal{A})\mathcal{V}\|$ among all monic polynomial of degree m , so that the numerator of $f_m(z)$ satisfies

$$\|f_m(\mathcal{E}, \mathcal{A})\mathcal{B}\| = \min_{\lambda_1, \dots, \lambda_m} \left\| \prod_{j=1}^m (\mathcal{A} - \lambda_j\mathcal{E})(\mathcal{A} - \mu_j\mathcal{E})^{-1}\mathcal{B} \right\|.$$

With this result, it was proposed in [84] that the next shift μ_{m+1} can be selected for symmetric matrix as

$$\mu_{m+1} = \arg \left(\max_{\mu \in [-\lambda_{max}, -\lambda_{min}]} \frac{1}{|f_m(\mu)|} \right),$$

where, $[\lambda_{min}, \lambda_{max}]$ is an estimated of $(\mathcal{E}, \mathcal{A})$'s spectral interval. During working with non-symmetric matrix, the interpolating points λ_j and μ_j are nominated on complex plane and the next shift can be selected as

$$\mu_{m+1} = \arg \left(\max_{\mu \in \partial\Lambda_m} \frac{1}{|f_m(\mu)|} \right),$$

where, $\Lambda_m \subset \mathbb{C}$ is the mirrored spectral region of $(\mathcal{E}, \mathcal{A})$ and $\partial\Lambda_m$ is its border. It has been narrated in [6] that Krylov based method like RKSM may be accurate at local level only. As a result, with a view to finding global convergences, in [83], Equi-Distributed Sequences (EDS) of shift parameters were computed by the classical Zolotaryov solution what were generated with some probability densities corresponding to the equilibrium charge distribution of the condenser with positive and negative plates $[-\lambda_{max}, -\lambda_{min}]$ and $[\lambda_{min}, \lambda_{max}]$ respectively.

For dealing with both symmetric and non-symmetric cases, according to [34] we calculate the shift parameters in an iterative manner by maximizing $\frac{1}{|f_m(\mu)|}$ over certain spectral interval, where the zeros of f_m are rational Ritz values while the poles of f_m are the previously computed shifts.

4.3 Computation of Matrix Exponential

Computation of matrix exponential is one of the key operations and most probably the main challenging part in computing the solution of time restricted Lyapunov equation. Although

Algorithm 7: Computation of Matrix Exponential.

Input: $\mathcal{A}_s = (\mathcal{E}^{-1}\mathcal{A})t_f$ (t_f endpoint of time interval), $0 < nztol \ll 1$ (Non-zero tolerance value), $0 < stol \ll 1$ (sparsity tolerance value), $0 < Ctol \ll 1$ (Convergence value), \mathcal{I} (Identity matrix having size of (\mathcal{A}_s)).

Output: $\text{ExpM} = e^{\mathcal{A}_s}$.

- 1 $Cc = 1$ (Flag for Convergence check)
- 2 $sf = 2^{\text{ceil}(\log_2(\|\mathcal{A}_s\|))}$ (Scaling factor)
- 3 $\mathcal{A}_s = sf \mathcal{A}_s$
- 4 $\mathcal{A}_s = nztol(\text{round}(\frac{1}{nztol}))\mathcal{A}_s$
- 5 $\text{ExpM} = \mathcal{I}$; $nT = \mathcal{I}$
- 6 $Rn = \frac{\text{No. of Non-Zero Element}}{\text{No. of total element}}$
- 7 **if** $Rn > stol$ **then**
- 8 | $\text{ExpM} = \mathbf{V}e^{\mathbf{J}}\mathbf{V}^T$ by eigenvalue decomposition
- 9 **else**
- 10 | $i = 1$
- 11 | **while** $Cc > Ctol$ **do**
- 12 | | $nT = \frac{1}{i}\mathcal{A}_s nT$
- 13 | | $nT = nztol(\text{round}(\frac{1}{nztol})nT)$
- 14 | | $Cc = \|nT\|$
- 15 | | $\text{ExpM} = \text{ExpM} + nT$
- 16 | | $i = i + 1$
- 17 | $\text{ExpM} = nztol(\text{round}(\frac{1}{nztol})\text{ExpM})$
- 18 | $\text{ExpM} = (\text{ExpM})^2$

by eigenvalue decomposition, the exponent of small dense matrix can easily be computed (see Subsubsection (2.2.4.1)), it is impossible to calculate matrix exponential of large sparse matrix by eigenvalue decomposition due to time and memory limitation. As a result, there are different kinds of algorithm been developed around last decades for finding the convergence result of matrix computation. In [85, 86] Krylov subspace based algorithm have been developed for computing matrix exponential. On the other hand, the scaling and squaring method, what is vastly used in computing exponential, is described elaborately in [87]. There, the author established an explicit relation of exponential of matrix \mathcal{A}_s as

$$e^{\mathcal{A}_s} = e^{\frac{\mathcal{A}_s}{\sigma}} \sigma,$$

where, $e^{\mathcal{A}_s}$ was approximated near the origin by Padé approximation $r_{km}(x)$ and σ was chosen as integral power of 2, i.e. $\sigma = 2^i$. $r_{km}(x)$ can be calculated as $r_{km}(x) = \frac{P_{km}(x)}{Q_{km}(x)}$, where,

$$P_{km}(x) = \sum_{j=0}^k \frac{(k+m-j)!k!}{(k+m)!(k-j)!j!} x^j, \quad Q_{km}(x) = \sum_{j=0}^m \frac{(k+m-j)!m!}{(k+m)!(m-j)!j!} (-x)^j$$

Then, the author showed that $r_{mk}(2^{-i}\mathcal{A}_s)^{2^i} = e^{\mathcal{A}_s}$ and the scaling factor can be determined by $i = \log_2 \frac{\|\mathcal{A}_s\|}{\theta_m}$ if $\|\mathcal{A}_s\| \geq \theta_m$ and zero otherwise, where $\theta_m := \left\| 2^{-i} r_m \right\|$.

On the contrary, in [41], the traditional Taylor series expansion (see Subsubsection (2.2.4.2)) at origin was considered for calculating the matrix exponential by scaling and squaring method. There, the authors reduced the calculation of the scaling factor by ceiling the operation by taking the maximum values of $2^{\log_2(\|\mathcal{A}_s\|)}$ and neglected the higher-order Taylor polynomial. In

Table 4.1: Computational time of Matrix Exponential

Model	$nztol$	T1	T2	Norm
BIPS-606	1×10^{-10}	5.799	0.867	5.215
	1×10^{-16}	6.50	1.028	5.04×10^{-6}
	1×10^{-20}	8.78	1.062	5.74×10^{-8}
	1×10^{-25}	9.27	1.85	8.35×10^{-8}
	1×10^{-30}	10.25	2.05	1.27×10^{-10}
BIPS-1142	1×10^{-10}	35.35	3.098	2935.28
	1×10^{-16}	36.50	3.7801	0.0044
	1×10^{-20}	38.28	3.895	3.69×10^{-5}
	1×10^{-25}	39.27	4.09	3.00×10^{-7}
	1×10^{-30}	40.95	4.27	4.07×10^{-9}
BIPS-1693	1×10^{-10}	89.54	8.9299	2807.60
	1×10^{-16}	90.20	11.33	0.0015
	1×10^{-20}	91.05	12.01	3.45×10^{-5}
	1×10^{-25}	91.95	12.97	2.71×10^{-6}
	1×10^{-30}	92.75	13.10	3.27×10^{-8}
Piezo Tonpilz	1×10^{-10}	76.299	5.15	1596.28
	1×10^{-16}	77.50	6.86	1.1×10^{-2}
	1×10^{-20}	78.28	6.94	8.52×10^{-10}
	1×10^{-25}	79.001	8.71	7.96×10^{-14}
	1×10^{-30}	79.80	9.125	7.82×10^{-15}

this thesis, we modify their proposed algorithm. In order to speed up the calculation, we use three types of tolerance values and combine eigenvalue decomposition for the dense matrix exponential computation. As a result, this algorithm easily switches to any mode of operation based on the nature of matrix and may reduce the unnecessary computational time. Another good reason to choose this algorithm is that this algorithm is highly customizable and users can increase the computational speed based on size and sparsity ratio of the given matrix. Algorithm (7) shows the entire computational procedure of matrix exponential. In line (6), we compute sparsity ratio to classify the input matrix by its nature and will calculate the matrix exponent by eigenvalue decomposition if the matrix is dense without going through Taylor series iterative process. Therefore, it may reduce time if the matrix is dense. We set the sparsity ratio as 3 : 1 for mode switching to get good result what can be changed in accordance of the sparsity pattern of the system matrices. In addition, we do rounding up the non-zero entities of the input matrix to their nearer mantissa values plugging in the tolerance values what increases the calculation speed by rounding the negligible parts. We generally consider the standard machine precision (10^{-16}) as common tolerance value with a view to getting desirable result what may vary based on the sparsity of the input matrices. However, it is noted that with the increment of the tolerance values, the requirement of the computational time is also increased. Table (4.1) illustrates the comparison between the traditional methods what are basically used by typical simulation software and our proposed algorithm. The tolerance values, we considered, for testing purposes are included in column $nztol$. T1 column shows the required time by the traditional methods and T2 column represents the time required by our proposed algorithm for calculating matrix exponential what clearly indicates that the algorithm, we proposed, successfully boosts up the entire computation.

It is also observed from the *Norm* column that the computational accuracy of our proposed algorithm is gradually upgraded with the minimal increment of time requirement. As a result, the proposed algorithm becomes more efficient comparing with the existing algorithm.

4.4 Calculating Residual Norm

Calculating residual norm is the prime analytical step of any iterative algorithm like (6) for checking the convergence rate of the iterative solution at every stage compared with the original solution as $\|\mathcal{P} - \tilde{\mathcal{P}}\|$. Among different types of norm calculation methods, it has been observed in [25, 34] that Frobenius norm measurement is appropriate in RKSM method. In this section, we modify that norm calculation for the computation on finite time interval $[0, t_f]$ written as

$$\frac{\|\mathbf{R}(\tilde{\mathcal{P}})\|_F}{\|\mathcal{B}_t \mathcal{B}_t^T\|_F + \|\mathcal{A}\|_F \|\mathcal{P}\|_F \|\mathcal{E}\|_F},$$

where, $\|\cdot\|_F$ denotes Frobenius norm, the residual at m_{it} th iteration step is

$$\mathbf{R}(\tilde{\mathcal{P}}) = \mathcal{A} \mathcal{R}_{\mathcal{P}} \mathcal{R}_{\mathcal{P}}^T \mathcal{E}^T + \mathcal{E} \mathcal{R}_{\mathcal{P}} \mathcal{R}_{\mathcal{P}}^T \mathcal{A}^T + \mathcal{B}_t \mathcal{B}_t^T,$$

where,

$$\mathcal{B}_t \mathcal{B}_t^T = \mathcal{B} \mathcal{B}^T - \mathcal{E} e^{(\mathcal{E}^{-1} \mathcal{A}) t_f} (\mathcal{E}^{-1} \mathcal{B}) (\mathcal{E}^{-1} \mathcal{B})^T e^{(\mathcal{E}^{-1} \mathcal{A})^T t_f} \mathcal{E}^T.$$

However, the computation of the norm of approximate solution $\tilde{\mathcal{P}}$ is expensive if the system matrices are large in dimension. Hence, in order to compute the residual norm cheaply, we follow the below observation enclosed in [34].

Theorem 4.1. *Let, \mathcal{V}_m be the orthogonal basis of the Rational Krylov Subspace \mathcal{K}_m and $\mathcal{P} = \mathcal{V}_m \tilde{\mathcal{P}} \mathcal{V}_m^T$ be the solution of the time restricted Lyapunov equation (2.19a). Then the residual \mathbf{R}_m can be computed as*

$$\|\mathbf{R}_m\|_F = \|S J S^T\|_F, \quad J = \begin{bmatrix} 0 & 1 & 0 \\ 1 & 0 & 1 \\ 0 & 1 & 0 \end{bmatrix},$$

where, S is the upper triangular matrix in the QR factorization of

$$\mathbf{U} = \left[v_{m+1} \mu_{m+1}, \mathcal{E} \mathcal{V} \mathcal{P} \mathcal{H}_m^{-T} e_m h_{m+1,m} - (\mathcal{I} - \mathcal{V}_m \mathcal{V}_m^T) \mathcal{A} v_{m+1} \right],$$

where, \mathcal{H}_m is a block upper Hessenberg matrix and e_m be the matrix formed by the last p columns of $m p \times m p$ identity matrix.

Proof. The proof can be found in [11, 34]. ■

4.5 Formulation and Solution of Time Restricted Index-I Descriptor System

Descriptor system (see Subsection (2.1.4)) is special type of dynamic system having the determinant of \mathcal{E} as zero. This section elaborately describes how to formulate one class of descriptor system known as index-I system and find the low-rank solution of Lyapunov equation constructing around index-I system on definite time interval by RKSM method.

Recalling the index-I descriptor system (2.10) represented as

$$\underbrace{\begin{bmatrix} \mathcal{E}_i & \mathcal{E}_{ii} \\ 0 & 0 \end{bmatrix}}_{\mathcal{E}} \underbrace{\begin{bmatrix} \dot{g}(t) \\ \dot{r}(t) \end{bmatrix}}_{\dot{x}(t)} = \underbrace{\begin{bmatrix} \mathcal{A}_i & \mathcal{A}_{ii} \\ \mathcal{A}_{iii} & \mathcal{A}_{iv} \end{bmatrix}}_{\mathcal{A}} \underbrace{\begin{bmatrix} g(t) \\ r(t) \end{bmatrix}}_{x(t)} + \underbrace{\begin{bmatrix} \mathcal{B}_i \\ \mathcal{B}_{ii} \end{bmatrix}}_{\mathcal{B}} u(t)$$

$$y(t) = \underbrace{\begin{bmatrix} \mathcal{C}_i & \mathcal{C}_{ii} \end{bmatrix}}_{\mathcal{C}} \underbrace{\begin{bmatrix} g(t) \\ r(t) \end{bmatrix}}_{x(t)} + \mathcal{D}u(t)$$

These equations are equivalent to the differential-algebraic equations written as:

$$\mathcal{E}_i \dot{g}(t) + \mathcal{E}_{ii} \dot{r}(t) = \mathcal{A}_i g(t) + \mathcal{A}_{ii} r(t) + \mathcal{B}_i u(t), \quad (4.5a)$$

$$0 = \mathcal{A}_{iii} g(t) + \mathcal{A}_{iv} r(t) + \mathcal{B}_{ii} u(t), \quad (4.5b)$$

$$y(t) = \mathcal{C}_i g(t) + \mathcal{C}_{ii} r(t) + \mathcal{D}u(t). \quad (4.5c)$$

Since \mathcal{A}_{iv} is non-singular block matrix, the system (2.10) is claimed as index-I descriptor system what is also represented as semi-explicit system in [88]. Since Equation (4.5b) contains no differential term, it is totally an algebraic equation and from there, we obtain the algebraic part as

$$r(t) = -\mathcal{A}_{iv}^{-1} \mathcal{A}_{iii} g(t) - \mathcal{A}_{iv}^{-1} \mathcal{B}_{ii} u(t) \quad (4.6)$$

Substituting the value of $r(t)$ in (4.5a), we obtain new state-space equation eliminating algebraic part as

$$\underbrace{(\mathcal{E}_i - \mathcal{E}_{ii} \mathcal{A}_{iv}^{-1} \mathcal{A}_{iii})}_{\mathcal{E}} \dot{g}(t) = \underbrace{(\mathcal{A}_i - \mathcal{A}_{ii} \mathcal{A}_{iv}^{-1} \mathcal{A}_{iii})}_{\mathcal{A}} g(t) + \underbrace{\begin{bmatrix} \mathcal{B}_i - \mathcal{A}_{ii} \mathcal{A}_{iv}^{-1} \mathcal{B}_{ii} \\ \mathcal{E}_{ii} \mathcal{A}_{iv}^{-1} \mathcal{B}_{ii} \end{bmatrix}}_{\mathcal{B}} \underbrace{\begin{bmatrix} u^T(t) & \dot{u}^T(t) \end{bmatrix}}_{\bar{u}(t)} \quad (4.7a)$$

$$y(t) = \underbrace{(\mathcal{C}_i - \mathcal{C}_{ii} \mathcal{A}_{iv}^{-1} \mathcal{A}_{iii})}_{\mathcal{C}} g(t) + \underbrace{\begin{bmatrix} \mathcal{D} - \mathcal{C}_{ii} \mathcal{A}_{iv}^{-1} \mathcal{B}_{ii} \\ 0 \end{bmatrix}}_{\mathcal{D}} \underbrace{\begin{bmatrix} u^T(t) & \dot{u}^T(t) \end{bmatrix}}_{\bar{u}(t)}. \quad (4.7b)$$

which has relations with generalised state-space equation (2.2) as

$$\mathcal{E} := \mathcal{E}_i - \mathcal{E}_{ii} \mathcal{A}_{iv}^{-1} \mathcal{A}_{iii}, \quad \mathcal{A} := \mathcal{A}_i - \mathcal{A}_{ii} \mathcal{A}_{iv}^{-1} \mathcal{A}_{iii}, \quad \mathcal{B} := \begin{bmatrix} \mathcal{B}_i - \mathcal{A}_{ii} \mathcal{A}_{iv}^{-1} \mathcal{B}_{ii} \\ \mathcal{E}_{ii} \mathcal{A}_{iv}^{-1} \mathcal{B}_{ii} \end{bmatrix}$$

$$\mathcal{C} := \mathcal{C}_i - \mathcal{C}_{ii} \mathcal{A}_{iv}^{-1} \mathcal{A}_{iii}, \quad \mathcal{D} := \begin{bmatrix} \mathcal{D} - \mathcal{C}_{ii} \mathcal{A}_{iv}^{-1} \mathcal{B}_{ii} \\ 0 \end{bmatrix}, \quad \bar{u}(t) := \begin{bmatrix} u^T(t) & \dot{u}^T(t) \end{bmatrix}$$

Algorithm 8: RKSM for solving time-restricted controllability Gramian (2.19a) of index-I system (2.10) on time interval $[0, t_f]$.

Input: $\mathcal{E}_i, \mathcal{E}_{ii}, \mathcal{A}_i, \mathcal{A}_{ii}, \mathcal{A}_{iii}, \mathcal{A}_{iv}, \mathcal{B}_i, \mathcal{B}_{ii}, m_{it}$ (no. of iteration), t_f (endpoint of time interval), $0 < tol \ll 1$ (tolerance value), μ_1 (initial shift parameter).

Output: $\mathcal{R}_{\mathcal{P}} \in \mathbb{R}^{n \times z}$ such that $\mathcal{R}_{\mathcal{P}} \mathcal{R}_{\mathcal{P}}^T \approx \mathcal{P}$, where $z \ll n$.

1 set initial basis vector $v_1 = \begin{bmatrix} \mathcal{A}_i - \mu_1 \mathcal{E}_i & \mathcal{A}_{ii} - \mu_1 \mathcal{E}_{ii} \\ \mathcal{A}_{iii} & \mathcal{A}_{iv} \end{bmatrix}^{-1} \begin{bmatrix} \mathcal{B}_i \\ \mathcal{B}_{ii} \end{bmatrix}$, $\mathcal{V}_1 = \frac{v}{\|v\|}$

2 **while** $j \leq m_{it}$ **do**

3 Find the next basis matrix by solving linear system

$$\begin{bmatrix} \mathcal{A}_i - \mu_j \mathcal{E}_i & \mathcal{A}_{ii} - \mu_j \mathcal{E}_{ii} \\ \mathcal{A}_{iii} & \mathcal{A}_{iv} \end{bmatrix} \begin{bmatrix} v_{j+1} \\ * \end{bmatrix} = \begin{bmatrix} \mathcal{V}_j \\ \mathbf{0} \end{bmatrix}. \quad (4.8)$$

4 Construct orthonormal vector set $\mathcal{V}_{j+1} = [\mathcal{V}_j, v_{j+1}]$ by QR decomposition (see Subsection (2.2.3.3)) using Algorithm (2).

5 Solve the projected controllability Lyapunov equation (4.1)

$$\tilde{\mathcal{A}}_{j+1} \tilde{\mathcal{P}} \tilde{\mathcal{E}}_{j+1}^T + \tilde{\mathcal{E}}_{j+1} \tilde{\mathcal{P}} \tilde{\mathcal{A}}_{j+1}^T + \tilde{\mathcal{B}}_{j+1} \tilde{\mathcal{B}}_{j+1}^T - \tilde{\mathcal{E}}_{j+1} e^{\tilde{\mathcal{E}}_{j+1}^{-1} \tilde{\mathcal{A}}_{j+1} t_f} \tilde{\mathcal{E}}_{j+1}^{-1} \tilde{\mathcal{B}}_{j+1} (\tilde{\mathcal{E}}_{j+1}^{-1} \tilde{\mathcal{B}}_{j+1})^T e^{(\tilde{\mathcal{E}}_{j+1}^{-1} \tilde{\mathcal{A}}_{j+1})^T t_f} \tilde{\mathcal{E}}_{j+1}^T = \mathbf{0}$$

for finding small-scale CG \tilde{P} Where, $\tilde{\mathcal{E}}_{j+1} = \mathcal{V}_{j+1}^T \mathcal{E}_i \mathcal{V}_{j+1} - (\mathcal{V}_{j+1}^T \mathcal{E}_{ii}) \mathcal{A}_{iv}^{-1} (\mathcal{A}_{iii} \mathcal{V}_{j+1})$,

$$\tilde{\mathcal{A}}_{j+1} = \mathcal{V}_{j+1}^T \mathcal{A}_i \mathcal{V}_{j+1} - (\mathcal{V}_{j+1}^T \mathcal{A}_{ii}) \mathcal{A}_{iv}^{-1} (\mathcal{A}_{iii} \mathcal{V}_{j+1}), \tilde{\mathcal{B}}_{j+1} = \begin{bmatrix} \mathcal{V}_{j+1}^T \mathcal{B}_i - (\mathcal{V}_{j+1}^T \mathcal{A}_{ii}) \mathcal{A}_{iv}^{-1} \mathcal{B}_{ii} \\ (\mathcal{V}_{j+1}^T \mathcal{E}_{ii}) \mathcal{A}_{iv}^{-1} \mathcal{B}_{ii} \end{bmatrix}.$$

7 Compute next shift parameter μ (see Section (4.2))

8 Compute residual norm (see Section (4.4))

9 **if** residual norm $\leq tol$ **then**

10 | Stop Rational Krylov iteration.

11 Operate eigenvalue decomposition as (4.3).

12 Establish low-rank controllability Gramian factor $\mathcal{R}_{\mathcal{P}}$ as (4.4).

Therefore, the index-I descriptor system (2.10) can be converted to the generalised system (2.2) through the above connection. However, it is matter of concern that the explicit conversion of system matrices of (4.7) makes the entire system dense. As a result, it increases the computational cost during finding the solution of Lyapunov equation on finite time interval. To overcome this complexity, we take two major steps like [89]. First, we retain the sparsity patterns of the system matrices at the time of solving linear system (4.8) instead of doing explicit conversion of the system matrices likewise the system matrices of (4.7) which is essential to construct the basis matrix of rational Krylov subspace. Secondly, We solve the projected Lyapunov equation after projecting the system matrices implicitly without forming explicit structure highlighted in line (6) inside the Algorithm (8) representing the entire process of solving time-restricted controllability Lyapunov equation (2.19a) established based on index-I descriptor system (2.10).

Similarly, by taking the transpose of the system matrices and replacing $\mathcal{E}_i, \mathcal{E}_{ii}, \mathcal{A}_i, \mathcal{A}_{ii}, \mathcal{A}_{iii}, \mathcal{A}_{iv}, \mathcal{B}_i$, and \mathcal{B}_{ii} by $\mathcal{E}_i^T, \mathcal{E}_{ii}^T, \mathcal{A}_i^T, \mathcal{A}_{iii}^T, \mathcal{A}_{ii}^T, \mathcal{A}_{iv}^T, \mathcal{C}_i^T$, and \mathcal{C}_{ii}^T in Algorithm (8), we can find the observability Gramian factor $\mathcal{L}_{\mathcal{Q}}$ by solving projected Lyapunov equation (4.2) whose projector is

constructed from the basis matrix found by solving the linear system

$$\begin{bmatrix} \mathcal{A}_i^T - \mu_j \mathcal{E}_i^T & \mathcal{A}_{iii}^T \\ \mathcal{A}_{ii}^T - \mu_j \mathcal{E}_{ii}^T & \mathcal{A}_{iv}^T \end{bmatrix} \begin{bmatrix} v_{j+1} \\ * \end{bmatrix} = \begin{bmatrix} \mathcal{V}_j \\ 0 \end{bmatrix} \quad (4.9)$$

Special Case 1 : When $\mathcal{E}_{ii} = 0$ in the system (2.10), the index-I system can be represented by

$$\underbrace{\begin{bmatrix} \mathcal{E}_i & 0 \\ 0 & 0 \end{bmatrix}}_{\mathcal{E}} \underbrace{\begin{bmatrix} \dot{g}(t) \\ \dot{r}(t) \end{bmatrix}}_{\dot{x}(t)} = \underbrace{\begin{bmatrix} \mathcal{A}_i & \mathcal{A}_{ii} \\ \mathcal{A}_{iii} & \mathcal{A}_{iv} \end{bmatrix}}_{\mathcal{A}} \underbrace{\begin{bmatrix} g(t) \\ r(t) \end{bmatrix}}_{x(t)} + \underbrace{\begin{bmatrix} \mathcal{B}_i \\ \mathcal{B}_{ii} \end{bmatrix}}_{\mathcal{B}} u(t)$$

$$y(t) = \underbrace{\begin{bmatrix} \mathcal{C}_i & \mathcal{C}_{ii} \end{bmatrix}}_{\mathcal{C}} \underbrace{\begin{bmatrix} g(t) \\ r(t) \end{bmatrix}}_{x(t)} + \mathcal{D}u(t),$$

what is equivalent to the following differential-algebraic equation of the system

$$\begin{aligned} \mathcal{E}_i \dot{g}(t) &= \mathcal{A}_i g(t) + \mathcal{A}_{ii} r(t) + \mathcal{B}_i u(t), \\ 0 &= \mathcal{A}_{iii} g(t) + \mathcal{A}_{iv} r(t) + \mathcal{B}_{ii} u(t), \\ y(t) &= \mathcal{C}_i g(t) + \mathcal{C}_{ii} r(t) + \mathcal{D}u(t). \end{aligned}$$

After conversion from descriptor system to generalised system, we get the following relation

$$\begin{aligned} \mathcal{E} &:= \mathcal{E}_i, \quad \mathcal{A} := \mathcal{A}_i - \mathcal{A}_{ii} \mathcal{A}_{iv}^{-1} \mathcal{A}_{iii}, \quad \mathcal{B} := \mathcal{B}_i - \mathcal{A}_{ii} \mathcal{A}_{iv}^{-1} \mathcal{B}_{ii} \\ \mathcal{C} &:= \mathcal{C}_i - \mathcal{C}_{ii} \mathcal{A}_{iv}^{-1} \mathcal{A}_{iii}, \quad \mathcal{D} := \mathcal{D} - \mathcal{C}_{ii} \mathcal{A}_{iv}^{-1} \mathcal{B}_{ii} \end{aligned}$$

Therefore, the basis of the rational Krylov subspace can be generated for finding CG by solving the linear system

$$\begin{bmatrix} \mathcal{A}_i - \mu_j \mathcal{E}_i & \mathcal{A}_{ii} \\ \mathcal{A}_{iii} & \mathcal{A}_{iv} \end{bmatrix} \begin{bmatrix} v_{j+1} \\ * \end{bmatrix} = \begin{bmatrix} \mathcal{V}_j \\ 0 \end{bmatrix}.$$

In the similar way, we can construct the basis matrix with a view to finding OG by solving the linear system

$$\begin{bmatrix} \mathcal{A}_i^T - \mu_j \mathcal{E}_i^T & \mathcal{A}_{iii}^T \\ \mathcal{A}_{ii}^T & \mathcal{A}_{iv}^T \end{bmatrix} \begin{bmatrix} v_{j+1} \\ * \end{bmatrix} = \begin{bmatrix} \mathcal{V}_j \\ 0 \end{bmatrix}$$

Special Case 2 : When \mathcal{E}_{ii} and \mathcal{A}_{ii} both are zero, the system (2.10) becomes

$$\underbrace{\begin{bmatrix} \mathcal{E}_i & 0 \\ 0 & 0 \end{bmatrix}}_{\mathcal{E}} \underbrace{\begin{bmatrix} \dot{g}(t) \\ \dot{r}(t) \end{bmatrix}}_{\dot{x}(t)} = \underbrace{\begin{bmatrix} \mathcal{A}_i & 0 \\ \mathcal{A}_{iii} & \mathcal{A}_{iv} \end{bmatrix}}_{\mathcal{A}} \underbrace{\begin{bmatrix} g(t) \\ r(t) \end{bmatrix}}_{x(t)} + \underbrace{\begin{bmatrix} \mathcal{B}_i \\ \mathcal{B}_{ii} \end{bmatrix}}_{\mathcal{B}} u(t)$$

$$y(t) = \underbrace{\begin{bmatrix} \mathcal{C}_i & \mathcal{C}_{ii} \end{bmatrix}}_{\mathcal{C}} \underbrace{\begin{bmatrix} g(t) \\ r(t) \end{bmatrix}}_{x(t)} + \mathcal{D}u(t),$$

Then, the system matrices of the new converted system become

$$\begin{aligned}\mathcal{E} &:= \mathcal{E}_i, \quad \mathcal{A} := \mathcal{A}_i, \quad \mathcal{B} := \mathcal{B}_i \\ \mathcal{C} &:= \mathcal{C}_i - \mathcal{C}_{ii}\mathcal{A}_{iv}^{-1}\mathcal{A}_{iii}, \quad \mathcal{D} := \mathcal{D} - \mathcal{C}_{ii}\mathcal{A}_{iv}^{-1}\mathcal{B}_{ii},\end{aligned}$$

and the basis of the rational Krylov subspace can be generated for finding CG and OG by solving the linear system

$$\begin{bmatrix} \mathcal{A}_i - \mu_j \mathcal{E}_i & 0 \\ \mathcal{A}_{iii} & \mathcal{A}_{iv} \end{bmatrix} \begin{bmatrix} v_{j+1} \\ * \end{bmatrix} = \begin{bmatrix} \mathcal{V}_j \\ 0 \end{bmatrix}.$$

and

$$\begin{bmatrix} \mathcal{A}_i^T - \mu_j \mathcal{E}_i^T & \mathcal{A}_{iii}^T \\ 0 & \mathcal{A}_{iv}^T \end{bmatrix} \begin{bmatrix} v_{j+1} \\ * \end{bmatrix} = \begin{bmatrix} \mathcal{V}_j \\ 0 \end{bmatrix}$$

respectively.

Special Case 3 : When \mathcal{E}_{ii} , \mathcal{A}_{ii} , and \mathcal{A}_{iii} are zero, the system (2.10) becomes

$$\begin{aligned}\underbrace{\begin{bmatrix} \mathcal{E}_i & 0 \\ 0 & 0 \end{bmatrix}}_{\mathcal{E}} \underbrace{\begin{bmatrix} \dot{g}(t) \\ \dot{r}(t) \end{bmatrix}}_{x(t)} &= \underbrace{\begin{bmatrix} \mathcal{A}_i & 0 \\ 0 & \mathcal{A}_{iv} \end{bmatrix}}_{\mathcal{A}} \underbrace{\begin{bmatrix} g(t) \\ r(t) \end{bmatrix}}_{x(t)} + \underbrace{\begin{bmatrix} \mathcal{B}_i \\ \mathcal{B}_{ii} \end{bmatrix}}_{\mathcal{B}} u(t) \\ y(t) &= \underbrace{\begin{bmatrix} \mathcal{C}_i & \mathcal{C}_{ii} \end{bmatrix}}_{\mathcal{C}} \underbrace{\begin{bmatrix} g(t) \\ r(t) \end{bmatrix}}_{x(t)} + \mathcal{D}u(t),\end{aligned}$$

Then, the system matrices of the new converted system become

$$\begin{aligned}\mathcal{E} &:= \mathcal{E}_i, \quad \mathcal{A} := \mathcal{A}_i, \quad \mathcal{B} := \mathcal{B}_i \\ \mathcal{C} &:= \mathcal{C}_i, \quad \mathcal{D} := \mathcal{D} - \mathcal{C}_{ii}\mathcal{A}_{iv}^{-1}\mathcal{B}_{ii},\end{aligned}$$

and the basis of the rational Krylov subspace can be generated for finding CG and OG by solving the linear system

$$\begin{bmatrix} \mathcal{A}_i - \mu_j \mathcal{E}_i & 0 \\ 0 & \mathcal{A}_{iv} \end{bmatrix} \begin{bmatrix} v_{j+1} \\ * \end{bmatrix} = \begin{bmatrix} \mathcal{V}_j \\ 0 \end{bmatrix}.$$

and

$$\begin{bmatrix} \mathcal{A}_i^T - \mu_j \mathcal{E}_i^T & 0 \\ 0 & \mathcal{A}_{iv}^T \end{bmatrix} \begin{bmatrix} v_{j+1} \\ * \end{bmatrix} = \begin{bmatrix} \mathcal{V}_j \\ 0 \end{bmatrix}$$

respectively.

4.5.1 Investigation on Solving Time Restricted Index-I Descriptor System with Non-homogeneous Initial Condition

Till now, we have talked about solving the Lyapunov equations (2.19) on limited time interval having initial value as zero. Now, we extend our idea to solve the Lyapunov equations on finite time interval $[t_0, t_f]$ stapled with non-homogeneous initial condition, i.e., $t_0 \neq 0$. Recalling the Lyapunov equations (2.17) and (2.18) on time interval $[t_0, t_f]$

$$\begin{aligned} \mathcal{A}\mathcal{P}\mathcal{E}^T + \mathcal{E}\mathcal{P}\mathcal{A}^T + \mathcal{E}e^{\mathcal{E}^{-1}\mathcal{A}t_0}\mathcal{E}^{-1}\mathcal{B}(\mathcal{E}^{-1}\mathcal{B})^T e^{(\mathcal{E}^{-1}\mathcal{A})^T t_0}\mathcal{E}^T - \mathcal{E}e^{\mathcal{E}^{-1}\mathcal{A}t_f}\mathcal{E}^{-1}\mathcal{B}(\mathcal{E}^{-1}\mathcal{B})^T e^{(\mathcal{E}^{-1}\mathcal{A})^T t_f}\mathcal{E}^T &= 0, \\ \mathcal{A}^T\mathcal{Q}\mathcal{E} + \mathcal{E}^T\mathcal{Q}\mathcal{A} + e^{(\mathcal{E}^{-1}\mathcal{A})^T t_0}\mathcal{C}^T\mathcal{C}e^{\mathcal{E}^{-1}\mathcal{A}t_0} - e^{(\mathcal{E}^{-1}\mathcal{A})^T t_f}\mathcal{C}^T\mathcal{C}e^{\mathcal{E}^{-1}\mathcal{A}t_f} &= 0, \end{aligned}$$

and the output equation (2.5) from the Duhamel's principle (see Subsection 2.1.2)

$$y(t) = \mathcal{C}e^{\mathcal{E}^{-1}\mathcal{A}t}x_0 + \int_0^{t_f} \mathcal{C}e^{\mathcal{E}^{-1}\mathcal{A}(t-\tau)}(\mathcal{E}^{-1}\mathcal{B})u(\tau)d\tau + \mathcal{D}u(t),$$

where x_0 is the initial condition, i.e., $x(t_0) = x_0$. Unfortunately, we do not find convergent solution by directly solving time restricted Lyapunov equations (2.17) and (2.18). Hence, it needs to be modified. In [90], the authors extended the input matrix \mathcal{B} by creating an augmented form $[\mathcal{B} \ \mathcal{B}_0] \in \mathbb{R}^{k+q}$ where the non-zero initial value $x_0 \in Im(\mathcal{B}_0)$ contained the subspace of \mathcal{K}_0 spanned by $\mathcal{B}_0 \in \mathbb{R}^q$. As a result, the general state-space equation 2.2 were modified as

$$\begin{aligned} \mathcal{E}\dot{x}(t) &= \mathcal{A}x(t) + \underbrace{[\mathcal{B} \ \mathcal{B}_0]}_{\mathcal{B}} \underbrace{\begin{bmatrix} u^T(t) \\ u_0^T(t) \end{bmatrix}}_{u(t)}; \quad x(t_0) = x_0, \quad t \geq t_0, \\ y(t) &= \mathcal{C}x(t) + \mathcal{D}u(t). \end{aligned} \tag{4.10}$$

On the other hand, the authors in [91] reformed the non-homogeneous initial condition $x(t_0) = x_0$ as $x_0 = \mathcal{B}_0\mathcal{K}_0$ where \mathcal{K}_0 was spanned by \mathcal{B}_0 , and evaluated the output $y(t)$ using Duhamel formula as

$$y(t) = \underbrace{\mathcal{C}e^{\mathcal{E}^{-1}\mathcal{A}t}x_0}_{y(0)} + \underbrace{\int_0^{t_f} \mathcal{C}e^{\mathcal{E}^{-1}\mathcal{A}(t-\tau)}(\mathcal{E}^{-1}\mathcal{B})u(\tau)d\tau}_{y(t)} + \mathcal{D}u(t), \tag{4.11}$$

It is closely observed that $y(0)$ term of (4.11) is the response of the system to the initial condition x_0 with $u(t) = 0$ and $y(t)$ term is the response of the system to the $u(t)$ with homogeneous initial condition, i.e. $x(t_0) = 0$. On the based of the output relation, the authors of [91] splitted the state-space (4.10) into two state-space equation written as

$$\begin{aligned} \mathcal{E}\dot{x}_0(t) &= \mathcal{A}x_0(t) + \mathcal{B}_0u_0(t); \quad x_0(t_0) = 0, \\ y(t) &= \mathcal{C}x_0(t) + \mathcal{D}u_0(t), \end{aligned} \tag{4.12}$$

and

$$\begin{aligned} \mathcal{E}\dot{x}(t) &= \mathcal{A}x(t) + \mathcal{B}u(t); \quad x(t_0) = 0, \\ y(t) &= \mathcal{C}x(t) + \mathcal{D}u_0(t), \end{aligned} \tag{4.13}$$

where, $u_0(t) = \mathcal{K}_0\delta(t)$ and $\delta(t)$ is the Dirac delta distribution function.

As opposed to efficiently deal with the non-homogeneous initial condition, we build an orthogonal

basis matrix \mathcal{B}_0 like [92] in such a way that $\mathcal{B}_0 \mathcal{K}_0 = 0$. As a result, term $y(0)$ of (4.11) is diminished and the only term $y(t)$ remains responding to input $u(t)$ as the form of

$$y(t) = \int_0^{t_f} \mathcal{C} e^{\mathcal{E}^{-1} \mathcal{A}(t-\tau)} (\mathcal{E}^{-1} \mathcal{B}) u(\tau) d\tau + \mathcal{D} u(t),$$

Hence, the output relation is developed on shifted homogeneous time interval and it is enough to compute the system matrices of the state-space equation (4.13) only. Here, we directly evaluate our idea for index-I descriptor system (2.10). For spanning the null space, we assume two basis sub-matrices \mathcal{B}_{x_1} and \mathcal{B}_{x_2} as

$$\mathcal{B}_{x_i} := e^{\mathcal{B}_i t_0}, \quad \mathcal{B}_{x_{ii}} := e^{\mathcal{B}_{ii} t_0}$$

and extract orthonormal basis conducting QR decomposition (see Subsubsection 2.2.3.3) of \mathcal{B}_{x_1} and \mathcal{B}_{x_2} through forming two augmented sub-matrices as follows

$$\mathcal{B}_{aug_i} := \begin{bmatrix} \mathcal{B}_i & \mathcal{B}_{x_i} \end{bmatrix}, \quad \mathcal{B}_{aug_{ii}} := \begin{bmatrix} \mathcal{B}_{ii} & \mathcal{B}_{x_{ii}} \end{bmatrix}$$

Therefore, the index-I system (2.10) can be reformed as

$$\underbrace{\begin{bmatrix} \mathcal{E}_i & \mathcal{E}_{ii} \\ 0 & 0 \end{bmatrix}}_{\mathcal{E}} \underbrace{\begin{bmatrix} \dot{g}(t) \\ \dot{r}(t) \end{bmatrix}}_{x(t)} = \underbrace{\begin{bmatrix} \mathcal{A}_i & \mathcal{A}_{ii} \\ \mathcal{A}_{iii} & \mathcal{A}_{iv} \end{bmatrix}}_{\mathcal{A}} \underbrace{\begin{bmatrix} g(t) \\ r(t) \end{bmatrix}}_{x(t)} + \underbrace{\begin{bmatrix} \mathcal{B}_{aug_i} \\ \mathcal{B}_{aug_{ii}} \end{bmatrix}}_{\mathcal{B}} u(t) \quad (4.14)$$

$$y(t) = \underbrace{\begin{bmatrix} \mathcal{C}_i & \mathcal{C}_{ii} \end{bmatrix}}_{\mathcal{C}} \underbrace{\begin{bmatrix} g(t) \\ r(t) \end{bmatrix}}_{x(t)} + \mathcal{D} u(t).$$

Hence, the relation can be grown up with generalised system (2.2) as

$$\mathcal{E} := \mathcal{E}_i - \mathcal{E}_{ii} \mathcal{A}_{iv}^{-1} \mathcal{A}_{iii}, \quad \mathcal{A} := \mathcal{A}_i - \mathcal{A}_{ii} \mathcal{A}_{iv}^{-1} \mathcal{A}_{iii}, \quad \mathcal{B}_{aug} := \begin{bmatrix} \mathcal{B}_{aug_i} - \mathcal{A}_{ii} \mathcal{A}_{iv}^{-1} \mathcal{B}_{aug_{ii}} \\ \mathcal{E}_{ii} \mathcal{A}_{iv}^{-1} \mathcal{B}_{aug_{ii}} \end{bmatrix}$$

$$\mathcal{C} := \mathcal{C}_i - \mathcal{C}_{ii} \mathcal{A}_{iv}^{-1} \mathcal{A}_{iii}, \quad \mathcal{D} := \begin{bmatrix} \mathcal{D} - \mathcal{C}_{ii} \mathcal{A}_{iv}^{-1} \mathcal{B}_{aug_{ii}} \\ 0 \end{bmatrix}$$

and the controllable Lyapunov equation of the above system is written as

$$\mathcal{A} \mathcal{P} \mathcal{E}^T + \mathcal{E} \mathcal{P} \mathcal{A}^T + \mathcal{B}_{aug} \mathcal{B}_{aug}^T - \mathcal{E} e^{\mathcal{E}^{-1} \mathcal{A} t_f} \mathcal{E}^{-1} \mathcal{B}_{aug} (\mathcal{E}^{-1} \mathcal{B}_{aug})^T e^{(\mathcal{E}^{-1} \mathcal{A})^T t_f} \mathcal{E}^T = 0. \quad (4.15)$$

Since the matrix extension is only occupied in \mathcal{B} what relates with the corresponding output of the system (2.10) on the time interval $[0, t_f]$, there is no modification needed in observability Lyapunov equation (2.19b). For solving the above equations through RKSM, we need to form projected controllable Lyapunov equation as

$$\tilde{\mathcal{A}} \tilde{\mathcal{P}} \tilde{\mathcal{E}}^T + \tilde{\mathcal{E}} \tilde{\mathcal{P}} \tilde{\mathcal{A}}^T + \tilde{\mathcal{B}}_{aug} \tilde{\mathcal{B}}_{aug}^T - \tilde{\mathcal{E}} e^{\tilde{\mathcal{E}}^{-1} \tilde{\mathcal{A}} t_f} \tilde{\mathcal{E}}^{-1} \tilde{\mathcal{B}}_{aug} (\tilde{\mathcal{E}}^{-1} \tilde{\mathcal{B}}_{aug})^T e^{(\tilde{\mathcal{E}}^{-1} \tilde{\mathcal{A}})^T t_f} \tilde{\mathcal{E}}^T = 0 \quad (4.16)$$

and observable Lyapunov equation as (4.2).

The controllability Gramian can be found by solving (4.15) using Algorithm (8) after slight modification what are highlighted in Algorithm (9). As there is no change occurred in observable Lyapunov equation (2.19b), we can directly solve it using Algorithm (8) by taking transpose of the system sub-blocks and solving the linear system (4.9).

Algorithm 9: Change in Algorithm (8) for solving time-restricted controllability Gramian (4.15) of index-I system (2.10) on time interval $[t_0, t_f]$.

Input: $\mathcal{E}_i, \mathcal{E}_{ii}, \mathcal{A}_i, \mathcal{A}_{ii}, \mathcal{A}_{iii}, \mathcal{A}_{iv}, \mathcal{B}_i, \mathcal{B}_{ii}, m_{it}$ (no. of iteration), t_f (endpoint of time interval), $0 < tol \ll 1$ (tolerance value), μ_1 (initial shift parameter).

Output: $\mathcal{R}_{\mathcal{P}} \in \mathbb{R}^{n \times z}$ such that $\mathcal{R}_{\mathcal{P}} \mathcal{R}_{\mathcal{P}}^T \approx \mathcal{P}$, where $z \ll n$.

1 set initial basis vector $v_1 = \begin{bmatrix} \mathcal{A}_i - \mu_1 \mathcal{E}_i & \mathcal{A}_{ii} - \mu_1 \mathcal{E}_{ii} \\ \mathcal{A}_{iii} & \mathcal{A}_{iv} \end{bmatrix}^{-1} \begin{bmatrix} \mathcal{B}_{aug_i} \\ \mathcal{B}_{aug_{ii}} \end{bmatrix}$, $\mathcal{V}_1 = \frac{v}{\|v\|}$

2 **while** $j \leq m_{it}$ **do**

3 Solve the projected controllability Lyapunov equation (4.16)

$$\tilde{\mathcal{A}}_{j+1} \tilde{\mathcal{P}} \tilde{\mathcal{E}}_{j+1}^T + \tilde{\mathcal{E}}_{j+1} \tilde{\mathcal{P}} \tilde{\mathcal{A}}_{j+1}^T + \tilde{\mathcal{B}}_{aug_{j+1}} \tilde{\mathcal{B}}_{aug_{j+1}}^T - \tilde{\mathcal{E}}_{j+1} e^{\tilde{\mathcal{E}}_{j+1}^{-1} \tilde{\mathcal{A}}_{j+1} t_f} \tilde{\mathcal{E}}_{j+1}^{-1} \tilde{\mathcal{B}}_{aug_{j+1}} (\tilde{\mathcal{E}}_{j+1}^{-1} \tilde{\mathcal{B}}_{aug_{j+1}})^T e^{(\tilde{\mathcal{E}}_{j+1}^{-1} \tilde{\mathcal{A}}_{j+1})^T t_f} \tilde{\mathcal{E}}_{j+1}^T = 0$$

for finding small-scale CG $\tilde{\mathcal{P}}$ Where, $\tilde{\mathcal{B}}_{aug_{j+1}} = \begin{bmatrix} \mathcal{V}_{j+1}^T \mathcal{B}_{aug_i} - (\mathcal{V}_{j+1}^T \mathcal{A}_{ii}) \mathcal{A}_{iv}^{-1} \mathcal{B}_{aug_{ii}} \\ (\mathcal{V}_{j+1}^T \mathcal{E}_{ii}) \mathcal{A}_{iv}^{-1} \mathcal{B}_{aug_{ii}} \end{bmatrix}$.

4.6 Formulation and Solution of Time Restricted Index-II Descriptor System

Index-II (2.11) is another special type of descriptor system (see Subsection 2.1.4) arisen in various practical sector written in the form

$$\underbrace{\begin{bmatrix} \mathcal{E}_i & 0 \\ 0 & 0 \end{bmatrix}}_{\mathcal{E}} \underbrace{\begin{bmatrix} \dot{g}(t) \\ \dot{r}(t) \end{bmatrix}}_{x(t)} = \underbrace{\begin{bmatrix} \mathcal{A}_i & \mathcal{A}_{ii} \\ \mathcal{A}_{iii} & 0 \end{bmatrix}}_{\mathcal{A}} \underbrace{\begin{bmatrix} g(t) \\ r(t) \end{bmatrix}}_{x(t)} + \underbrace{\begin{bmatrix} \mathcal{B}_i \\ \mathcal{B}_{ii} \end{bmatrix}}_{\mathcal{B}} u(t),$$

$$y(t) = \underbrace{\begin{bmatrix} \mathcal{C}_i & \mathcal{C}_{ii} \end{bmatrix}}_{\mathcal{C}} \underbrace{\begin{bmatrix} g(t) \\ r(t) \end{bmatrix}}_{x(t)} + \mathcal{D}u(t),$$

what is equivalent to the differential-algebraic equation of the form

$$\mathcal{E}_i \dot{g}(t) = \mathcal{A}_i g(t) + \mathcal{A}_{ii} r(t) + \mathcal{B}_i u(t), \quad (4.17a)$$

$$0 = \mathcal{A}_{iii} g(t) + \mathcal{B}_{ii} u(t), \quad (4.17b)$$

$$y(t) = \mathcal{C}_i g(t) + \mathcal{C}_{ii} r(t) + \mathcal{D}u(t). \quad (4.17c)$$

In order to convert to the generalised presentation like (2.2), the authors in [93] enforced the algebraic part $r(t)$ of the above equations by expressing the differential part $g(t)$ as the combination of its complimentary and particular solution written as

$$g(t) = g_c(t) + g_p(t) \quad (4.18)$$

It has been observed in [93] that the particular solution can be written as

$$g_p(t) = -\mathcal{E}_i^{-1} \mathcal{A}_{ii} \mathcal{B}_{ii} u(t),$$

where, $\Xi = (\mathcal{A}_{iii}\mathcal{E}_i^{-1}\mathcal{A}_{ii})^{-1}$. Putting all together in (4.17) and eliminating algebraic part $r(t)$ by taking as

$$r(t) = -\Xi(\mathcal{A}_{iii}\mathcal{E}_i^{-1}\mathcal{A}_{ii})g_c(t) - \Xi\mathcal{A}_{iii}\mathcal{E}_i^{-1}(\mathcal{B}_i - \mathcal{A}_i\mathcal{E}_i^{-1}\mathcal{A}_{ii}\Xi\mathcal{B}_{ii})u(t) - \Xi\mathcal{B}_{ii}\dot{u}(t),$$

we get

$$\underbrace{\mathcal{E}_i}_{\mathcal{E}} \dot{g}_c(t) = \underbrace{\left[\mathcal{A}_i - \mathcal{A}_{ii}\Xi(\mathcal{A}_{iii}\mathcal{E}_i^{-1}\mathcal{A}_{ii}) \right]}_{\mathcal{A}} g_c(t) + \underbrace{\left[\begin{array}{c} \mathcal{B}_i - \mathcal{A}_i\mathcal{E}_i^{-1}\mathcal{A}_{ii}\Xi\mathcal{B}_{ii} - \mathcal{A}_{ii}\Xi\mathcal{A}_{iii}\mathcal{E}_i^{-1}(\mathcal{B}_i - \mathcal{A}_i\mathcal{E}_i^{-1}\mathcal{A}_{ii}\Xi\mathcal{B}_{ii}) \\ \mathcal{A}_{ii}\Xi\mathcal{B}_{ii} - \mathcal{A}_{ii}\Xi\mathcal{B}_{ii} \end{array} \right]}_{\mathcal{B}} \underbrace{\left[\begin{array}{c} u^T(t) \\ \dot{u}^T(t) \end{array} \right]}_{\bar{u}(t)}, \quad (4.19)$$

and

$$y = \underbrace{\left[\mathcal{C}_i - \mathcal{C}_{ii}\Xi(\mathcal{A}_{iii}\mathcal{E}_i^{-1}\mathcal{A}_{ii}) \right]}_{\mathcal{C}} g_c(t) + \underbrace{\left[\begin{array}{c} \mathcal{D} - \mathcal{C}_i\mathcal{E}_i^{-1}\mathcal{A}_{ii}\Xi\mathcal{B}_{ii} - \mathcal{C}_{ii}\Xi\mathcal{A}_{iii}\mathcal{E}_i^{-1}(\mathcal{B}_i - \mathcal{A}_i\mathcal{E}_i^{-1}\mathcal{A}_{ii}\Xi\mathcal{B}_{ii}) \\ -\mathcal{C}_{ii}\Xi\mathcal{B}_{ii} \end{array} \right]}_{\mathcal{D}} \underbrace{\left[\begin{array}{c} u^T(t) \\ \dot{u}^T(t) \end{array} \right]}_{\bar{u}(t)}. \quad (4.20)$$

Equations (4.19) and (4.20) are the equivalent representations of the general state-space equation (2.2). Now, the setup is completed to solve the time-restricted Lyapunov equation by RKSM. Like index-I, the sparsity of the system matrices are highly preserved during solving the linear system (4.21) mandatory to construct the basis matrix of rational subspace and no explicit structure has been formed of the system matrices at the time of solving projected Lyapunov equation (4.1). Algorithm (10) summarizes the total procedure of solving time-restricted controllable Lyapunov equation centered into index-II descriptor system (2.11) and of formulating low-rank controllability Gramian factor $\mathcal{R}_{\mathcal{D}}$. However, same algorithm can be applicable during solving index-II observable Lyapunov equation to find observability Gramian factor $\mathcal{L}_{\mathcal{Q}}$ after taking transposes of the system sub-matrices. At that time, the basis matrix of the Krylov subspace can be generated by solving linear system

$$\begin{bmatrix} \mathcal{A}_i^T - \mu_j\mathcal{E}_i^T & \mathcal{A}_{iii}^T \\ \mathcal{A}_{ii}^T & 0 \end{bmatrix} \begin{bmatrix} v_{j+1} \\ * \end{bmatrix} = \begin{bmatrix} \mathcal{V}_j \\ 0 \end{bmatrix} \quad (4.22)$$

Special Case 1 : When $\mathcal{B}_{ii} = 0$ in the system (2.11), the index-II system is expressed as

$$\underbrace{\begin{bmatrix} \mathcal{E}_i & 0 \\ 0 & 0 \end{bmatrix}}_{\mathcal{E}} \underbrace{\begin{bmatrix} \dot{g}(t) \\ \dot{r}(t) \end{bmatrix}}_{\dot{x}(t)} = \underbrace{\begin{bmatrix} \mathcal{A}_i & \mathcal{A}_{ii} \\ \mathcal{A}_{iii} & 0 \end{bmatrix}}_{\mathcal{A}} \underbrace{\begin{bmatrix} g(t) \\ r(t) \end{bmatrix}}_{x(t)} + \underbrace{\begin{bmatrix} \mathcal{B}_i \\ 0 \end{bmatrix}}_{\mathcal{B}} u(t),$$

$$y(t) = \underbrace{\begin{bmatrix} \mathcal{C}_i & \mathcal{C}_{ii} \end{bmatrix}}_{\mathcal{C}} \underbrace{\begin{bmatrix} g(t) \\ r(t) \end{bmatrix}}_{x(t)} + \mathcal{D}u(t),$$

Algorithm 10: RKSM for solving time-restricted controllability Gramian (2.19a) of index-II system (2.11) on time interval $[0, t_f]$.

Input: $\mathcal{E}_i, \mathcal{A}_i, \mathcal{A}_{ii}, \mathcal{A}_{iii}, \mathcal{B}_i, \mathcal{B}_{ii}, m_{it}$ (no. of iteration), t_f (endpoint of time interval), $0 < tol \ll 1$ (tolerance value), μ_1 (initial shift parameter).

Output: $\mathcal{R}_{\mathcal{P}} \in \mathbb{R}^{n \times z}$ such that $\mathcal{R}_{\mathcal{P}} \mathcal{R}_{\mathcal{P}}^T \approx \mathcal{P}$, where $z \ll n$.

1 set initial basis vector $v_1 = \begin{bmatrix} \mathcal{A}_i - \mu_1 \mathcal{E}_i & \mathcal{A}_{ii} \\ \mathcal{A}_{iii} & 0 \end{bmatrix}^{-1} \begin{bmatrix} \mathcal{B}_i \\ \mathcal{B}_{ii} \end{bmatrix}$, $\mathcal{V}_1 = \frac{v}{\|v\|}$

2 **while** $j \leq m_{it}$ **do**

3 Find the next basis matrix by solving linear system

$$\begin{bmatrix} \mathcal{A}_i - \mu_j \mathcal{E}_i & \mathcal{A}_{ii} \\ \mathcal{A}_{iii} & 0 \end{bmatrix} \begin{bmatrix} v_{j+1} \\ * \end{bmatrix} = \begin{bmatrix} \mathcal{V}_j \\ 0 \end{bmatrix}. \quad (4.21)$$

4 Construct orthonormal vector set $\mathcal{V}_{j+1} = [\mathcal{V}_j, v_{j+1}]$ by QR decomposition (see Subsection (2.2.3.3)) using Algorithm (2).

5 Solve the projected controllability Lyapunov equation (4.1)

$$\tilde{\mathcal{A}}_{j+1} \tilde{\mathcal{P}} \tilde{\mathcal{E}}_{j+1}^T + \tilde{\mathcal{E}}_{j+1} \tilde{\mathcal{P}} \tilde{\mathcal{A}}_{j+1}^T + \tilde{\mathcal{B}}_{j+1} \tilde{\mathcal{B}}_{j+1}^T - \tilde{\mathcal{E}}_{j+1} e^{\tilde{\mathcal{E}}_{j+1}^{-1} \tilde{\mathcal{A}}_{j+1} t_f} \tilde{\mathcal{E}}_{j+1}^{-1} \tilde{\mathcal{B}}_{j+1} (\tilde{\mathcal{E}}_{j+1}^{-1} \tilde{\mathcal{B}}_{j+1})^T e^{(\tilde{\mathcal{E}}_{j+1}^{-1} \tilde{\mathcal{A}}_{j+1})^T t_f} \tilde{\mathcal{E}}_{j+1}^T = 0$$

for finding small-scale CG \tilde{P} Where, $\tilde{\mathcal{E}}_{j+1} = \mathcal{V}_{j+1}^T \mathcal{E}_i \mathcal{V}_{j+1}$,

$$\tilde{\mathcal{A}}_{j+1} = \mathcal{V}_{j+1}^T \mathcal{A}_i \mathcal{V}_{j+1} - (\mathcal{V}_{j+1}^T \mathcal{A}_{ii}) \Xi (\mathcal{A}_{iii} \mathcal{E}_i^{-1} (\mathcal{A}_i \mathcal{V}_{j+1})),$$

$$\tilde{\mathcal{B}}_{j+1} = \begin{bmatrix} (\mathcal{V}_{j+1}^T \mathcal{B}_i) - (\mathcal{V}_{j+1}^T \mathcal{A}_i) \mathcal{E}_i^{-1} \mathcal{A}_{ii} \Xi \mathcal{B}_{ii} - (\mathcal{V}_{j+1}^T \mathcal{A}_{ii}) \Xi \mathcal{A}_{iii} \mathcal{E}_i^{-1} (\mathcal{B}_i - \mathcal{A}_i \mathcal{E}_i^{-1} \mathcal{A}_{ii} \Xi \mathcal{B}_{ii}) \\ (\mathcal{V}_{j+1}^T \mathcal{A}_{ii}) \Xi \mathcal{B}_{ii} - (\mathcal{V}_{j+1}^T \mathcal{A}_i) \Xi \mathcal{B}_{ii} \end{bmatrix}.$$

7 Compute next shift parameter μ (see Section (4.2))

8 Compute residual norm (see Section (4.4))

9 **if** residual norm $\leq tol$ **then**

10 | Stop Rational Krylov iteration.

11 Operate eigenvalue decomposition as (4.3).

12 Establish low-rank controllability Gramian factor $\mathcal{R}_{\mathcal{P}}$ as (4.4).

what is equivalent to the differential-algebraic equation of the form

$$\mathcal{E}_i \dot{g}(t) = \mathcal{A}_i g(t) + \mathcal{A}_{ii} r(t) + \mathcal{B}_i u(t),$$

$$0 = \mathcal{A}_{iii} g(t),$$

$$y(t) = \mathcal{C}_i g(t) + \mathcal{C}_{ii} r(t) + \mathcal{D} u(t).$$

After conversion from descriptor system to generalised system, the following relations are established

$$\mathcal{E} := \mathcal{E}_i, \quad \mathcal{A} := \mathcal{A}_i - \mathcal{A}_{ii} \Xi \mathcal{A}_{iii} \mathcal{E}_i^{-1} \mathcal{A}_i, \quad \mathcal{B} := \mathcal{B}_i - \mathcal{A}_{ii} \Xi \mathcal{A}_{iii} \mathcal{E}_i^{-1} \mathcal{B}_i,$$

$$\mathcal{C} := \mathcal{C}_i - \mathcal{C}_{ii} \Xi \mathcal{A}_{iii} \mathcal{E}_i^{-1} \mathcal{A}_i, \quad \mathcal{D} := \mathcal{D} - \mathcal{C}_{ii} \Xi \mathcal{A}_{iii} \mathcal{E}_i^{-1} \mathcal{B}_i.$$

Special Case 2 : When \mathcal{B}_{ii} and \mathcal{C}_{ii} both are zero in the system (2.11), the index-II system is expressed as

$$\underbrace{\begin{bmatrix} \mathcal{E}_i & 0 \\ 0 & 0 \end{bmatrix}}_{\mathcal{E}} \underbrace{\begin{bmatrix} \dot{g}(t) \\ \dot{r}(t) \end{bmatrix}}_{\dot{x}(t)} = \underbrace{\begin{bmatrix} \mathcal{A}_i & \mathcal{A}_{ii} \\ \mathcal{A}_{iii} & 0 \end{bmatrix}}_{\mathcal{A}} \underbrace{\begin{bmatrix} g(t) \\ r(t) \end{bmatrix}}_{x(t)} + \underbrace{\begin{bmatrix} \mathcal{B}_i \\ 0 \end{bmatrix}}_{\mathcal{B}} u(t),$$

$$y(t) = \underbrace{\begin{bmatrix} \mathcal{C}_i & 0 \end{bmatrix}}_{\mathcal{C}} \underbrace{\begin{bmatrix} g(t) \\ r(t) \end{bmatrix}}_{x(t)} + \mathcal{D}u(t),$$

what is equivalent to the differential-algebraic equation of the form

$$\begin{aligned} \mathcal{E}_i \dot{g}(t) &= \mathcal{A}_i g(t) + \mathcal{A}_{ii} r(t) + \mathcal{B}_i u(t), \\ 0 &= \mathcal{A}_{iii} g(t), \\ y(t) &= \mathcal{C}_i g(t) + \mathcal{D}u(t). \end{aligned}$$

After conversion from descriptor system to generalised system, the following relations are established

$$\begin{aligned} \mathcal{E} &:= \mathcal{E}_i, \quad \mathcal{A} := \mathcal{A}_i - \mathcal{A}_{ii} \Xi \mathcal{A}_{iii} \mathcal{E}_i^{-1} \mathcal{A}_i, \\ \mathcal{B} &:= \mathcal{B}_i - \mathcal{A}_{ii} \Xi \mathcal{A}_{iii} \mathcal{E}_i^{-1} \mathcal{B}_i, \quad \mathcal{C} := \mathcal{C}_i, \quad \mathcal{D} := \mathcal{D}. \end{aligned}$$

4.7 Numerical Outcomes

In this section, we assess our proposed methods on different finite time intervals applying on both index-I and index-II descriptor data models and analysis how efficient our algorithms are by calculating the required time. We also observe the convergence tendency of the iterative solution of the time-restricted Lyapunov equations by computing residual norms at each iteration and numerical error of time-restricted and unrestricted solutions of the Lyapunov equations on our nominated time segments.

All of the following results are carried out on the computational machine comprised of Intel® Core™ i5 1.80 GHz base clock speed with RAM 8 GB.

4.7.1 Numerical Results from Index-I Descriptor System

In this subsection, we attach the numerical outcomes found after solving the time-restricted Lyapunov equations of index-I systems by proposed Algorithm (8) on time interval $[0, t_f]$. The dimensions of our generated and selected data models have already are enlisted in Tables (3.1), (3.2), and (3.3).

The sparsity and dense patterns of the state matrix \mathcal{A} of some of our nominated data models are illustrated in Figures (4.1), (4.2), and (4.3). If we closely look into the figures, it will be visible that number of non-zero quantities, indicated by nz in figures, of dense matrices is greater than that of the sparse matrices. As a result, the computational time is increased during dealing with dense matrix. However, we develop the Algorithm (8) for not only minimizing the error on

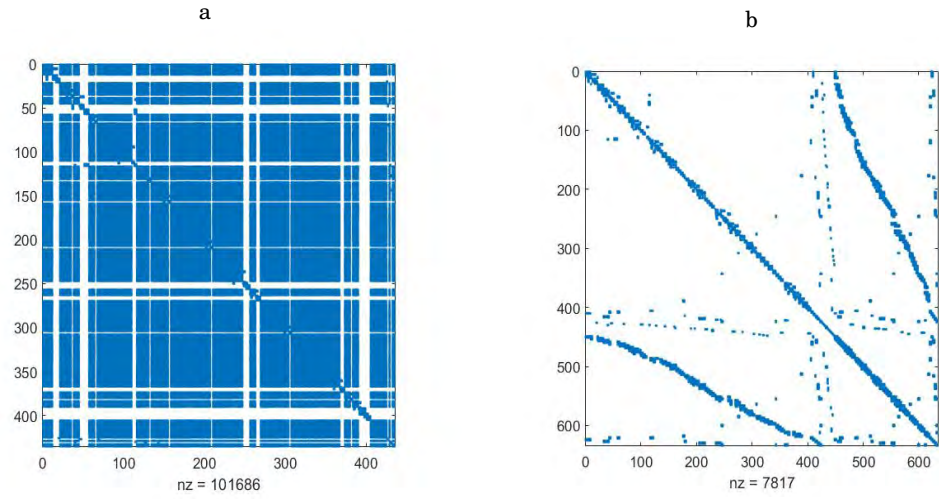


Figure 4.1: (a) Dense Pattern and (b) Sparse Pattern of Power system model

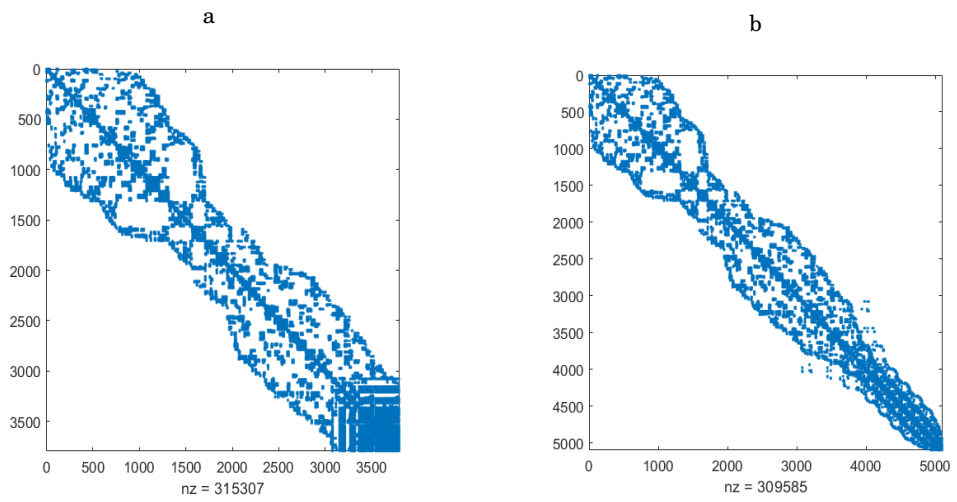


Figure 4.2: (a) Dense Pattern and (b) Sparse Pattern of Piezoelectric Tonpilz Transducer model

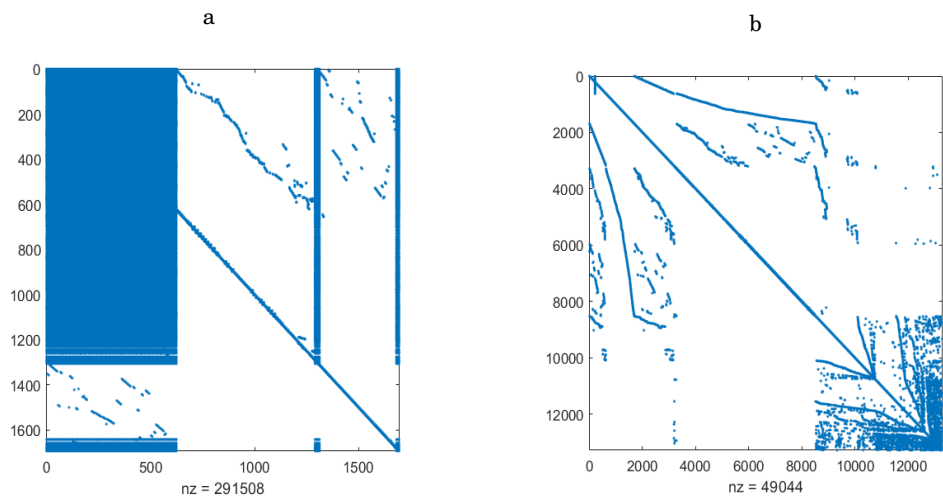


Figure 4.3: (a) Dense Pattern and (b) Sparse Pattern of BIPS-1693 model

restricted time interval but reducing the calculation period also.

To minimize the calculating period, our proposed algorithm solves the linear system as (4.8) strongly retaining the sparsity of the system matrices. Looking attentively at Table (4.2), it is

Table 4.2: Required Time for the computation of linear systems of sparse and dense system

Model	Required Time (Sec)				Saving time (%)	
	CG		OG		CG	OG
	Sparse	Dense	Sparse	Dense		
BIPS-606	0.1618	0.8213	0.105	0.586	19.7	17.91
BIPS-1142	0.1325	1.25	0.126	.95	10.6	13.26
BIPS-1693	0.45	1.95	0.56	1.98	23.07	28.28
Power System	0.24	0.87	0.35	0.97	27.58	36.08
Piezo Tonpilz Transducer	0.72	0.92	0.611	0.75	78.26	81.4

easily observed that the linear system of sparse system calculating by our proposed algorithm reduces the computational time at every case and thus the entire calculation process boosts up.

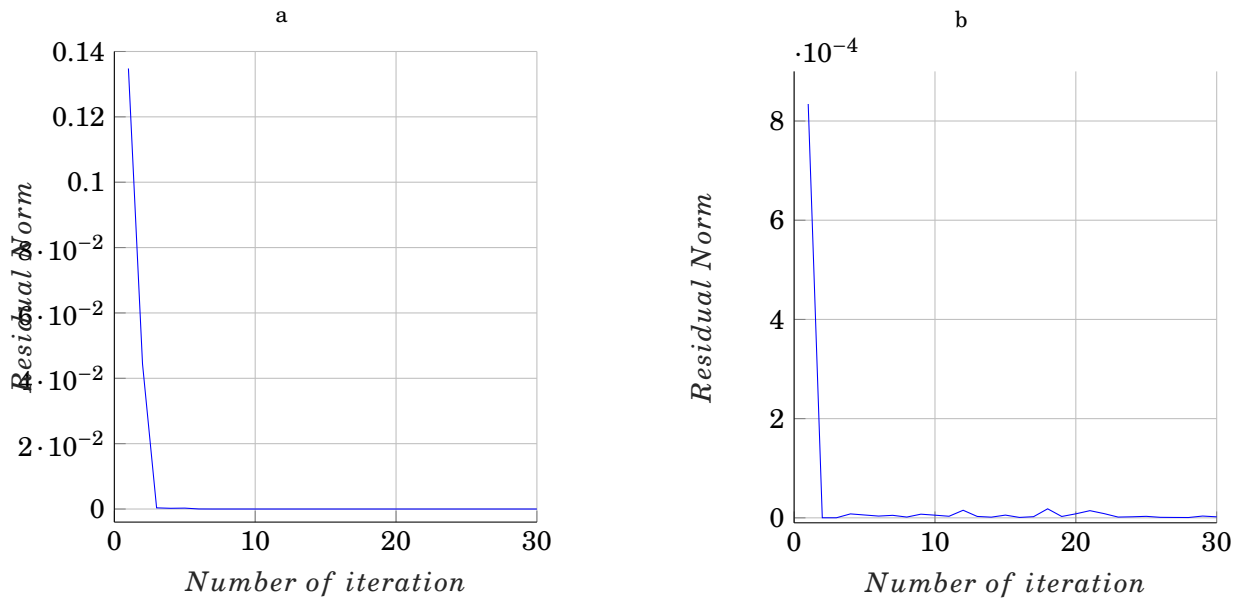


Figure 4.4: Convergence tendency of (a) CG and (b) OG of BIPS-606

Figures (4.4), (4.5), (4.6), and (4.7) demonstrate the convergence tendency of controllability and observability Gramians on restricted time intervals found by imposing our Algorithm (8). Since the total process largely depends on proper selection of shift parameters, we try to apply the best shift selection method (see Section 4.2) for finding fast convergence solution within minimal iterations. If we see the convergence figures, it will be noticed that in most of the cases averagely we can get better low-rank solution within 30 iterations. It is also visible that averagely after 10 – 15 iterations, the residual norms become so closed to zero that the line graph fluctuates little. As a result, it is also proposed that one can choose less number of iteration than ours by setting up the tolerance value high. But the sparsity patterns of the system matrices may vary the number of iterations.

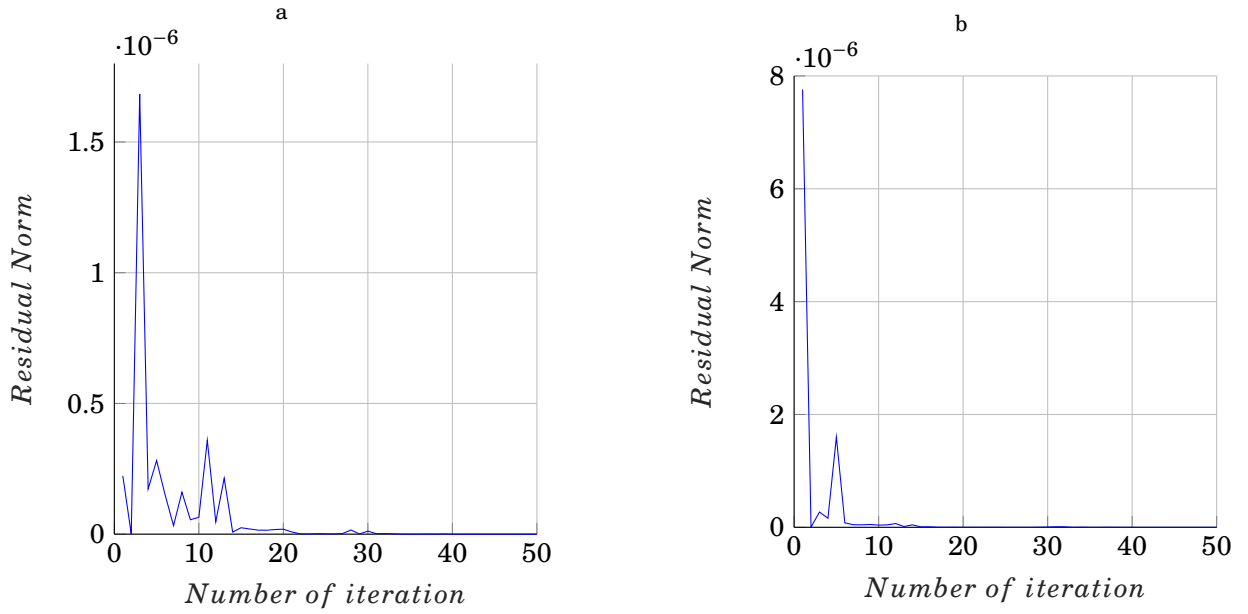


Figure 4.5: Convergence tendency of (a) CG and (b) OG of BIPS-1142

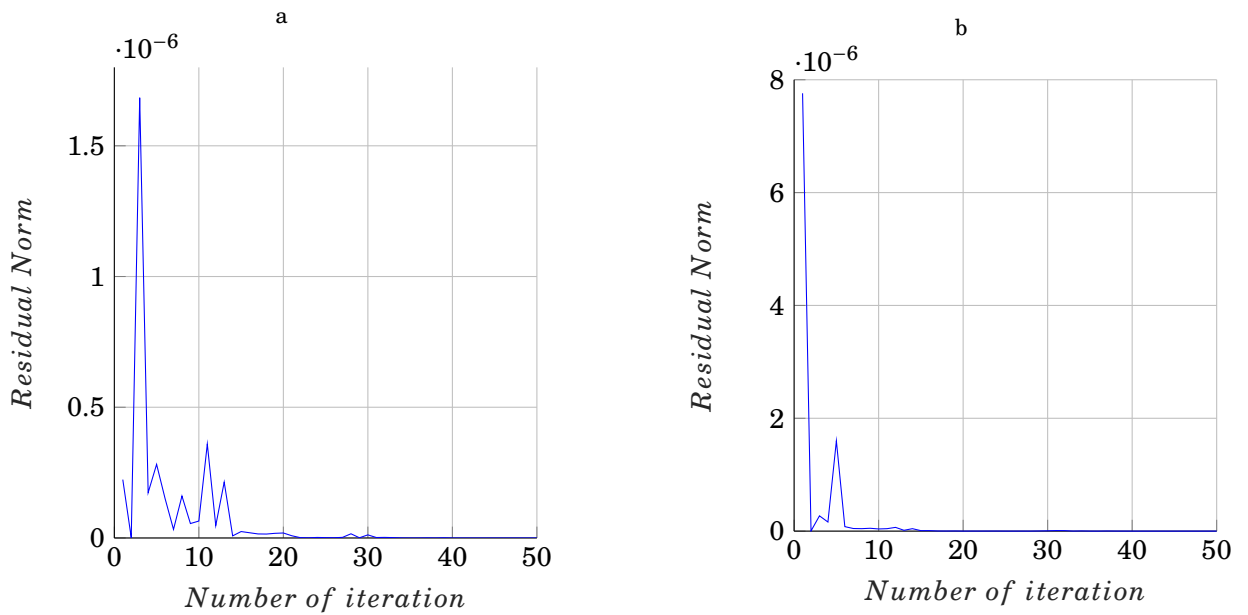


Figure 4.6: Convergence tendency of (a) CG and (b) OG of BIPS-1693

Moreover, we calculate the residual norms of the time-restricted CG and OG following the process described in Section (4.4) on finite time intervals and compare them with the time infinite low-rank CG and OG. Table (4.3) includes the comparison between the residual norms what clearly reflects that on finite time intervals time-restricted solutions of Lyapunov equations minimize more residual norm, i.e., more convergence than the solutions of time infinite Lyapunov equations. Therefore, our proposed algorithm gives more accurate approximated solutions of the original solutions of Lyapunov equations on nominated time intervals.

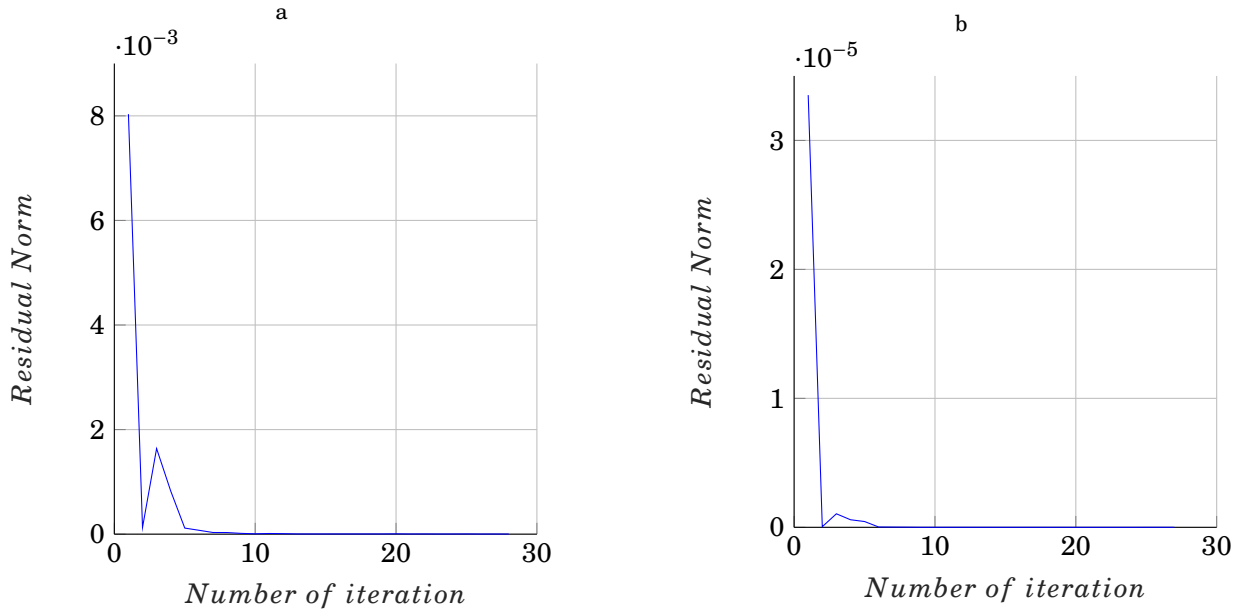


Figure 4.7: Convergence tendency of (a) CG and (b) OG of Piezo Tonpiliz Transducer

Table 4.3: Residual norms of time restricted and unrestricted CG and OG on nominated time intervals

Model	Time Interval	Residual Norm			
		CG		OG	
		t	∞	t	∞
BIPS-606	[0,4]	2.1×10^{-2}	2.10	1.23×10^{-4}	3.5×10^{-2}
BIPS-1142	[0,5]	1.5×10^{-5}	2.22×10^{-4}	2.01×10^{-6}	5.6×10^{-3}
BIPS-1693	[0,7]	3.7×10^{-4}	1×10^{-2}	2.9×10^{-4}	1×10^{-3}
Piezo Tonpiliz Transducer	[0,5]	8.5×10^{-3}	1.063×10^{-1}	1.23×10^{-4}	5.37×10^{-2}

4.7.2 Numerical Results from Index-I Descriptor System on Non-homogeneous Time intervals

This subsection consists of the numerical outcomes of the solutions of the time-restricted Lyapunov equations on non-homogeneous time intervals $[t_0, t_f]$ for testing the efficiency of our proposed Algorithm (9).

Figures (4.8) and (4.9) illustrate the convergence tendency of CG and OG on non-homogeneous time interval applying our proposed Algorithm (9). Unlike the convergence histories of the time-restricted CG and OG on homogeneous time intervals, it is seen from the figures that the solutions are not fast converged. Therefore, we need to run more iterative loops to find convergent solutions what makes the entire procedures slightly slow. While the controllability Gramians have strong tendency to converge to zero gradually by declining the line graph to the zero with the increment of iterations, the observability Gramians have less tendency to become convergent. Hence, computing OG needs more iterative loops rather than CG computation. However, looking at the Table (4.4), it is undoubtedly said that like the solutions of Lyapunov equations on homogeneous time intervals, the time-restricted low-rank CG and OG also minimize the norms

on non-homogeneous time segments. Therefore, our proposed algorithm for the treatment of the solutions of Lyapunov equations on time intervals having non-zero initial conditions also gives satisfactory low-rank approximated solutions of the original solutions of the Lyapunov equations.

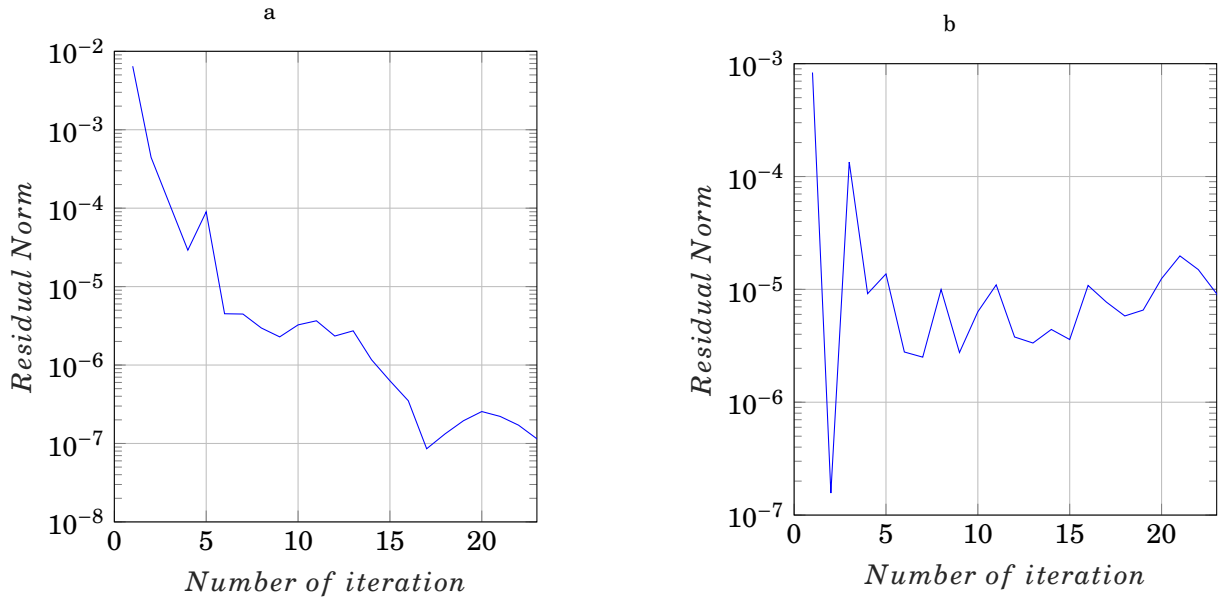


Figure 4.8: Convergence tendency of (a) CG and (b) OG of BIPS-606 on non-homogeneous time interval

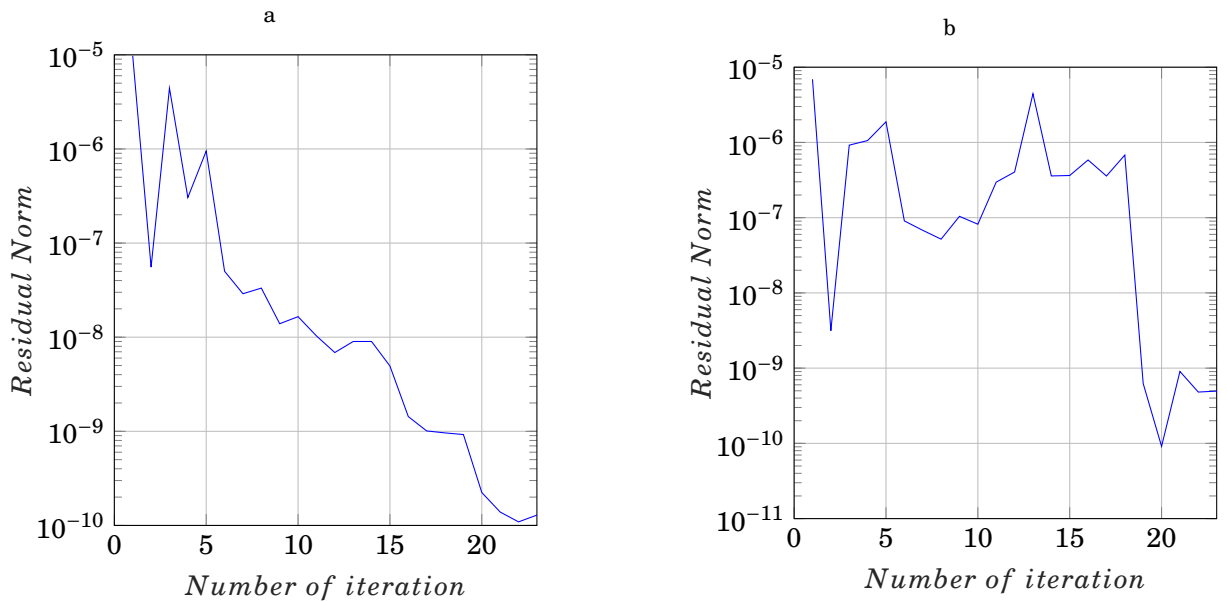


Figure 4.9: Convergence tendency of (a) CG and (b) OG of BIPS-606 on non-homogeneous time interval

4.7.3 Numerical Results from Index-II Descriptor System

The numerical outcomes on finite time segments of another important class of descriptor system known as index-II system are included in this subsection whose dimensions are described

Table 4.4: Residual norms of time restricted and unrestricted CG and OG on nominated time intervals

Model	Time Interval	Residual Norm			
		CG		OG	
		t	∞	t	∞
BIPS-606	[2,4]	0.00647	0.0648	0.00084	0.0073
BIPS-1693	[1,3]	1.07×10^{-5}	3.46×10^{-4}	8.6×10^{-6}	7.04×10^{-5}

in Table (3.4).

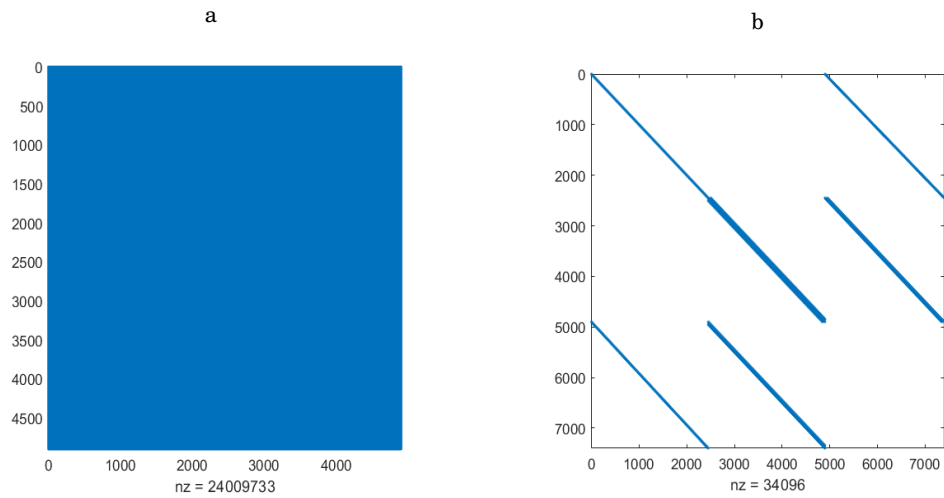


Figure 4.10: (a) Dense Pattern and (b) Sparse Pattern of Ossen model

To retain the sparsity without making the linear system denser with a view to dealing with less amount of non-zero elements, we propose another Algorithm (10) what successfully reduces the entire computational time along with minimizing the residual norms. Table (4.5) upholds the same image in front of us indicating around 97% of total computational time is reduced by our algorithm.

Table 4.5: Required Time for the computation of linear systems of sparse and dense index-II system

Model	Required Time (Sec)				Saving time (%)	
	CG		OG		CG	OG
	Sparse	Dense	Sparse	Dense		
Ossen model	0.0801	2.9025	0.125	4.503	97.24	97.22

Table 4.6: Residual norms of time restricted and unrestricted CG and OG on nominated time intervals

Model	Time Interval	Residual Norm			
		CG		OG	
		t	∞	t	∞
Ossen	[0,5]	0.00038	0.0053	0.00881	0.0925

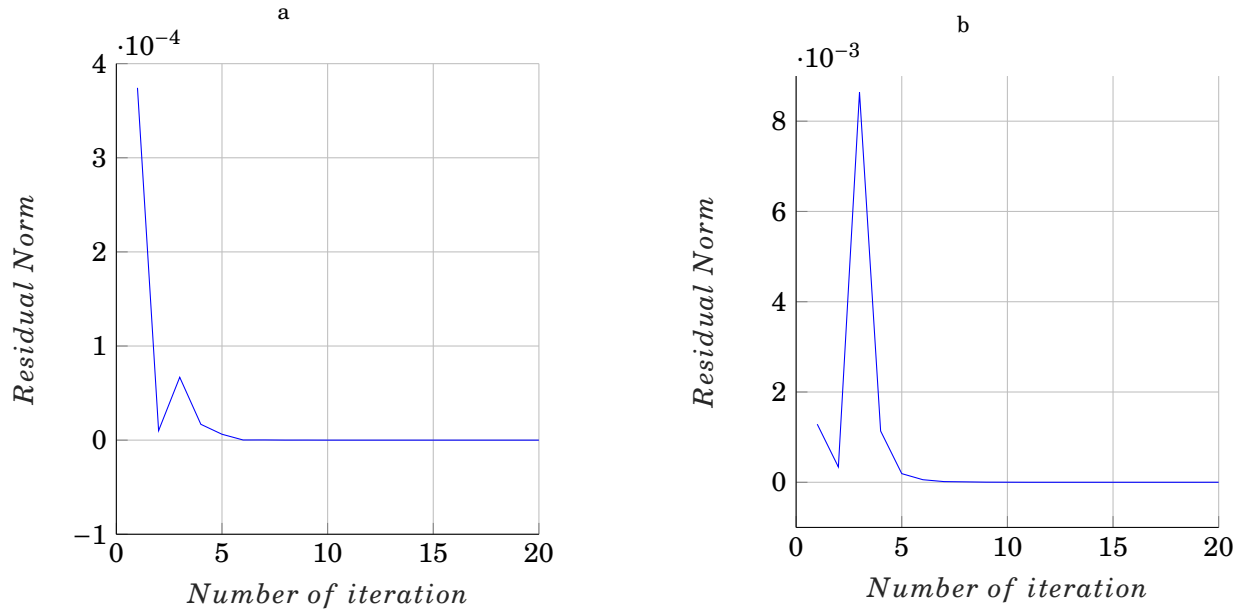


Figure 4.11: Convergence tendency of (a) CG and (b) OG of Ossen model

In addition, after convergence analysis and observing the Figure (4.11) like index-I system, our proposed algorithm also find convergent solution of Lyapunov equations of index-II data model on limited time intervals within shortest possible iteration what may change based on the nature of the system matrices and may speed up more by taking tolerance value higher.

Finally, Table (4.6) enlists the comparison between the residual norms of the time-restricted and time-unrestricted CG and OG what visualizes that like, index-I, our Algorithm (10) successfully minimizes the norms of the solutions of Lyapunov equations of index-II system on limited time intervals than the infinite Gramians of Lyapunov equations. Hence, the solutions got from our algorithm surely gives more accurate low-rank solutions of the original full-rank solution.

SOLUTION OF LYAPUNOV EQUATIONS ON RESTRICTED FREQUENCY INTERVALS BY ITERATIVE METHOD

Introduction

Like the solution of time-restricted Lyapunov equations, it is also important to solve Lyapunov equation on restricted frequency interval to deal with practical problems, especially signal processing analysis. Although few works have been taken place to find the solution of Lyapunov equation of dense small standard or generalised state-space systems on finite frequency interval [12, 37, 39] what are the previous topics of our discussion (see Section 2.3), no work has till done on the solution of the Lyapunov equations constructed on large-sparse dynamic system. In this chapter, we mainly focus on the efficient computation procedure of the low-rank solution of large-scale Lyapunov equations on finite frequency intervals constructed around two special types of large-scale sparse descriptor systems of the form (2.10) and (2.11) known as index-I and index-II descriptor system respectively. Like previous chapter, at here we also pay our attention on RKSM for its efficiency during solving large-scale systems. We propose algorithms for finding the Gramian of large-scale index-I and index-II descriptor systems on finite frequency interval. Since we deal with large-scale system, to increase the computational efficiency we compute low-rank solution factors instead of finding full-rank solution. Proper selection of shift parameters is a vital operation in RKSM method. For that reason, we introduce a new approach of finding shift parameters using renowned genetic algorithm with a view to finding best approximation and less faulty solutions on restricted frequency intervals. We also inspect the procedure of computing matrix logarithm inevitable part for solving frequency restricted Lyapunov equation in order to increase the efficiency of the computational algorithms.

5.1 Rational Krylov Subspace Method for Generalised Frequency-restricted Lyapunov Equation

Since we have already discussed the basic properties of RKSM method (see Section 4.1), at here we start with recalling the frequency restricted Lyapunov equation pairs on frequency

interval $[\Omega_0, \Omega_f]$ (2.33a) and (2.33b)

$$\begin{aligned} \mathcal{A} \mathcal{M} \mathcal{E}^T + \mathcal{E} \mathcal{M} \mathcal{A}^T + \mathcal{E} \phi(i\omega) \mathcal{B} \mathcal{B}^T + \mathcal{B} \mathcal{B}^T \phi^*(i\omega) \mathcal{E}^T &= 0 \\ \mathcal{A}^T \mathcal{N} \mathcal{E} + \mathcal{E}^T \mathcal{N} \mathcal{A} + \xi^*(i\omega) \mathcal{E}^T \mathcal{C}^T \mathcal{C} + \mathcal{C}^T \mathcal{C} \xi(i\omega) &= 0 \end{aligned}$$

where, $\phi(i\omega) = (\phi(i\Omega_f) - \phi(i\Omega_0))$, $\xi(i\omega) = (\xi(i\Omega_f) - \xi(i\Omega_0))$, $\phi(i\Omega) = \frac{i}{2\pi} [\ln(-i\Omega \mathcal{E} - \mathcal{A}) - \ln(i\Omega \mathcal{E} - \mathcal{A})] \mathcal{E}^{-1}$, and $\xi(i\Omega) = \frac{i}{2\pi} \mathcal{E}^{-1} [\ln(-\mathcal{E} i\Omega - \mathcal{A}) - \ln(\mathcal{E} i\Omega - \mathcal{A})]$.

Applying the Galerkin condition on frequency-restricted Controllability Lyapunov equation (2.33a), we can write the projected frequency-restricted controllability equation as

$$\tilde{\mathcal{A}} \tilde{\mathcal{M}} \tilde{\mathcal{E}}^T + \tilde{\mathcal{E}} \tilde{\mathcal{M}} \tilde{\mathcal{A}}^T + \tilde{\mathcal{E}} \tilde{\phi}(i\omega) \tilde{\mathcal{B}} \tilde{\mathcal{B}}^T + \tilde{\mathcal{B}} \tilde{\mathcal{B}}^T \tilde{\phi}^*(i\omega) \tilde{\mathcal{E}}^T = 0, \quad (5.1)$$

where, $\tilde{\mathcal{M}} = \mathcal{V}^T \mathcal{M} \mathcal{V}$, $\tilde{\mathcal{E}} = \mathcal{V}^T \mathcal{E} \mathcal{V}$, $\tilde{\mathcal{A}} = \mathcal{V}^T \mathcal{A} \mathcal{V}$, $\tilde{\mathcal{B}} = \mathcal{V}^T \mathcal{B}$, $\tilde{\phi}(i\omega) = (\tilde{\phi}(i\Omega_f) - \tilde{\phi}(i\Omega_0))$, and $\tilde{\phi}(i\Omega) = \frac{i}{2\pi} [\ln(i\Omega \tilde{\mathcal{E}} - \tilde{\mathcal{A}}) - \ln(-i\Omega \tilde{\mathcal{E}} - \tilde{\mathcal{A}})] \tilde{\mathcal{E}}^{-1}$. Here, \mathcal{V} is the orthogonal basis of rational Krylov subspace. Similarly, the projected observability Lyapunov equation can be reformed from (2.33b) as

$$\tilde{\mathcal{A}}^T \tilde{\mathcal{N}} \tilde{\mathcal{E}} + \tilde{\mathcal{E}}^T \tilde{\mathcal{N}} \tilde{\mathcal{A}} + \xi^*(i\omega) \tilde{\mathcal{E}}^T \tilde{\mathcal{C}}^T \tilde{\mathcal{C}} + \tilde{\mathcal{C}}^T \tilde{\mathcal{C}} \xi(i\omega) = 0, \quad (5.2)$$

where, $\tilde{\mathcal{C}} = \mathcal{C} \mathcal{V}$, $\tilde{\xi}(i\omega) = (\tilde{\xi}(i\Omega_f) - \tilde{\xi}(i\Omega_0))$, and $\tilde{\xi}(i\Omega) = \frac{i}{2\pi} \tilde{\mathcal{E}}^{-1} [\ln(-\tilde{\mathcal{E}} i\Omega - \tilde{\mathcal{A}}) - \ln(\tilde{\mathcal{E}} i\Omega - \tilde{\mathcal{A}})]$. Likewise, time-limited Lyapunov equations, due to the small-scale conversion of the projected equation (5.1), it can be solved directly. As it is low-rank solution, we can retrieve the original solution by Gaussian back substitution as

$$\mathcal{M} = \mathcal{V} \tilde{\mathcal{M}} \mathcal{V}^T$$

where, $\tilde{\mathcal{M}}$ is the low-rank solution of frequency-restricted controllable Lyapunov equation found by RKSM method and conducting eigenvalue decomposition as

$$\tilde{\mathcal{M}} = (\mathbf{V} \Lambda^{\frac{1}{2}}) (\mathbf{V} \Lambda^{\frac{1}{2}})^T$$

Combining altogether, we can get the low-rank controllable Gramian factor $\mathcal{R}_{\mathcal{M}}$ as

$$\begin{aligned} \mathcal{M} &= (\mathcal{V} \mathbf{V} \Lambda^{\frac{1}{2}}) (\mathbf{V} \Lambda^{\frac{1}{2}} \mathcal{V}^T)^T \\ &= \mathcal{R}_{\mathcal{M}} \mathcal{R}_{\mathcal{M}}^T, \end{aligned}$$

Since the observable Lyapunov equation is dual of the controllable equation, we just take the transposes of the system matrices during solving the projected observable Lyapunov equation (5.2) on restricted frequency interval using the same Algorithm (11) and then get the low-rank observability Gramian factor $\mathcal{L}_{\mathcal{N}}$ written as $\mathcal{N} = \mathcal{L}_{\mathcal{N}} \mathcal{L}_{\mathcal{N}}^T$.

5.2 Selection of Shift Parameters Using Genetic Algorithm

Error minimization and fast convergence solutions of system's equations by RKSM method are largely depended on the proper selection of shift parameters. But unfortunately, there is no definite exact method introduced for shift parameter computations. Many works have been done [22, 34, 65] in search of shift parameters. We have already discussed one of the shift parameter selection processes (see Section 4.2) what we have partially applied in this thesis. However, with

Algorithm 11: RKSM for solving frequency-restricted controllability Gramian (2.33a) of generalised system (2.2) on frequency interval $[\Omega_0, \Omega_f]$.

Input: $\mathcal{E}, \mathcal{A}, \mathcal{B}, m_{it}$ (no. of iteration), Ω_0 (initial point of frequency interval), Ω_f (endpoint of frequency interval), $0 < tol \ll 1$ (tolerance value), μ_1 (initial shift parameter).

Output: $\mathcal{R}_{\mathcal{M}} \in \mathbb{R}^{n \times z}$ such that $\mathcal{R}_{\mathcal{M}} \mathcal{R}_{\mathcal{M}}^T \approx \mathcal{M}$, where $z \ll n$.

1 set initial basis vector $v_1 = (\mathcal{A} - \mu_1 \mathcal{E})^{-1} \mathcal{B}$, $\mathcal{V}_1 = \frac{v}{\|v\|}$

2 **while** $j \leq m_{it}$ **do**

3 Find the next basis matrix by solving linear system $(\mathcal{A} - \mu_j \mathcal{E}) v_{j+1} = \mathcal{V}_j$.

4 Construct orthonormal vector set $\mathcal{V}_{j+1} = [\mathcal{V}_j, v_{j+1}]$ by QR decomposition (see Subsection (2.2.3.3)) using Algorithm (2).

5 Solve the projected controllability Lyapunov equation (5.1)

$$\tilde{\mathcal{A}}_{j+1} \tilde{\mathcal{M}} \tilde{\mathcal{E}}_{j+1}^T + \tilde{\mathcal{E}}_{j+1} \tilde{\mathcal{M}} \tilde{\mathcal{A}}_{j+1}^T + \tilde{\mathcal{E}}_{j+1} \tilde{\Phi}_{j+1}(i\omega) \tilde{\mathcal{B}}_{j+1} \tilde{\mathcal{B}}_{j+1}^T + \tilde{\mathcal{B}}_{j+1} \tilde{\mathcal{B}}_{j+1}^T \tilde{\Phi}_{j+1}^*(i\omega) \tilde{\mathcal{E}}_{j+1}^T = 0$$

for finding small-scale CG $\tilde{\mathcal{M}}$ Where, $\tilde{\mathcal{E}}_{j+1} = \mathcal{V}_{j+1}^T \mathcal{E} \mathcal{V}_{j+1}$, $\tilde{\mathcal{A}}_{j+1} = \mathcal{V}_{j+1}^T \mathcal{A} \mathcal{V}_{j+1}$,

$$\tilde{\mathcal{B}}_{j+1} = \mathcal{V}_{j+1}^T \mathcal{B}.$$

6 Compute next shift parameter μ (see Section (5.2))

7 Compute residual norm (see Section (5.4))

8 **if** residual norm $\leq tol$ **then**

9 Stop Rational Krylov iteration.

10 Operate eigenvalue decomposition

$$\tilde{\mathcal{M}} = \begin{bmatrix} \mathbf{V}_1 & \mathbf{V}_2 \end{bmatrix} \begin{bmatrix} \Lambda_1 & \\ & \Lambda_2 \end{bmatrix} \begin{bmatrix} \mathbf{V}_1 & \mathbf{V}_2 \end{bmatrix}^T \quad (5.3)$$

11 Establish low-rank controllability Gramian factor

$$\mathcal{R}_{\mathcal{M}} = \mathcal{V}_{j+1} \mathbf{V}_1 \Lambda_1^{\frac{1}{2}} \quad (5.4)$$

after truncating less effective eigenvalues Λ_2 .

a view to minimizing error more by maximizing the efficiency of the computation, we introduce a new shift parameter selection approach here using the evolutionary algorithm what is more specifically known as genetic algorithm.

Genetic algorithm is commonly used to generate solutions to optimization and search problems what is developed inspired from the biological doctrine 'Theory of Evolution' relying on biological operators selection, crossover, and mutation [94–96]. It is a metaheuristic algorithm what is largely functioned using various probabilistic parameters to find the convergent solutions through gradually updating and analysing the patterns of inserting data. The algorithm is primarily initiated with generating random search space (called population) whose properties (called chromosome) are evaluated through fitness function. The unsatisfactory population go through the selection process to find the best fit couples (known as parents) for crossover operation with a view to generating new candidate solution (known as Off-springs) what are participated to mutation process for maintaining the genetic diversity from one generation to another. Then they merge to the previous population for upgrading the search space and take part into evolution process. In these steps, the iterative loop (called generation) is run until a satisfactory fitness

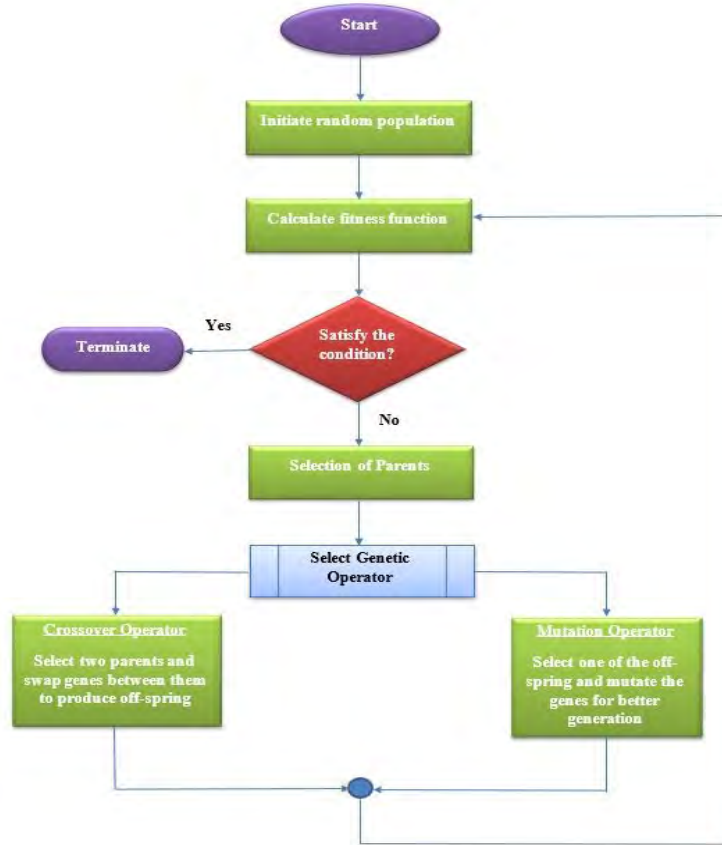


Figure 5.1: Flow chart of genetic algorithm

level has been reached. Flow chart (5.1) illustrates the whole procedure of genetic algorithm. However, we apply this total idea in search of generating proper shift parameters during solving linear system (4.8, 4.9, 4.21, 4.22) in order to minimize error more on finite frequency interval. We have taken classical min-max problem describing in [65] written as

$$\min_{\alpha_1, \dots, \alpha_m} \left\| \max_{1 \leq l \leq n} \prod_{j=1}^m \frac{\alpha_j - \lambda_l}{\alpha_j + \lambda_l} \right\|. \quad (5.5)$$

as our fitness function to evaluate the population of the search space, where λ is the Ritz values of the projected small-scale system matrices $(\Lambda(\tilde{\mathcal{A}}, \tilde{\mathcal{E}}))$. But computing Ritz values at each iteration makes the entire computational process costly. As a result, we have taken the total numbers of Ritz values, we required, at the initial stage computing by Algorithm (2). As it is a probabilistic algorithm, the effectiveness largely depends on the population size, the distribution density function, the mean and variance of the crossover and mutation processes. We follow uniform distribution function here during crossover for creating off-springs and normal distribution having σ variance and 0 mean for mutation. The reason behind choosing these functions is for ensuring each and every possible candidate solution inside our predefined Ritz value intervals so that nothing exceeds the Ritz value domain. However, one can change the parameters and take other types of distribution function for analytical purpose. Algorithm (12) summarizes the step by step procedure of the calculating shift parameter by genetic algorithm. One of the key operations of

Algorithm 12: Selection of Shift Parameters using Genetic Algorithm

Input: nP (No. of Population), σ (Variance of distribution), nC (No. of off-springs), gc (Mutation Parameter), β (permutation rate), ub (Ritz Value of largest Magnitude), lb (Ritz Value of smallest Magnitude), λ (Predefined Ritz values)

Output: μ

```

1 Initiate search space  $nP$  no. of rows and 1 column containing candidate solutions.
2 for  $i = 1 : nP$  do
3   Choose random interpolate points  $\alpha$  in the intervals  $lb \leq \alpha \leq ub$  as candidate solutions.
4   Evaluate each  $\alpha$  by min-max problem (5.5) and calculate  $Cost$  .
5   Set best solution  $bs = inf$ .
6   if  $Cost < bs$  then
7     Update best solution as  $bs = Cost$ .
8      $\mu_i = \alpha$ .
9   else
10    Initiate matrix of off-spring having  $nC$  rows and 2 columns.
11    for  $k = 1 : nC$  do
12      Select best couples  $P1$  and  $P2$  from search space for crossover.
13      Generate random matrix  $p$  of size  $P1$  or  $P2$  having permutation rate  $\beta$ .
14      Produce off-spring as
          
$$pC(k,1) = pP1 + (1-p)P2,$$

          
$$pC(k,2) = pP2 + (1-p)P1.$$

15      for  $l = 1 : 2$  do
16        Create random matrix of logical values  $L$  of size  $pC$  less than  $gc$ .
17        Perform mutation as
          
$$MpC(:,l) = pC(L) + \sigma rand(size(L))$$

18      Update Search space merging new mutants, sorting and truncating unfit population.
19      Again, choose random interpolate points  $\alpha$  in the intervals  $lb \leq \alpha \leq ub$  from updating search space.
20      repeat the process of line (4).
21      if  $Cost < bs$  then
22        Update best solution as  $bs = Cost$ .
23         $\mu_i = \alpha$ .

```

this algorithm is to select best couples $P1$ and $P2$ in line (12). One can pick them randomly in each iteration. However, it is not a good way of selection. At here, we pick the two best candidate solutions $P1$ and $P2$ as best parents and cross them over each other using uniform distribution functions as line (14) to produce two off-springs $pC1$ and $pC2$.

We assign uniform distribution function to perform crossover. Then we conduct mutation process to modify the off-springs through Gaussian distribution function. To keep the off-spring into our nominated range, we take zero mean with σ variance what may be varied according to the nature of the system data. Finally, we combine our newly produced off-spring to the existing population and update them by truncating less fit candidate solution. This process is repeated

until finding our desired number of shift parameters.

5.3 Computation of Matrix Logarithm

One of the most critical part in computing the solution of frequency restricted Lyapunov equation is the computation of matrix logarithm. There are several works been done during last few decades for finding the efficient computation of matrix logarithm. Although all of them are appropriate for computing the logarithm of dense matrix, unfortunately none of them is perfectly applicable on large-scale sparse matrix. In this thesis, we inspect two existing logarithmic algorithms and apply them during finding the solution of Lyapunov equations on limited frequency intervals. Firstly, we impose the algorithm described in [42, 97]. There, the authors applied inverse scaling and squaring method written as

$$\log(\mathcal{A}) = 2^s \log(\mathcal{A}^{\frac{1}{2^s}}),$$

what is just opposite to the the scaling and squaring method, we applied during the computation of matrix exponential. Then they applied Padé approximation of matrix logarithm [98] written as partial fraction form

$$r_m(x) = \frac{P_m(x)}{Q_m(x)} = \sum_{j=1}^m \frac{\alpha_j^{(m)} x}{\beta_j^{(m)} x - 1},$$

where, $\alpha_j^{(m)}$ are the weights and the $\beta_j^{(m)}$ are the nodes of the mid-point found using Gauss-Legendre quadrature rule [99, 100]. They used Denman-Beavers [60] method (see Subsubsection 2.2.5.3) to compute the square root of the matrices. However, their proposed method works well for dense matrices but is not efficient for computing the logarithm of sparse matrices since the square root method, they followed, needs explicit inversion of the inserted matrix. As a result, the entire process becomes costly. In addition, although the algorithm proposed in [98] is appropriate of the real matrices, it approximates poorly the logarithm of complex matrix having the real part of the eigenvalues are on the negative x-half plane. Nevertheless, we apply their algorithm for few of our data models having eigenvalues of positive real part during finding the solution of the Lyapunov equation on frequency intervals with a view to minimizing error more on finite frequency interval since Padé approach gives better approximation of the matrix logarithm than typical algorithm. Since we need to find out the logarithm of complex matrices $(i\Omega\mathcal{E} - \mathcal{A})$ and $(-i\Omega\mathcal{E} - \mathcal{A})$ and there is no guarantee of the system matrices having eigenvalues of positive real part, we need to compute general value logarithm (see Subsection 2.2.6) most of the time rather than computing principle value logarithm. As a result, we follow eigenvalue decomposition (see Subsubsection 2.2.6.1) as an alternative way to deal with matrix logarithm having no eigenvalue restriction. The main problem of this method is that it makes the entire system matrices dense before computing logarithm. Therefore, it increases the cost of the algorithm with respect of memory. However, this process of computation requires less time comparing with the Padé approximation process stapled in [42, 98]. The reason is that it is a direct decomposition method while Padé approximation is an iterative searching method. We, basically, impose both of these processes in this thesis based on the nature and sparsity patterns of the data models.

Algorithm 13: RKSM for solving frequency-restricted controllability Gramian (2.33a) of index-I system (2.10) on frequency interval $[\Omega_0, \Omega_f]$.

Input: $\mathcal{E}_i, \mathcal{E}_{ii}, \mathcal{A}_i, \mathcal{A}_{ii}, \mathcal{A}_{iii}, \mathcal{A}_{iv}, \mathcal{B}_i, \mathcal{B}_{ii}, m_{it}$ (no. of iteration), Ω_0 (initial point of frequency interval), Ω_f (endpoint of frequency interval), $0 < tol \ll 1$ (tolerance value), μ_1 (initial shift parameter).

Output: $\mathcal{R}_{\mathcal{M}} \in \mathbb{R}^{n \times z}$ such that $\mathcal{R}_{\mathcal{M}} \mathcal{R}_{\mathcal{M}}^T \approx \mathcal{M}$, where $z \ll n$.

1 set initial basis vector $v_1 = \begin{bmatrix} \mathcal{A}_i - \mu_1 \mathcal{E}_i & \mathcal{A}_{ii} - \mu_1 \mathcal{E}_{ii} \\ \mathcal{A}_{iii} & \mathcal{A}_{iv} \end{bmatrix}^{-1} \begin{bmatrix} \mathcal{B}_i \\ \mathcal{B}_{ii} \end{bmatrix}$, $\mathcal{V}_1 = \frac{v}{\|v\|}$

2 **while** $j \leq m_{it}$ **do**

3 Find the next basis matrix by solving linear system

$$\begin{bmatrix} \mathcal{A}_i - \mu_j \mathcal{E}_i & \mathcal{A}_{ii} - \mu_j \mathcal{E}_{ii} \\ \mathcal{A}_{iii} & \mathcal{A}_{iv} \end{bmatrix} \begin{bmatrix} v_{j+1} \\ * \end{bmatrix} = \begin{bmatrix} \mathcal{V}_j \\ \mathbf{0} \end{bmatrix}.$$

4 Construct orthonormal vector set $\mathcal{V}_{j+1} = [\mathcal{V}_j, v_{j+1}]$ by QR decomposition (see Subsection (2.2.3.3)) using Algorithm (2).

5 Solve the projected controllability Lyapunov equation (5.1)

$$\tilde{\mathcal{A}}_{j+1} \tilde{\mathcal{M}} \tilde{\mathcal{E}}_{j+1}^T + \tilde{\mathcal{E}}_{j+1} \tilde{\mathcal{M}} \tilde{\mathcal{A}}_{j+1}^T + \tilde{\mathcal{E}}_{j+1} \tilde{\phi}_{j+1}(i\omega) \tilde{\mathcal{B}}_{j+1} \tilde{\mathcal{B}}_{j+1}^T + \tilde{\mathcal{B}}_{j+1} \tilde{\mathcal{B}}_{j+1}^T \tilde{\phi}_{j+1}^*(i\omega) \tilde{\mathcal{E}}_{j+1}^T = \mathbf{0}$$

for finding small-scale CG $\tilde{\mathcal{M}}$ Where, $\tilde{\mathcal{E}}_{j+1} = \mathcal{V}_{j+1}^T \mathcal{E}_i \mathcal{V}_{j+1} - (\mathcal{V}_{j+1}^T \mathcal{E}_{ii}) \mathcal{A}_{iv}^{-1} (\mathcal{A}_{iii} \mathcal{V}_{j+1})$,

$$\tilde{\mathcal{A}}_{j+1} = \mathcal{V}_{j+1}^T \mathcal{A}_i \mathcal{V}_{j+1} - (\mathcal{V}_{j+1}^T \mathcal{A}_{ii}) \mathcal{A}_{iv}^{-1} (\mathcal{A}_{iii} \mathcal{V}_{j+1}), \tilde{\mathcal{B}}_{j+1} = \begin{bmatrix} \mathcal{V}_{j+1}^T \mathcal{B}_i - (\mathcal{V}_{j+1}^T \mathcal{A}_{ii}) \mathcal{A}_{iv}^{-1} \mathcal{B}_{ii} \\ (\mathcal{V}_{j+1}^T \mathcal{E}_{ii}) \mathcal{A}_{iv}^{-1} \mathcal{B}_{ii} \end{bmatrix},$$

$$\tilde{\phi}(i\omega) = (\tilde{\phi}(i\Omega_f) - \tilde{\phi}(i\Omega_0)), \text{ and } \tilde{\phi}(i\Omega) = \frac{i}{2\pi} [\ln(i\Omega \tilde{\mathcal{E}} - \tilde{\mathcal{A}}) - \ln(-i\Omega \tilde{\mathcal{E}} - \tilde{\mathcal{A}})] \tilde{\mathcal{E}}^{-1}.$$

6 Compute next shift parameter μ (see Section (5.2))

7 Compute residual norm (see Section (5.4))

8 **if** residual norm $\leq tol$ **then**

9 Stop Rational Krylov iteration.

10 Operate eigenvalue decomposition as (5.3).

11 Establish low-rank controllability Gramian factor $\mathcal{R}_{\mathcal{M}}$ as (5.4).

5.4 Calculating Residual Norm

The detailed description of residual norm of time limited low-rank Gramian has been given in Section (4.4) of Chapter (4). We just modify that norm formation in order to compute on finite frequency interval $[\Omega_0, \Omega_f]$ written as

$$\frac{\|\mathbf{R}(\tilde{\mathcal{M}})\|_F}{\left\| \mathcal{B}_\Omega \mathcal{B}_\Omega^T \right\|_F + \|\mathcal{A}\|_F \|\mathcal{M}\|_F \|\mathcal{E}\|_F},$$

where, $\|\cdot\|_F$ denotes Frobenius norm, the residual at m_{it} th iteration step is

$$\mathbf{R}(\tilde{\mathcal{M}}) = \mathcal{A} \mathcal{R}_{\mathcal{M}} \mathcal{R}_{\mathcal{M}}^T \mathcal{E}^T + \mathcal{E} \mathcal{R}_{\mathcal{M}} \mathcal{R}_{\mathcal{M}}^T \mathcal{A}^T + \mathcal{B}_\Omega \mathcal{B}_\Omega^T,$$

and

$$\mathcal{B}_\Omega \mathcal{B}_\Omega^T = \mathcal{E} \phi(i\omega) \mathcal{B} \mathcal{B}^T + \mathcal{B} \mathcal{B}^T \phi^*(i\omega) \mathcal{E}^T.$$

5.5 Solution of Frequency Restricted Index-I Descriptor System

The formulation of index-I descriptor system has already been described in Chapter (4) Section (4.5). At here, we consider only the solution of frequency restricted Lyapunov equations constructed on index-I descriptor system. The RKSM procedure, we applied during solving time restricted Lyapunov equation, is almost same. The difference is that we need to compute matrix logarithm by the processes described in Section (5.3). Then we need to find the low-rank solution of the projected frequency-restricted Lyapunov equations (5.1) and (5.2). Algorithm (13) summarizes the step by step procedures of finding low-rank controllability Gramian factor $\mathcal{R}_{\mathcal{M}}$ on finite frequency interval by solving frequency-restricted projected controllable Lyapunov equation (5.1).

In the mean time, we can find the low-rank observability Gramian factor $\mathcal{L}_{\mathcal{N}}$ on finite frequency interval using same Algorithm (13) after solving projected observable Lyapunov equation (5.2) and taking transpose of the matrices of the system (2.10). At that time, the basis matrices of the RKSM subspace are computed by solving the linear system (4.9).

5.6 Solution of Frequency Restricted Index-II Descriptor System

Like index-I descriptor system, the index-II descriptor system has also been formulated in Chapter (4) Section (4.6). In this section, we only discuss the solution of Lyapunov equation of index-II system on nominated frequency intervals. After converting index-II system (2.11) to the generalised system (2.2) through the procedure described in Section (4.6), we solve the frequency restricted projected Lyapunov equation (5.1) by the Algorithm (14) creating projector on rational Krylov subspace. At final stage, we form the low-rank controllable Gramian factors $\mathcal{R}_{\mathcal{M}}$ instead of full rank solution with a view to saving the machine's memory.

Likewise, the frequency-restricted low-rank observability Gramian factor $\mathcal{L}_{\mathcal{N}}$ can also be calculated by taking transposes of the system matrices and solving observable Lyapunov equation (5.2) using the same Algorithm (14) when the basis of the rational Krylov subspace are computed by solving Linear system (4.22).

5.7 Numerical Outcomes

In this section, our proposed methods on different finite frequency intervals are evaluated applying on both index-I and index-II descriptor data models and are also analyzed the efficiency of our proposed algorithms by calculating the required time. The convergence tendency of the iterative solution of the frequency-restricted Lyapunov equations are also observed by computing residual norms at each iteration and numerical error of frequency-restricted and unrestricted solutions of the Lyapunov equations on finite frequency segments.

Algorithm 14: RKSM for solving frequency-restricted controllability Gramian (2.33a) of index-II system (2.11) on frequency interval $[\Omega_0, \Omega_f]$.

Input: $\mathcal{E}_i, \mathcal{A}_i, \mathcal{A}_{ii}, \mathcal{A}_{iii}, \mathcal{B}_i, \mathcal{B}_{ii}, m_{it}$ (no. of iteration), Ω_0 (initial point of frequency interval), Ω_f (endpoint of frequency interval), $0 < tol \ll 1$ (tolerance value), μ_1 (initial shift parameter).

Output: $\mathcal{R}_{\mathcal{M}} \in \mathbb{R}^{n \times z}$ such that $\mathcal{R}_{\mathcal{M}} \mathcal{R}_{\mathcal{M}}^T \approx \mathcal{M}$, where $z \ll n$.

1 set initial basis vector $v_1 = \begin{bmatrix} \mathcal{A}_i - \mu_1 \mathcal{E}_i & \mathcal{A}_{ii} \\ \mathcal{A}_{iii} & 0 \end{bmatrix}^{-1} \begin{bmatrix} \mathcal{B}_i \\ \mathcal{B}_{ii} \end{bmatrix}$, $\mathcal{V}_1 = \frac{v}{\|v\|}$

2 **while** $j \leq m_{it}$ **do**

3 Find the next basis matrix by solving linear system

$$\begin{bmatrix} \mathcal{A}_i - \mu_j \mathcal{E}_i & \mathcal{A}_{ii} \\ \mathcal{A}_{iii} & 0 \end{bmatrix} \begin{bmatrix} v_{j+1} \\ * \end{bmatrix} = \begin{bmatrix} \mathcal{V}_j \\ 0 \end{bmatrix}.$$

4 Construct orthonormal vector set $\mathcal{V}_{j+1} = [\mathcal{V}_j, v_{j+1}]$ by QR decomposition (see Subsection (2.2.3.3)) using Algorithm (2).

5 Solve the projected controllability Lyapunov equation (5.1)

$$\tilde{\mathcal{A}}_{j+1} \tilde{\mathcal{M}} \tilde{\mathcal{E}}_{j+1}^T + \tilde{\mathcal{E}}_{j+1} \tilde{\mathcal{M}} \tilde{\mathcal{A}}_{j+1}^T + \tilde{\mathcal{E}}_{j+1} \tilde{\phi}_{j+1}(i\omega) \tilde{\mathcal{B}}_{j+1} \tilde{\mathcal{B}}_{j+1}^T + \tilde{\mathcal{B}}_{j+1} \tilde{\mathcal{B}}_{j+1}^T \tilde{\phi}_{j+1}^*(i\omega) \tilde{\mathcal{E}}_{j+1}^T = 0$$

for finding small-scale CG $\tilde{\mathcal{M}}$ Where, $\tilde{\mathcal{E}}_{j+1} = \mathcal{V}_{j+1}^T \mathcal{E}_i \mathcal{V}_{j+1}$,

$$\tilde{\mathcal{A}}_{j+1} = \mathcal{V}_{j+1}^T \mathcal{A}_i \mathcal{V}_{j+1} - (\mathcal{V}_{j+1}^T \mathcal{A}_{ii}) \Xi (\mathcal{A}_{iii} \mathcal{E}_i^{-1} (\mathcal{A}_i \mathcal{V}_{j+1})),$$

$$\tilde{\mathcal{B}}_{j+1} = \begin{bmatrix} (\mathcal{V}_{j+1}^T \mathcal{B}_i) - (\mathcal{V}_{j+1}^T \mathcal{A}_i) \mathcal{E}_i^{-1} \mathcal{A}_{ii} \Xi \mathcal{B}_{ii} - (\mathcal{V}_{j+1}^T \mathcal{A}_{ii}) \Xi \mathcal{A}_{iii} \mathcal{E}_i^{-1} (\mathcal{B}_i - \mathcal{A}_i \mathcal{E}_i^{-1} \mathcal{A}_{ii} \Xi \mathcal{B}_{ii}) \\ (\mathcal{V}_{j+1}^T \mathcal{A}_{ii}) \Xi \mathcal{B}_{ii} - (\mathcal{V}_{j+1}^T \mathcal{A}_i) \Xi \mathcal{B}_{ii} \end{bmatrix},$$

$$\Xi = (\mathcal{A}_{iii} \mathcal{E}_i^{-1} \mathcal{A}_{ii})^{-1}, \quad \tilde{\phi}(i\omega) = (\tilde{\phi}(i\Omega_f) - \tilde{\phi}(i\Omega_0)), \text{ and}$$

$$\tilde{\phi}(i\Omega) = \frac{i}{2\pi} [\ln(i\Omega \tilde{\mathcal{E}} - \tilde{\mathcal{A}}) - \ln(-i\Omega \tilde{\mathcal{E}} - \tilde{\mathcal{A}})] \tilde{\mathcal{E}}^{-1}.$$

6 Compute next shift parameter μ (see Section (5.2))

7 Compute residual norm (see Section (5.4))

8 **if** residual norm $\leq tol$ **then**

9 | Stop Rational Krylov iteration.

10 Operate eigenvalue decomposition as (5.3).

11 Establish low-rank controllability Gramian factor $\mathcal{R}_{\mathcal{M}}$ as (5.4).

5.7.1 Numerical Results from Index-I Descriptor System

At here, we highlight the numerical outcomes found after solving frequency-restricted Lyapunov equations of index-I systems by proposed Algorithm (13) on frequency interval $[\Omega_0, \Omega_f]$. Tables (3.1), (3.2), and (3.3) includes the dimension of our generated and selected data models. Figures (5.2), (5.3), (5.4), and (5.5) illustrate the convergence pattern of controllability and observability Gramians on restricted frequency intervals found by applying our Algorithm (13). Each of the figures shows that with respect of time and iteration, our proposed algorithm gradually find the convergence solution of the controllable and observable Lyapunov equations on finite frequency intervals. It will be more accurate by taking more iteration. Averagely, we get better result taking 25 iterations. Moreover, we calculate the residual norms of the frequency-restricted CG and OG following the process described in Section (5.4) on finite frequency intervals and compare them with the frequency infinite low-rank CG and OG. Table (5.1)

Table 5.1: Residual norms of frequency restricted and unrestricted CG and OG on nominated frequency intervals

Model	Frequency Interval	Residual Norm			
		CG		OG	
		Ω	∞	Ω	∞
BIPS-606	[10,13]	1×10^{-5}	2.35×10^{-4}	1.05×10^{-6}	2.9×10^{-5}
BIPS-1142	[-2,2]	3.5×10^{-2}	7.5×10^{-1}	2.75×10^{-4}	1.25×10^{-3}
BIPS-1693	[4,7]	1.07×10^{-6}	9.7×10^{-4}	1.5×10^{-5}	2.39×10^{-4}
Piezo Tonpilz Transducer	[-1,4]	2.08×10^{-4}	1.11×10^{-3}	3.05×10^{-4}	1.17×10^{-2}

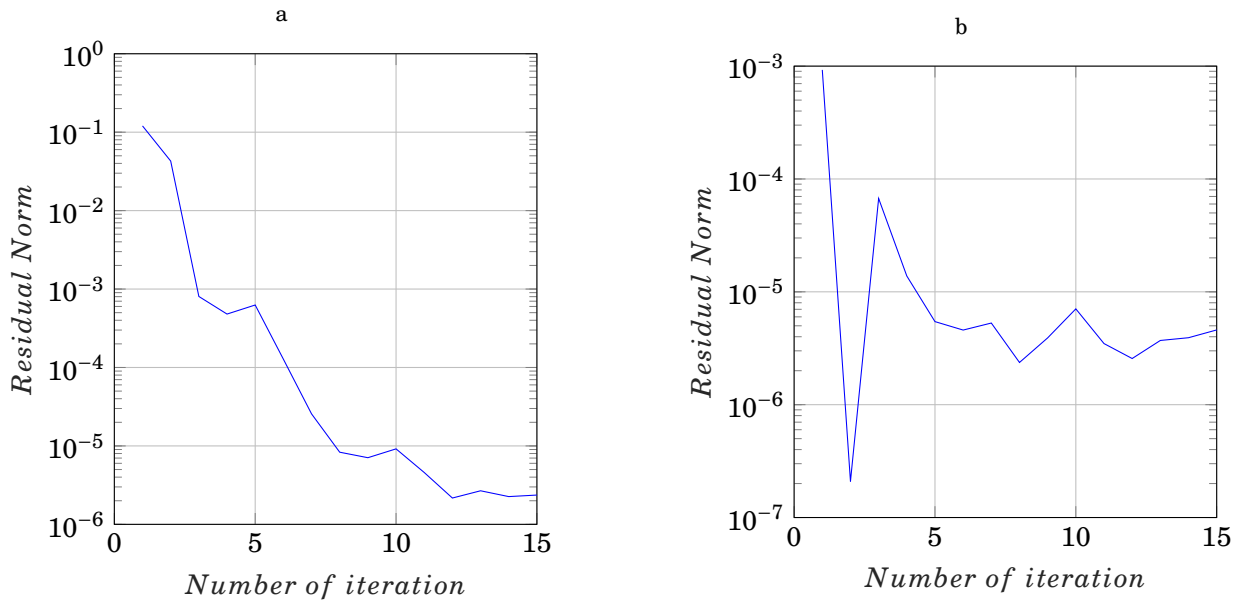


Figure 5.2: Convergence tendency of (a) CG and (b) OG of BIPS-606

highlights the comparison between the residual norms what clearly shows that on nominated frequency intervals, frequency-restricted solutions of Lyapunov equations minimize residual more than infinite Gramians, that means, frequency-restricted Gramians is more convergent than infinite Gramians on finite frequency intervals. Hence, it is clearly declared that our proposed algorithm for the treatment of the solutions of Lyapunov equations on frequency intervals gives satisfactory low-rank approximation of the original solutions of the Lyapunov equations.

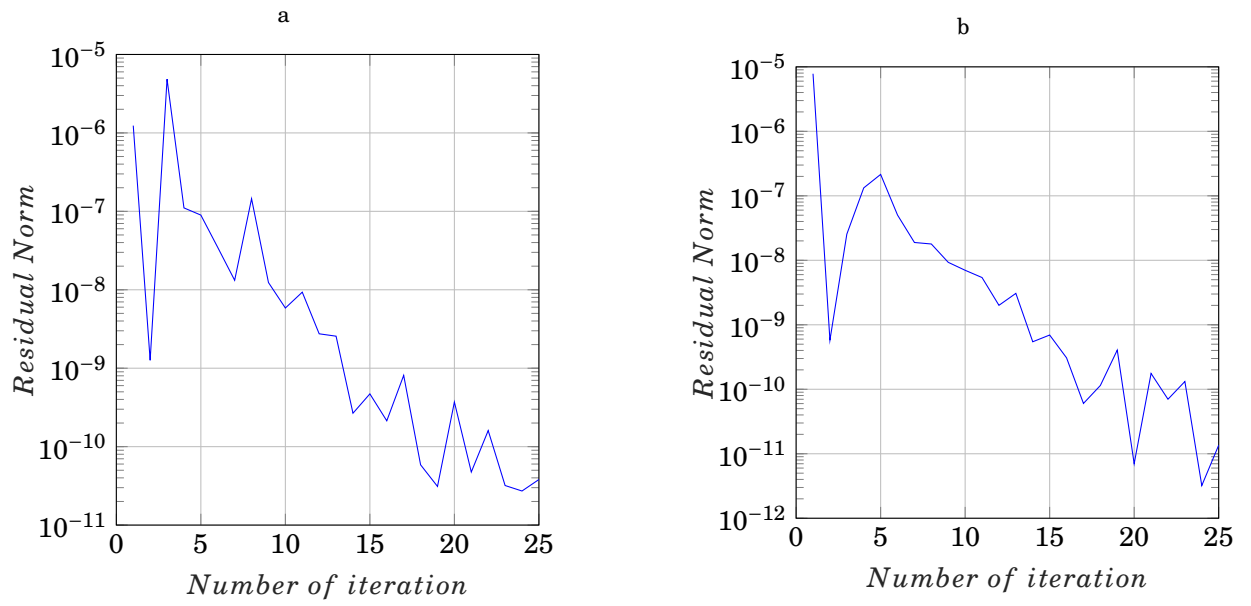


Figure 5.3: Convergence tendency of (a) CG and (b) OG of BIPS-1142

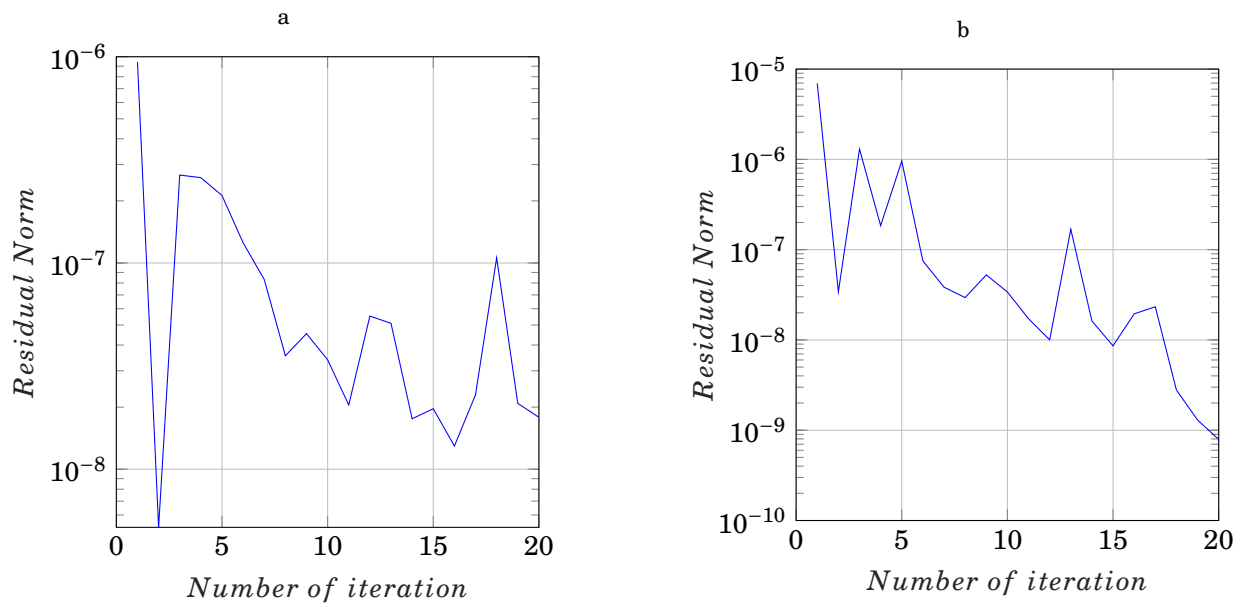


Figure 5.4: Convergence tendency of (a) CG and (b) OG of BIPS-1693

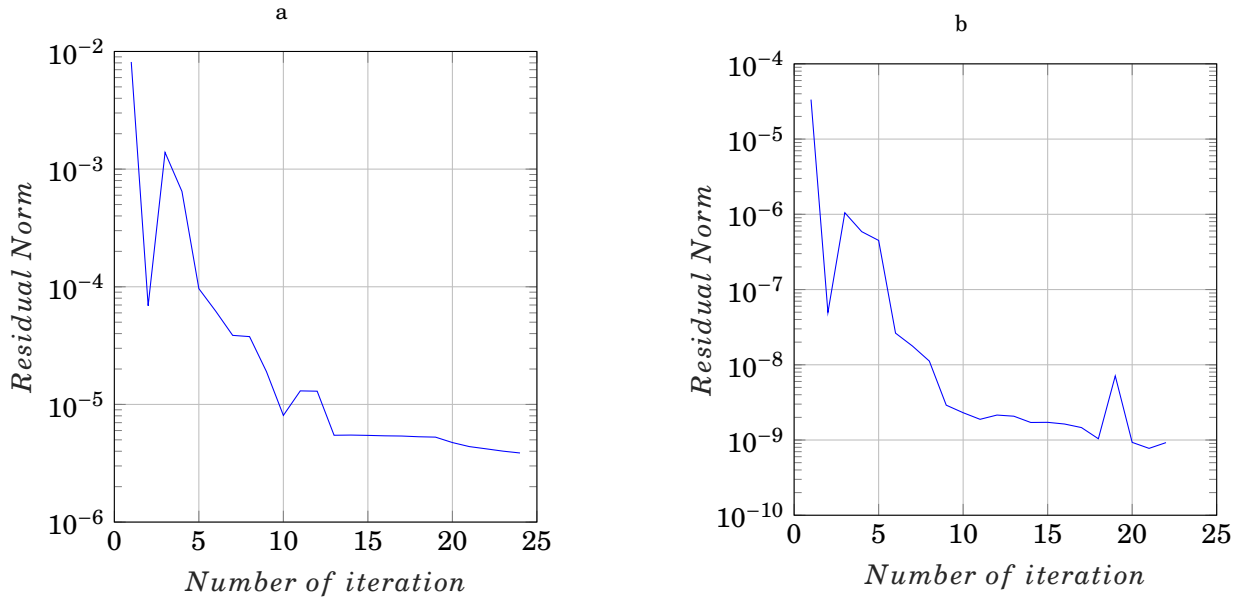


Figure 5.5: Convergence tendency of (a) CG and (b) OG of Piezo Tonpilz Transducer

5.7.2 Numerical Results from Index-II Descriptor System

In this subsection, the numerical outcomes on finite frequency intervals of index-II system are included whose dimension are added in Table (3.4). Like index-I system, we also analysis the convergence tendency of the solution of the controllability and observability Lyapunov equations constructing around index-II system by imposing our proposed Algorithm (14). Figure (5.6) shows the convergence tendency of the controllable and observable Gramians where it is observed that with respect of iteration, the CG becomes gradually convergent. But OG fluctuates little bit upwards after a certain interval with the increment of time what may need more iteration to find convergent observable Gramian. But since we find our satisfactory outcomes with minimum residual norm, we keep our iteration size limited with a view to minimizing the error. Table (5.2) highlights the comparison between the residual norm of the frequency-restricted and unrestricted CG and OG what visualizes that our Algorithm (14) minimizes the norms of the solutions of the Lyapunov equations of index-II system on limited frequency intervals than the infinite Gramians of Lyapunov equations. As a result, the solution, got from our algorithm, surely gives more accurate low-rank solutions of the original solutions.

Table 5.2: Residual norms of frequency restricted and unrestricted CG and OG on nominated frequency intervals

Model	Frequency Interval	Residual Norm			
		CG		OG	
		Ω	∞	Ω	∞
Ossen	[-2,2]	1.69×10^{-3}	8.12×10^{-1}	0.023	0.15

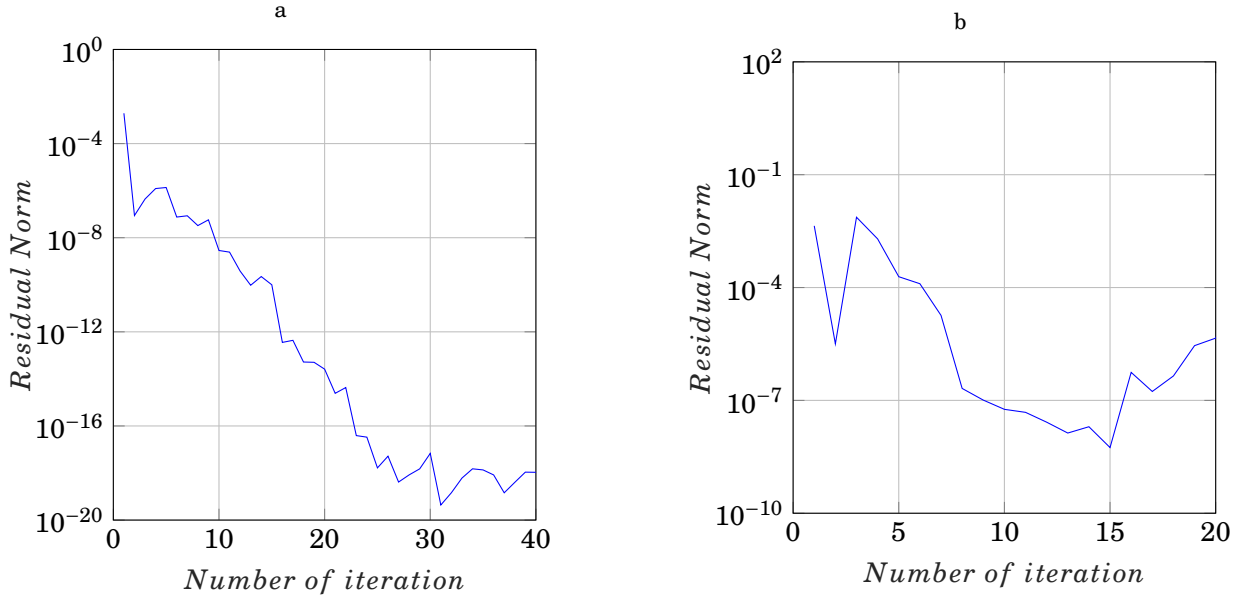


Figure 5.6: Convergence tendency of (a) CG and (b) OG of Ossen model

5.7.3 Numerical Results after Plugging in Gene Shift Parameters

It has already been described that the convergence tendencies of the solutions largely depend on the proper selection of the shift parameter, especially during solving the linear system (4.8), (4.9), (4.21), and (4.22). By the way, there is no definite procedure of selecting shift parameter. However, we have proposed a shift parameter selection procedure using genetic algorithm (See Section 5.2) with a view to minimizing error on nominated frequency interval whose outcomes are attached in this subsection.

Table 5.3: Residual norms of frequency restricted and unrestricted CG and OG on nominated frequency intervals

Model	Frequency Interval	Residual Norm			
		CG		OG	
		Gene Shift	RKSM Shift	Gene Shift	RKSM Shift
BIPS-606	[-1,3]	2.25×10^{-10}	1.25×10^{-4}	4.02×10^{-5}	3.19×10^{-5}
Piezo Tonpiliz Transducer	[-3,0]	3.53×10^{-5}	2.01×10^{-4}	7.39×10^{-5}	4.87×10^{-5}

If we look at the Table (5.3), it will be clearly visible that the solutions, we found by plugging in the shift parameters by our proposed Algorithm (12) minimize the norms on nominated frequency interval. Especially, the solution of the controllable frequency-restricted Lyapunov equation minimizes the residual norm more than observability gramian. Since the entire process is based on various kinds of probabilistic parameters, we make a thorough analysis on this to find the better convergence solution. It has been observed from the Table (5.4) that with the development of population size nP and mutation rate gc , we can get better convergence solution whereas we maintain a minimum improvement of the permutation rate β during picking up off-spring for a balanced convergence rate. However, we have to concern about calculation time requirement also

Table 5.4: Effect of various key parameters on selecting shift parameters

nP	gc	β	Residual Norm	
			CG	OG
15	0.15	1	1×10^{-4}	5.01×10^{-3}
15	0.20	1	2.01×10^{-4}	7.05×10^{-4}
15	0.25	1	5.26×10^{-6}	8.01×10^{-4}
15	0.30	1	1.57×10^{-8}	1.39×10^{-5}
15	0.35	1	2.25×10^{-10}	4.02×10^{-5}
15	0.30	1.05	1.02×10^{-7}	1.17×10^{-5}
15	0.30	1.15	3.11×10^{-4}	2.22×10^{-4}
15	0.30	1.25	5.07×10^{-4}	4.45×10^{-3}
15	0.30	1.30	5.95×10^{-3}	1.806×10^{-3}
15	0.30	1.35	9.12×10^{-3}	3.34×10^{-1}
20	0.30	1	2×10^{-8}	3.01×10^{-5}
25	0.30	1	3.95×10^{-8}	2.24×10^{-6}
30	0.30	1	5.07×10^{-9}	3.33×10^{-6}
35	0.30	1	7.77×10^{-9}	8.78×10^{-6}
40	0.30	1	8.81×10^{-9}	1.25×10^{-8}

what may increase with the increment of the population size. As result, for finding better solution with the minimum time requirement, we take the population size as 15, mutation rate as 0.35, and permutation rate as 1. However, these parametric values will be changed according to the nature, sparsity pattern of data models and convergence tendency of the solutions.

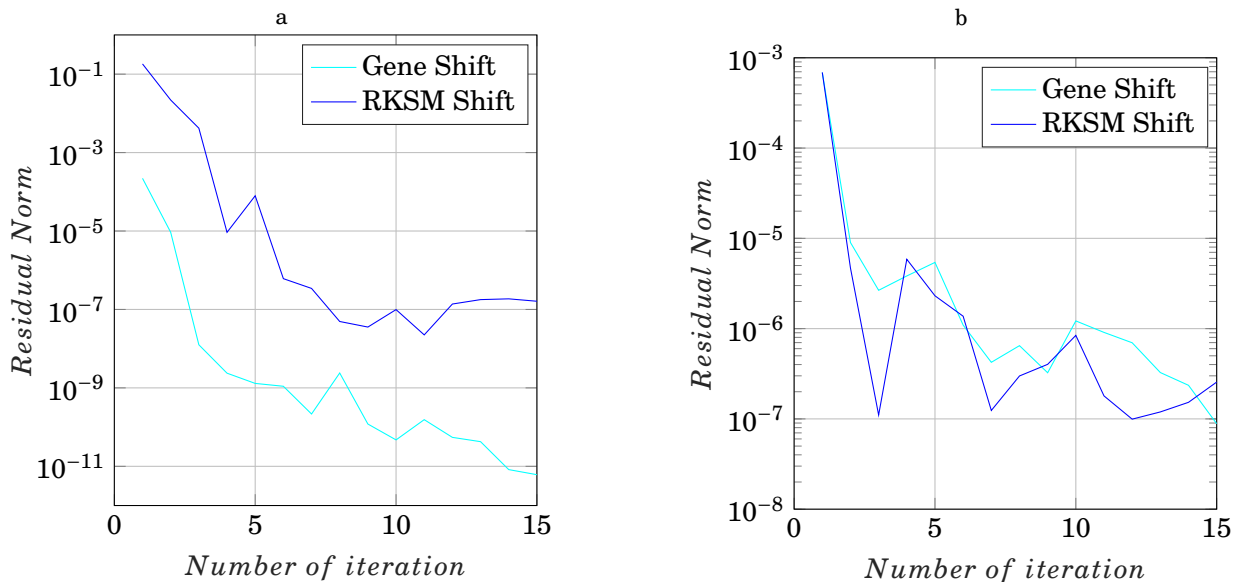


Figure 5.7: Convergence tendency of (a) CG and (b) OG of BIPS-606 by Gene Shift

Figures (5.7) and (5.8) show the comparison of the convergence tendency of the solutions using existing shift parameter and our proposed shift parameter. In both of the cases, we get convergent controllability Gramian within minimum possible time whereas we need to take population size little bit larger to get convergent observability Gramian as they are slowly converted.

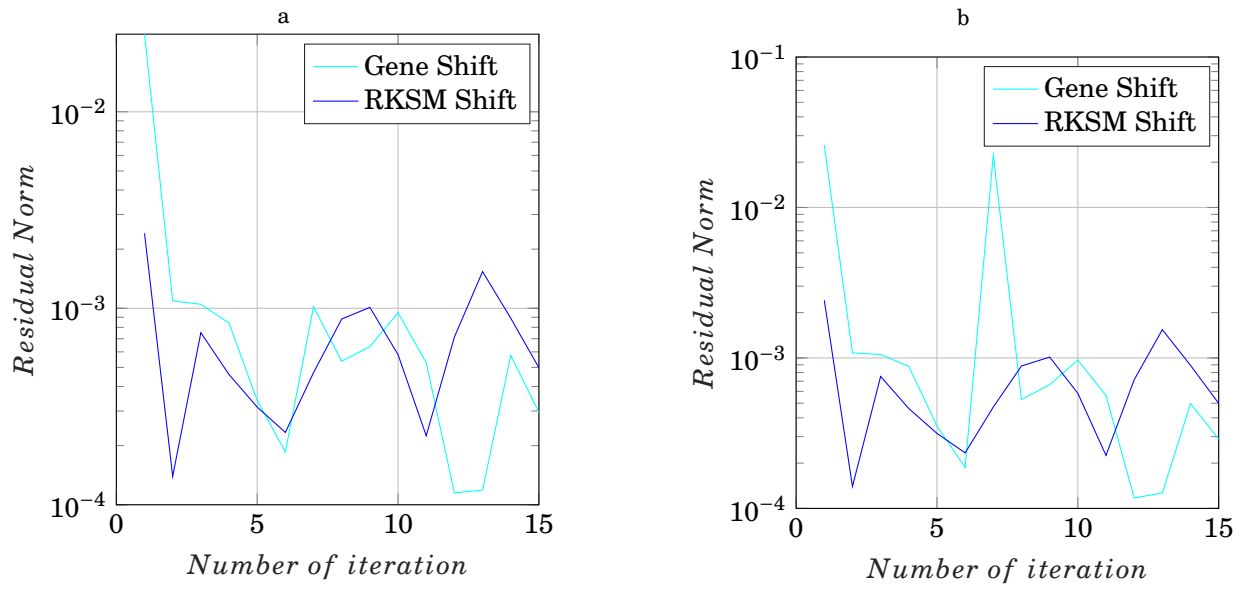


Figure 5.8: Convergence tendency of (a) CG and (b) OG of Piezo Tonpiliz Transducer by Gene Shift

ERROR MINIMIZATION OF REDUCED ORDER MODEL USING THE SOLUTIONS OF LYAPUNOV EQUATIONS

Introduction

The application of the solutions of the Lyapunov equations is huge in the field of control theory and optimization. In this chapter, we use the low-rank solutions of the Lyapunov equations, we previously found by our proposed algorithms, in order to eliminate the dimensions of the original data models to form the equivalent reduced order models (2.43) written as

$$\begin{aligned}\tilde{\mathcal{E}}\dot{\tilde{x}}(t) &= \tilde{\mathcal{A}}\tilde{x}(t) + \tilde{\mathcal{B}}u(t), \\ \tilde{y}(t) &= \tilde{\mathcal{C}}\tilde{x}(t) + \tilde{\mathcal{D}}u(t).\end{aligned}$$

Among various types of well-established model order reduction techniques, we use square-root balanced truncation (see Chapter 2 Subsection 2.4.1) what needs the solution of the Lyapunov equations, we have already discussed in the previous Chapters 4 and 5. As we deal with two special types of descriptor systems, we modify the generalised square root BT technique for index-I and index-II systems. Since we solve the Lyapunov equations on restricted time and frequency intervals, we mainly focus on the error minimization on the finite time and frequency intervals whereas the domains out the nominated time and frequency intervals are not our prior concern. Since there is no guarantee to preserve the stability of the reduced order models due to the negative definiteness of the solutions of the Lyapunov equations, at here we propose an algorithm as the remedy of this problem so that our reduced order models not only minimize error on the finite time and frequency segments but also preserve stability.

However, the concept of model order reduction has already been discussed in Chapter 2 Section 2.4. Hence, we start our discussion here from the Balanced Truncation (BT) of the descriptor systems.

6.1 Square Root Balanced Truncation of Index-I System

We have known that BT is a Gramian-based model reduction technique. As a result, we need to solve Lyapunov equations to find out Gramians. Since we mainly focus on model order reduction on limited time intervals, so we need to solve time-restricted controllable and observable Lyapunov equations (2.19a) and (2.19b) to find out low-rank CG and OG $\mathcal{R}_{\mathcal{D}}$ and $\mathcal{L}_{\mathcal{D}}$ respectively to apply BT technique for MOR. We modify the generalised BT Algorithm (4) for reducing the

Algorithm 15: Square root balanced truncation for index-I system (2.10)

Input: Low rank factors $\mathcal{R}_{\mathcal{P}}$ and $\mathcal{L}_{\mathcal{Q}}$ of \mathcal{P} and \mathcal{Q} respectively, $\mathcal{E}_i, \mathcal{E}_{ii}, \mathcal{A}_i, \mathcal{A}_{ii}, \mathcal{A}_{iii}, \mathcal{A}_{iv}, \mathcal{B}_i, \mathcal{B}_{ii}, \mathcal{C}_i, \mathcal{C}_{ii}, \mathcal{D}$

Output: Reduced order system matrices $\tilde{\mathcal{E}}, \tilde{\mathcal{A}}, \tilde{\mathcal{B}}, \tilde{\mathcal{C}}, \tilde{\mathcal{D}}$

1 Compute and partition a (thin) Singular Value Decomposition (SVD) (2.47) as

$$\mathcal{L}_{\mathcal{Q}}^T \mathcal{R}_{\mathcal{P}} = \begin{bmatrix} \mathbf{U}_i & \mathbf{U}_{ii} \end{bmatrix} \begin{bmatrix} \Sigma_i & \\ & \Sigma_{ii} \end{bmatrix} \begin{bmatrix} \mathbf{V}_i & \mathbf{V}_{ii} \end{bmatrix}^T,$$

where $\Sigma_i = \text{diag}(\sigma_1, \dots, \sigma_r)$ contains the largest r HSVs.

2 Construct the left and right balancing transformation matrices as (2.48)

$$\mathcal{T}_L := \mathcal{R}_{\mathcal{P}} \mathbf{V}_i \Sigma_i^{-\frac{1}{2}}, \quad \mathcal{T}_R := \mathcal{L}_{\mathcal{Q}} \mathbf{U}_i \Sigma_i^{-\frac{1}{2}},$$

3 Generate reduced order system matrices as

$$\begin{aligned} \tilde{\mathcal{E}} &:= \mathcal{T}_R^T \mathcal{E}_i \mathcal{T}_L - \mathcal{T}_R^T \mathcal{E}_{ii} \mathcal{A}_{iv}^{-1} \mathcal{A}_{iii} \mathcal{T}_L, \\ \tilde{\mathcal{A}} &:= \mathcal{T}_R^T \mathcal{A}_i \mathcal{T}_L - \mathcal{T}_R^T \mathcal{A}_{ii} \mathcal{A}_{iv}^{-1} \mathcal{A}_{iii} \mathcal{T}_L, \\ \tilde{\mathcal{B}} &:= \begin{bmatrix} \mathcal{T}_R^T \mathcal{B}_i - \mathcal{T}_R^T \mathcal{A}_{ii} \mathcal{A}_{iv}^{-1} \mathcal{B}_{ii} \\ \mathcal{T}_R^T \mathcal{E}_{ii} \mathcal{A}_{iv}^{-1} \mathcal{B}_{ii} \end{bmatrix}, \\ \tilde{\mathcal{C}} &:= \mathcal{C}_i \mathcal{T}_L - \mathcal{C}_{ii} \mathcal{A}_{iv}^{-1} \mathcal{A}_{iii} \mathcal{T}_L, \quad \tilde{\mathcal{D}} := \begin{bmatrix} \mathcal{D} - \mathcal{C}_{ii} \mathcal{A}_{iv}^{-1} \mathcal{B}_{ii} \\ 0 \end{bmatrix} \end{aligned} \quad (6.1)$$

dimensions of the system matrices of index-I descriptor system. Algorithm (15) summarizes the total procedures of BT for index-I system. The main modification, we did, is that the generation of the reduced order sub-blocks of the system matrices (6.1) by balancing transformation matrices \mathcal{T}_L and \mathcal{T}_R .

From the reduced order system matrices $\tilde{\mathcal{E}}, \tilde{\mathcal{A}}, \tilde{\mathcal{B}}, \tilde{\mathcal{C}},$ and $\tilde{\mathcal{D}}$, we can reform the reduced order descriptor systems having index-I structure as

$$\begin{aligned} \begin{bmatrix} \tilde{\mathcal{E}}_i & \tilde{\mathcal{E}}_{ii} \\ 0 & 0 \end{bmatrix} \begin{bmatrix} \dot{\tilde{\mathbf{g}}}(t) \\ \dot{\mathbf{r}}(t) \end{bmatrix} &= \begin{bmatrix} \tilde{\mathcal{A}}_i & \tilde{\mathcal{A}}_{ii} \\ \tilde{\mathcal{A}}_{iii} & \mathcal{A}_{iv} \end{bmatrix} \begin{bmatrix} \tilde{\mathbf{g}}(t) \\ \mathbf{r}(t) \end{bmatrix} + \begin{bmatrix} \tilde{\mathcal{B}}_i \\ \mathcal{B}_{ii} \end{bmatrix} \mathbf{u}(t) \\ \tilde{\mathbf{y}}(t) &= \begin{bmatrix} \tilde{\mathcal{C}}_i & \mathcal{C}_{ii} \end{bmatrix} \begin{bmatrix} \tilde{\mathbf{g}}(t) \\ \mathbf{r}(t) \end{bmatrix} + \mathcal{D} \mathbf{u}(t) \end{aligned} \quad (6.2)$$

where $\tilde{\mathcal{E}}_i := \mathcal{T}_R^T \mathcal{E}_i \mathcal{T}_L$, $\tilde{\mathcal{E}}_{ii} := \mathcal{T}_R^T \mathcal{E}_{ii}$, $\tilde{\mathcal{A}}_i := \mathcal{T}_R^T \mathcal{A}_i \mathcal{T}_L$, $\tilde{\mathcal{A}}_{ii} := \mathcal{T}_R^T \mathcal{A}_{ii}$, $\tilde{\mathcal{A}}_{iii} := \mathcal{A}_{iii} \mathcal{T}_L$, $\tilde{\mathcal{B}}_i := \mathcal{T}_R^T \mathcal{B}_i$, $\tilde{\mathcal{C}}_i := \mathcal{C}_i \mathcal{T}_L$. The dimension of the sub-blocks become $(\mathcal{T}_L, \mathcal{T}_R) \in \mathbb{R}^{n_i \times r}$, $\tilde{\mathcal{E}}_i \in \mathbb{R}^{r \times r}$, $\tilde{\mathcal{E}}_{ii} \in \mathbb{R}^{r \times n_{ii}}$, $\tilde{\mathcal{A}}_i \in \mathbb{R}^{r \times r}$, $\tilde{\mathcal{A}}_{ii} \in \mathbb{R}^{r \times n_{ii}}$, $\tilde{\mathcal{A}}_{iii} \in \mathbb{R}^{n_{ii} \times r}$, $\tilde{\mathcal{B}}_i \in \mathbb{R}^{r \times k}$, $\tilde{\mathcal{C}}_i \in \mathbb{R}^{l \times r}$, where $r \ll n = (n_i + n_{ii})$ is the dimension of reduced matrices.

Same Algorithm (15) is applicable for MOR on limited frequency intervals where the left and right transformation matrices \mathcal{T}_L and \mathcal{T}_R are constructed from the SVD of $\mathcal{L}_{\mathcal{N}}^T \mathcal{R}_{\mathcal{M}}$ as like as (2.47). It is noted that $\mathcal{R}_{\mathcal{M}}$ and $\mathcal{L}_{\mathcal{N}}$ are the low-rank controllability and observability Gramian factors of the frequency-restricted controllable and observable Lyapunov equations (2.33a) and (2.33b) what are formed by applying our proposed Algorithm (13).

6.2 Square Root Balanced Truncation of Index-II System

For the reduction of the system matrices of index-II system (2.11) on finite time and frequency intervals through BT, we also need to solve time and frequency restricted Lyapunov equations. Likewise index-I, for reducing the order of index-II we modify the generalised BT algorithm suitable for index-II system.

Algorithm 16: Square root balanced truncation for index-II system (2.11)

Input: Low rank factors $\mathcal{R}_{\mathcal{P}}$ and $\mathcal{L}_{\mathcal{Q}}$ of \mathcal{P} and \mathcal{Q} respectively, $\mathcal{E}_i, \mathcal{A}_i, \mathcal{A}_{ii}, \mathcal{A}_{iii}, \mathcal{B}_i, \mathcal{B}_{ii}, \mathcal{C}_i, \mathcal{C}_{ii}, \mathcal{D}$

Output: Reduced order system matrices $\tilde{\mathcal{E}}, \tilde{\mathcal{A}}, \tilde{\mathcal{B}}, \tilde{\mathcal{C}}, \tilde{\mathcal{D}}$

1 Compute and partition a (thin) Singular Value Decomposition (SVD) (2.47) as

$$\mathcal{L}_{\mathcal{Q}}^T \mathcal{R}_{\mathcal{P}} = \begin{bmatrix} \mathbf{U}_i & \mathbf{U}_{ii} \end{bmatrix} \begin{bmatrix} \Sigma_i & \\ & \Sigma_{ii} \end{bmatrix} \begin{bmatrix} \mathbf{V}_i & \mathbf{V}_{ii} \end{bmatrix}^T,$$

where $\Sigma_i = \text{diag}(\sigma_1, \dots, \sigma_r)$ contains the largest r HSVs.

2 Construct the left and right balancing transformation matrices as (2.48)

$$\mathcal{T}_L := \mathcal{R}_{\mathcal{P}} \mathbf{V}_i \Sigma_i^{-\frac{1}{2}}, \quad \mathcal{T}_R := \mathcal{L}_{\mathcal{Q}} \mathbf{U}_i \Sigma_i^{-\frac{1}{2}},$$

3 Generate reduced order system matrices as

$$\begin{aligned} \tilde{\mathcal{E}} &:= \mathcal{T}_R^T \mathcal{E}_i \mathcal{T}_L, \\ \tilde{\mathcal{A}} &:= \mathcal{T}_R^T \mathcal{A}_i \mathcal{T}_L - \mathcal{T}_R^T \mathcal{A}_{ii} \Xi \mathcal{A}_{iii} \mathcal{E}_i^{-1} \mathcal{A}_i \mathcal{T}_L, \\ \tilde{\mathcal{B}} &:= \begin{bmatrix} \mathcal{T}_R^T \mathcal{B}_i - \mathcal{T}_R^T \mathcal{A}_i \mathcal{E}_i^{-1} \mathcal{A}_{ii} \Xi \mathcal{B}_{ii} - \mathcal{T}_R^T \mathcal{A}_{ii} \Xi \mathcal{A}_{iii} \mathcal{E}_i^{-1} (\mathcal{B}_i - \mathcal{A}_i \mathcal{E}_i^{-1} \mathcal{A}_{ii} \Xi \mathcal{B}_{ii}) \\ \mathcal{T}_R^T \mathcal{A}_{ii} \Xi \mathcal{B}_{ii} - \mathcal{T}_R^T \mathcal{A}_{ii} \Xi \mathcal{B}_{ii} \end{bmatrix}, \\ \tilde{\mathcal{C}} &:= \mathcal{C}_i \mathcal{T}_L - \mathcal{C}_{ii} \Xi \mathcal{A}_{iii} \mathcal{E}_i^{-1} \mathcal{A}_i \mathcal{T}_L, \\ \tilde{\mathcal{D}} &:= \begin{bmatrix} \mathcal{D} - \mathcal{C}_i \mathcal{E}_i^{-1} \mathcal{A}_{ii} \Xi \mathcal{B}_{ii} - \mathcal{C}_{ii} \Xi \mathcal{A}_{iii} \mathcal{E}_i^{-1} (\mathcal{B}_i - \mathcal{A}_i \mathcal{E}_i^{-1} \mathcal{A}_{ii} \Xi \mathcal{B}_{ii}) \\ -\mathcal{C}_{ii} \Xi \mathcal{B}_{ii} \end{bmatrix} \end{aligned} \quad (6.3)$$

where, $\Xi = (\mathcal{A}_{iii} \mathcal{E}_i^{-1} \mathcal{A}_{ii})^{-1}$.

Algorithm (16) summarizes the step by step procedures of BT technique for index-II system where only the change is occurred during the generation of the reduced order system matrices (6.3) of the index-II system.

After plugging in the frequency-restricted low-rank controllability and observability Gramians $\mathcal{R}_{\mathcal{M}}$ and $\mathcal{L}_{\mathcal{N}}$ solving controllable and observable Lyapunov equations (2.33a) and (2.33b) respectively by our proposed Algorithm (14) in the replacement of $\mathcal{R}_{\mathcal{P}}$ and $\mathcal{L}_{\mathcal{Q}}$, we can use the same Algorithm (16) for the model order reduction of the index-II system on finite frequency intervals.

6.3 Retrieve of the Stability of the Reduced Order Models

We have already discussed on the instability difficulties of the time and frequency-restricted Lyapunov equations in the Chapter 2 Subsection 2.1.9. As a result, the reduced order models in

Algorithm 17: Stability preservation of reduced order index-I and index-II system matrices (6.1) and (6.3)

Input: Unstable balanced reduced matrices $\tilde{\mathcal{E}}, \tilde{\mathcal{A}}, \tilde{\mathcal{B}}, \tilde{\mathcal{C}}, \tilde{\mathcal{D}}$.

Output: Stable balanced reduced matrices $\hat{\mathcal{E}}, \hat{\mathcal{A}}, \hat{\mathcal{B}}, \hat{\mathcal{C}}, \hat{\mathcal{D}}$.

- 1 Operate eigenvalue decomposition of $(\tilde{\mathcal{A}}, \tilde{\mathcal{E}})$, and $(\tilde{\mathcal{A}}^T, \tilde{\mathcal{E}}^T)$ to find out (K, M) , and (K^T, M^T) respectively.
- 2 Construct left, and right projector S_L, S_R from the eigenvectors of the corresponding eigenvalues containing negative real parts as

$$S_L := K^T(:, \text{real}(M^T < 0)), \quad S_R := K(:, \text{real}(M < 0))$$

- 3 Establish stable balanced reduced matrices as

$$\begin{aligned} \hat{\mathcal{E}} &:= S_L \tilde{\mathcal{E}} S_R, \quad \hat{\mathcal{A}} := S_L \tilde{\mathcal{A}} S_R, \\ \hat{\mathcal{B}} &:= S_L \tilde{\mathcal{B}}, \quad \hat{\mathcal{C}} := \tilde{\mathcal{C}} S_R, \quad \hat{\mathcal{D}} := \tilde{\mathcal{D}} \end{aligned}$$

limited time and frequency intervals fail to preserve the stability due to the positive indefiniteness of the system matrices, that means, some of the eigenvalues of the system matrices are on the positive x-half plane after order reduction. Therefore, it causes serious issue on system's stability and total reduced system becomes unstable in spite of the full system being stable. In order to overcome that difficulty, we propose an stability retrieving algorithm like [101] where we create two projectors S_L and S_R used for truncating the unstable less-important eigenvalues in order to make the system stable concerning about the minimization of error on nominated time and frequency intervals. Algorithm (17) shows the process how to create projectors and make the unstable reduced order system matrices $\tilde{\mathcal{E}}, \tilde{\mathcal{A}}, \tilde{\mathcal{B}}, \tilde{\mathcal{C}}, \tilde{\mathcal{D}}$ to stable system matrices $\hat{\mathcal{E}}, \hat{\mathcal{A}}, \hat{\mathcal{B}}, \hat{\mathcal{C}}, \hat{\mathcal{D}}$. This reduced order system matrices not only make the reduced system stable but minimize error also comparing with infinite Gramians on finite time and frequency intervals what will be shown in the numerical section.

6.4 Error Calculation of Reduced Order Systems

In this section, we describe the error computational process, we followed in this thesis. There are several techniques to compute the norm (2.45) of the system of the reduce order systems comparing with full order models.

6.4.1 Error Calculation of Index-I Reduced Order Model

In [17], the author introduced \mathbb{H}_∞ -approximation error calculation process. However, at here we apply \mathbb{H}_2 -norm calculation processes. The time-restricted \mathbb{H}_2 -norm error calculation process was described in [102] by partitioning the balanced realization $(\mathcal{T} \mathcal{E} \mathcal{T}^{-1}, \mathcal{T} \mathcal{A} \mathcal{T}^{-1}, \mathcal{T} \mathcal{B}, \mathcal{C} \mathcal{T}^{-1})$ as follows:

$$\mathcal{T} \mathcal{E} \mathcal{T}^{-1} = \begin{bmatrix} \tilde{\mathcal{E}}_i & \tilde{\mathcal{E}}_{ii} \\ 0 & 0 \end{bmatrix} \begin{bmatrix} \dot{\tilde{g}}(t) \\ \dot{r}(t) \end{bmatrix}, \quad \mathcal{T} \mathcal{A} \mathcal{T}^{-1} = \begin{bmatrix} \tilde{\mathcal{A}}_i & \tilde{\mathcal{A}}_{ii} \\ \tilde{\mathcal{A}}_{iii} & \tilde{\mathcal{A}}_{iv} \end{bmatrix}, \quad \mathcal{T} \mathcal{B} = \begin{bmatrix} \tilde{\mathcal{B}}_i \\ \mathcal{B}_{ii} \end{bmatrix}, \quad \mathcal{C} \mathcal{T}^{-1} = \begin{bmatrix} \tilde{\mathcal{C}}_i & \mathcal{C}_{ii} \end{bmatrix}$$

and by partitioning the time-restricted controllability Lyapunov equations of reduced order systems as

$$\begin{bmatrix} \tilde{\mathcal{A}}_i & \tilde{\mathcal{A}}_{ii} \\ \tilde{\mathcal{A}}_{iii} & \tilde{\mathcal{A}}_{iv} \end{bmatrix} \begin{bmatrix} \Sigma_i & \\ & \Sigma_{ii} \end{bmatrix} \begin{bmatrix} \tilde{\mathcal{E}}_i^T & 0 \\ \tilde{\mathcal{E}}_{ii}^T & 0 \end{bmatrix} + \begin{bmatrix} \tilde{\mathcal{E}}_i & \tilde{\mathcal{E}}_{ii} \\ 0 & 0 \end{bmatrix} \begin{bmatrix} \Sigma_i & \\ & \Sigma_{ii} \end{bmatrix} \begin{bmatrix} \tilde{\mathcal{A}}_i^T & \tilde{\mathcal{A}}_{iii}^T \\ \tilde{\mathcal{A}}_{ii}^T & \tilde{\mathcal{A}}_{iv}^T \end{bmatrix} = \\ \begin{bmatrix} e^{\tilde{\mathcal{E}}_i^{-1} \tilde{\mathcal{A}}_i t_f} \tilde{\mathcal{B}}_i \tilde{\mathcal{B}}_i^T (e^{\tilde{\mathcal{E}}_i^{-1} \tilde{\mathcal{A}}_i t_f})^T & e^{\tilde{\mathcal{E}}_i^{-1} \tilde{\mathcal{A}}_i t_f} \tilde{\mathcal{B}}_i \tilde{\mathcal{B}}_{ii}^T e^{\tilde{\mathcal{A}}_{iv}^T t_f} \\ e^{\tilde{\mathcal{A}}_{iv} t_f} \tilde{\mathcal{B}}_{ii} \tilde{\mathcal{B}}_i^T (e^{\tilde{\mathcal{E}}_i^{-1} \tilde{\mathcal{A}}_i t_f})^T & e^{\tilde{\mathcal{A}}_{iv} t_f} \tilde{\mathcal{B}}_{ii} \tilde{\mathcal{B}}_{ii}^T e^{\tilde{\mathcal{A}}_{iv}^T t_f} \end{bmatrix} - \begin{bmatrix} \tilde{\mathcal{B}}_i \tilde{\mathcal{B}}_i^T & \tilde{\mathcal{B}}_i \tilde{\mathcal{B}}_{ii}^T \\ \tilde{\mathcal{B}}_{ii} \tilde{\mathcal{B}}_i^T & \tilde{\mathcal{B}}_{ii} \tilde{\mathcal{B}}_{ii}^T \end{bmatrix}.$$

Then, applying Cauchy-Schwarz inequality on Frobenius norm $\|\cdot\|_F$ and linearity of the Duhamel's integral, the $\|H\|_{\mathbb{H}_2}$ -norm error was calculated as follows:

$$\|H\|_{\mathbb{H}_2} = \sqrt{\text{tr}(\mathcal{C} \mathcal{P} \mathcal{C}^T) + \text{tr}(\tilde{\mathcal{C}}_i \hat{\mathcal{P}} \tilde{\mathcal{C}}_i^T) - 2\text{tr}(\mathcal{C} \mathcal{P}_i \tilde{\mathcal{C}}_i^T)}, \quad (6.4)$$

where, tr is the trace of the system matrices, $\mathcal{P} = \mathcal{E} \int_0^{t_f} e^{\mathcal{E}^{-1} \mathcal{A} \tau} \mathcal{B} \mathcal{B}^T e^{(\mathcal{E}^{-1} \mathcal{A})^T \tau} \mathcal{E}^T d\tau$, $\hat{\mathcal{P}} = \tilde{\mathcal{E}} \int_0^{t_f} e^{\tilde{\mathcal{E}}_i^{-1} \tilde{\mathcal{A}}_i \tau} \tilde{\mathcal{B}}_i \tilde{\mathcal{B}}_i^T e^{(\tilde{\mathcal{E}}_i^{-1} \tilde{\mathcal{A}}_i)^T \tau} \tilde{\mathcal{E}}_i^T d\tau$, and $\mathcal{P}_i = \mathcal{E} \int_0^{t_f} e^{\mathcal{E}^{-1} \mathcal{A} \tau} \mathcal{B} \tilde{\mathcal{B}}_i^T e^{(\tilde{\mathcal{E}}_i^{-1} \tilde{\mathcal{A}}_i)^T \tau} \tilde{\mathcal{E}}_i^T d\tau$.

Similarly, partitioning the time-restricted observability Lyapunov equations of reduced order systems as

$$\begin{bmatrix} \tilde{\mathcal{A}}_i^T & \tilde{\mathcal{A}}_{iii}^T \\ \tilde{\mathcal{A}}_{ii}^T & \tilde{\mathcal{A}}_{iv}^T \end{bmatrix} \begin{bmatrix} \Sigma_i & \\ & \Sigma_{ii} \end{bmatrix} \begin{bmatrix} \tilde{\mathcal{E}}_i & \tilde{\mathcal{E}}_{ii} \\ 0 & 0 \end{bmatrix} + \begin{bmatrix} \tilde{\mathcal{E}}_i^T & 0 \\ \tilde{\mathcal{E}}_{ii}^T & 0 \end{bmatrix} \begin{bmatrix} \Sigma_i & \\ & \Sigma_{ii} \end{bmatrix} \begin{bmatrix} \tilde{\mathcal{A}}_i & \tilde{\mathcal{A}}_{ii} \\ \tilde{\mathcal{A}}_{iii} & \tilde{\mathcal{A}}_{iv} \end{bmatrix} = \\ \begin{bmatrix} (e^{\tilde{\mathcal{E}}_i^{-1} \tilde{\mathcal{A}}_i t_f})^T \tilde{\mathcal{C}}_i^T \tilde{\mathcal{C}}_i e^{\tilde{\mathcal{E}}_i^{-1} \tilde{\mathcal{A}}_i t_f} & (e^{\tilde{\mathcal{E}}_i^{-1} \tilde{\mathcal{A}}_i t_f})^T \tilde{\mathcal{C}}_i^T \mathcal{C}_{ii} e^{\tilde{\mathcal{A}}_{iv} t_f} \\ (e^{\tilde{\mathcal{A}}_{iv} t_f})^T \mathcal{C}_{ii}^T \tilde{\mathcal{C}}_i e^{\tilde{\mathcal{E}}_i^{-1} \tilde{\mathcal{A}}_i t_f} & (e^{\tilde{\mathcal{A}}_{iv} t_f})^T \mathcal{C}_{ii}^T \mathcal{C}_{ii} e^{\tilde{\mathcal{A}}_{iv} t_f} \end{bmatrix} - \begin{bmatrix} \tilde{\mathcal{C}}_i^T \tilde{\mathcal{C}}_i & \tilde{\mathcal{C}}_i^T \mathcal{C}_{ii} \\ \mathcal{C}_{ii}^T \tilde{\mathcal{C}}_i & \mathcal{C}_{ii}^T \mathcal{C}_{ii} \end{bmatrix}.$$

it can be shown that the $\|H\|_{\mathbb{H}_2}$ -norm error can be calculated as follows:

$$\|H\|_{\mathbb{H}_2} = \sqrt{\text{tr}(\mathcal{B}^T \mathcal{Q} \mathcal{B}) + \text{tr}(\tilde{\mathcal{B}}_i^T \hat{\mathcal{Q}} \tilde{\mathcal{B}}_i) + 2\text{tr}(\mathcal{B}^T \mathcal{Q}_i \tilde{\mathcal{B}}_i)}.$$

\mathcal{Q} , $\hat{\mathcal{Q}}$, and \mathcal{Q}_i can be calculated by taking transposes of \mathcal{P} , $\hat{\mathcal{P}}$, and \mathcal{P}_i . However, in [6, 73], the authors have been observed that the $\|H\|_{\mathbb{H}_2}$ -norm on frequency interval was given by

$$\|H\|_{\mathbb{H}_2}^2 = \frac{1}{2\pi} \int_{-\omega}^{\omega} \text{tr}(\mathcal{G}(-i\omega) \mathcal{G}(i\omega)^T) d\omega \quad (6.5)$$

and proved in [73] that on frequency domain,

$$\int_{-\omega}^{\omega} \text{tr}(\mathcal{G}(-i\omega) \mathcal{G}(i\omega)^T) d\omega = 2\pi \mathcal{C} \mathcal{M} \mathcal{C}^T$$

where, \mathcal{M} is the solution of the controllability Lyapunov equation. Imposing balanced realization and partitioning the frequency-restricted controllability and observability Lyapunov equations (2.50a) and (2.50b) of reduced order models, the $\|H\|_{\mathbb{H}_2}$ -norm error can be calculated for controllability Gramian as

$$\|H\|_{\mathbb{H}_2} = \sqrt{\text{tr}(\mathcal{C} \mathcal{M} \mathcal{C}^T) + \text{tr}(\tilde{\mathcal{C}}_i \hat{\mathcal{M}} \tilde{\mathcal{C}}_i^T) - 2\text{tr}(\mathcal{C} \mathcal{M}_i \tilde{\mathcal{C}}_i^T)}, \quad (6.6)$$

and for observability Gramian as

$$\|H\|_{\mathbb{H}_2} = \sqrt{\text{tr}(\mathcal{B}^T \mathcal{N} \mathcal{B}) + \text{tr}(\tilde{\mathcal{B}}_i^T \hat{\mathcal{N}} \tilde{\mathcal{B}}_i) + 2\text{tr}(\mathcal{B}^T \mathcal{N}_i \tilde{\mathcal{B}}_i)},$$

where, tr is the trace of the system matrices, $\mathcal{M} = \frac{\mathcal{E}}{2\pi} \int_{-\Omega}^{\Omega} \Phi(i\Omega) \mathcal{B} \mathcal{B}^T \Phi^*(i\Omega) d\Omega \mathcal{E}^T$, $\hat{\mathcal{M}} = \frac{\tilde{\mathcal{E}}}{2\pi} \int_{-\Omega}^{\Omega} \tilde{\Phi}(i\Omega) \mathcal{B} \mathcal{B}^T \tilde{\Phi}^*(i\Omega) d\Omega \tilde{\mathcal{E}}^T$, and $\mathcal{M}_i = \frac{\mathcal{E}}{2\pi} \int_{-\Omega}^{\Omega} \Phi(i\Omega) \mathcal{B} \tilde{\mathcal{B}}^T \tilde{\Phi}^*(i\Omega) d\Omega \mathcal{E}^T$, $\Phi(i\Omega) = (i\Omega \mathcal{E} - \mathcal{A})^{-1}$, and $\tilde{\Phi}(i\Omega) = (i\Omega \tilde{\mathcal{E}} - \tilde{\mathcal{A}})^{-1}$. \mathcal{N} , $\hat{\mathcal{N}}$, and \mathcal{N}_i can also be estimated by taking transposes of \mathcal{M} , $\hat{\mathcal{M}}$, and \mathcal{M}_i .

However, the absolute error of the reduced order system can be computed as

$$AbsoluteError = \left\| H - \hat{H} \right\|$$

and, the relative error can be calculated by

$$RelativeError = \frac{\left\| H - \hat{H} \right\|}{\left\| H \right\|}$$

6.4.2 Error Calculation of Index-II Reduced Order Model

It has been closely observed in [82, 90] that for index-II system, a relation can be built up with the balancing left and right projection matrices as:

$$\mathcal{T}_R := \Pi^T \mathcal{T}_R, \quad \mathcal{T}_L := \Pi^T \tilde{\mathcal{T}}_L$$

where, $\Pi = \mathcal{I} - \mathcal{A}_{ii}(\mathcal{A}_{iii}\mathcal{E}_i^{-1}\mathcal{A}_{ii})^{-1}\mathcal{A}_{iii}\mathcal{E}_i^{-1}$. Therefore, it can be easily shown that the state and output equations of index-II system (2.11a) and (2.11b) can be reformed as:

$$\begin{aligned} \mathcal{T}_R^T \mathcal{E}_i \mathcal{T}_L \dot{\tilde{x}}(t) &= \mathcal{T}_R^T \mathcal{A}_i \mathcal{T}_L \tilde{x}(t) + \mathcal{T}_R^T \mathcal{B} u(t), \\ \tilde{y}(t) &= \mathcal{C} \mathcal{T}_L \tilde{x}(t) \end{aligned}$$

where, $\mathcal{B} = \mathcal{B}_i - \mathcal{A}_i \mathcal{E}_i^{-1} \mathcal{A}_{ii} \Xi \mathcal{B}_{ii}$, $\mathcal{C} := \mathcal{C}_i - \mathcal{C}_{ii} \Xi \mathcal{A}_{iii} \mathcal{E}_i^{-1} \mathcal{A}_i$. The above relation can be expressed as same as the reduced order system (2.43), and hence, the absolute error between the original and the reduced order systems can be measured by calculating $\|H\|_{\mathbb{H}_\infty}$ as:

$$\left\| H - \hat{H} \right\|_{\mathbb{H}_\infty} = \left\| \mathcal{C}(s\mathcal{E} - \mathcal{A})^{-1} \mathcal{B} - \tilde{\mathcal{C}}(s\tilde{\mathcal{E}} - \tilde{\mathcal{A}})^{-1} \tilde{\mathcal{B}} \right\|$$

where, $\tilde{\mathcal{E}} = \mathcal{T}_R^T \mathcal{E}_i \mathcal{T}_L$, $\tilde{\mathcal{A}} = \mathcal{T}_R^T \mathcal{A}_i \mathcal{T}_L$, $\tilde{\mathcal{B}} = \mathcal{T}_R^T \mathcal{B}_i - \mathcal{T}_R^T \mathcal{A}_i \mathcal{E}_i^{-1} \mathcal{A}_{ii} \Xi \mathcal{B}_{ii}$, and $\tilde{\mathcal{C}} = \mathcal{C}_i \mathcal{T}_L - \mathcal{C}_{ii} \Xi \mathcal{A}_{iii} \mathcal{E}_i^{-1} \mathcal{A}_i \mathcal{T}_L$.

6.5 Numerical Outcomes

The error comparisons of the reduced order models on finite time and frequency intervals with full order models and infinite reduced order models are illustrated in this section. The efficiency of our proposed algorithms have been evaluated by constructing better reduced order approximation of the full order models on the nominated time and frequency intervals than the time and frequency infinite reduced order models. Since our main concern is to reduce the models on small time and frequency segments, therefore the numerical outcomes out of the restricted time and frequency intervals is not included in our investigation. For time domain analysis, we compute step responses of the input and output of the system using implicit Euler's method summarized in Algorithm (1) whereas for frequency domain analysis, we establish the transfer functions (2.9) from the input-output relation of the dynamical system. However, we compute the error on the

Table 6.1: Competitive numerical analysis on absolute & relative errors of the time-restricted (t) and time-unrestricted (∞) Gramians under nominated time intervals

Model	Interval	Dimension		Error			
		Reduced DP	Reduced TP	Absolute		Relative	
				t	∞	t	∞
BIPS-606	[0,2]	50	6579	4×10^{-7}	1.2×10^{-5}	2.3×10^{-5}	1×10^{-4}
BIPS-1142	[0,5]	70	8663	5.01×10^{-3}	0.123	1.83×10^{-3}	0.550
BIPS-1693	[0,7]	60	11642	7.23×10^{-5}	2.3×10^{-2}	2.55×10^{-6}	8×10^{-4}
Piezo Tonpilz	[0,10]	90	6165	7.95×10^{-5}	2.03×10^{-2}	1.16×10^{-3}	0.23

Table 6.2: Competitive numerical analysis on absolute & relative errors of the time-restricted (t) and time-unrestricted (∞) Gramians under non-homogeneous time intervals

Model	Interval	Dimension		Error			
		Reduced DP	Reduced TP	Absolute		Relative	
				t	∞	t	∞
BIPS-606	[2,5]	70	6599	6.2×10^{-4}	1.10×10^{-1}	2.32×10^{-5}	8.75×10^{-1}
BIPS-1693	[1,3]	70	11652	9.95×10^{-7}	8.23×10^{-3}	2.52×10^{-5}	6.66×10^{-2}

nominated time and frequency intervals using the procedures describing in the immediate above section. In each of the error analysis data table, we indicate the reduced differential dimensions of the system matrices using the column **Reduced DP** and entire reduced dimensions by the column **Reduced TP**.

6.5.1 Error of Index-I system on Restricted Time Intervals

For model order reduction of index-I descriptor system on time domains, at first we compute the controllability and observability solutions of the time-restricted Lyapunov equations using our proposed Algorithm (8) solving shifted linear systems in sparse forms. Then we apply balanced truncation MOR technique to reduce the dimensions of the original models. We truncate the less impacted singular values of the system. Normally, we ignore the singular values having numerical value 10^{-3} . After model order reduction, we plot step responses of the full and reduced order systems on time domain using the Algorithm (1) to illustrate the comparisons of the errors of the reduced order on nominated time intervals. Tables (6.1) and (6.2) show the errors of reduced order models using time-restricted and time-unrestricted Gramians on finite time intervals having homogeneous and non-homogeneous initial conditions respectively.

t column enlists the error of the time-restricted reduced order models whereas ∞ is error of time-infinite reduced order models. It has been observed that on both homogeneous and non-homogeneous time intervals, the models reduced by our proposed Algorithm (15) what use low-rank Gramians factors computed by our Algorithms (8) and (9), minimize errors more comparing with the time-unrestricted reduced models. We have taken several time intervals to examine the adaptability of our proposed algorithms with different time intervals and it has been successfully shown that on different time intervals, the reduced order models by our algorithms approximate

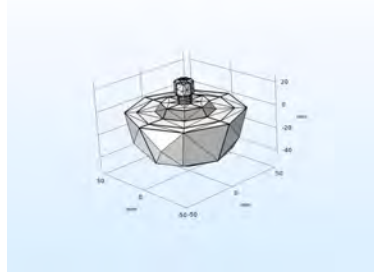


Figure 6.1: Mesh of reduced order Piezoelectric Tonpilz Transducer



Figure 6.2: Acoustic field pressure on output Probe points Vs. Time [0-10 sec] of reduced order Piezo Tonpilz Transducer

the original full models better than time unrestricted reduced order models. Closely looking at the Figures (6.3), (6.6), (6.8), it is clearly visible that on nominated time intervals time-restricted reduced order models minimize error more by approximating more accurate full order models. Figure (6.1) is the reduced order meshing structure of our generated Piezo Tonpilz Transducer after reducing it to **6165** dimensions from **9140** dimensions. The physical outcomes of the reduced order Piezo Tonpilz Transducer model have been shown by Figures (6.2), (6.4), (6.7), and (6.5).

6.5.2 Error of Index-II system on Restricted Time Intervals

We extend our error analysis of reduced order models on time domain for index-II descriptor systems what are reduced by Algorithm (16). The low-rank time-restricted Gramian factors, what are required here, are computed by Algorithm (10). For index-II system, we simply ignore the singular values less than 10^{-4} of the reduced order model. The below Table (6.3) shows the error of the ossen model on finite time interval where it is clearly shown that on nominated time intervals time-restricted reduced order model minimizes both absolute and relative error and give better approximation of original model illustrated in Figure (6.9 (a)). Figures (6.9 (b)) and (6.9 (c)) illustrate the absolute and relative errors respectively on finite time intervals by which it is visibly proven that the time-restricted ossen model gives more accurate approximation of full model by minimizing both absolute and relative errors comparing with time-unrestricted reduced order model.

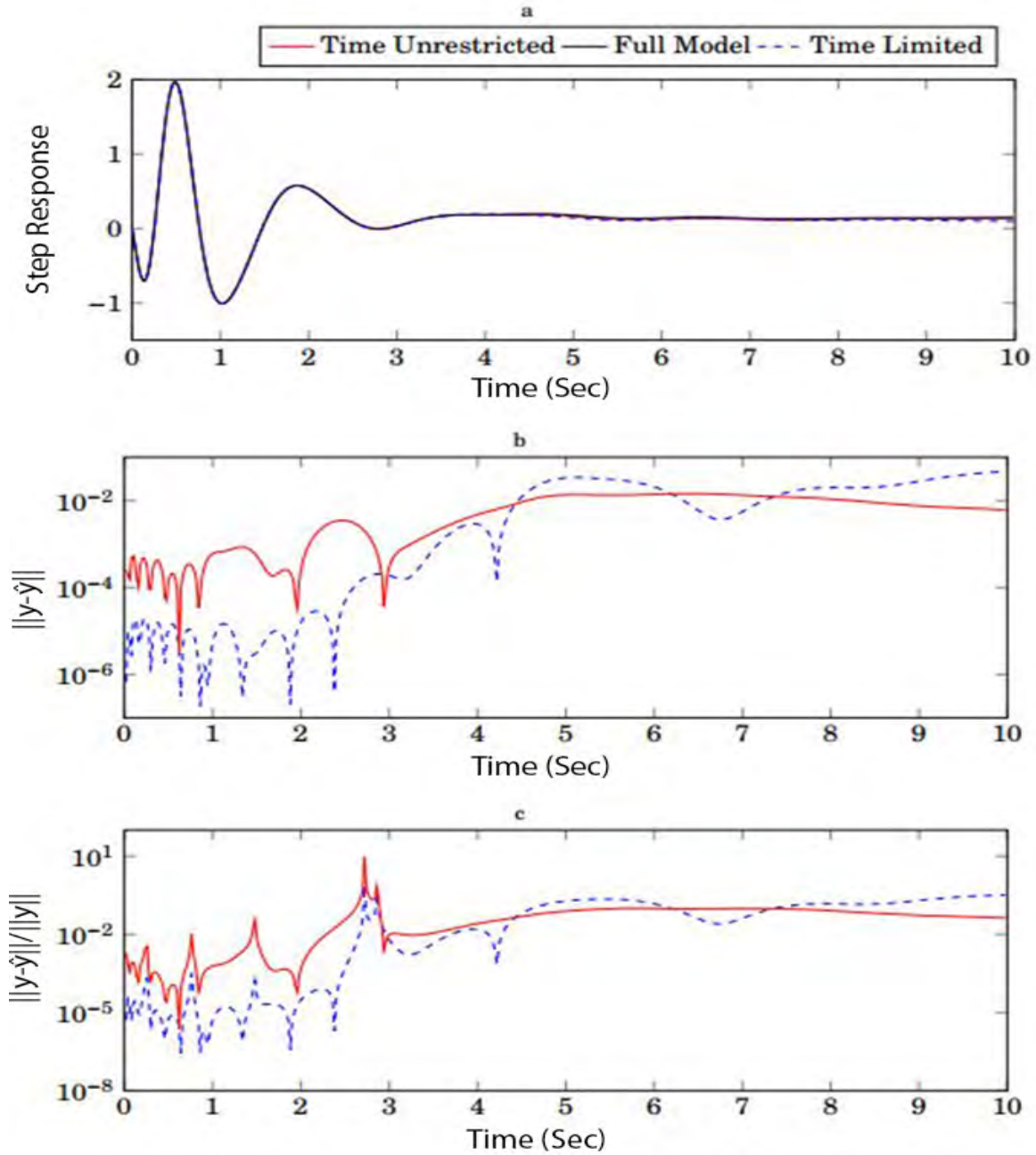


Figure 6.3: (a) Approximation of full models and (b) Absolute (c) Relative errors of reduced order BIPS-1142 Model on time interval [0,5]

Table 6.3: Competitive numerical analysis on absolute & relative errors of the time-restricted (t) and time-unrestricted (∞) Gramians under nominated time intervals

Model	Interval	Dimension		Error			
		Reduced DP	Reduced TP	Absolute		Relative	
				t	∞	t	∞
Ossen	[0,6]	60	2559	7.1×10^{-3}	5×10^{-1}	2.96×10^{-2}	4.45×10^{-1}

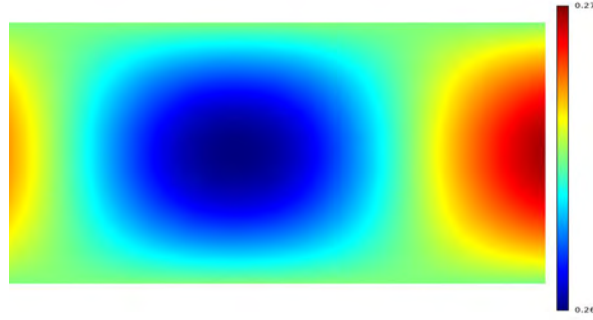


Figure 6.4: External field pressure of reduced order Piezo Tonpilz Transducer

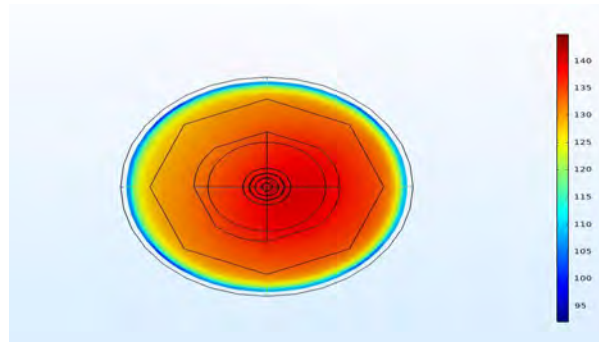


Figure 6.5: Sound pressure of reduced order Piezo Tonpilz Transducer

6.5.3 Error of Index-I system on Restricted Frequency Intervals

We also analysis the MOR on limited frequency intervals using balanced truncation technique. Hence, it is mandatory to compute low-rank controllability and observability Gramian factors what we are computed by our proposed Algorithm (13). We reduce the order of the index-I models on frequency intervals by eliminating the singular values less than 10^{-3} . For frequency domain analysis, we plot the transfer function (2.7) of the full and reduced order systems. Table (6.4) includes the errors of the reduced order systems using frequency-restricted and unrestricted Gramians on finite frequency intervals. Ω column indicates the error of the frequency-restricted reduced order models whereas ∞ is error of frequency-infinite reduced order models. The reduced order models found by our proposed algorithm are examined on different frequency segments and on every intervals the frequency restricted reduced order models give more accurate approximation of the original systems and minimize error more than frequency unrestricted reduced order models. Figures (6.10) and (6.11) are the visual proof of our numerical outcomes what clearly show on restricted frequency intervals our reduced order models work better.

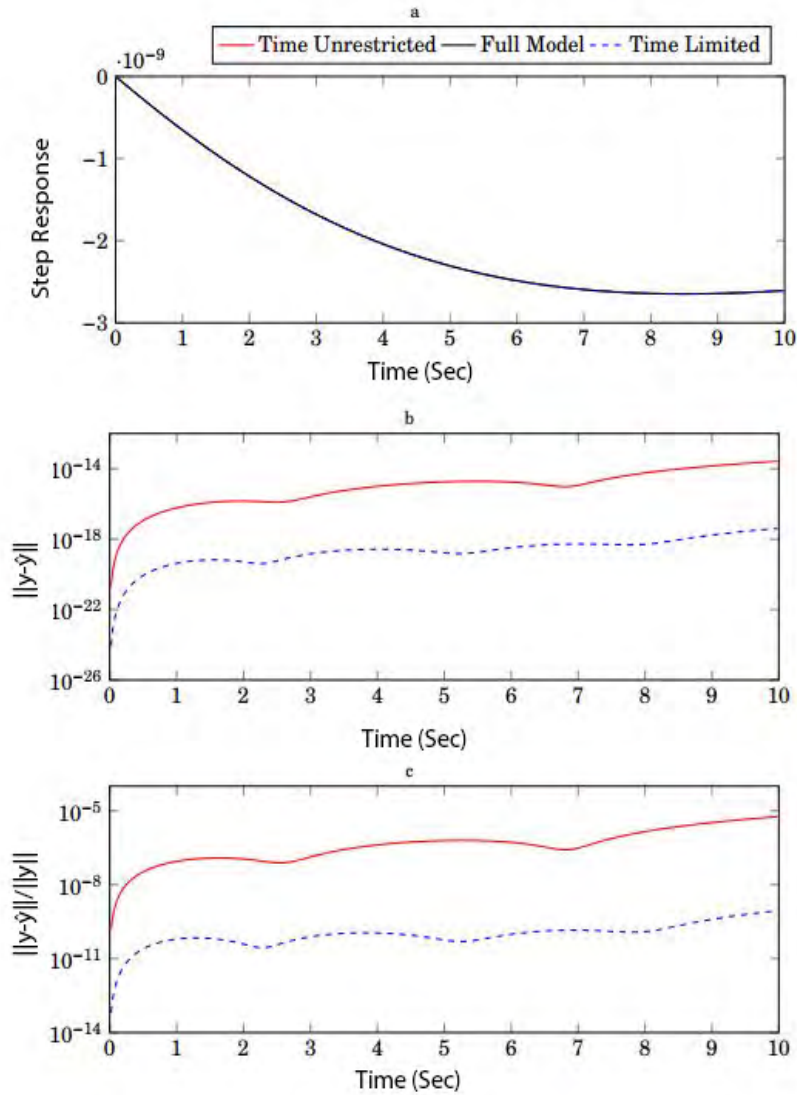


Figure 6.6: (a) Approximation of full models and (b) Absolute (c) Relative errors of reduced order Piezo Tonpilz Transducer Model on time interval [0,10]

Table 6.4: Competitive numerical analysis on absolute & relative errors of the frequency-restricted (Ω) and frequency-unrestricted (∞) Gramians under nominated frequency intervals

Model	Interval	Dimension		Error			
		Reduced DP	Reduced TP	Absolute		Relative	
				Ω	∞	Ω	∞
BIPS-606	[10,14]	40	6569	3.31×10^{-5}	4×10^{-2}	3.78×10^{-4}	2.91×10^{-2}
BIPS-1142	[-2,2]	60	8653	2.55×10^{-8}	3.69×10^{-5}	2.29×10^{-6}	1.45×10^{-4}
BIPS-1693	[3,7]	80	11662	4.54×10^{-2}	.054	8.89×10^{-3}	1.15×10^{-2}
Piezo Tonpilz	[-1,4]	70	6145	2.23×10^{-6}	7.53×10^{-4}	1.21×10^{-5}	5.2×10^{-4}
Power system	[0,5]	30	229	2.32×10^{-1}	0.61	1.23×10^{-5}	1.98×10^{-3}

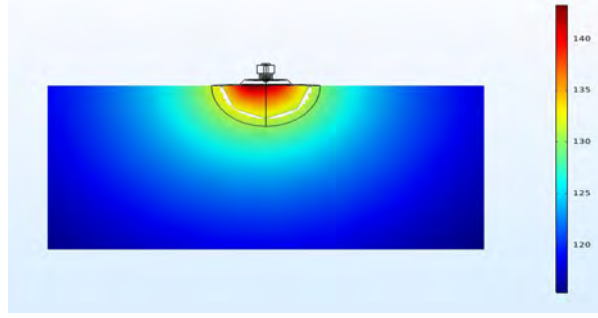


Figure 6.7: External fluid pressure of reduced order Piezo Tonpiliz Transducer

Table 6.5: Competitive numerical analysis on absolute & relative errors of the frequency-restricted (Ω) Gramians between Gene shift and RKSM shift under nominated frequency intervals

Model	Interval	Error			
		Absolute		Relative	
		Gene Shift	RKSM Shift	Gene Shift	RKSM Shift
BIPS-606	[-2,2]	9.10×10^{-2}	0.78	2.22×10^{-4}	1.1×10^{-1}
Piezo Tonpiliz	[-5,0]	1.52×10^{-4}	4.2×10^{-2}	3.96×10^{-4}	5.01×10^{-3}

In addition, Table (6.5) give the comparative numerical results of the two shift parameters, we have used. One of them is computed by our proposed Algorithm (12) whose numerical outcomes are indicated by the column **Gene Shift**. Another is computed by existing method describing in Chapter 4 Section 4.2 whose numerical errors are highlighted by the column **RKSM Shift**. Attentively looking at the numerical values of error analysis, we can come to an end that the reduced order models which are generated from the low-rank Gramians solving linear system (see Chapter 5 Section 5.5) plugged in the Gene shift parameters minimize both absolute and relative errors more than the reduced order models found form the low-rank Gramians computed by the linear system inserting existing RKSM shift.

However, since the procedure, we followed to compute the shift parameters, is based on different kinds of parametric values of governing parameters, sometimes based on the nature of the data models, error minimization largely depends on the proper choice of the values of the parameters. We get better result by taking population size as 15, mutation rate as 0.35 and the permutation rate of the off-spring generation as 1. Figures (6.12) demonstrates that efficiency of the shift parameters selected by our proposed Algorithm (12). The reduced order models found by inserting our shift parameters minimizes errors more and give far better approximation of the full model on nominated frequency intervals.

6.5.4 Error of Index-II system on Restricted Frequency Intervals

Like index-I system, we extend our research for index-II data model also and reduce the model by Algorithm (16) where we need to find out the frequency-restricted low-rank Gramian factors by our Algorithm (14). Singular value less than 10^{-4} are simply truncated with a view to reducing dimensions of the model. Table (6.6) show the error of the ossen model on finite

Table 6.6: Competitive numerical analysis on absolute & relative errors of the frequency-restricted (Ω) and frequency-unrestricted (∞) Gramians under nominated frequency intervals

Model	Interval	Dimension		Error			
		Reduced DP	Reduced TP	Absolute		Relative	
				Ω	∞	Ω	∞
Ossen	[-3,3]	50	2549	3.63×10^{-13}	1.12×10^{-10}	7.78×10^{-12}	5.63×10^{-9}

frequency interval by which it is shown that on finite frequency intervals frequency-restricted reduced order models minimize both absolute and relative error by giving more accuracy during the approximation of the full model. Looking at the Figure (6.13), we can say that like time-limited reduced order model, frequency restricted ROM give more accurate approximation by minimizing errors on nominated frequency intervals. As a result, alongside numerical data, more accurate approximation of original index-II models by frequency-restricted reduced order models on selected frequency intervals are also be visually proven.

6.5.5 Error of Stable system

Since there is no guarantee to ensure the preservation of stability of the time and frequency restricted reduced order models due to the positive indefiniteness of the system matrices, we propose a stability retrieving Algorithm (17) what successfully ensures the stability of the reduced order model as well as minimizes the error more on restricted intervals. It has already been known to us that the eigenvalues of the state matrices (\mathcal{A}, \mathcal{E}) of a stable dynamic systems are on the negative x-half plane.

Unfortunately, some of the eigenvalues of the system matrices of the time and frequency restricted reduced order models are on the positive x-half plane despite the original systems are stable. Due to this unexpected situation, the entire reduced order systems become unstable. If we look at the Figure (6.15), it will be visible to us some of the eigenvalues of the unstable reduced order models indicated by **blue** * are on the right x-half plane. However, after applying our Algorithm (17), we observe from the Figure (6.15) that all of the eigenvalues of our stable reduced order models symbolized as **green** \diamond are on the negative x-half plane, that means, our proposed algorithm successfully retrieve the stability of the reduced order system. Figure (6.14) shows the time domain analysis of the stable reduced order system where it is clearly visible that the stable reduced system indicated by **green** curve is marginally stable with respect of time whereas the unstable reduced system indicated by **blue** curve becomes diverse after a certain period of time. However, the stable reduced order models by our proposed algorithm also minimizes the error on restricted intervals more than the unrestricted reduced order models. Looking at the Figure (6.16), we can come to the end saying that the stable reduced order model on restricted intervals indicated by **green** curve minimizes error more than unrestricted reduced order models indicated by **red** curve. Therefore, our stability retrieving Algorithm (17) not only retrieves system stability but also minimizes error on finite intervals.

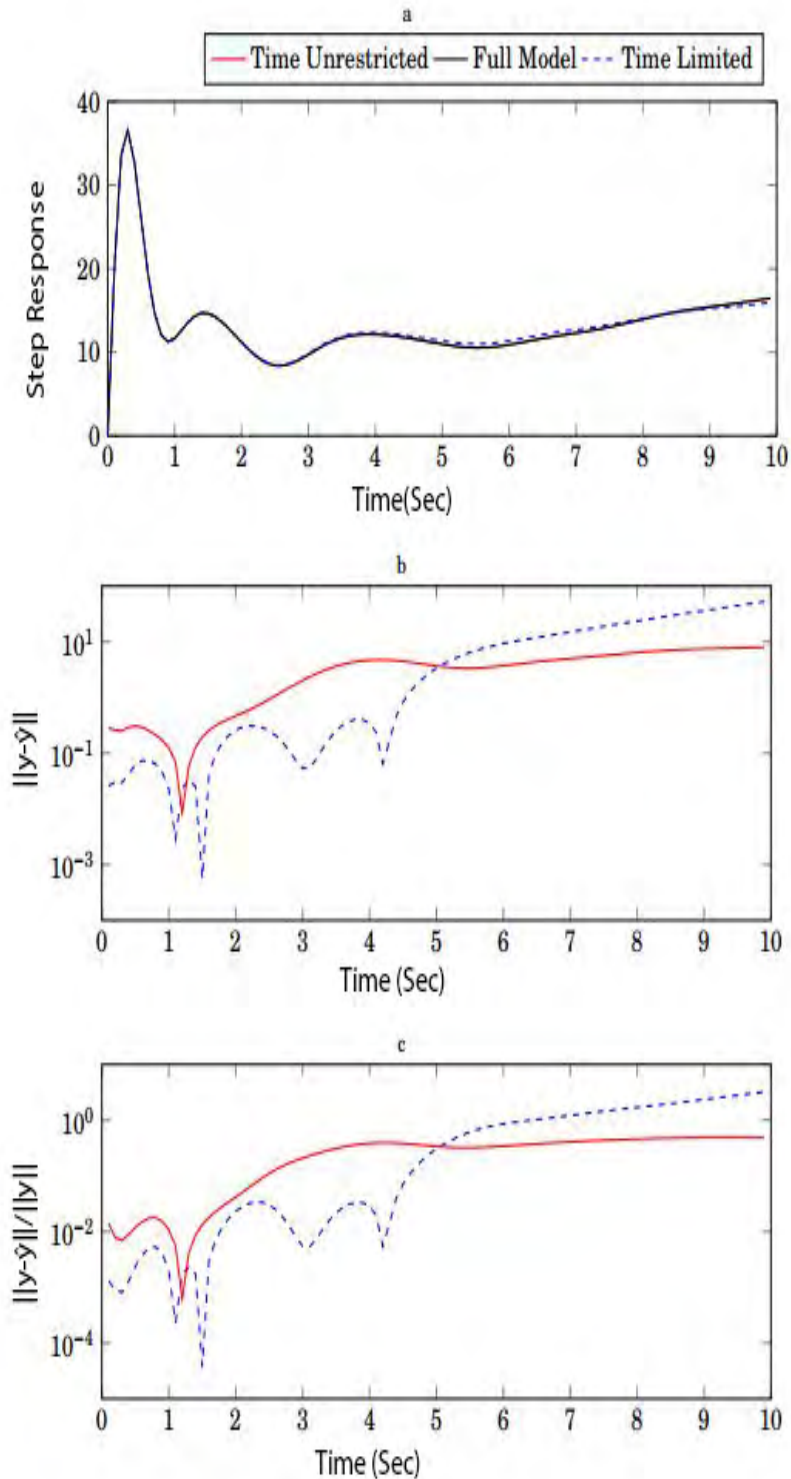


Figure 6.8: (a) Approximation of full models and (b) Absolute (c) Relative errors of reduced order BIPS-606 Model on time interval [2,5]

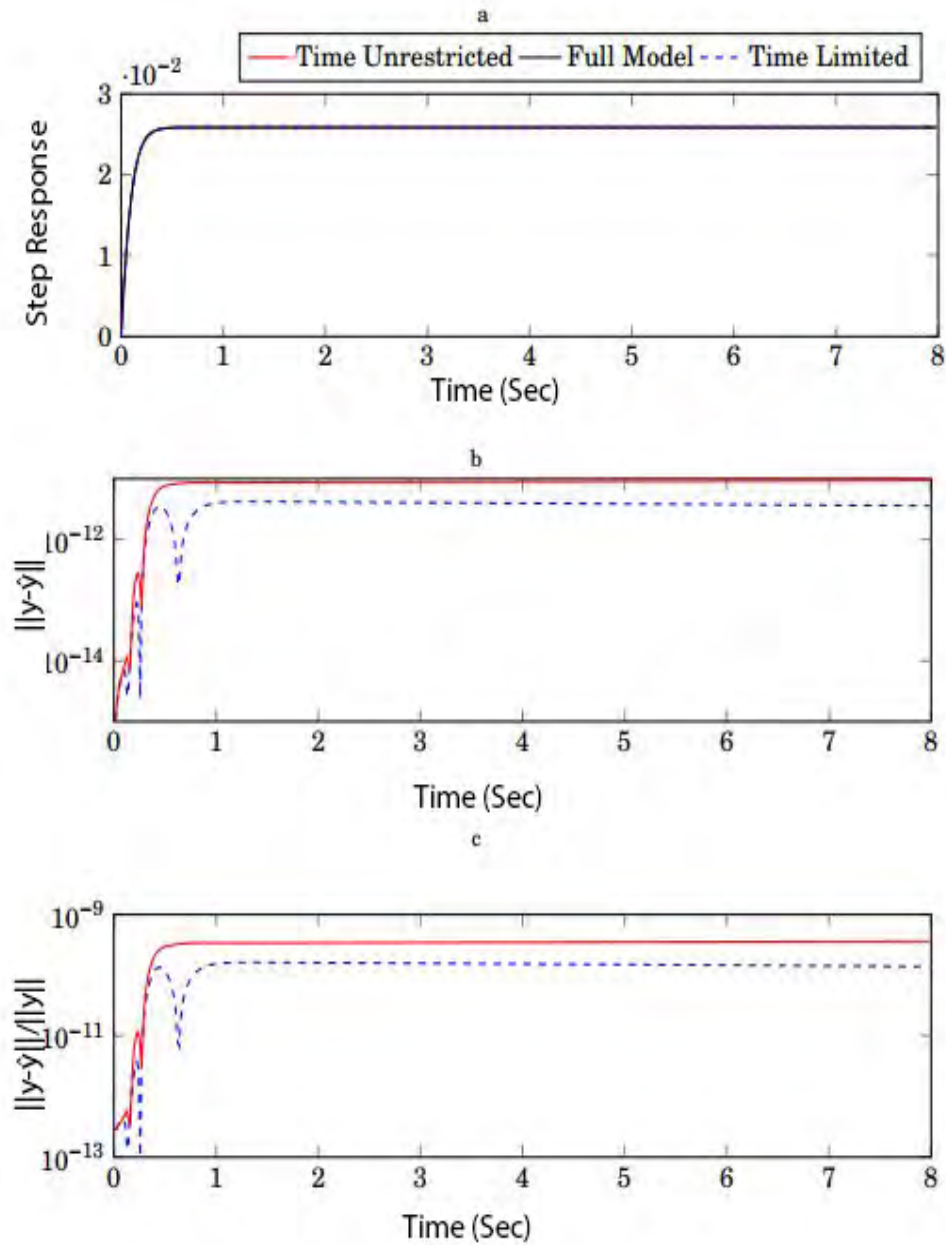


Figure 6.9: (a) Approximation of full models and (b) Absolute (c) Relative errors of reduced order Ossen Model on time interval $[0,6]$

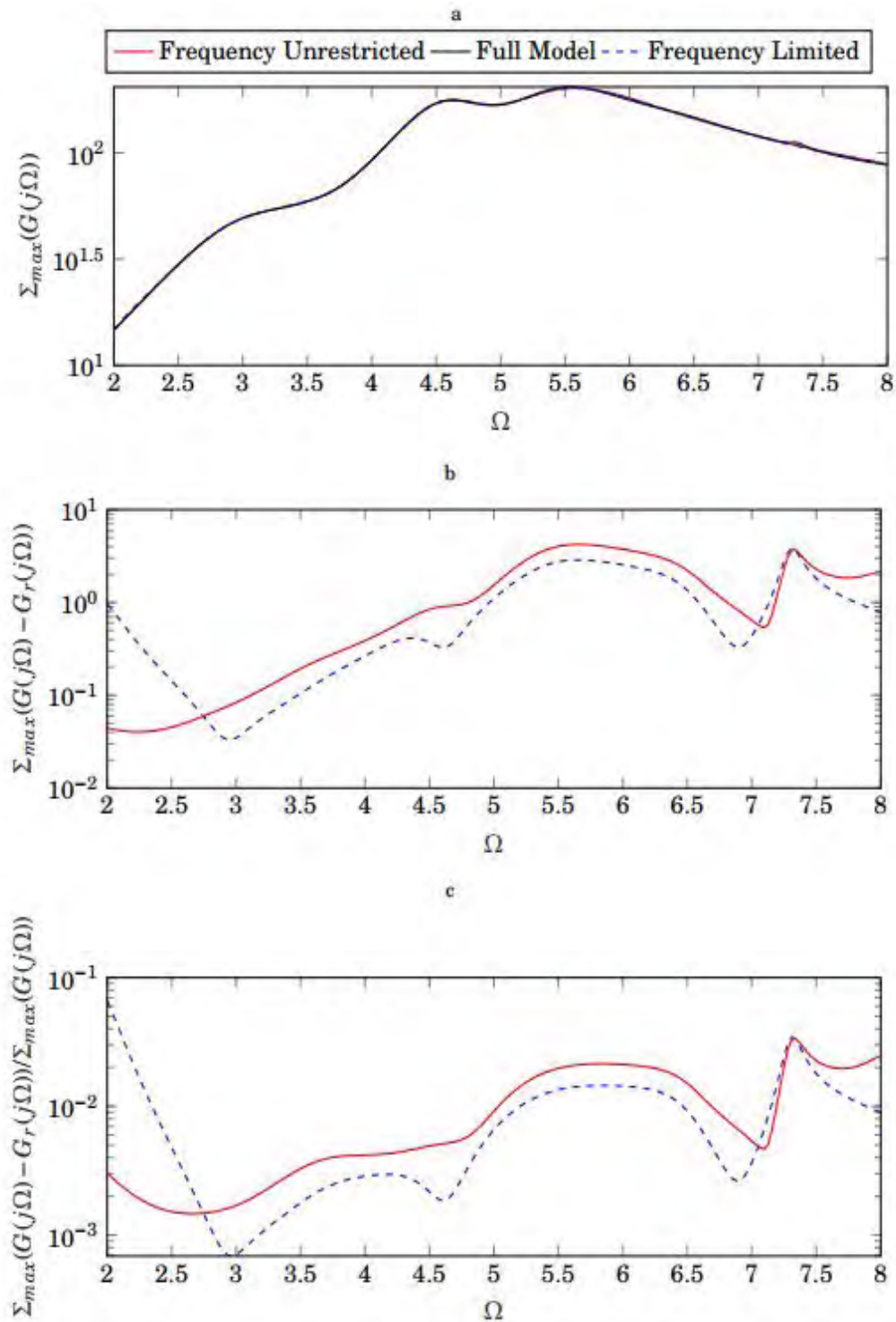


Figure 6.10: (a) Approximation of full models and (b) Absolute (c) Relative errors of reduced order BIPS-1693 Model on frequency interval [3,7]

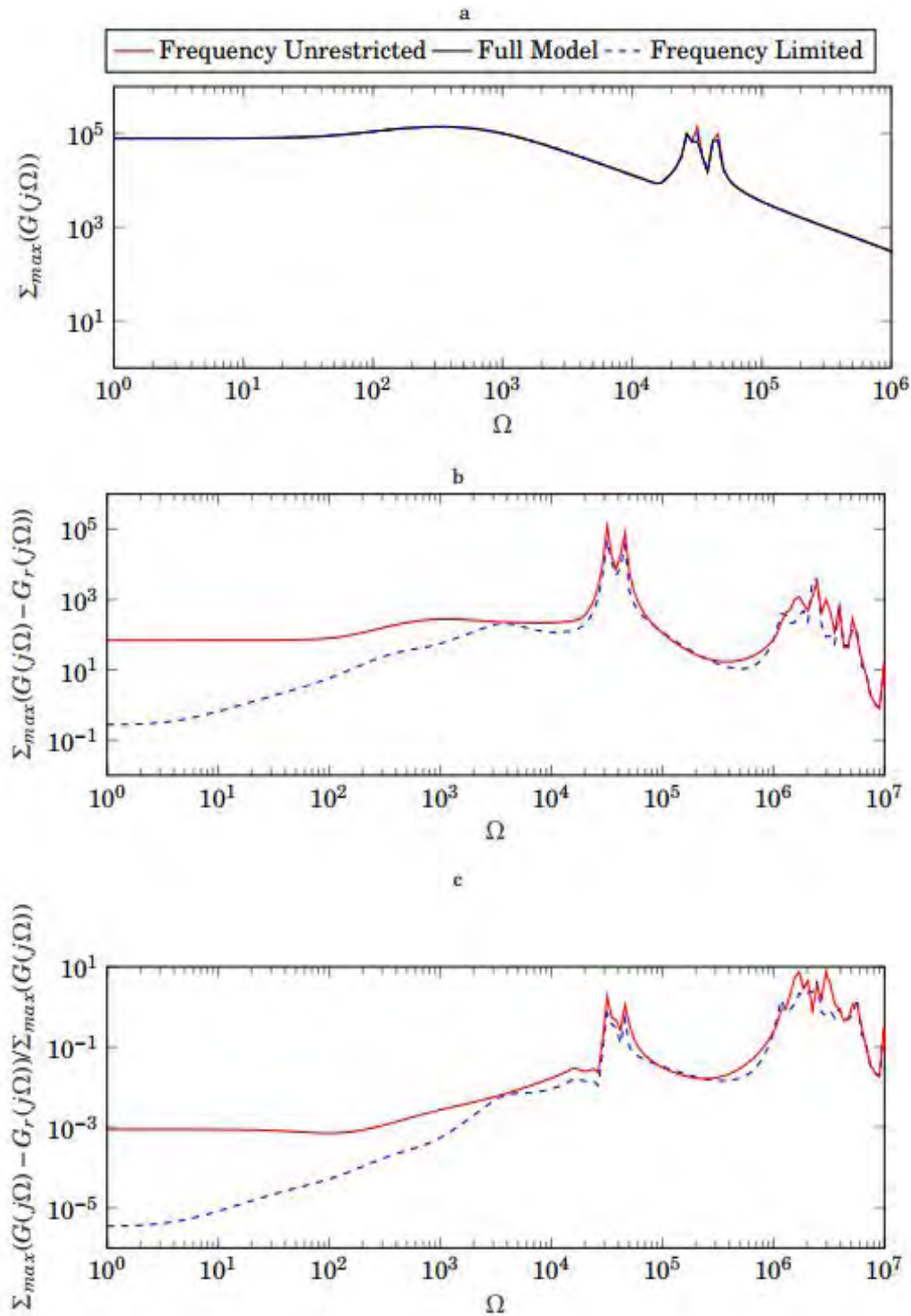


Figure 6.11: (a) Approximation of full models and (b) Absolute (c) Relative errors of reduced order Power System Model on frequency interval $[0, 5]$

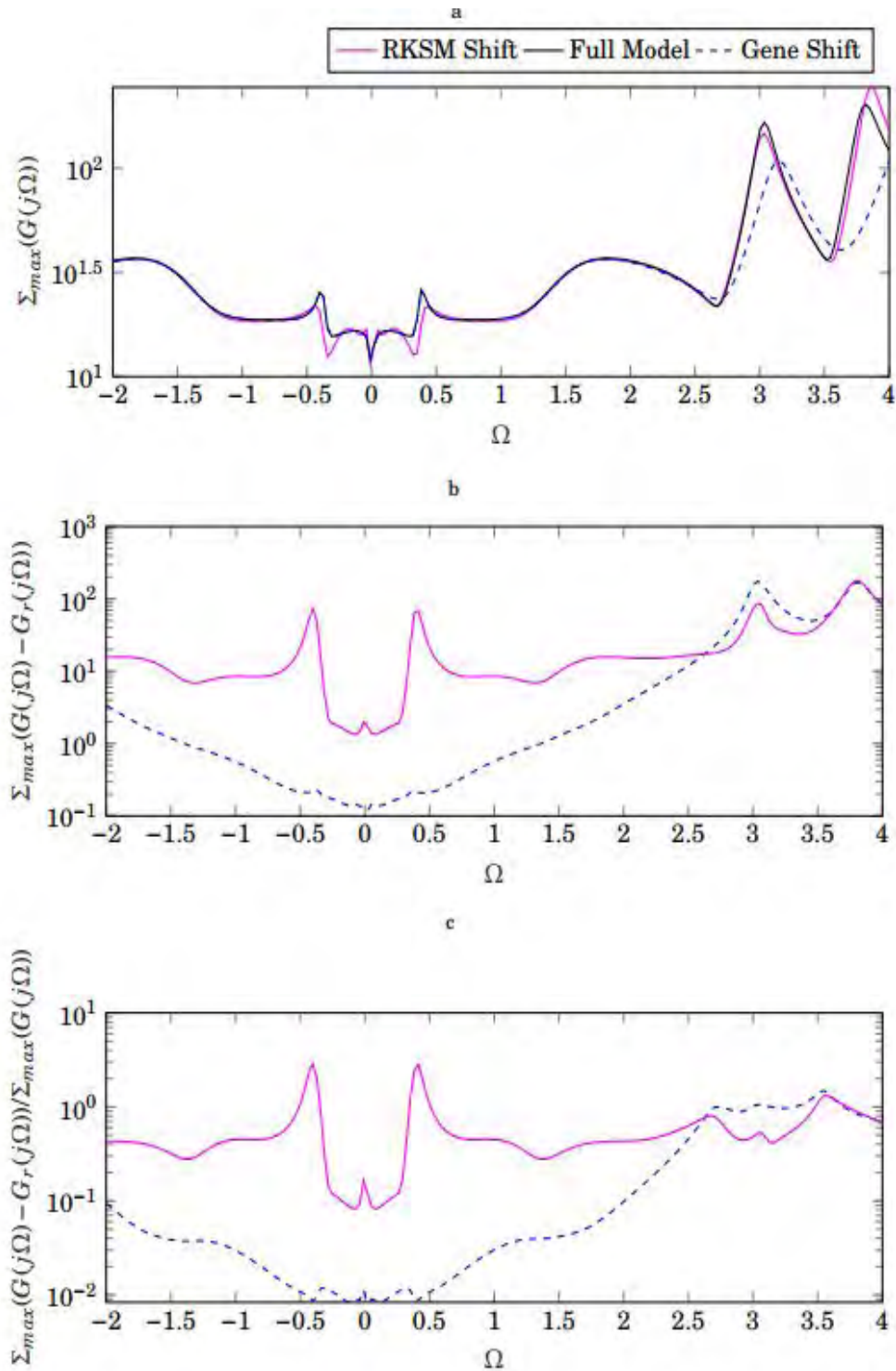


Figure 6.12: Comparative error analysis between full and reduced order models using existing RKSM shift and proposed Gene shift on frequency interval [-2,2]

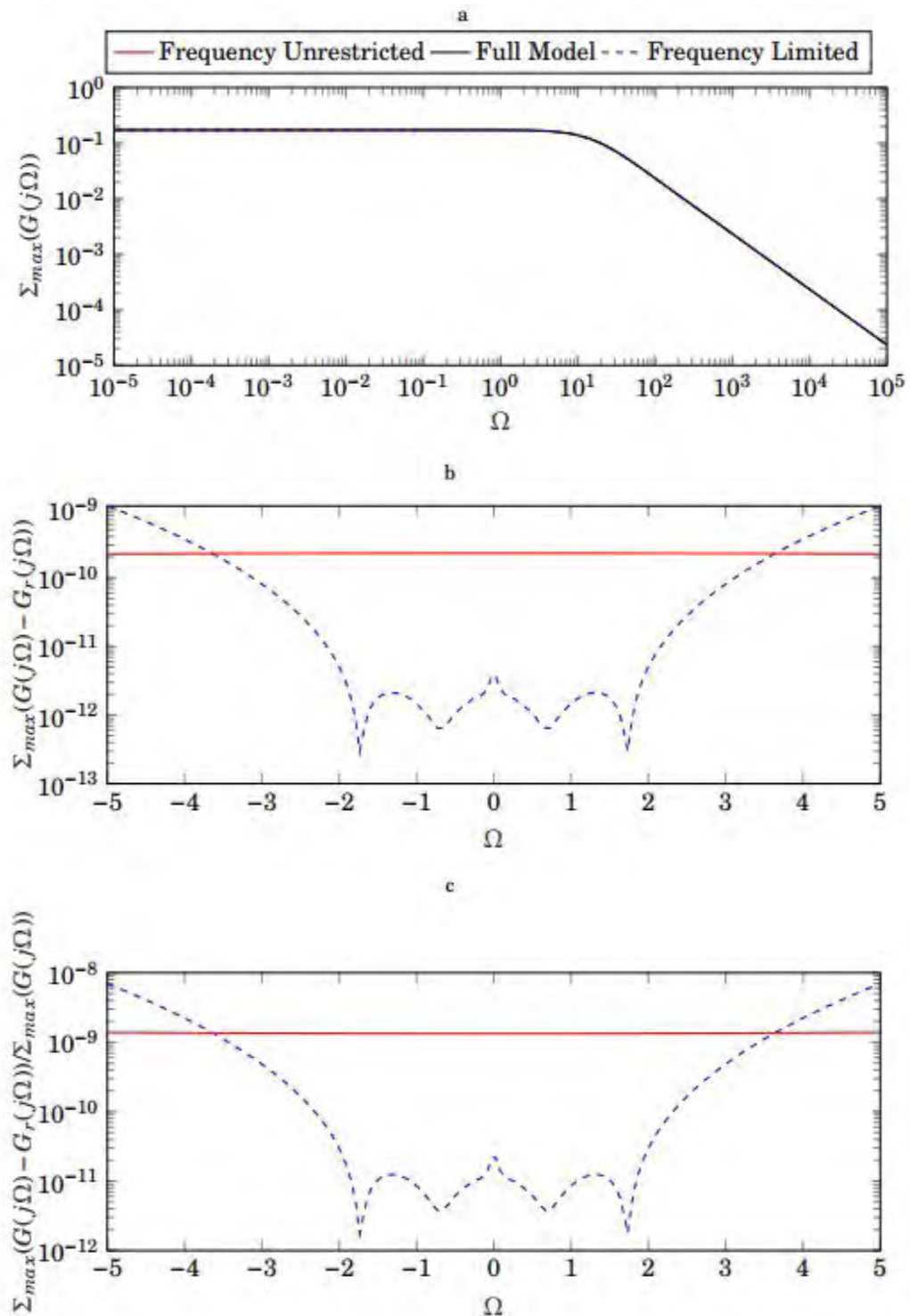


Figure 6.13: (a) Approximation of full models and (b) Absolute (c) Relative errors of reduced order Ossen Model on frequency interval $[-3,3]$

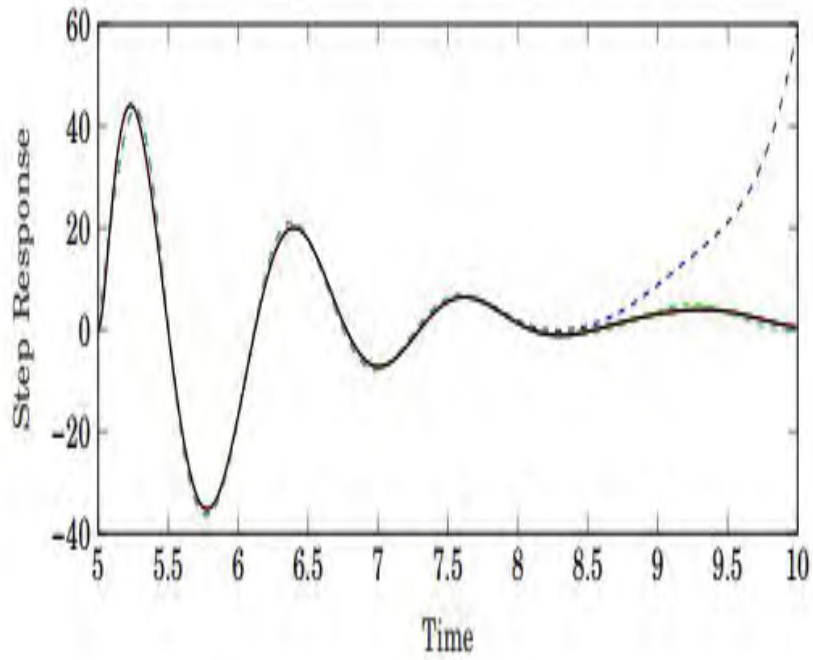


Figure 6.14: Time domain analysis of stable and unstable reduced order system

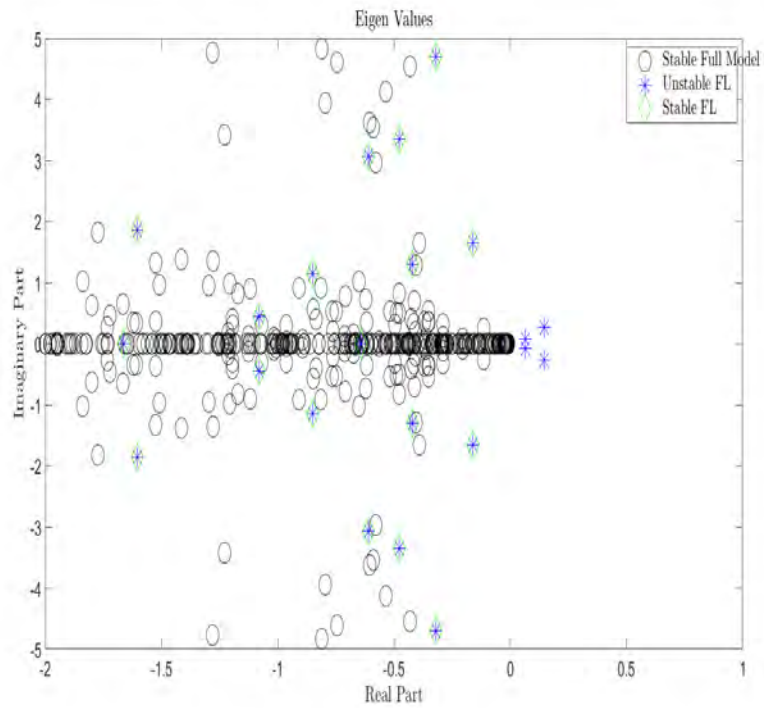


Figure 6.15: Eigenvalues observation of stable and unstable reduced order models

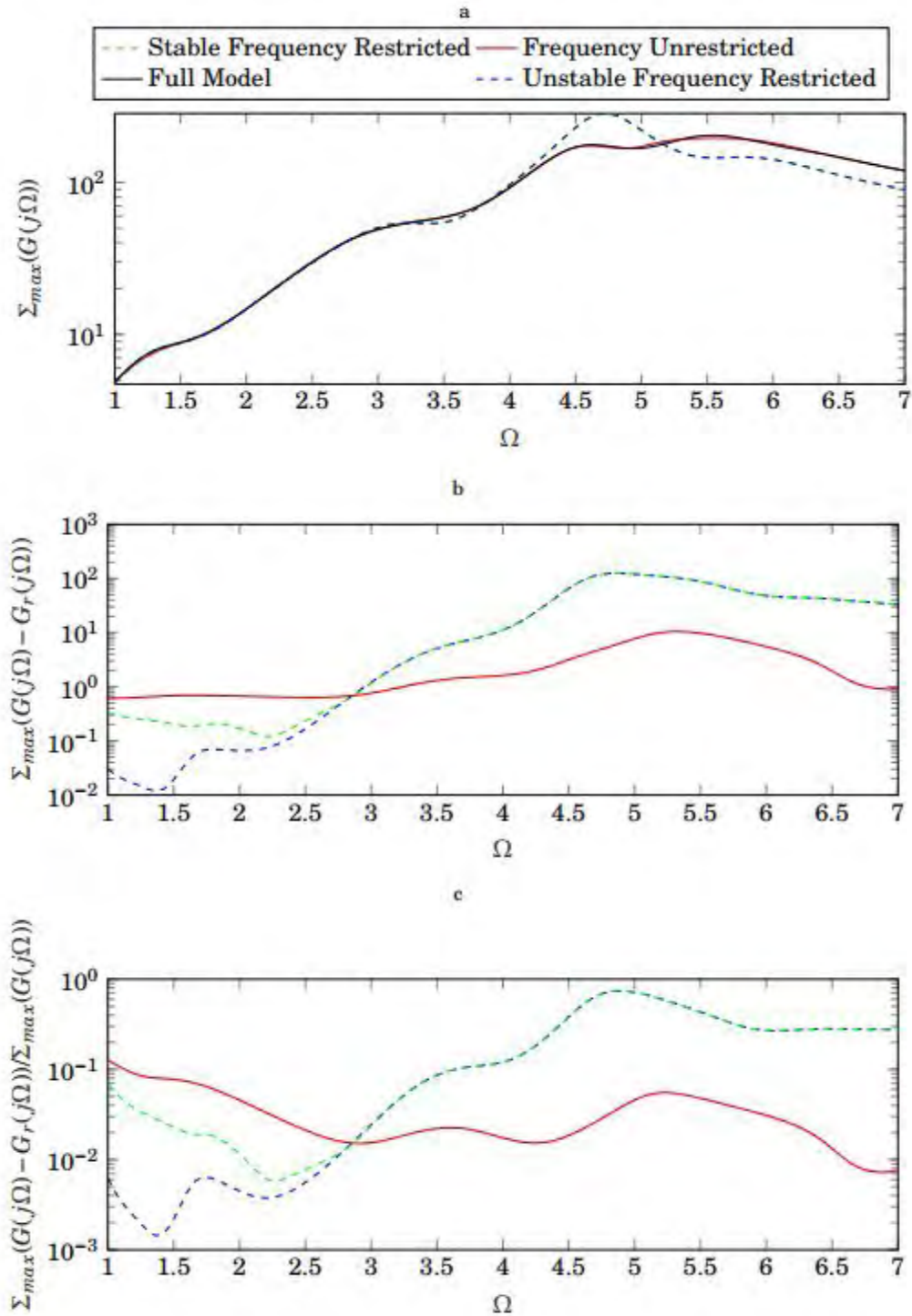


Figure 6.16: Comparison between unstable and stable model on frequency intervals [1,3]

CONCLUSION AND FUTURE WORK

7.1 Conclusion

In all over this thesis, basically four important issues have been elaborately presented. First of all, the generation of the data models from the physical models has discussed in Chapter 3 arisen in two major practical oriented topics: Electrodynamics and Fluid dynamics because data models are recognised as the life-blood of the control and optimization analyses. Since this thesis is based on the model order reduction optimization techniques for efficient data modelling and it is an important necessity in the field of engineering during data modelling and optimization to reduce the dimensions of the models on finite time and frequency intervals for time and frequency domain analyses, we have mainly focused on the model order reduction of the dynamic models on restricted time and frequency intervals. For that reasons, we have discussed on the efficient solution of the controllable and observable Lyapunov equations on restricted time intervals in Chapter 4 and on restricted frequency intervals in Chapter 5 using Rational Krylov Subspace Method (RKSM). Finally, we have reduced the order of the models analysing the equivalency of the original full order models using square-root Balanced Truncation (BT) technique describing in Chapter 6.

Firstly, we have generated data models from the physical models arisen in two different types of real-life related problems. We have applied proper governing equations and initial and boundary conditions to create physical models and then, extracted data from those physical models after simulation. We have rearranged the extracted data to form the state-space equations and used those data as system matrices of those formulated equations.

Since our prime concern is to deal with large-scale sparse descriptor data models, we have proposed algorithms for solving Lyapunov equations on time and frequency intervals constructing around sparse large-scale descriptor models of two classes known as index-I and index-II systems after modifying the existing RKSM methods for generalised system. For increasing the efficiency of our proposed algorithms, we have solved the linear systems necessary for creating projections of the Krylov subspaces keeping the sparsity patterns of the system matrices as same as original. We have proposed an algorithm for solving matrix exponential keeping the state matrices sparse what is one of the major computational hindrance during solving the time-restricted Lyapunov equations. However, we have conducted an analytical discussion on the computational methods of the matrix logarithm for imposing the best procedure during logarithm computation what is mandatory for solving Lyapunov equations on nominated frequency intervals. Since selection of

shift parameters is a vital steps during computation of the solution of the Lyapunov equations and there is no definite process of the selection of shift parameters, we have also proposed a process of shift parameter selection using evolutionary algorithm commonly known as genetic algorithm. Since it is a probabilistic algorithm, we have done a thorough analysis on the impact of the different key parameters used for the selection of shift parameters by genetic algorithm. As RKSM is an iterative method, so we have applied a normalized residual technique to break the iterative loop after beyond the satisfactory residual norm.

Finally, we have imposed balancing based projection technique known as Balanced Truncation (BT) for model order reduction of descriptor system after modifying the existing procedure suitable for descriptor systems. Since the reduced order models on restricted time and frequency intervals give no guarantee of the system's stability, we have proposed stability retrieving technique what not only retains the system's stability but also minimizes error on finite time and frequency intervals. In concluding stage, the accuracy of our proposed methods has been discussed by a vast numerical analysis on reduced system's errors, frequency responses and time domain responses for several test systems. The final analytical observations give a conclusion that on restricted time and frequency intervals our proposed methods produce more accurate approximation of the original system comparing with time and frequency unrestricted reduced order models.

7.2 Future Work

A wide range of futuristic research possibilities on system and control optimization may be extended from this presented research work. Some of them are theoretical whereas some others relate to the computational scientific aspects. The techniques, we have proposed here, can be efficiently used to solve many practical oriented problems as well as for dynamic systems of large-scale system. Since we have discussed two special types of indexing systems, what are frequently available in our daily life, our techniques can be easily adaptable in various field of engineering problems. However, there are few topics in this thesis what may be extended directly in future research.

- Although we have proposed an efficient process to solve matrix exponential, we do not give a proper remedy to calculate complex matrix logarithm having negative real parts, i.e. general value logarithm due to the abnormal behaviour of the matrix logarithm on complex plane. So in future, we may do a thorough analysis on it and try to find better process based on iterative or general residual process.
- We have proposed an algorithm, what deals with time intervals having non-homogeneous initial conditions. However, we have proposed it only for one special class of descriptor system known as index-I system. We did not do any analysis on no-homogeneous time domain for index-II data models. So it is our another plan to do a analysis on this topic in future.
- We have proposed a shift parameter selection process by genetic algorithm what is affected by the change of different types of probabilistic parameters. However, at here we have done our analysis by inserting some static values of the parameters. So we have to change the

value of the parameters manually during analysis. In future, we may try to modify our algorithm in the sense of adapting with the nature of the data so that the value of the parameters can be automatically upgraded. Hopefully, it will be more efficient then.

- Despite index-III descriptor system is rarely found in practical life, to some extent the physical systems are turned into this special kind of data structure. This thesis does not concern with the index-III system. However, in the future, our study will be extended for this system.
- We want to extend our idea to solve the algebraic Riccati equations on finite time and frequency intervals so that it can be efficient to design Linear Quadratic Regulator (LQR) to regulate any dynamic system on finite time and frequency intervals.

BIBLIOGRAPHY

- [1] W. H. A. Schilders, H. A. van der Vorst, and J. Rommes, *Model Order Reduction: Theory, Research Aspects and Applications*. Berlin, Heidelberg: Springer-Verlag, 2008.
- [2] M. M. Uddin, “Computational methods for model reduction of large-scale sparse structured descriptor systems,” Ph.D. Thesis, OVGU, Magdeburg, Germany, 2015. [Online]. Available: <http://nbn-resolving.de/urn:nbn:de:gbv:ma9:1-6535>
- [3] A. C. Antoulas, D. C. Sorensen, and S. Gugercin, “A survey of model reduction methods for large-scale systems,” *ContempMath*, vol. 280, pp. 193–219, 2001.
- [4] P. Benner, V. Mehrmann, and D. C. Sorensen, *Dimension Reduction of Large-Scale Systems*, ser. LNCSE. Springer-Verlag, Berlin/Heidelberg, Germany, 2005.
- [5] M. M. Uddin, “Model reduction for piezo-mechanical systems using Balanced Truncation,” Master’s thesis, Stockholm University, Stockholm, Sweden, 2011. [Online]. Available: http://www.qucosa.de/fileadmin/data/qucosa/documents/7822/Master_Thesis_Uddin.pdf
- [6] A. Antoulas, *Approximation of Large-Scale Dynamical Systems*, ser. Advances in Design and Control. Philadelphia, PA: SIAMPub, 2005.
- [7] P. Benner, M. Hinze, and E. J. W. ter Maten, Eds., *Model Reduction for Circuit Simulation*, ser. Lecture Notes in Electrical Engineering. Dordrecht: Springer, 2011.
- [8] Z.-Q. Qu, *Model Order Reduction Techniques with Applications in Finite Element Analysis: With Applications in Finite Element Analysis*. London: Springer-Verlag, 2004.
- [9] M. M. Uddin, *Computational Methods for Approximation of Large-Scale Dynamical Systems*. New York, USA: Chapman and Hall/CRC, 2019.
- [10] B. N. Datta, *Numerical Methods for Linear Control Systems*. California, USA: Elsevier Academic Press, 2004.
- [11] M. S. Hossain, “Efficient solution of lyapunov equation for descriptor system and application to model order reduction,” 2017. [Online]. Available: <http://lib.buet.ac.bd:8080/xmlui/handle/123456789/4758>
- [12] W. Gawronski and J. Juang, “Model reduction in limited time and frequency intervals,” *Int. J. Syst. Sci.*, vol. 21, no. 2, pp. 349–376, 1990.

-
- [13] K. Fernando and H. Nicholson, "Singular perturbational model reduction of balanced systems," *IEEE Transactions on Automatic Control*, vol. 27, no. 2, pp. 466–468, 1982.
- [14] K. Glover, "All optimal hankel-norm approximations of linear multivariable systems and their l₂-error bounds," *International journal of control*, vol. 39, no. 6, pp. 1115–1193, 1984.
- [15] I. M. Elfadel and D. D. Ling, "A block rational Arnoldi algorithm for multipoint passive model-order reduction of multiport RLC networks," in *Proceedings of the 1997 IEEE/ACM international conference on Computer-aided design*. IEEE Computer Society, 1997, pp. 66–71.
- [16] R. W. Freund, "Krylov-subspace methods for reduced-order modeling in circuit simulation," *Journal of Computational and Applied Mathematics*, vol. 123, no. 1-2, pp. 395–421, 2000.
- [17] B. Moore, "Principal component analysis in linear systems: Controllability, observability, and model reduction," *IEEE transactions on automatic control*, vol. 26, no. 1, pp. 17–32, 1981.
- [18] M. G. Safonov and R. Chiang, "A Schur method for balanced-truncation model reduction," *IEEE Transactions on Automatic Control*, vol. 34, no. 7, pp. 729–733, 1989.
- [19] K. Jbilou, "ADI preconditioned Krylov methods for large Lyapunov matrix equations," *Linear algebra and its applications*, vol. 432, no. 10, pp. 2473–2485, 2010.
- [20] J.-R. Li and J. White, "Low rank solution of Lyapunov equations," *SIAM Journal on Matrix Analysis and Applications*, vol. 24, no. 1, pp. 260–280, 2002.
- [21] S. Gugercin, D. C. Sorensen, and A. C. Antoulas, "A modified low-rank Smith method for large-scale Lyapunov equations," *Numerical Algorithms*, vol. 32, no. 1, pp. 27–55, 2003.
- [22] T. Penzl, "A cyclic low rank Smith method for large sparse Lyapunov equations," *SIAM SciComp*, vol. 21, no. 4, pp. 1401–1418, 2000.
- [23] I. M. Jaimoukha and E. M. Kasenally, "Krylov subspace methods for solving large Lyapunov equations," *SIAM Journal on Numerical Analysis*, vol. 31, no. 1, pp. 227–251, 1994.
- [24] K. Jbilou and A. Riquet, "Projection methods for large Lyapunov matrix equations," *Linear Algebra and its Applications*, vol. 415, no. 2-3, pp. 344–358, 2006.
- [25] V. Simoncini, "A new iterative method for solving large-scale Lyapunov matrix equations," *SIAM Journal on Scientific Computing*, vol. 29, no. 3, pp. 1268–1288, 2007.
- [26] Y. Saad, "Numerical solution of large Lyapunov equation," in *Signal Processing, Scattering, Operator Theory and Numerical Methods*, M. A. Kaashoek, J. H. van Schuppen, and A. C. M. Ran, Eds. Birkhauser, 1990, pp. 503–511.

-
- [27] P. Benner, E. S. Quintana-Ortí, and G. Quintana-Ortí, “Balanced truncation model reduction of large-scale dense systems on parallel computers,” *Mathematical and Computer Modelling of Dynamical Systems*, vol. 6, no. 4, pp. 383–405, 2000.
- [28] C. Kenney and A. J. Laub, “Rational iterative methods for the matrix sign function,” *SIAM Journal on Matrix Analysis and Applications*, vol. 12, no. 2, pp. 273–291, 1991.
- [29] R. H. Bartels and G. W. Stewart, “Solution of the matrix equation $AX + XB = C$: Algorithm 432,” *CACM*, vol. 15, pp. 820–826, 1972.
- [30] D. C. Sorensen and Y. Zhou, “Direct methods for matrix Sylvester and Lyapunov equations,” *Journal of Applied Mathematics*, vol. 2003, no. 6, pp. 277–303, 2003.
- [31] D. Kressner, “Block variants of Hammarling’s method for solving Lyapunov equations,” *ACM Transactions on Mathematical Software (TOMS)*, vol. 34, no. 1, pp. 1–15, 2008.
- [32] T. Penzl, “Numerical solution of generalized Lyapunov equations,” *Advances in Computational Mathematics*, vol. 8, no. 1, pp. 33–48, 1998.
- [33] A. Ruhe, “Rational Krylov sequence methods for eigenvalue computation,” *Linear Algebra and its Applications*, vol. 58, pp. 391–405, 1984.
- [34] V. Druskin and V. Simoncini, “Adaptive rational Krylov subspaces for large-scale dynamical systems,” *Systems & Control Letters*, vol. 60, no. 8, pp. 546–560, 2011.
- [35] M. M. Uddin, M. S. Hossain, and M. F. Uddin, “Rational Krylov subspace method (RKSM) for solving the lyapunov equations of index-1 descriptor systems and application to balancing based model reduction,” in *2016 9th International Conference on Electrical and Computer Engineering (ICECE)*. IEEE, 2016, pp. 451–454.
- [36] M. S. Hossain and M. M. Uddin, “Iterative methods for solving large sparse Lyapunov equations and application to model reduction of index 1 differential-algebraic-equations,” *Numerical Algebra, Control & Optimization*, vol. 9, no. 2, p. 173, 2019.
- [37] M. Imran and A. Ghafoor, “Frequency limited model reduction techniques with error bounds,” *IEEE Transactions on Circuits and Systems II: Express Briefs*, vol. 65, no. 1, pp. 86–90, 2017.
- [38] K. S. Haider, A. Ghafoor, M. Imran, and F. M. Malik, “Model reduction of large scale descriptor systems using time limited gramians,” *Asian Journal of Control*, vol. 19, no. 3, pp. 1217–1227, 2017.
- [39] P. Benner, P. Kürschner, and J. Saak, “Frequency-limited balanced truncation with low-rank approximations,” *SIAM Journal on Scientific Computing*, vol. 38, no. 1, pp. A471–A499, 2016.
- [40] P. Kürschner, “Balanced truncation model order reduction in limited time intervals for large systems,” *Advances in Computational Mathematics*, vol. 44, no. 6, pp. 1821–1844, 2018.

-
- [41] J. Sastre, J. Ibáñez, E. Defez, and P. Ruiz, “New scaling-squaring Taylor algorithms for computing the matrix exponential,” *SIAM Journal on Scientific Computing*, vol. 37, no. 1, pp. A439–A455, 2015.
- [42] A. H. Al-Mohy and N. J. Higham, “Improved inverse scaling and squaring algorithms for the matrix logarithm,” *SIAM Journal of Scientific Computing*, vol. 34, no. 4, pp. C153–C169, 2012.
- [43] S. Gugercin and A. C. Antoulas, “A survey of model reduction by balanced truncation and some new results,” *IntControl*, vol. 77, no. 8, pp. 748–766, 2004.
- [44] N. W. McLachlan, *Laplace transforms and their applications to differential equations*. New York, USA: Dover Publication, 2014.
- [45] T. Stykel, “Analysis and numerical solution of generalized Lyapunov equations,” Ph.D. Thesis, Technische Universität Berlin, Berlin, 2002.
- [46] P. Kunkel and V. Mehrmann, *Differential-algebraic equations: analysis and numerical solution*. Switzerland: European Mathematical Society, 2006.
- [47] M. Green and D. J. Limebeer, *Linear robust control*. New York, USA: Dover Publication, 2012.
- [48] J. R. Leigh, *Functional analysis and linear control theory*. New York, USA: Dover Publication, 2007.
- [49] T. Kailath, *Linear systems*. Englewood Cliffs, NJ: Prentice-Hall, 1980.
- [50] Z. Gajic and M. T. J. Qureshi, *Lyapunov matrix equation in system stability and control*. New York, USA: Dover Publication, 2008.
- [51] D. Petersson, “A nonlinear optimization approach to \mathcal{H}_2 -optimal modeling and control,” Ph.D. dissertation, Linköping University Electronic Press, 2013.
- [52] A. Laub, M. Heath, C. Paige, and R. Ward, “Computation of system balancing transformations and other applications of simultaneous diagonalization algorithms,” *IEEE Transactions on Automatic Control*, vol. 32, no. 2, pp. 115–122, 1987.
- [53] L. N. Trefethen and D. Bau III, *Numerical linear algebra*. Philadelphia, USA: SIAM, 1997.
- [54] R. A. Horn and C. R. Johnson, *Matrix analysis*. New York, USA: Cambridge university press, 2012.
- [55] G. Strang, *Introduction to linear algebra*. Wellesley, MA: Wellesley-Cambridge Press, 1993.
- [56] N. J. Higham, *Functions of matrices: theory and computation*. Philadelphia, USA: SIAM, 2008.
- [57] S. L. Brunton and J. N. Kutz, *Data-driven science and engineering: Machine learning, dynamical systems, and control*. New York, USA: Cambridge University Press, 2019.

-
- [58] W. E. Arnoldi, "The principle of minimized iterations in the solution of the matrix eigenvalue problem," *Quarterly of applied mathematics*, vol. 9, no. 1, pp. 17–29, 1951.
- [59] R. B. Lehoucq, D. C. Sorensen, and C. Yang, *ARPACK users' guide: solution of large-scale eigenvalue problems with implicitly restarted Arnoldi methods*. Philadelphia, USA: SIAM, 1998.
- [60] E. D. Denman and A. N. Beavers Jr, "The matrix sign function and computations in systems," *Applied mathematics and Computation*, vol. 2, no. 1, pp. 63–94, 1976.
- [61] C. S. Kenney and A. J. Laub, "The matrix sign function," *IEEE Transactions on Automatic Control*, vol. 40, no. 8, pp. 1330–1348, 1995.
- [62] P. Benner and E. S. Quintana-Ortí, "Solving stable generalized Lyapunov equations with the matrix sign function," *Numerical Algorithms*, vol. 20, no. 1, pp. 75–100, 1999.
- [63] U. Baur and P. Benner, "Factorized solution of Lyapunov equations based on hierarchical matrix arithmetic," *Computing*, vol. 78, no. 3, pp. 211–234, 2006.
- [64] A. Lu and E. L. Wachspress, "Solution of Lyapunov equations by alternating direction implicit iteration," *Computers & Mathematics with Applications*, vol. 21, no. 9, pp. 43–58, 1991.
- [65] P. Benner, P. Kürschner, and J. Saak, "Self-generating and efficient shift parameters in ADI methods for large Lyapunov and Sylvester equations," *Electronic Transactions on Numerical Analysis (ETNA)*, vol. 43, pp. 142–162, 2014.
- [66] J.-R. Li and J. White, "Low rank solution of Lyapunov equations," *SIAM Journal on Matrix Analysis and Applications*, vol. 24, no. 1, pp. 260–280, 2002.
- [67] N. Lang, H. Mena, and J. Saak, "On the benefits of the LDL^T factorization for large-scale differential matrix equation solvers," *Linear Algebra and its Applications*, vol. 480, pp. 44–71, 2015.
- [68] P. Benner, P. Kürschner, and J. Saak, "Efficient handling of complex shift parameters in the low-rank Cholesky factor ADI method," *Numerical Algorithms*, vol. 62, no. 2, pp. 225–251, 2013.
- [69] V. Simoncini and V. Druskin, "Convergence analysis of projection methods for the numerical solution of large Lyapunov equations," *SIAM Journal on Numerical Analysis*, vol. 47, no. 2, pp. 828–843, 2009.
- [70] D. Kressner, "Memory-efficient Krylov subspace techniques for solving large-scale Lyapunov equations," in *2008 IEEE International Conference on Computer-Aided Control Systems*. IEEE, 2008, pp. 613–618.
- [71] T. Penzl, "Algorithms for model reduction of large dynamical systems," *Linear algebra and its applications*, vol. 415, no. 2-3, pp. 322–343, 2006.

-
- [72] K. Gallivan, A. Vandendorpe, and P. Van Dooren, “Model reduction of MIMO systems via tangential interpolation,” *SIAM Journal on Matrix Analysis and Applications*, vol. 26, no. 2, pp. 328–349, 2004.
- [73] S. Gugercin, A. C. Antoulas, and C. Beattie, “ \mathcal{H}_2 model reduction for large-scale linear dynamical systems,” *SIAM journal on matrix analysis and applications*, vol. 30, no. 2, pp. 609–638, 2008.
- [74] S. Gugercin, “An iterative SVD-Krylov based method for model reduction of large-scale dynamical systems,” *Linear Algebra and its Applications*, vol. 428, no. 8-9, pp. 1964–1986, 2008.
- [75] O. B. Wilson, *Introduction to theory and design of sonar transducers*. USA: Peninsula Pub, 1988.
- [76] Piezoelectric Tonpilz Transducer, author=COMSOL, url= <https://www.comsol.com/model/piezoelectric-tonpilz-transducer-11478>, note = Online; accessed: 2021-01-23.
- [77] L. E. Kinsler, A. R. Frey, A. B. Coppens, and J. V. Sanders, *Fundamentals of acoustics*. USA: John wiley & sons, 1999.
- [78] T. Ikeda, *Fundamentals of Piezoelectricity*. UK: Oxford university press, 1996.
- [79] Resources, author=IEEE PES AMPS DSAS Test Feeder Working Group, year=1992, url=<https://site.ieee.org/pes-testfeeders/resources/>, note = Online; accessed: 2020-11-20.
- [80] H. Saadat, *Power system analysis*. New York, USA: McGraw-hill, 1999.
- [81] Software, author=J. Rommes, year = 2008, url=https://sites.google.com/site/rommes/software/?fbclid=iwar3yckibt9zbbuzbyawwrkqwzltjieivqinjz_k4gmln_obf3aoc-h6dade, note = Online; accessed: 2020-02-10.
- [82] T. Stykel, “Balanced truncation model reduction for semidiscretized Stokes equation,” *Linear Algebra and its Applications*, vol. 415, no. 2-3, pp. 262–289, 2006.
- [83] V. Druskin, L. Knizhnerman, and M. Zaslavsky, “Solution of large scale evolutionary problems using rational Krylov subspaces with optimized shifts,” *SIAM Journal on Scientific Computing*, vol. 31, no. 5, pp. 3760–3780, 2009.
- [84] V. Druskin, C. Lieberman, and M. Zaslavsky, “On adaptive choice of shifts in rational Krylov subspace reduction of evolutionary problems,” *SIAM Journal on Scientific Computing*, vol. 32, no. 5, pp. 2485–2496, 2010.
- [85] M. Hochbruck and C. Lubich, “On Krylov subspace approximations to the matrix exponential operator,” *SIAM Journal on Numerical Analysis*, vol. 34, no. 5, pp. 1911–1925, 1997.
- [86] Y. Saad, “Analysis of some Krylov subspace approximations to the matrix exponential operator,” *SIAM Journal on Numerical Analysis*, vol. 29, no. 1, pp. 209–228, 1992.

-
- [87] N. J. Higham, “The scaling and squaring method for the matrix exponential revisited,” *SIAM Journal on Matrix Analysis and Applications*, vol. 26, no. 4, pp. 1179–1193, 2005.
- [88] S. Gugercin, T. Stykel, and S. Wyatt, “Model reduction of descriptor systems by interpolatory projection methods,” *SIAM Journal on Scientific Computing*, vol. 35, no. 5, pp. B1010–B1033, 2013.
- [89] K. I. B. Iqbal, M. M. Uddin, and M. F. Uddin, “In search of frequency-limited low-rank gramian factors for the balancing based model reduction of large-scale sparse descriptor system,” in *2020 23rd International Conference on Computer and Information Technology (ICCIT)*, 2020, pp. 1–5.
- [90] M. Heinkenschloss, T. Reis, and A. C. Antoulas, “Balanced truncation model reduction for systems with inhomogeneous initial conditions,” *Automatica*, vol. 47, no. 3, pp. 559–564, 2011.
- [91] C. Beattie, S. Gugercin, and V. Mehrmann, “Model reduction for systems with inhomogeneous initial conditions,” *Systems & Control Letters*, vol. 99, pp. 99–106, 2017.
- [92] K. I. B. Iqbal, X. Du, M. M. Uddin, and M. F. Uddin, “Time restricted balanced truncation for index-I descriptor systems with non-homogeneous initial condition,” in *Algorithms for Intelligent Systems*. Springer Singapore, 2021, pp. 179–190. [Online]. Available: https://doi.org/10.1007%2F978-981-16-0586-4_15
- [93] M. Heinkenschloss, D. C. Sorensen, and K. Sun, “Balanced truncation model reduction for a class of descriptor systems with application to the Oseen equations,” *SIAM Journal on Scientific Computing*, vol. 30, no. 2, pp. 1038–1063, 2008.
- [94] M. Mitchell, *An introduction to genetic algorithms*. Cambridge, USA: MIT press, 1998.
- [95] D. Whitley, “A genetic algorithm tutorial,” *Statistics and computing*, vol. 4, no. 2, pp. 65–85, 1994.
- [96] D. E. Goldberg, *Genetic algorithms in search, optimization, and Machine Learning*. MA, USA: Addison Wesley Publishing Co. Inc., 1989.
- [97] S. H. Cheng, N. J. Higham, C. S. Kenney, and A. J. Laub, “Approximating the logarithm of a matrix to specified accuracy,” *SIAM Journal on Matrix Analysis and Applications*, vol. 22, no. 4, pp. 1112–1125, 2001.
- [98] N. J. Higham, “Evaluating Padé approximants of the matrix logarithm,” *SIAM Journal on Matrix Analysis and Applications*, vol. 22, no. 4, pp. 1126–1135, 2001.
- [99] L. Dieci, B. Morini, and A. Papini, “Computational techniques for real logarithms of matrices,” *SIAM Journal on Matrix Analysis and Applications*, vol. 17, no. 3, pp. 570–593, 1996.
- [100] P. J. Davis and P. Rabinowitz, *Methods of numerical integration*. California, USA: Elsevier Academic Press, 1984.

- [101] K. I. B. Iqbal, M. M. Uddin, and M. F. Uddin, “Stability preservation of frequency-limited balancing based reduced order model of large scale index-1 descriptor system,” in *2020 11th International Conference on Electrical and Computer Engineering (ICECE)*, 2020, pp. 57–60.
- [102] M. Redmann and P. Kürschner, “An \mathcal{H}_2 -type error bound for time-limited balanced truncation,” *arXiv: Optimization and Control*, 2017.